Re-wiring the mTORC1 Pathway Using Mouse Models of Breast Cancer

by

Bin Xiao

A thesis submitted to McGill University in partial fulfillment of the requirements of the degree of Doctor of Philosophy

Department of Biochemistry

McGill University

Montreal, QC, Canada

Dec 2020

Table of Contents

Abstract

Mammary tumorigenesis is an evolutionary progression which enriches for cellular processes crucial for tumor growth and survival, thus the cancer cell biology during early stages of tumor initiation can differ from that exhibited within the end-stage established tumors. mTORC1 is a master regulator of cell growth, and prominent regulator of mRNA translation through the modulation of 4EBPs and S6 Kinase. While mTORC1 activity is central for the maintenance of breast cancer, the contribution of mTORC1 function during early stages of tumor initiation remains unexplored.

Given that genetically engineered mouse models (GEMMs) of breast cancer faithfully recapitulate the complexity of tumor initiation, two transgenic model systems were employed throughout my thesis work to evaluate the contribution of mTORC1 function during the early stages of tumorigenesis. I demonstrated that genetic ablation of the obligatory activator of mTORC1 Rheb1, within the pre-neoplastic epithelia stalls tumor progression within the early stages until compensation for the loss of Rheb1 is established. While mTORC1 activation is diminished within the Rheb1-deficient pre-neoplastic mammary epithelium, mTORC1 activity is ultimately restored within the Rheb1-deficient tumors. While eIF4E function is consequently restored within the arising Rheb1-deficient tumors, I demonstrated that solely rescuing the eIF4E signaling axis through genetic ablation of both 4EBP1 and 4EBP2 only partially alleviated the defect in tumor initiation attributed to Rheb1 ablation. This observation suggests the importance of other processes downstream of mTORC1, distinct from the regulation of cap-dependent translation initiation, which are additionally required in PyV mT-driven tumor initiation. Taking advantage of an *in vitro* model system of PyV mT-driven tumor initiation, we further evaluated the relative contribution of S6 kinase function in this process.

In attempts to dissect the underlying molecular mechanism of mTORC1 re-activation within the Rheb1-deficient tumors, we uncovered hyperactivating mTOR mutations within a subset of the Rheb1-deficient tumors which contributed to mTORC1 re-activation. We also observed the dependence of alternative small GTPases, such as RalB, in mediating mTORC1 activation. Taken together this thesis work emphasizes the importance of mTORC1 function within mammary tumor initiation, while unraveling the plasticity of the mTORC1 pathway upon perturbation of the upstream component Rheb1, within a biologically relevant *in vivo* context.

Abrégé

Tumogenèse mammaire est un processus évolutif où les processus cellulaires cruciaux pour la croissance et la survie de la tumeur sont sélectionnés et enrichis dans une tumeur. La biologie des cellules tumorales au cours des premiers stades de l'initiation de la tumeur peut être très différente de celle d'une tumeur établie au stade terminal. mTORC1 est un régulateur principal de la croissance cellulaire et joue un rôle bien établi dans la régulation de la traduction de l'ARNm par la régulation des 4EBP et de la S6 kinase. À ces regards mTORC1 contribue aux processus cruciaux pour la croissance et la survie des cellules tumorales. Bien que mTORC1 est centrale pour le maintien du cancer du sein, sa contribution au cours des premiers stades de l'inititiation tumorale n'a pas encore été explorée.

Étant donné que les modèles murins génétiquement modifiés (GEMM) du cancer du sein récapitulent fidèlement la complexité de l'initiation tumorale, deux systèmes de modèles transgéniques ont été utilisés tout au long de mon travail de thèse pour évaluer la contribution de la fonction mTORC1 au cours des premiers stades de la tumorigenèse. J'ai démontré que l'ablation génétique de l'activateur obligatoire de mTORC1 Rheb1, dans l'épithélium pré-néoplasique, bloque la progression tumorale dans les premiers stades jusqu'à ce qu'une compensation pour la perte de Rheb1 soit établie. Alors que l'activation de mTORC1 est diminuée dans l'épithélium mammaire pré-néoplasique déficient en Rheb1, l'activité de mTORC1 est finalement restaurée dans les tumeurs déficientes en Rheb1. Alors que la fonction eIF4E est par conséquent restaurée dans les tumeurs déficientes en Rheb1, j'ai démontré que le seul sauvetage de l'axe de signalisation eIF4E par l'ablation génétique de 4EBP1 et 4EBP2 n'a que partiellement atténué le défaut d'initiation tumorale attribué à l'ablation de Rheb1. Cette observation suggère l'importance d'autres processus en aval de mTORC1, distincts de la régulation de l'initiation de la traduction cap-dépendante, qui sont en outre nécessaires dans l'initiation de la tumeur PyV mT. Profitant d'un système de modèle in vitro d'initiation tumorale PyV mT, nous avons en outre évalué la contribution relative de la fonction kinase S6 dans ce processus.

En essayant de disséquer le mécanisme moléculaire sous-jacent de la réactivation de mTORC1 dans les tumeurs déficientes en Rheb1, nous avons découvert des mutations mTOR hyperactivantes dans un sous-ensemble des tumeurs déficientes en Rheb1 qui ont contribué à la réactivation de mTORC1. Nous avons également observé la dépendance d'autres petites

GTPases, telles que RalB, dans la médiation de l'activation de mTORC1. Pris ensemble, ce travail de thèse souligne l'importance de la fonction mTORC1 dans l'initiation des tumeurs mammaires, tout en révélant la plasticité de la voie mTORC1 lors de la perturbation du composant amont Rheb1, dans un contexte in vivo biologiquement pertinent.

Acknowledgments

My training was supported by MICRTP studentship, studentships from McGill University Health Centre, the McGill Faculty of Medicine, and the Fonds de la Recherche en Santé du Quebec (FRSQ). I would like to thank my supervisor Dr. William Muller for granting us the freedom to pursue our own scientific interests. I would like to thank my advisory committee, Dr. Josie Urisini-Siegel and Dr. Ivan Topisirovic who have provided inspiration, constructive feedback and advice throughout my thesis work. Many thanks to Tung Bui for critical review of my thesis, and Gabriella Johnson for help with translating my abstract into French.

It has been an honor and privilege to have been part of the Muller research group. I would like to extend my gratitude to all past and present lab members for their contributions with experimental troubleshooting, the numerous intriguing discussions, both scientific non-scientific, and for laying the foundations for such a positive, lively and enriching learning environment. My experience in the lab would not have been as been the same without everyone. I would like to extend thanks to past students Jason Turpin and Trisha Rao for their encouragement during my initial transition period into the lab, and into graduate studies. I would like to thank Vasilios Papavasiliou, Cynthia Lavoie, Virginie Sanguin-Gendreau and Dongmei Zuo for their technical help both within the mouse room and on the bench. I would like to thank Harvey Smith for his immeasurable patience and answering my mountains of questions over the years, and the many suggestions throughout my training. I would like to thank my past summer students, Frank Telfer and Sally Xiao for their help with my project. To Chen Ling, Arlan Walsh, Laura Jones, Alison Hirukawa, Tung Bui and Alexandra Simond, I am eternally grateful for the many adventures and memories we created together throughout our PhD training both inside and outside of the lab. Our shared experiences have helped shape me into the better adult that I am today. To Ippy Nandi, Linshan Liu, Sherif Attalla, Tarek Taifour, Yu Gu, Gabriella Johnson, and Vincent Li, I want to thank all of you for bringing fun and excitement into the lab during my descent into old age… I mean, my 30s. You guys always remind me that I am still young at heart. I wish you the best with your future studies.

Lastly, I would also like to thank my parents and my sister for all their insurmountable support, patience and encouragement over the years.

Preface

This thesis is written following the manuscript-based format, whereby Chapter 2 and Chapter 3 are composed of a published peer-reviewed, original research article and a manuscript in preparation, respectively. Chapter 1 is composed of a general introduction and literature review, while Chapter 4 encompasses a general discussion of the results present within Chapter 2 and 3.

First author publications arising from thesis work:

1. "Rheb1-independent Activation of mTORC1 in Mammary Tumors Occurs Through Activating Mutations in mTOR." **Xiao B**, Zuo D, Hirukawa A, Cardiff RD, Lamb R, Sonenberg N, Muller WJ. Cell Rep. 2020 April 28; 31(4): 107571.

2. "Rheb1-deficient ErbB2 mammary tumors switch dependency to alternative GTPase for mTORC1 activation" **Xiao B**, Liu L, Zuo D, Hollern D, Sonenberg N, Andrechek E, and Muller WJ. (Manuscript in preparation.)

3. Parts of Chapter 1 have been extracted for a mini-review entitled "Deregulating the mTORC1 pathway during mammary tumor initiation" **Xiao B** and Muller WJ. *Endocrinology*. (Manuscript in preparation)

Contribution of Authors

Chapter 2: R Lamb provided the conditional Rheb1 knockout mouse strain. N Sonenberg provided the conditional Raptor and mTOR knockout mouse strain. RD Cardiff analyzed the tumor pathology for Figure 2.4 D, and Figure 2.9 B. A Hirukawa designed Figure 2.16 E. D Zuo performed staining for Figure 2.4 B-E, Figure 2.6 A-B, Figure 2.7 A-B, Figure 2.10 A, and I analyzed the data for Figure 2.4 A-C,E-F, Figure 2.6 C-D, Figure 2.7 C-F, and Figure 2.10 B-E. I performed and analyzed data related to Figures 2.1 A-G, Figure 2.2 A-C, Figure 2.3 A-C, Figure 2.4 A-C, E-F. Figure 2.8 A-E, Figure 2.9 A-D, Figure 2.11 A-G, Figure 2.12 A-C, Figure 2.13 A-D, Figure 2.14 A-C, Figure 2.15 A-B, and Figure 2.16 A-D. I wrote the original draft of the manuscript. WJ Muller, Sonenberg N and A Hirukawa provided edits to the manuscript.

Chapter 3: Sonenberg N provided the conditional 4EBP1 and 4EBP2 knockout mouse strain. D Zuo performed staining for Figure 3.3 E-F, Figure 3.7A, and I analyzed the data for Figure 3.3E & G, Figure 3.7B. L Liu performed organoid growth and staining for Figure 3.5B-C. L Liu performed RNA collection for Fig 3.5D, and I analyzed the data for Figure 3.5E. L Liu performed organoid growth and staining for Figure 3.7C-D. I analyzed the data for Figure 3.7C-E. D Hollern and E Andrechek performed bioinformatics analysis for Figure 3.10A, while I performed RNA collection and microarray analysis for Figure 3.10A. I performed and analyzed data for Figure 3.1 A-D, Figure 3.2A, Figure 3.3 A-E and G, Figure 3.4A-B, Figure 3.5A, Figure 3.8A-D, Figure 3.10B-F, and Figure 3.11A. I wrote the original draft of the manuscript, and WJ Muller provided edits to the manuscript.

General Discussion: I performed and analyzed the data for Figure 4.1A-G.

List of Figures

Chapter 1 – General Introduction and Literature Review

Chapter 2 - Rheb1-independent Activation of mTORC1 in Mammary Tumors Occurs through Activating Mutations in mTOR

Chapter 3 - Rheb1-deficient ErbB2 tumors switch dependency to alternative GTPases for mTORC1 activation

Chapter 4 – General Discussion

List of Abbreviations

4EBP1-3 Eukaryotic translation initiation factor 4E-binding protein 1-3
5'UTR - 5' Untranslated region
Akt - v-akt thymoma viral oncogene homolog
AMP - Adenosine monophosphate
AMPK - AMP-activated protein kinase
ATF4 - Activating transcription factor 4
ATP - Adenosine Triphosphate
BCL XL - B-cell lymphoma 2 XL
BrdU - Bromodeoxyuridine
BSA - Bovine Serum Albumin
cDNA - complementary DNA
CK - Cytokeratin
DAPI - 4',6-diamidino-2-phenylindole
DMEM - Dulbecco's modified eagle's medium
DMSO - Dimethyl sulfoxide
DNA - Deoxyribonucleic acid
Dox - Doxycycline
ECM - Extracellular matrix
eEF2 - eukaryotic elongation factor 2 kinase
eEF2K - eukaryotic elongation factor 2 kinase
EGFR - Epidermal growth factor receptor
eIF-4B/4H/4G/4E/2a - eukaryotic intiation factor 4B/4H/4G/4E/2a
ERBB2 - Erythroblastic oncogene B2
ERBB3 - Erythroblastic oncogene B3
Erk - Extracellular-signal-regulated kinase
FBS - Fetal bovine serum
FVB - Friend virus B
Gab1 - Grb2 associated binder 1
GAP - GTPase-activation protein
GEF - Guanine Exchange Factor
GEMM - Genetically engineered mouse model
GFP - Green fluorescent protein
GRB2 - Growth Factor Receptor-bound protein 2
GSK3 - Glycogen synthase kinase 3
GTP - Guanine Triphosphate
GTRosa - gene trap ROSA 26
H&E - Hematoxylin and eosin
HER2 - Human Epidermal Growth Factor Receptor 2
HIF-1α - Hypoxia-inducible factor 1α
IF - Immunofluorescence
IHC - Immunohistochemistry
IHF - Immunohistofluorescence
IRES - internal ribosome entry site
IRS - insulin receptor substrate
Krt14 - Keratin14

Krt5 - Keratin 5
MAPK - Mitogen Activated Protein Kinase
Mek - Mitogen activated protein kinase kinase
Met-tRNAi - Methionine initiator tRNA
MMTV - Mouse mammary tumor virus
MMTV-LTR - Mouse mammary tumor virus long terminal repeat
mRNA - messenger RNA
mTORC1 - Mammalian target of rapamycin complex 1
mTORC2 - Mammalian target of rapamycin complex 2
Myc - v-myc avian myelocytomatosis viral oncogene homolog
NDL - Neu deletion
NIC - NeuNDL IRES Cre
PABP - Poly-A binding protein
PBS - Phosphate buffered saline
PDCD4 - Programmed cell death 4
PDK1 - phosphoinositide-dependent kinase 1
PI3K - Phosphatidylinositol 3-kinase
PR - progesterone receptor
RSK - p90 Ribosomal S6 Kinase
PRAS40 - proline-rich Akt substrate of 40 kilodaltons
PTEN - phosphatase and tensin homologue on chromosome 10
PVDF - Polyvinylidene difluoride
PyV mT - Polyomavirus middle T antigen
Rheb1- Ras Enriched in Brain
RIPA - Radioimmunoprecipitation assay buffer
RNA - Ribonucleic Acid
RNAi - RNA interference
RTK - Receptor tyrosine kinase
RT-PCR - Reverse transcription polymerase chain reaction
rtTA - Reverse tetracycline transactivator
S6K - Ribosomal protein S6 kinase
SDS - Sodium dodecyl sulphate
SEM - Standard error of the mea
SHC - Src homology 2 domain containing
SHIP2 - SH2 Domain-Containing Inositol 5'-Phosphatase
shRNA - Short hairpin RNA
SOS - Son of Sevenless
Src - v-src sarcoma viral oncogene homolog
SREBP - Sterol Regulatory Element Binding Protein
TEB - Terminal End Buds
TetO - Tet Operator, a portion of the tet-responsive element
TSC - Tuberin sclerosis complex
VEGF - Vascular endothelial growth factor
WAP - Whey Acidic Protein

Original Contribution to Knowledge

1. This is the first report of the acute effects of Rheb1 ablation within mammary tumorigenesis whereby loss of Rheb1 stalls tumor progression at early stages of tumor initiation within both an ErbB2-driven model system and a PyV mT-driven model system.
2. We demonstrated within the context of inhibited mTORC1 activity as a consequence of Rheb1 ablation, that restoring eIF4E activation alone is insufficient to permit mammary tumor initiation.
3. We identified that Rheb1-deficient mammary tumors that develop retain mTORC1 activation in a Rheb1-independent manner. This observation emphasizes the crucial role of mTORC1 during tumor progression.
4. We demonstrated that mTOR function is indispensable for ErbB2-driven mammary tumor initiation, as genetic ablation of the kinase completely abolishes tumor formation.
5. We identified spontaneous hyperactivating mutations within a subset of Rheb1-deficient mammary tumors. We provided supporting evidence that these hyperactivating mTOR mutation contribute to driving Rheb1-independency within mTORC1 activation.
6. We provided evidence of that alternative small GTPases such as Ral GTPase is capable of maintaining mTORC1 activation within a Rheb1-independent manner.

Chapter 1 - Literature Review

1.1 Breast Cancer

1.1.1 Epidemiology of Breast Cancer

Breast cancer is a disease characterized by uncontrolled growth of abnormal cells derived from the mammary epithelia, which eventually develop the capacity to invade distal sites and cause lethality. With the development and implementation of more efficient adjuvant therapies, chances of survival has dramatically improved (1). Despite this, breast cancer still presents the highest incidence of cancer (25%) and the second highest incidence of cancer-related deaths (12.9%) within Canadian women (2). Breast cancer is quite a heterogeneous disease both at the histological and molecular level, which plays a large role in hindering the efficacy of therapeutic interventions.

1.1.2 Histopathological Subtypes of Breast Cancer

Given the heterogeneous nature of breast cancer, the development of patient classification systems have allowed for prognosis prediction, and implementation of therapeutic regimes. Early classification system for stratifying patients utilized a combination of clinical parameter, such as tumor size, node metastasis status, and histological grade along with presence of pathological markers such as KI67 positivity, estrogen receptor (ER) status, progesterone receptor (PR) status and HER2 status by immunohistochemistry (3, 4). While practical within the clinical setting, these parameters can only partly encompass the heterogeneous nature of breast cancer.

1.1.3 Intrinsic Molecular Subtypes of Breast Cancer:

With the advent of high-throughput global gene expression profiling, gene expression analyses have become an instrumental in furthering the molecular taxonomy of breast cancer. With the use of 496 genes, deemed the “intrinsic” gene subset, patient breast tumors were initially categorized into four different molecular subtypes; Basal-like, HER2-enriched, Luminal and Normal-like (5). This classification system was further refined to the PAM50 subtype indicator, a set of only 50 genes which were used to classify breast tumors into these molecular intrinsic subtypes (6) Although, it is uncertain if the Normal-like class is mainly an artifact of having a high percentage of normal tissue mixed in with the tumor specimen (6). A new breast cancer intrinsic subtype referred to as the Claudin-low subtype was more recently identified in

both human tumors and mouse tumors (7). The Luminal subtype was further subdivided into a Luminal A and Luminal B class through the use of a larger subset of patient tumors (8).

1.1.4 Luminal A and B subtypes

The luminal intrinsic subset of tumors is highly heterogeneous in nature (6). Two main subclasses of luminal tumors have gained much research interest, the Luminal A and Luminal B tumor subtypes are both predominantly populated by ER/PR-positive tumors. As such, therapeutic interventions for these ER-positive tumors include anti-estrogen treatment such as Tamoxifen. The Luminal A subtypes of breast tumors, of all the intrinsic subtypes, exhibited the good prognosis as patients that fall within this subtype exhibit low-risk of relapse (6). The prominent difference between these two classes of tumors is that Luminal B tumors exhibit a higher proliferative index as measured by Ki-67 expression. Although a large portion of Luminal B tumors are hormone receptor positive and HER2-negative, a small fraction of Luminal B tumors (20%) also exhibit HER2 overexpression (9).

1.1.5 HER2-enriched subtype

Tumors within the HER2-enriched subtype were characterized by increased expression of several genes within the ERBB2 amplicon including *ERBB2* and *GRB7*, and are commonly ER- and PR-negative (4). HER2 overexpression within the tumor correlates with poorer patient prognosis with a decreased 5-year survival rate of 76% from 95% (6). Despite this, patient survival outcomes have greatly improved with the development of HER2-targeted therapeutic agents such as the HER2-targeting antibodies trastuzumab and pertuzumab, as well as the oral tyrosine kinase inhibitor Lapatinib (10). Although most tumors pertaining to the HER2-enriched subtype are HER2-positive (60-88%), a small fraction of tumors are HER2-negative which suggests for alternative mechanisms of enhanced HER2 function aside from receptor overexpression.

1.1.6 Claudin-low subtype

The Claudin-low class of breast tumors was a recently identified molecular subtype within both human and mouse tumors (7), and presents poorer patient prognosis than the Luminal A subtype of tumors (11). While Claudin-low tumors are predominantly high grade and

negative for ER, PR and HER2, only a small portion of triple-negative tumors are actually classified within the Claudin-low subtype which illustrates a demand for more accurate representation of this molecular subtype by immunohistochemical profiling. In attempts to strengthen representation of the Claudin-low subtype of tumors with immunohistochemistry markers, other surrogate markers including low expression of Claudin 3, Claudin 4, Claudin 7 and E-cadherin were proposed as additions to ER, PR and HER2 (11). Molecularly, Claudin-low tumors exhibit high expression of mesenchymal genes, such as N-cadherin and Vimentin, and genes associated with immune cell infiltration and mammary stem cells/tumor initiating cells with concomitant lower expression of luminal genes (4).

1.1.7 Basal-like subtype

Basal-like is the other intrinsic subtype that populates 70-80% of triple-negative breast cancers defined by the lack of ER, PR and HER2 expression (12). Common characteristics of Basal-like tumors are defined by high expression of the basal cytokeratins 5, 14, and 17, and low expression of luminal-related genes such as keratin 8. Although most triple-negative breast cancers are classified as basal-like, the use of immunohistochemical markers ER, PR and HER2 remains inadequate to definitively identify this intrinsic subtype. As such, EGFR and cytokeratin 5/6 expression, were proposed as supplementary surrogate markers in addition to ER/PR/HER2-negativity for defining the Basal-like tumors (4).

1.2 The Architecture of the Murine Mammary Gland.

Despite the anatomical differences between the murine mammary gland and the human breast, the mouse mammary gland has become an instrumental model for studying the histological and molecular changes that occur during breast cancer. The murine mammary gland is a complex organ composed of a single ductal tree spanning across the entire fat pad, and a stromal component largely comprised of adipose cells, fibroblasts, immune cells and endothelial cells (Figure 1.1) (13). While multiple ductal networks emerge from the nipple in human breast in contrast to murine mammary gland, the ductal architecture are conserved between the two species. The mammary duct is composed of a lumen space encased by a single layer of luminal epithelial cells which are identified by expression of cytokeratin 8 (14). Surrounding the luminal epithelial cells is a layer of myoepithelial cells which can be identified by expression of smooth

muscle actin (15). These myoepithelial cells provide contractile motion necessary to move milk along the duct during lactation, and take part in establishing the basement membrane (Figure 1.1).

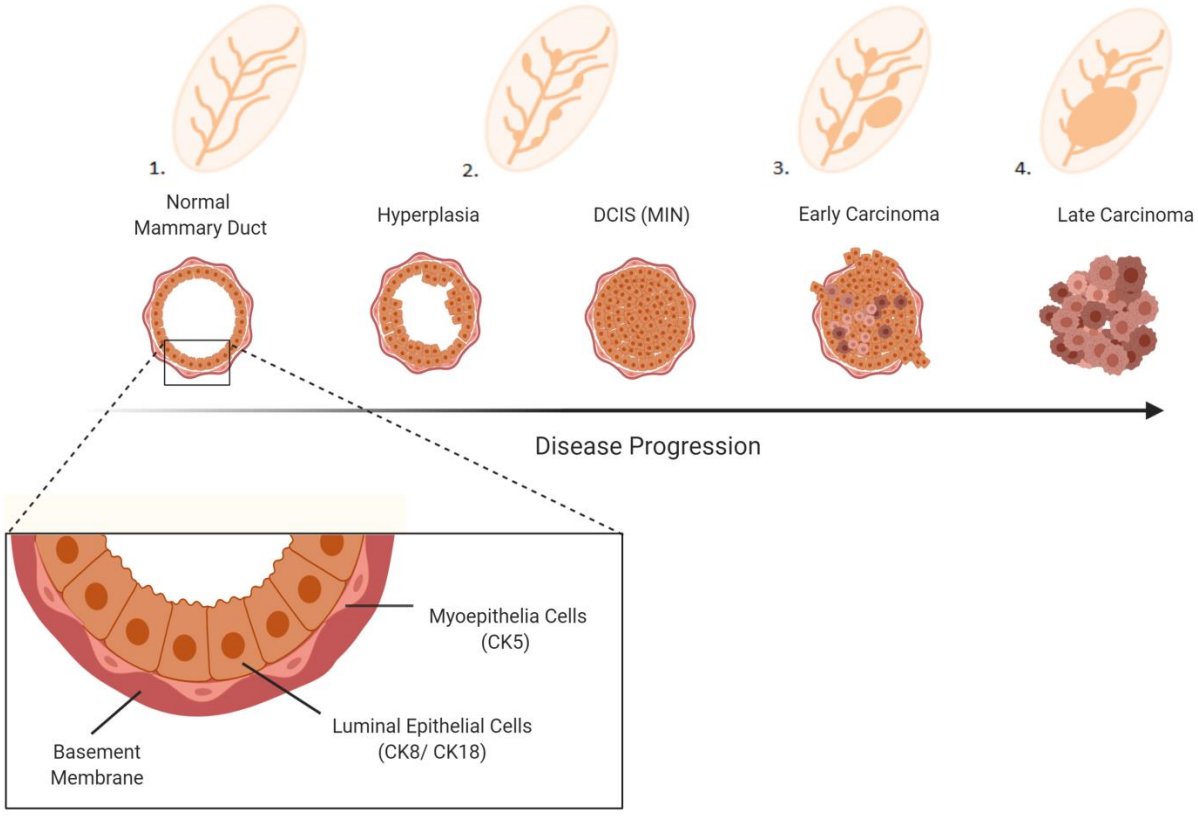

Figure 1.1 Perturbation of Normal Mammary Ductal Architecture During Mammary Tumorigenesis. The cartoon schematic illustrates the gradual stage-wise disruption of the normal architecture of the mammary duct (shown in zoomed-in panel) during mammary tumor progression; from normal ducts (1) to hyperplasia (2), murine *in situ* neoplasm (3), and eventually progressing into early and late-stage carcinomas (4).

1.3 Normal Mammary Gland Development and Mammary Tumor Progression.

The majority of the post-natal tissue development within the murine mammary gland occurs throughout puberty, whereby the rudimentary ductal tree undergoes massive expansion as

the terminal end buds (TEBs) extends across the fat pad. The TEBs are highly proliferative structures composed of body cells and cap cells that derive the mammary epithelium and myoepithelium respectively as the ductal branch extends across the fat-pad. During the ductal elongation process, the bifurcation of the TEBs generates additional side branches which undergo further elongation to establish an extensive ductal network. Expansion of the ductal networks stalls when the TEBs reach the edge of the fat-pad and lose their proliferative capacity. A prominent difference between the human and murine mammary gland is the formation of lobules during this pubertal period of development. Within human breast tissue, these lobules are formed at the ductal ends whereas similar lobule structures only arise within the murine mammary gland at the onset of pregnancy (16).

At the onset of pregnancy, increased ductal branching and development of alveolar buds can be observed within the murine mammary gland (13). As pregnancy progresses, the alveoli buds expand and segregate into individual alveoli structures which form the milk-producing lobules during lactation. By the end of alveologenesis, the fat pad of the mammary gland is largely filled with alveoli. Post-parturition, the epithelial cells start secreting milk proteins and lipids to fill the lumen of the alveoli. As mentioned previously, the myoepithelial layer surrounding the ductal epithelium contractile motions to aid the movement of milk out of the alveoli and along the duct during feeding. Once feeding is terminated and milk removal has ceased, involution is triggered within the mammary gland whereby massive apoptosis of the alveolar epithelial cells leads to the collapse of the alveoli and increased surrounding extracellular matrix deposition. As involution nears completion, both the epithelium and stroma undergo major remodeling and are reverted back to the pre-pregnant state (17).

Mammary stem cells are defined by their capacity to undergo self-renewal and differentiate into the epithelial components that construct the mammary duct. As such, these mammary stem cells play a large role in the major remodeling that occurs to the ductal tree through pregnancy, as well as the maintaining of architectural integrity of the virgin ductal tree. Given their characteristic to self-renew and persist within the mammary gland, mammary stem cells are modeled to be the pre-neoplastic cells, or the cell origin, that give rise to mammary tumors by accumulating genetic alterations that ultimately result in transformation. Since mouse models of breast cancer faithfully recapitulate the human disease, efforts have been made to define the cell of origin within various transgenic strains in attempts to understand the early

oncogenic events that lead to initiation of tumorigenesis (18-20). Following the initiation of tumorigenesis, tumor progression can be histologically described as the progressive filling of the mammary duct as the transformed epithelia transitions from hyperplasia to mammary intraepithelial neoplasia (MIN) (Figure 1.1). This stage-wise tumor progression culminates in heterogeneous malignancy that bypasses the basement membrane into the surrounding area.

1.3.1 Clonal Selection during Mammary Tumor Progression.

The source of tumor cell heterogeneity that accrued by tumors cells during progression can be partially described with two different models; the cancer stem cell model, and the clonal evolution hypothesis. The cancer stem cell model appoints the stem-like tumor cells that propagate tumor cells as the source of genetic variation. Novel genetic alteration arising in the bulk tumor originates only from the modifications derived within the cancer stem cells (CSC) as the progeny tumor cells do not exhibit capacity for self-renewal and expansion (21). The clonal evolution hypothesis describes the majority of the tumor cells within a bulk tumor as being plastic and having the ability to carry forward genetic and epigenetic alterations which are evolutionarily selected for based on the tumor environment (22). Taken together, the bulk tumors may be exhibiting a combination of both models whereby transition into the CSC state is bidirectional, thus allowing progeny tumor cells to adopt the CSC state (23-25). Consequentially, this phenomenon would grant propagation of genetic and epigenetic alterations adopted by the progeny cancer cells throughout the bulk tumor.

Genetic alterations within select population of neoplastic cells that confer a growth advantage will be enriched within the bulk tumor in a manner similar to the neo-Darwinian model of organism evolution (26). As such, inter- and intra-tumor heterogeneity arises as independent tumors are subjected to different selective pressures during disease progression (27, 28). This selective process is well demonstrated in transgenic tumors that develop in mouse models of breast cancer, particularly following genetic ablation of genes crucial for cell growth and survival. Following targeted gene ablation, the mammary tumors that develop are dominated by tumor cells that have established mechanisms to compensation for gene loss.

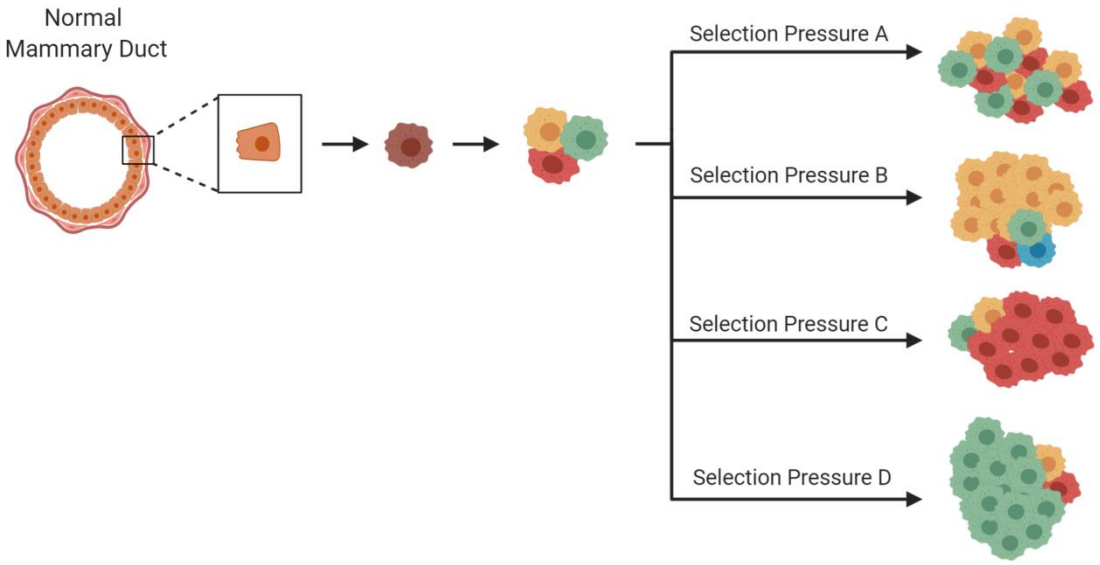

Figure 1.2 Tumor Progression is An Evolutionary Process Enriching for Cellular Traits Beneficial for Cell Proliferation and Survival. The cartoon schematic illustrates the selective nature of tumorigenesis which enriches for cells exhibiting molecular features that prove beneficial under the specific selective pressures placed on a cell population. The phenotypic profiles of distinct tumor cells are depicted by the differing color.

1.4 Genetically Engineered Mouse Models of Breast Cancer

Mouse models of breast cancer have recurrently demonstrated high capacity to faithfully recapitulate both the pathological stages of disease progression as well as recurring genetic alterations observed within human disease (29). By incorporating a Cre-LoxP system of targeted gene ablation, mouse models of breast cancer have become proliferative tools for studying gene function during disease progression.

1.4.1 Cre-LoxP System for Gene Targeting

The Cre-LoxP system derived from the P1 Bacteriophage (30) is frequently implemented as a gene targeting strategy for studying gene function *in vivo* (31). The strategy employs the use of two 34bp DNA sequences, composed of an 8bp asymmetric sequence flanked by two 13-bp palindromic sequences, called LoxP sites, and the Cre recombinase enzyme. Two parallel LoxP sites are introduced to flank a region crucial for proper gene expression within the targeted allele.

Gene ablation is subsequently achieved upon Cre Recombinase-mediated excision of the DNA sequence flanked by the two parallel LoxP sites (32). In addition to conditional gene ablation, the Cre-LoxP system has also been employed to elicit conditional expression of reporter genes including luciferase, β-galactosidase or GFP. With the incorporation of a stop cassette flanked by parallel LoxP sites upstream of the reporter gene, expression of Cre recombinase lead to gene expression of these various reporter genes (33-35).

1.4.2 Mammary-Specific promoters

Interrogation of gene function with the use of whole body gene knockout strategies has always been limited by the occasional issu of embryonic lethality. This limitation is circumvented through the coupling of the Cre-LoxP system with tissue-specific promoters (36-39). Various tissue-specific promoters such as the Krt8 promoter (40), Krt5 promoter (41), the whey acidic protein (WAP) promoter (42), and the Mouse Mammary Tumor Virus (MMTV) promoter have been used to drive mammary specific gene expression. The work described within this dissertation entails the use of the mammary specific promoter derived from the mouse mammary tumor virus which is an infectious retrovirus transmitted through the milk from mother to pup. The MMTV viral particles are known to spread into the mammary epithelium along its infection pathway after their initial amplification within lymphatic cells (30). Although the MMTV promoter demonstrates activity in both lymphatic and mammary epithelial cells, the 5' LTR segment of the MMTV promoter elicits greater exclusivity of expression to the mammary gland (43), with minimal activity in the salivary glands, kidney, and lymphoid tissue (44). As such, the MMTV-LTR sequence is incorporated in numerous transgenic mouse strains to drive mammary expression of various transgenes such as Cre recombinase (45) and various proto-oncogenes or oncogenes such as the Polyoma Virus middle T antigen (46), the activated Neu (NDL) (47), MET (48, 49), Wnt1 (50) and c-Myc (51, 52).

1.4.3 Tetracycline-inducible promoters

The tetracycline (Tet) inducible system commonly used to drive gene expression in mammalian cells was first derived from the Tn10 operon of *Escherichia coli*. In *E.Coli*, the tet-inducible system is adapted as a mechanism of tetracycline resistance by regulating the activity of the Tet operator upstream of the tetracycline efflux protein TetA, through the Tet repressor

TetR. Upon binding to tetracycline, TetR is dissociated from the Tet operator thus allowing induction of TetA expression (53, 54).

The transition of this prokaryotic system of gene expression regulation into the mammalian cell context involved; generating the tet-transactivator (tTA) through the fusion of the TetR with the VP16 viral transcription factor (55-57). Consequentially, gene expression downstream of the Tet promoter was induced in the absence of tetracycline or other derivatives such as doxycycline. Later iterations of the tet-inducible system assimilated the use of the reverse tet-transactivator (rtTA), a mutant variant of the tTA which allowed binding to the Tet promoters in the presence of tetracycline (58-60). The recent development of a transgenic mouse strain (MMTV-rtTA strain), where the rtTA element is incorporated downstream of the MMTV promoter (61), has opened new opportunities to allow temporal control of gene expression *in vivo* within the mammary epithelium upon tetracycline administration once interbred with mouse strains carrying the Tet-Operator (61-63)**.**

1.4.4 PyV mT-driven Mouse Models of Luminal Breast Cancer

The Polyoma virus middle T (PyV mT) antigen is a viral oncoprotein capable of inducing transformation in various tissue types. Although not observed in human breast cancer, PyV mT functions as a potent oncogene by activating signal pathways that drive cell growth and survival in a manner that mimics various human receptor tyrosine kinases (64). Despite lacking intrinsic kinase activity, PyV mT recruits Src to mediate phosphorylation of various tyrosine residues within the intracellular tail (64). These phosphorylated tyrosine residues act as docking site for various adaptors protein common to other receptor tyrosine kinases, such as ErbB2, to activate MAPK and PI3K signal transduction. The MMTV-PyV mT transgenic mouse strain closely recapitulates human breast cancer progression in a stage-wise manner, ultimately culminating in the formation of malignancy (46) that resembles human Luminal breast cancer (7). When assimilated with a LoxP-Cre gene targeting strategy, the MMTV-PyV mT strain becomes a powerful tool in evaluating the role of genes of interests during tumor progression (65).

One of the caveats of early bi-transgenic strains that carried both MMTV-PyV mT and MMTV-Cre, was the development of transgenic tumors exhibiting mosaic Cre expression and gene ablation was achieved within only a fraction of the tumor cells (66, 67). Later iterations of the PyV mT-driven model system (the MIC strain) circumvented this escapee phenomenon by

coupling Cre and PyV mT expression with an internal ribosome entry site (IRES) (62). The addition of a tetracycline-responsive system also allowed temporal control of oncogene expression and gene ablation upon Dox administration within the MIC strain (38) by incorporating a MMTV-rtTA construct (61) (Figure 1.3).

1.4.5 ErbB2/Neu-driven Mouse Models of HER2-positive Luminal Breast Cancer

HER2 is a member of the EGFR family of growth factor receptors which is observed amplified and over-expressed in 30% of breast cancer cases. Transgenic mouse models overexpressing the rat HER2/ErbB2 homolog Neu, within the mammary epithelium leads to formation of malignancy resembling HER2-positive luminal breast cancer (68). The MMTV-NIC mouse strain (Figure 1.3) employs an activated Neu (NDL) which exhibits deletions within the juxtamembrane domain that consequentially elicits an increase in receptor homo-dimerization (69) and an enhanced transforming potential (47, 70).Upon homo-dimerization, a series of tyrosine residues (Tyr1028, Tyr1144, Tyr1201, Tyr1227, and Tyr1253) within the Neu receptor are cross phosphorylated which initiates the recruitment of various adaptor proteins including Grb2 at Tyr1144, Crk at Tyr1201, and Shc at Tyr1227 (71, 72). Receptor binding of the Grb2 adaptor can potentiate both the PI3K-Akt pathway through recruitment of the docking protein Gab1, and the ERK1/2-MAPK pathway through recruitment of the Ras exchange factor SOS (73). Similarly, the receptor binding of the Shc docking protein can also potentiate the ERK1/2-MAPK pathway through the recruitment of the exchange factor Sos (71).

In addition, the MMTV-NIC strain allows co-expression of an activated Neu (NDL) with Cre recombinase within the mammary epithelium via an internal ribosome entry site (IRES) (74). By coupling Cre-mediated excision of LoxP-flanked DNA with NDL expression through a bicistronic expression system (74), we also circumvent the potential escapee phenomenon mentioned above. The MMTV-NIC strain becomes an informative tool in evaluating the function of genes of interest during Neu-tumor progression when assimilated with a LoxP-Cre gene targeting strategy.

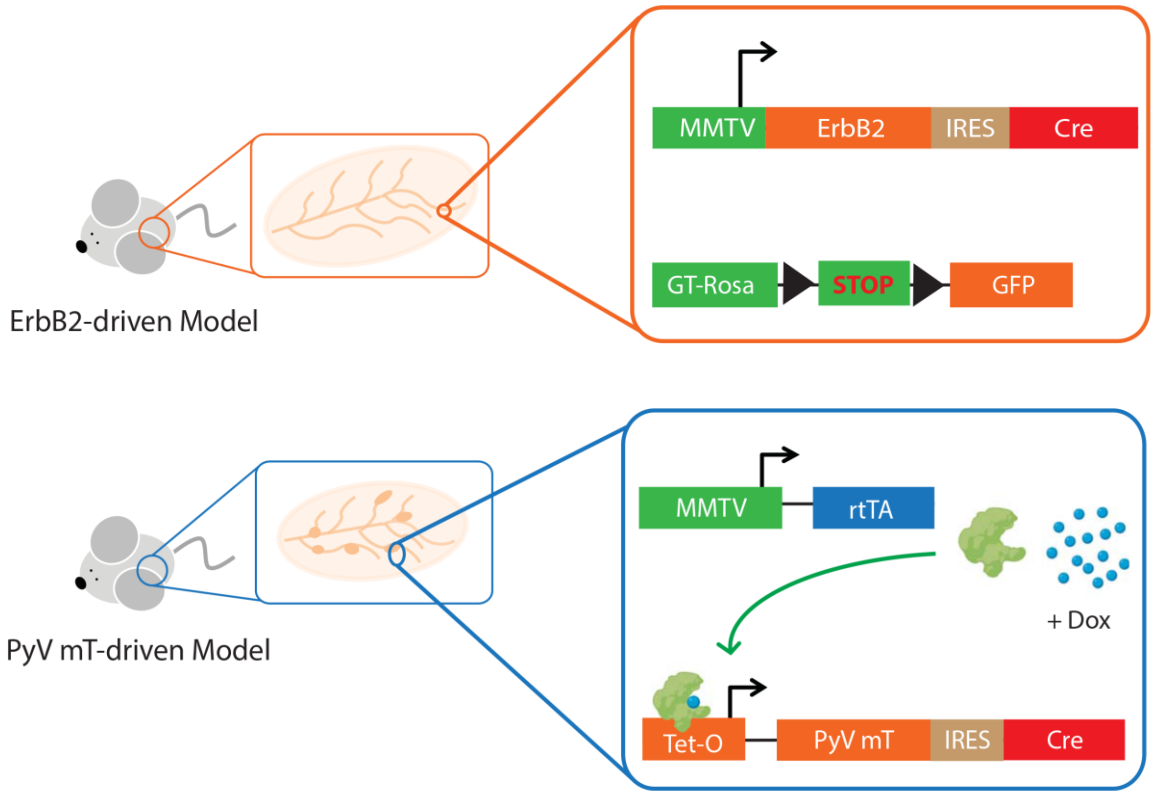

Figure 1.3 ErbB2-driven and PyV mT-driven Mouse Models of Breast Cancer. (Top) The Cartoon schematic illustrates a transgenic mouse model allowing mammary specific co-expression of ErbB2 and Cre recombinase via internal ribosomal entry site element (IRES), driven from the mouse mammary tumor virus promoter (MMTV). The use of tissue specific expression of Cre allows for targeted excision DNA flanked by LoxP sites (black arrows), allowing tissue specific gene disruption or reporter gene expression. **(Bottom)** The cartoon schematic illustrates a transgenic model system which allows for mammary specific, doxycycline-dependent co-expression of PyV mT and Cre from the Tet operator.

1.5 The Serine/Threonine Kinase MTOR

1.5.1 Initial Discovery of mTOR

Interest in mTOR was initially sparked from the isolation of the macrolide Rapamycin from *Streptomyces hygroscopicus* isolated from soil samples in Easter Island (Rapa Nui) (75). It was the discovery that Rapamycin possessed immunosuppressive properties (76-79) that drove the investigation into the drug's underlying mode of action. Much attention was placed on elucidating the molecular mechanism driving G1-arrest in yeast treated with Rapamycin in hopes of identifying a potential parallel mechanism responsible for the immunosuppressive effect within cytotoxic T-cells. To address this, multiple research groups had employed yeast mutagenesis screens in attempts to identify mutations that conferred resistance to cytostatic effects of Rapamycin (80-82). Two categories of mutations were detected from the screen; mutations within RBP1/FPR1, the yeast homologue of FKBP12, and mutation within the TOR1/2 proteins (80, 82). Although mutant RBP1 did confer resistance to Rapamycin treatment, only genetic disruption of both TOR1 and TOR2 recapitulated the G1 arrest caused by Rapamycin treatment (83). These observations suggested that RBP1 interacted with a protein eliciting G1-arrest in a Rapamycin-dependent manner. In attempts to isolate the protein interacting with FKBP12-Rapamycin complex within the mammalian context, various independent groups uncovered a large protein now referred to as the mechanistic Target of Rapamycin (mTOR), which shared homology with the yeast TOR proteins (84, 85). Further analysis of the mTOR protein demonstrated high similarity with other members of the PIKK lipid kinases including PI3K and VPS34 (81). Although mTOR was initially thought to be a lipid kinase, it was later elucidated to exhibit protein kinase functions (86, 87).

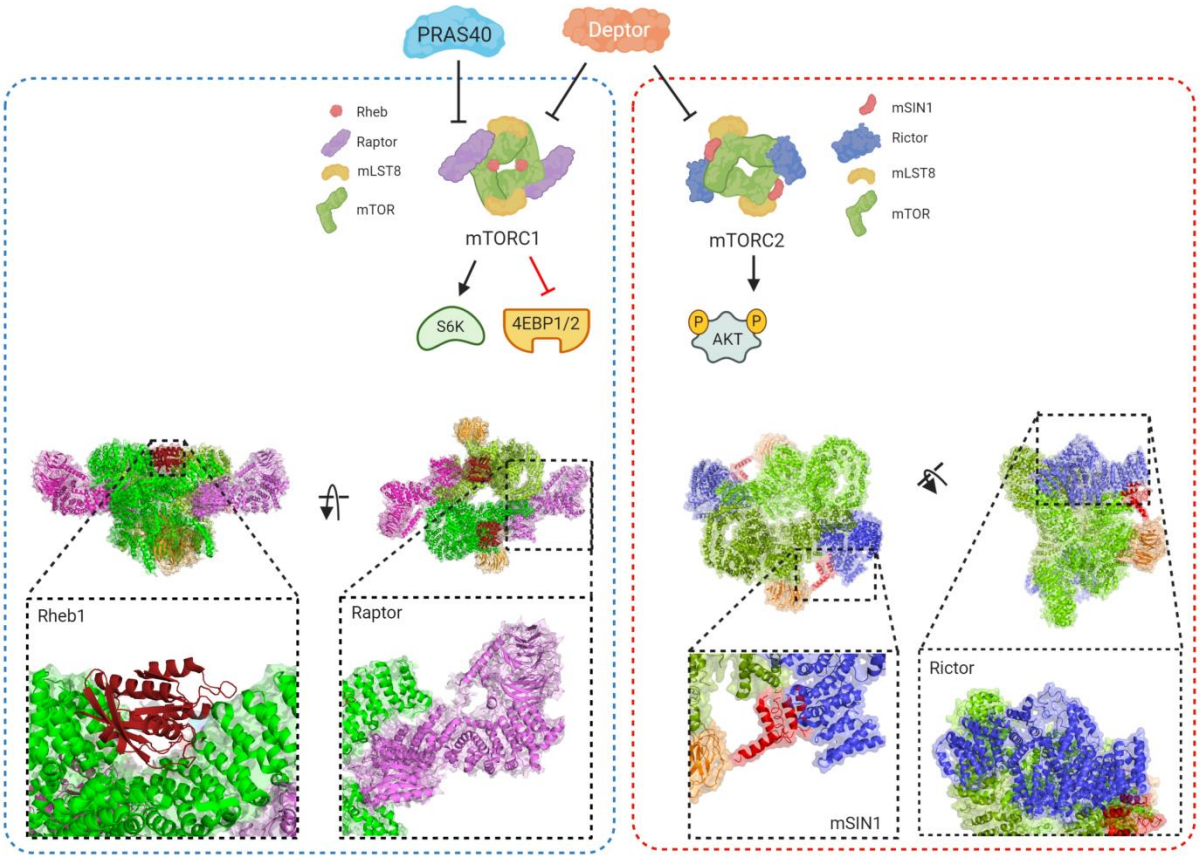

Figure 1.4 The mTOR kinase nucleates into two structurally and functionally distinct complexes, mTORC1 and mTORC2. Left: Cartoon representative of Cryo-EM structure of Rheb1-bound mTORC1. The components unique to mTORC1 are boxed in black; the scaffolding protein Raptor (Pink) and Rheb1 (Red). Right: Cartoon representation of Cryo-EM structure of mTORC2. The components unique to mTORC2 are boxed in black; the scaffolding protein Rictor (Blue) and mSin1 (Red). The structure of mTORC2 only illustrates a small fragment of the mSin1 protein. Images of mTORC1 and mTORC2 were derived using PyMol from published structures PDB 6BCU (88), and PDB 6ZWM (89) respectively.

1.5.2 Two Functional mTOR complexes: mTORC1 and mTORC2

While yeast cells carry two TOR genes TOR1 and TOR2, mammalian cells express only one mTOR which nucleates within two functional distinct complexes, mTORC1 and mTORC2 (90). The mTORC1 was demonstrated to exhibit sensitivity to the inhibitory effects of the FKBP12-Rapamycin complex through direct binding to the FRB domain (91). Although mTORC2 shows insensitivity to short-term Rapamycin treatment due to the inability of the FKBP12-Rapamycin complex to bind to mTORC2 (92), long-term Rapamycin treatment does inhibit mTORC2 assembly (93).

In addition to the catalytic subunit mTOR, mTORC1 is composed of the scaffolding subunit Raptor (94, 95), and mLST8 (Figure 1.4). Early Cryo-EM data coupled with biochemical evidence using Rapamycin treatment reveals that mTORC1 adopts a symmetrical functional dimer conformation (91, 96). mTORC1 is best known for its role in regulating mRNA translation through phosphorylation of p70 ribosomal S6 Kinase 1 (S6K1) and the eIF4E-binding proteins (4EBP1-3) (97-100). The Raptor subunit serves as a docking site for substrates such as 4EBP1 and S6K1 through their TOS motif (101-103). The mTORC1 inhibitor PRAS40 perturbs activity by directly blocking substrate recruitment by Raptor through directly interacting with its TOS motif and nearby hydrophobic regions (88, 104, 105). While Raptor assembles uniquely within mTORC1, mLST8 is mutually associated with both mTOR complexes and plays a stabilizing role (106, 107). Assembly of mLST8 into mTORC1 is regulated by the ubiquitination status of the seventh WD40 motif on mLST8 by TRAF2 or OUTD8B. Ubiquitination of the seventh WD40 motif (WD7) by TRAF2 blocks the interaction mLST8 with mSIN1, which consequentially shuttles mLST8 into mTORC1. De-ubiquitination of the WD7 motif shuttles mLST8 into mTORC2 (108), whereby it assembles with one of three isoforms of mSIN1 (109), and scaffolding protein Rictor (110) (Figure 1.4). While mTORC1 adopts symmetric dimer conformation, Cryo-EM structure reveals mTORC2 in a “hand” conformation (89). mTORC2 is best known for regulating Akt phosphorylation (111) and control of actin polymerization (112). Although Protor1/2 was identified as a unique interactor with mTORC2 through the Rictor subunit, its exact role in regulation of mTORC2 function is still undefined (113).

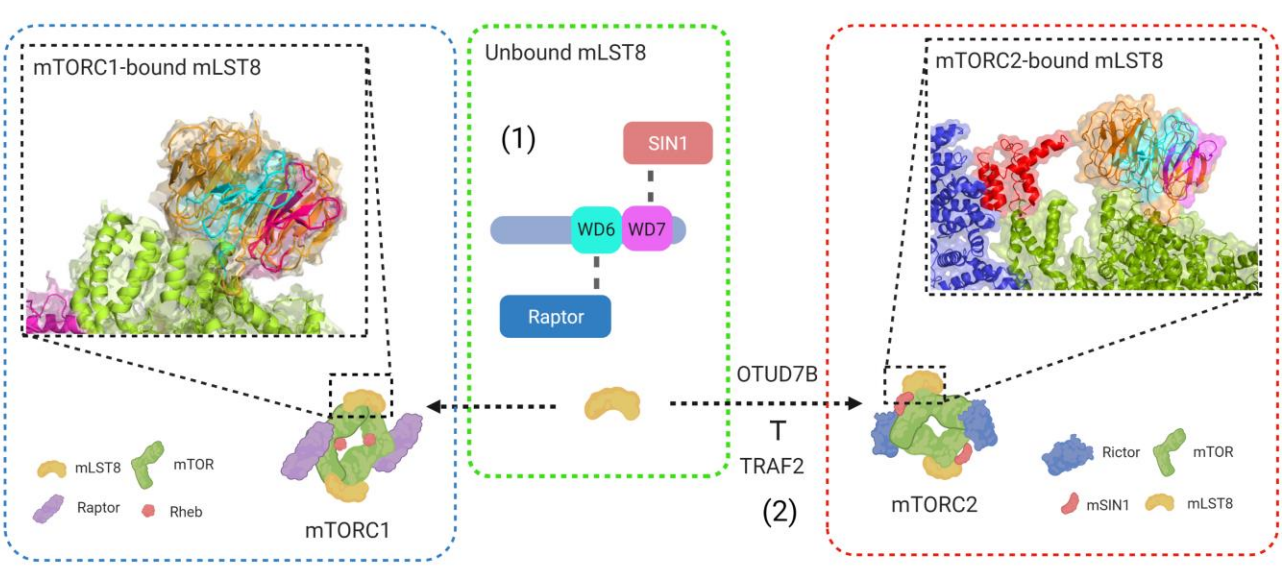

Figure 1.5 Ubiquitination of mLST8 blocks assembly of mTORC2. (1) mLST8 assembled within mTORC2 interacts with Sin1 via the WD7 domain while mLST8 assembled within mTORC1 interacts with Raptor via the WD6 domain. (2) Ubiquitination within the WD7 domain (Purple) of mLST8 by TRAF2 hinders mTORC2 assembly by disrupting the interaction between Sin1 (Red) and mLST8. Images of mTORC1 and mTORC2 were derived using PyMol from published structure PDB 6BCU (88), and PDB 6ZWM (89) respectively.

1.6 Signaling Downstream of mTORC1

Nutrient availability and growth factor stimulation elicit multifaceted roles in the regulation mTORC1 activation. Activation of the kinase complex stimulates anabolic processes including, mRNA translation and lipid biogenesis while concomitantly suppressing the catabolic process autophagy. mTORC1 activation and function is frequently observed dysregulated in various cancers including breast cancer, where affected processes downstream of mTORC1 contribute a prominent role in maintaining the cell growth and proliferation of cancer cells.

1.6.1 Regulation of Cap-dependent mRNA Translation by mTORC1

The translatome is a subset of mRNA transcripts actively undergoing translation within a cell, and is tightly regulated at the initiation phase as mRNA translation is an energetically costly process (114). Initiation of cap-dependent translation is heavily dependent on the efficient

assembly of the eIF4F complex which comprises of the mRNA cap-binding protein eIF4E, the scaffolding subunit eIF4G, and the helicase eIF4A. eIF4F complex assembly is largely regulated through the suppression of eIF4E-eIF4G interactions through competitive eIF4E-4EBP interactions (115, 116). Provided that the eIF4E-eIF4G interaction is fundamental for eIF4F assembly, therapeutic strategies targeting this interaction through competitive compounds such as the inhibitor 4EGI-1, have been developed and demonstrate anti-cancer effects (117-119). Following assembly of the eIF4F complex, the 40S ribosomal subunit is recruited to initiate scanning of 5'untranslated region (UTR) of the bound mRNA for the initiator AUG codon (120). The helicase activity of eIF4A improves the efficiency of ribosomal scanning by alleviating impeding secondary structure situated within the 5' UTR. Enhancement in ribosomal scanning of the 5'UTR correlates with improved translational efficiency of the targeted mRNA (121). Alternatively, mRNA translation can initiate in a cap-independent manner through Internal Ribosome Element sequences (IRES) by mediating RNP-dependent recruitment of ribosomes (122).

1.6.1.1 Regulation of the 4EBP1-eIF4E signaling axis by mTORC1

mTORC1 modulates cap-dependent mRNA translation through phosphorylation of 4EBPs in a sequential manner. The priming residues threonine 37, 46 are initially phosphorylated, followed by threonine 70, and ultimately serine 65 (123). Phosphorylation of all four mentioned residues on 4EBP1 liberates eIF4E to assemble into the eIF4F cap complex (124) through the initial recruitment of eIF4G. The eIF4E-eIF4G assembly generates a binding site for MNK1/2 kinase which mediates eIF4E S209 phosphorylation (125, 126). Although, the exact molecular mechanistic consequence of eIF4E phosphorylation is undefined, eIF4E S209 phosphorylation has been shown to preferentially drive translation of gene involved in cell invasion including MMP-3 and SNAIL (127). Although mTORC1 function prominently contributes to regulation of mRNA translation, only a small subset of the translatome has demonstrated sensitivity to mTORC1 inhibition (128). The subset of mTORC1-sensitive translatome is best identified empirically through polysome profiling following mTORC1 inhibitor, and complimented with 4EBP1/2 knockout (128). Currently there are two prominent working models for explaining mTORC1-sensitivity within the translatome. One working model is based on the complexity of the 5'UTR which defines the dependency for eIF4A-mediated unwinding of secondary structures that would improve efficiency of ribosome-scanning (121). With relevance to cancer, pro-

tumorigenic genes such as Cyclin D1 and D3 (129-131) frequently carry complex structured 5'UTRs which renders them translationally sensitive to mTORC1 inhibition. Such secondary structures include RNA G-quadruplexes which arise within 5'UTR regions rich in CGG content which rends efficient translation dependent on eIF4A function (132). The other proposed working model for identifying mTORC1-dependent mRNA is defined by the presence of TOP motifs and TOP-like motifs which are characteristic of 5-15 pyrimidines adjacent to 5' terminal cap. Although the exact molecular mechanism is still undefined within this model, mTORC1-dependency within these transcripts correlated with the presence these motifs (128).

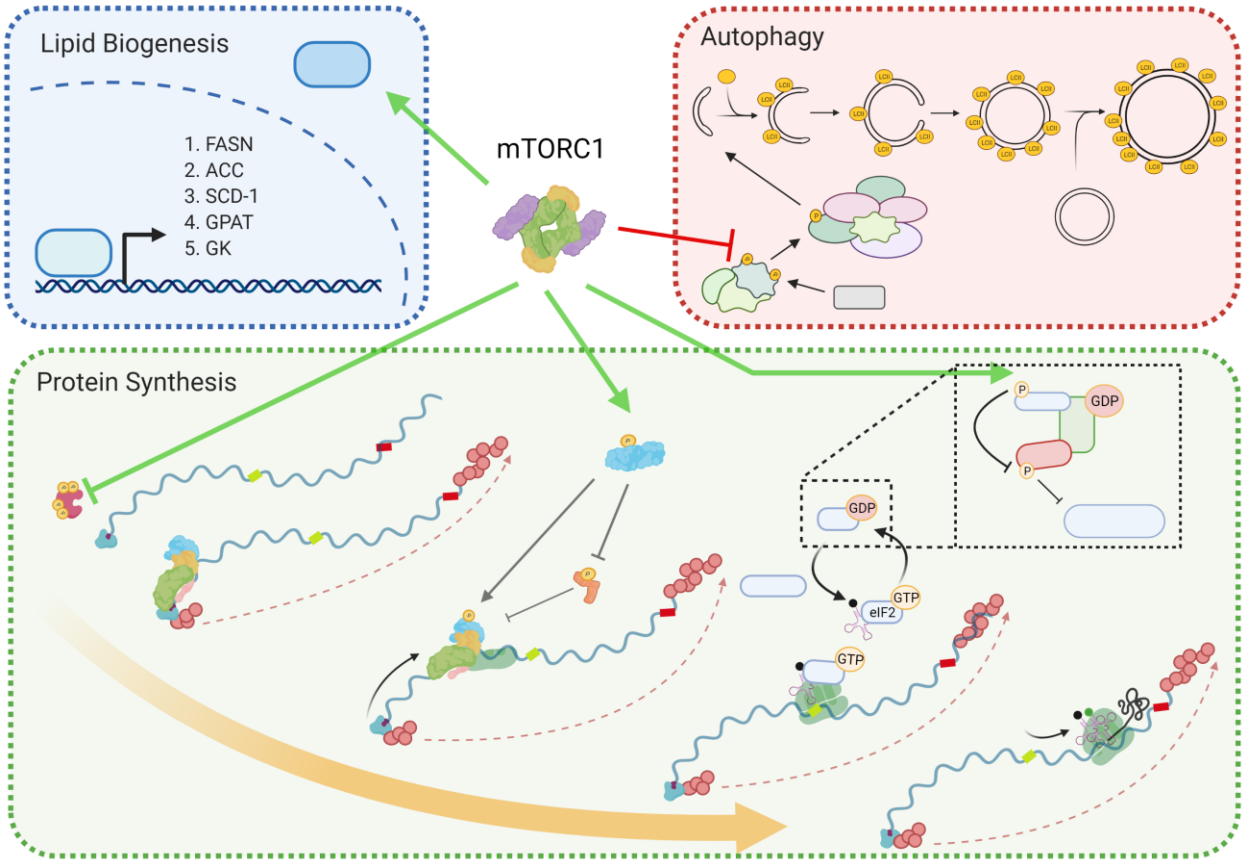

Figure 1. 6 mTORC1 is a Critical Node in the Regulation of Various Anabolic and Catabolic Cellular Processes. mTORC1 is a critical negative regulator of the catabolic process of autophagy (Red), while simultaneously contributing to the activation of anabolic processes such as lipid biogenesis (Blue), and protein synthesis (Green).

1.6.1.2 Regulation of p70 S6K by mTORC1

It is well-established that mTORC1 also contributes to the regulation of p70 ribosomal S6 Kinase activation. Full activation of the p70 S6 kinase is achieved through a series of sequential phosphorylation events elicited by various kinases including MAPKs, PDK1 and, mTORC1. Activation of p70 S6 kinase is initially primed by phosphorylation of a series of threonine residues (Thr404/405) located at the N-terminus by various MAP Kinases (133). This drives a conformation change which opens p70 S6 kinase to the subsequent phosphorylation of the Thr389 residue by mTORC1 (134), and phosphorylation of Thr229 by PDK1 (135). Upon full activation, S6K up-regulates protein synthesis through enhancing eIF4A activity through the phosphorylation of eIF4B (S206) (99), and the phosphorylation-mediated degradation of the eIF4A inhibitor PDCD4 (100). In adipocytes, p70 S6K has been shown to also mediate phosphorylation of Histone 2B (H2B) at residue Ser36 which elicits a transcriptional program essential for adipogenesis (136). H2B Ser36 phosphorylation was shown to be mediated by AMPK**,** where AMPK-mediated phosphorylation of H2B Ser36 elicited a stress response transcriptional program (137). p70 S6 kinase is also known to mediate phosphorylation of S6 at Ser235/236/ 240, and 244. While these targets are shared between the p90 ribosomal S6 kinases (RSK) (99, 138), S6 Ser240 and Ser244 are obligate p70 S6 kinase phosphorylation sites (139).

p70 S6K plays a prominent role in the regulation of cell size whereby genetic ablation of the closely related S6K isoforms, S6K1 and S6K2, results in smaller but viable mice (140). While the molecular consequences of rpS6 phosphorylation are still unclear, mice expressing a knock-in of S6 phospho-residue mutants also closely recapitulate a similar small cell size phenotype (141). Given that this small cell size phenotype is recapitulated with mTORC1 inhibition via Rapamycin treatment (142-145), this suggests that p70 S6K is a prominent downstream effector of mTORC1.

1.6.2 Regulation of Global Translational Rate by mTORC1

A crucial step for translation initiation involves the assembly of the eIF2:GTP: methionyl-tRNA (Met-tRNA$_i$) ternary complex (TC) (Figure 1.7), as this allows loading of the first methionine residue. The heterodimer eIF2 which is composed of eIF2α-, β-, and γ-subunits binds and delivers the Met-tRNA$_i$ to the P-site of a small 40S ribosomal subunit (Reviewed in (146)). Upon recruitment to the capped mRNA, the GTP is hydrolyzed and this ribosomal

complex initiates scanning of the 5' UTR for the first AUG codon and upon discovery, the GDP-bound eIF2 is released from the ribosomal subunit (reviewed in (146)). The 60S ribosomal subunit is subsequently incorporated by GTP-bound eIF5B to form the 80S ribosomal subunit which allows for progression into the initiation of translational elongation.

In order for progression of a subsequent round of translation initiation, the active eIF2-GTP must be replenished through the GEF function of eIF2B. Phosphorylation of eIF2α (Ser 51) subunit play a well-established role in suppression of the global translation rate, and is mediated by various kinases including PERK, GCN2 and PKR in response to variable stresses such as amino acid insufficiency, protein misfolding, and viral infections (146). eIF2α Ser 51 phosphorylation converts eIF2 into an allosteric inhibitor of eIF2B by inhibiting the GEF activity which consequentially depletes the amount of active GTP-bound eIF2 (147, 148).

As mentioned above, in the presence of growth factor stimulation the increase in mTORC1 activity drives elevated translation initiation through the assembly of eIF4F. This elevated rate of translation initiation puts forth the increased demand for eIF2 reloading in response. Correspondingly, mTORC1 demonstrates a role in acclimating this elevated demand by facilitating increased recycling of GDP-bound eIF2 through phosphorylation of the eIF2β (Ser 2 and Ser 67) subunit (149). eIF2β (Ser 2) phosphorylation consequentially drives NCK1-directed, PP1-mediated de-phosphorylation of eIF2α Ser 51. Taken together, this molecular mechanism allows for coordination in the elevation of both eIF4F-mediated translation initiation, and TC recycling.

While eIF2α Ser51 phosphorylation serves to suppress global translation during periods of cellular stress, it also concomitantly enhances translation of mRNA species containing inhibitory upstream open reading frames (uORFs) within the same transcript. The inadequate abundance of GTP-bound eIF2 reduces the efficacy of translation re-initiation of 5' ORFs. As a result, this allows the ribosomes to scan through these upstream inhibitory uORFs and initiate translation further downstream within gene such as activating transcription factor 4 (ATF4) (150, 151), IBTKα (152), and CCAAT-enhancer-binding protein homologous protein (CHOP) (152, 153). Both ATF4 and CHOP are transcription factors well-established of driving gene expression programs that focus on ameliorating cellular stress.

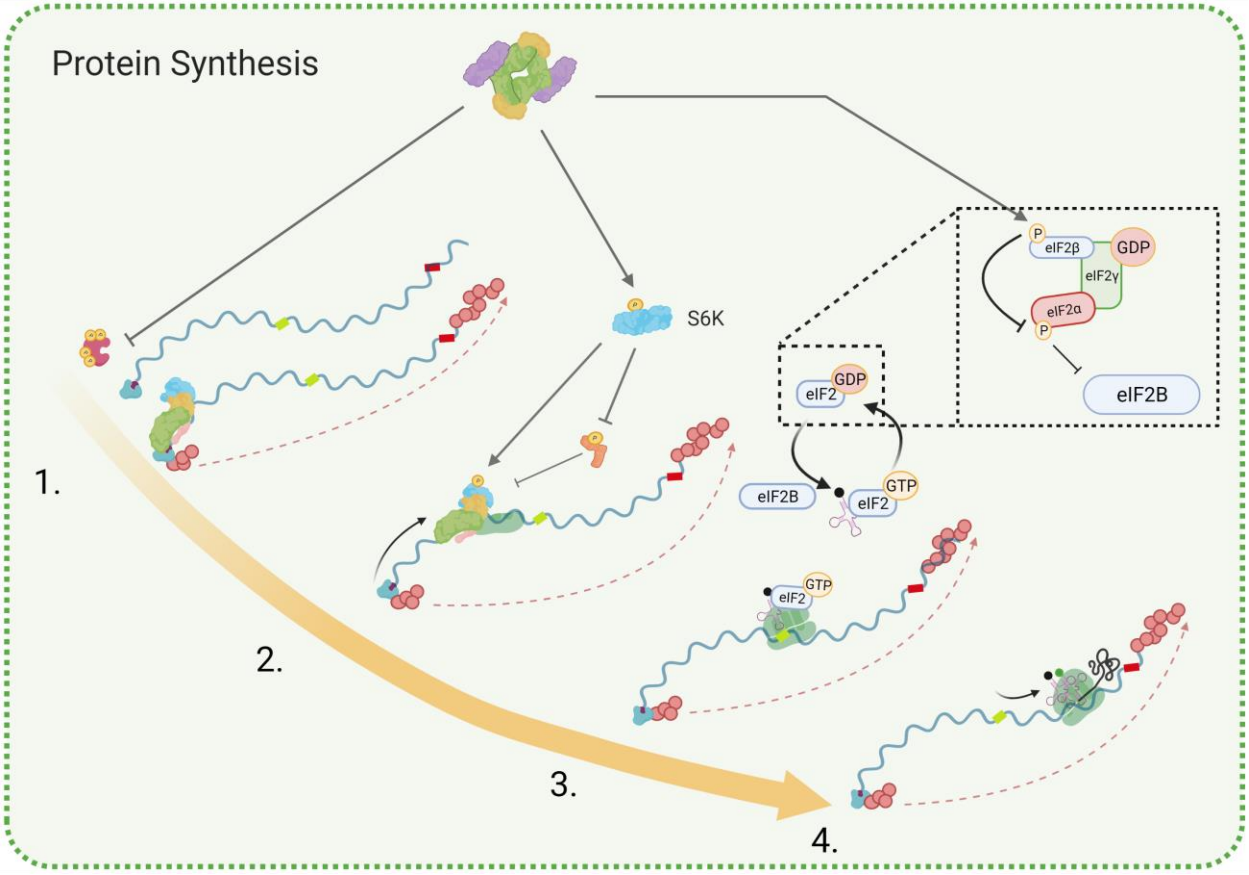

Figure 1. 7 mTORC1 initiates eIF4E-dependent mRNA translation through the regulation of 4EBP1 and p70 S6K. (1) mTORC1 facilitates eIF4F assembly by liberating eIF4E through phosphorylation of 4EBPs. (2) mTORC1 enhances the efficiency of ribosomal scanning through activation of S6K. (3) mTORC1 enhances eIF2-GTP recycling by mediating eIF2β phosphorylation. (4) mTORC1 also promotes translation elongation by driving S6K-dependent inhibition of eEF2K.

1.6.3 Regulation of Autophagy by mTORC1

Autophagy is the catabolic process whereby damaged organelles and cytosolic components are enveloped by the double-membrane autophagosome, and shuttled into the lysosome for degradation in attempts to recuperate macromolecules such as amino acids and fatty acids (154). The immediate molecular response triggered by the induction of autophagy is the assembly and activation of the ULK1-ATP13-FIP200 complex, which subsequently mediates activation of PI3KC3-complex 1 via phosphorylation of various subunits including VPS34 (Ser249), and AMBRA1 (Ser465/Ser635) (155). Consequentially, the activation of these two

complexes initiates nucleation of the phagophore, and triggers lipidation of LC3-I into LC3-II which decorates the phagophore to drive elongation into enclosed autophagosomes. After maturation, the autophagosome along with its subcellular cargo eventually fuses with the lysosome in a SNARE-dependent manner (154) to generate autophagolysosomes (Figure 1.8).

Although autophagy can play cytoprotective roles by maintaining cellular homeostasis during intervals of nutrient starvation and cellular stress, the catabolic process becomes counterproductive during periods of nutrient abundance, and states of increased cellular anabolic processes. While mTORC1 stimulates the up-regulation of various anabolic processes, including nucleotide synthesis (156, 157), lipid synthesis (158), and increased energy production (159-161) to accompany the increased cell growth, the kinase also suppresses the catabolic process of autophagy. mTORC1 suppresses autophagy partly by inhibiting the autophagy initiation machinery through phosphorylation of both ULK1 (Serine 757) (162), and ATG13 (163). Aside from autophagy initiation, mTORC1 also suppresses autophagosome maturation by inhibiting autophagosome-lysosome fusion through negative regulation of UVRAG (164).

In addition, mTORC1 also inhibits autophagy through suppression of the transcription factor EB (TFEB) which stimulates transcriptional programs that drive lysosomal biogenesis and autophagy during intervals of starvation (165-167). Upon recruitment to lysosome by active RagD GTPase, mTORC1-mediated phosphorylation of Ser142 and Ser211 on TFEB sequesters the transcription factor away from the nucleus (168, 169). Interestingly, TFEB has also been shown to transcriptionally regulate the expression of RagD GTPase activity which implicates a possible negative feedback mechanism to auto-regulate TFEB-dependent autophagy (170).

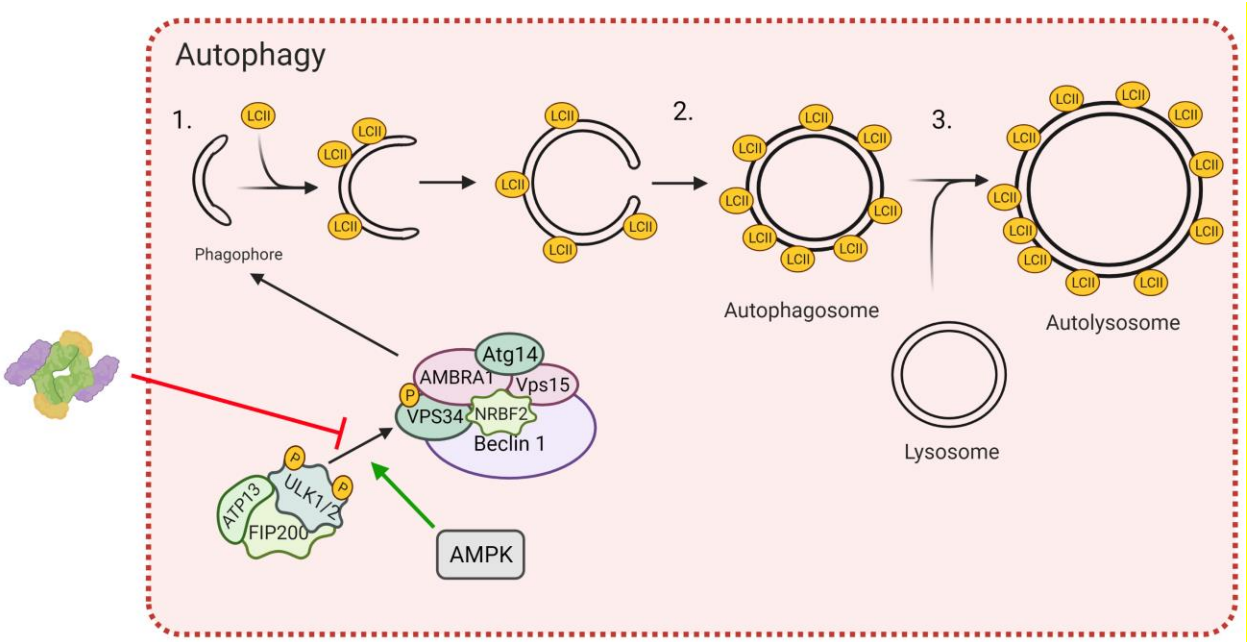

Figure 1. 8 mTORC1 suppresses autophagy initiation through ULK phosphorylation. ULK complex-mediated VPS34 complex activation leads to seeding of the phagophore (1), followed by elongation of the lipid bilayer accompanied by addition of LC3II. A closed autophagosome structure ultimately forms, which encases cellular content targeted for degradation (2). The enveloped cellular content within the autophagosome is broken down following formation of the autolysosome (3).

1.6.4 Regulation of Lipid Metabolism by mTORC1

Lipid metabolism is a major contributing factor in sustaining cancer growth by supplying materials for membrane biogenesis, and energy production in order to help maintain their proliferative nature. The SREBPs are a family of basic helix-loop-leucine zipper transcription factors comprised of three members; SREBP1a, SREBP1c and SREBP2 (171), which are master regulators of *de novo* lipid and cholesterol biosynthesis downstream of the PI3K-Akt pathway (172). The SREBPs are initially synthesized as inactive precursors and activated upon cleavage by a series of protease located on the Golgi apparatus. The maturation of SREBPs into nuclear SREBPs (nSREBPs) is facilitated by sterol cleavage activating proteins (SCAP) which escorts the inactive SREBP precursors from the ER membrane to the surface of the Golgi (171). Upon arrival at the Golgi membrane, the SREBPs are cleaved by the proteases Site-1 protease (S1P)

and Site-2 protease (S2P) into nSREBP thus granting nuclear entry and binding to sterol regulatory elements sequences found in promoters of genes involved in cholesterol and fatty acid biosynthesis (173). In the presence of sterol, feedback mechanisms involving the two proteins Insig-1 and Insig-2 are initiated to sequester of the SCAP-SREBP complex to the ER membrane thus preventing the nuclear entry of SREBPs (174-177).

The mTORC1-mediated maturation of nSREBP1 plays a prominent contribution in eliciting insulin-induced cell growth (172), while the exact mechanism is undefined, the downstream mTORC1 effector p70 S6K has demonstrated a direct role in the maturation process (159, 178). In addition to enhancing nSREBP maturation, mTORC1 has been demonstrated to augment SREBP activity by mediating nuclear exclusion of lipin-1 through phosphorylation of lipin-1 Ser106, Ser237 and Ser472 which induces nuclear exclusion of lipin-1 and allows for nuclear accumulation of SREBP1 (158, 179).

1.7 Signaling Upstream of mTORC1

1.7.1 Regulation of mTORC1 Activation by Growth Factors and Mitogens.

Adequate growth stimulation brought on by the presence of growth factors and hormones such as insulin, is required for robust mTORC1 activation. Stimulation of the insulin receptor and various growth factor receptors, including various members of the EGFR family of receptor tyrosine kinases (RTKs), initiates signal cascades such as the ERK1/2-MAPK and PI3K-Akt signaling pathway that culminate in cell growth, proliferation, and survival. The contribution of these signaling cascades to mTORC1 activation, downstream of RTKs, relies heavily on the regulation of the obligator activator Rheb1 through the suppression of the TSC complex. The TSC complex composed of the subunits TSC1, TSC2 and TBC1D7 functions by facilitating the hydrolysis of the GTP bound to Rheb1 into GDP (180) (181, 182). Phosphorylation of the TSC2 subunit on Ser664 and Ser540 by ERK1/2 (183-185), and Ser939 and Thr1462 by Akt (186-188) elicits the inhibition of the Rheb1 GAP function, and the dissociation of the TSC complex. The TBC1D7 subunit, which stabilizes the functional TSC complex, is also modulated by Akt activity whereby phosphorylation of Ser124 leads to sequestration by 14-3-3 (189). Upon accumulation of sufficient active Rheb1 and recruitment of mTORC1 the lysosomal surface, GTP-bound Rheb1 binds to mTOR to stimulating kinase activity. While it has been elusive for years, there is now direct insight into the molecular consequences what occur within mTORC1

upon docking of active Rheb1. When active Rheb1 is bound, mTOR undergoes a conformational change that re-aligns the catalytic pocket to better allow for ATP hydrolysis (88).

In addition to the abovementioned PI3K-Akt and ERK1/2-MAPK signaling cascades cumulating in mTORC1 activation, several feedback circuits are also periodically triggered in response mTORC1 activation which functions to hamper overall kinase activity. Activation of the p70 S6 Kinase (S6K1 and S6K2) elicits phosphorylation and degradation of the insulin receptor substrate docking proteins IRS-1 and IRS-2 (190-192), thus consequently diminishing insulin-driven Akt and mTORC1 activation (Figure 1.9). S6K1 also confers multiple roles in the suppression of Akt activity through the inhibition of mTORC2; firstly through the phosphorylation of the scaffolding subunit Rictor at Thr1135 (193), as well as phosphorylation of the stabilizing subunit mSin1 at Thr86 and Thr398 (194). Although phosphorylation of mSin1 at Thr86 by S6K is reported to inhibit mTORC2 (194), conflicting reports highlight that mSin1 Thr86 phosphorylation is mediated by Akt and this consequently elicits increased mTORC2 activity (195). Regardless, both proposed models of mSin1 phosphorylation highlight the suppression of mTORC2 upon mTORC1 activation (Figure 1.9), as Akt activity is also consequently suppressed upon activation of p70 S6K1 via the aforementioned S6K-IRS feedback loop.

With the addition of Grb10 to the repertoire of *bona fide* direct phosphorylation targets of mTORC1, an alternative feedback loop has been uncovered involving Grb10-mediated suppression of the insulin receptor (IR) (196). While various Grb10 phosphorylation sites demonstrate sensitivity to the mTOR inhibitor torin1 (197), mTORC1 phosphorylation of Grb10 at Ser501 and Ser503 induced stabilization of Grb10 which consequentially resulted in suppressed insulin-driven Akt activity (198). Alternatively, mTORC1-mediated phosphorylation of Grb10 Ser501/Ser503 has also been shown to elicit increased binding of Grb10 to the Raptor subunit, and directly quench mTORC1 activity (199). Taken together, the initiation of these feedback networks function as means of curtailing the degree of mTORC1 activation within homeostatic levels.

A common effect of mitogen stimulation is the initiation of the ERK1/2-MAPK pathway through the small GTPase Ras. The aforementioned signaling pathway is commonly downstream of various growth factor receptors including ErbB2 and EGFR (200). Upon activation of the small GTPase Ras, the Raf-MEK signal cascade is initiated and results in the propagation of

transcriptional programs engaging in cell growth, and cell cycle progression (201). While ERK1/2- mTORC1 feedback circuits have been minimally documented thus far (202), ERK1/2 activation is curtailed by the kinase itself through ERK1/2-mediated inhibition of the upstream effectors such as the Ras GEF Sos (203), and MEK1/2 (204). Concomitantly, elevation in the levels of the lipid second messenger phosphatidic acid (PA) can also be observed upon mitogen stimulation, such as in the presence of PDGF (205), and does elicit mitogenic properties. The production of PA accumulates from the hydrolysis of Phosphatidylcholine (PC) by the action of the two enzymes PLD1 and PLD2. While mitogen stimulation may induce mTORC1 activation through inhibition of TSC function upon triggering the ERK1/2-MAPK signal cascade, PA production has been shown to mediate mTORC1 activation by stimulating the dissociation of the inhibitor FKBP38 from mTORC1 (206). Additionally, PA has been shown to cause rapid dissociation of the inhibitor Deptor from mTOR (207). Deptor is also post-transcriptionally regulated through degradation and, interestingly, an initiating mTORC1-dependent phosphorylation event is required for the E3-ligase-driven process. This initiates a Deptor-mTORC1 positive feedback loop, which involves the initial degradation of Deptor that triggers more mTORC1-mediated Deptor phosphorylation events which further accentuates mTORC1 activation (208-210). Since PA can mediate dissociation Deptor dissociation from mTOR, and phosphorylation of Deptor Ser293/Ser299 is subsequent to dissociation from mTOR, it is feasible that this may be the initiating event for the positive feedback loop (207, 211). Interestingly, PLD1 has been shown to be a downstream effector of Rheb1 (212), and where active Rheb1 can stimulate production of PA within an *in vitro* PLD functional assay. While Rheb1 alone is sufficient to stimulate kinase activity within *in vitro* mTORC1 kinase assays (213), it is feasible to speculate that robust mTORC1 activation *in vivo* may require concomitant PLD1-mediated Deptor dissociation.

1.7.2 Regulation of mTORC1 Activation by Energy Stress and Hypoxia.

The rapid expansion of bulk tumor elicits increased consumption of limitedly available nutrients within the tumor microenvironment, and as such, tumor cells are commonly subjected to periods of nutrient starvation. mTORC1 activity is suppressed during periods of nutrient starvation whereby the cell undergoes energy stress as a result of ATP depletion which is consequentially coupled with the accumulation of AMP. Activation of AMP-activated protein

kinase (AMPK) is particularly sensitive to change in the ATP: AMP ratio, as elevated levels of AMP drives allosteric activation of the kinase through direct binding of the molecule (214, 215), in addition to priming it for LKB1-mediated AMPK Thr172 phosphorylation to further enhance activity (216, 217). AMPK-driven activation of the TSC complex serves as a classical mechanism by which mTORC1 activation is inhibited by energy stress. Elevated AMPK-dependent phosphorylation of TSC2 at T1227 and S1345 consequently drives increased Rheb1 GAP function (218, 219). Concomitantly, AMPK-mediated phosphorylation of Raptor at Thr792 also diminishes mTORC1 activity (220). While activation of AMPK hinders cell growth partially through inhibition of mTORC1, short-term autophagic response driven by AMPK either indirectly through the suppression of mTORC1 or directly through ULK1/2 phosphorylation, can serve as a survival response (218, 221-224).

Alternative mechanisms by which mTORC1 activation is inhibited during periods of energy stress include the direct phosphorylation and inhibition of Rheb1 by PRAK kinase (225, 226). PRAK-mediated Rheb1 Ser130 phosphorylation results in the dissociation of the guanosine nucleotide from the small GTPase (227). Additionally, cellular energy sufficiency can also regulate mTORC1 activity by modulating complex dimerization through the ATP-sensitive TTT-RUVBL1/2 complex, which is sensitive to alternating ATP levels. Given that mTORC1 is a functional dimer (228-230), the inhibition of mTORC1 dimerization can serve as an alternative molecular mechanism of suppressing of kinase activity during state of cellular energy stress (231, 232).

In addition to nutrient starvation and energy stress, tumor microenvironment distant from blood circuitry tends to be plagued by low levels of oxygen which results in hypoxia. Consequentially, low cellular oxygen readily results in the stabilization of the Hypoxia-inducible factor 1 (HIF-1) which can induce expression of pro-angiogenic genes including VEGF, VECF receptor, and erythropoietin (233-235). This triggered angiogenesis furthers mammary tumor progression by allowing replenishment of nutrient and oxygen supplies. Under hypoxia, Hif-1a also drives expression of REDD1 which initiates inhibition of mTORC1 activity through activation of the TSC complex and suppression of Rheb1 (236). Genetic deletion of REDD1 demonstrates ability to ablate hypoxia-mediated inhibition of mTORC1 within various cell types (218, 237-239), which can sensitize cells to apoptosis following prolong hypoxia.

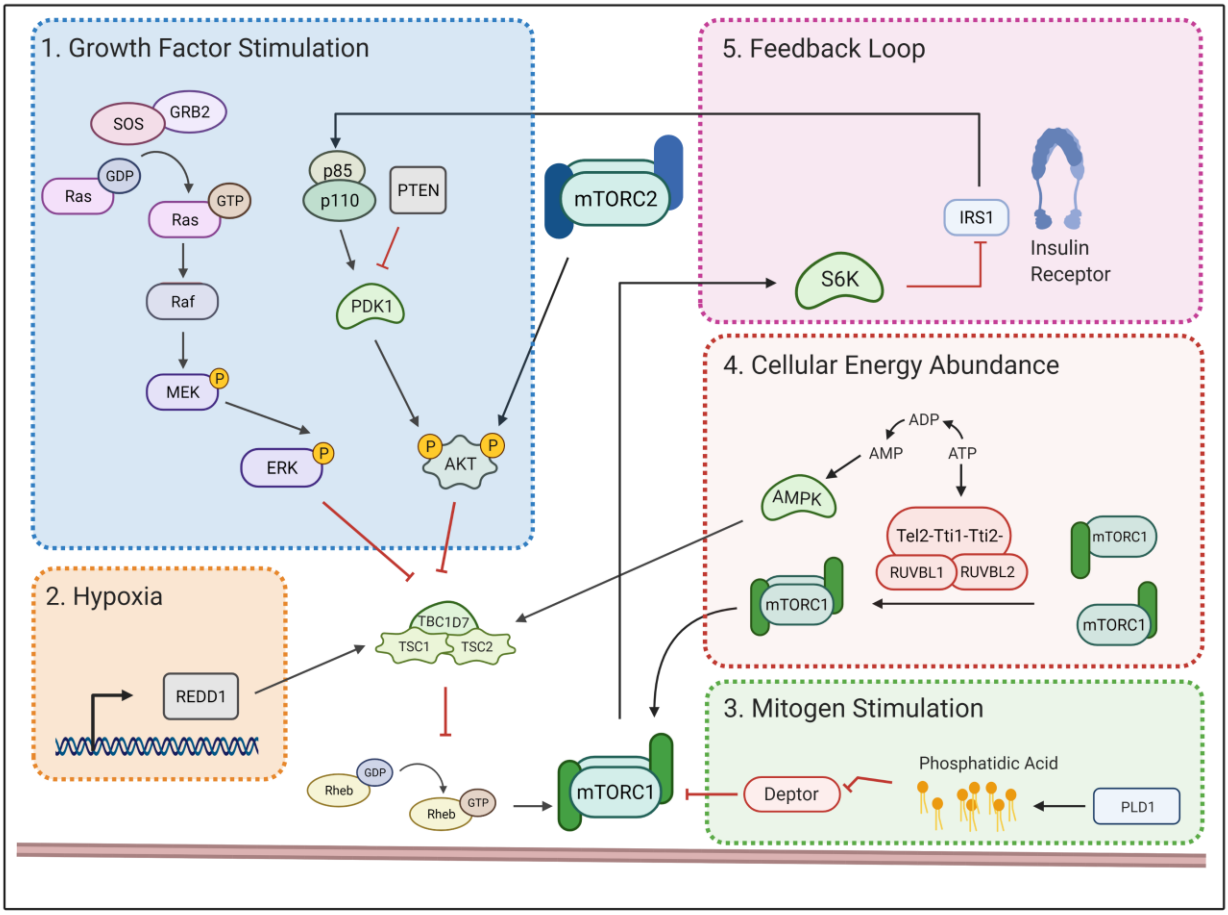

Figure 1. 9 mTORC1 is Regulated by a Network of Signalling Cascades Governed by Various Cellular Stimuli. mTORC1 activation is elicited through signalling cascades downstream of stimuli including growth factor stimulation (1), and mitogen stimulation (3). mTORC1 activation is hindered through signalling cascades downstream of stimuli such as hypoxia (2) and insufficient cellular energy (4), as well as various feedback loops involving the insulin receptor (5).

1.7.3 Regulation of mTORC1 by Amino Acids levels

Regulation of mTORC1 activation largely bifurcates into two predominantly separate signalling axes that converge at the lysosome surface; one axis governed by growth factor stimulation while the other is governed by amino acid sufficiency (Figure 1.9). While adequate

growth factor stimulation consequently amasses active GTP-bound Rheb1 at the lysosome, nutrient sufficiency controls lysosomal recruitment of mTORC1 in proximity of its obligate activator. These two parallel signaling axes ensure mTORC1 activation occurs only in the presence of both abundant nutrients and growth factors. Although amino acid starvation can trigger lysosomal localization of the TSC1/2 complex (240), the lysosomal recruitment of mTORC1 is TSC-independent (241) and is largely mediated by Rag GTPase-dependent tethering of the Raptor subunit to the lysosome-bound pentameric Ragulator complex (LAMTOR1-5; also known as, p18, p14, MP1, C7orf59, and HBXIP) (242, 243).

Rag GTPases function as obligate heterodimers and, within mammalian cells, are composed of a Rag A or B subunit (RagA/B) and a Rag C or D subunit (RagC/D) (244) while the equivalent heterodimer in yeast is composed of only two subunits, Gtr1p and Gtr2p (245). While the RagA/B GTPases demonstrate high homology and functional redundancy with Gtr1p, expression of RagC/D GTPases does not complement Gtr2p deficiency in yeast (246, 247). While activation of small GTPases are governed by the status of the guanine nucleotide bound, activation the obligate Rag heterodimers are dictated by the status of the guanine nucleotide bound to both subunits. The functional locked "ON" conformation, which permits interaction with the Raptor subunit, occurs within the Rag heterodimers only when both the RagA/B subunit is GTP-bound and the RagC/D subunit is GDP-bound. Conversely, the Rag heterodimers adopts a locked "OFF" conformation when both the RagA/B subunit is GDP-bound and RagC/D subunit is GTP-bound (248). Within either locked conformations, GTP-binding of one Rag subunit diminishes GTP binding and GTPase activity within the other subunit (249). This intrasubunit communication between Rag A/B and Rag C/D subunits, elicited through conformation changes within each subunit (246), allows for rapid coordinated transition between the locked "ON" and "OFF" states (Figure 1.9). Blockage of this intra-subunit communication consequentially disrupts the dynamic response of mTORC1 to fluctuations within amino acid levels (249).

A variety of Rag GEFs and GAPs have been identified that modulate mTORC1 activity in response to fluctuating amino acid levels, including the GATOR1/2 complex which is tethered to the lysosome through the KICSTOR complex (KPTN, ITFG2, C12orf66, and SZT2) (250). The GATOR1 complex, which is composed of DEPDC5, NPRL2 and NPRL3, elicits Rag A/B GAP activity (251) while the pentameric GATOR2 complex (Sec13, Seh1L, WDR24, WDR59

and Mios) provides suppression of GATOR1 function through an unknown mechanism (252). The FLCN-FNIP2 complex was identified to mediate RagC/D GAP activity in response to amino acid stimulation, which plays a crucial role in activating the Rag heterodimers (253). The Ragulator complex that functions as the lysosomal signaling platform for the Rag heterodimers elicits GAP-like activity towards RagC that, as a consequent of the intra-subunit communication, drives increased GTP-loading for the RagA/B (254, 255).

Amino acid-specific sensor proteins signal amino acid sufficiency (especially levels of arginine, and leucine) to the Rag heterodimers largely by regulating the activity of the Rag GAPs and GEFs mentioned above. The SLC38A9 transmembrane protein was determined to function as GEF for RagA thus facilitating activation of Rag heterodimers. The transmembrane protein was identified as a sensor for lysosomal arginine levels whereby the avidity of SLC38A9 towards GDP-bound RagA GTPase is increased, upon binding to arginine (254). When coupled with the Ragulator complex and the lysosomal v-ATPase proton pump, SLC38A9 provides inside-out amino acid signals on the lysosomal surface (256-259). While SLC38A9 responds to fluctuating lysosomal levels of arginine, CASTOR1 and CASTOR2 respond to changes in levels of cytosolic arginine by binding and inhibiting GATOR2 activity (260). Upon arginine starvation, CASTOR1 and CASTOR2 drive activation of GATOR1 through impeding GATOR2 function, which ultimately leads to the GDP-loaded RagA/B (261). In a similar manner, Sestrins1 and Sestrin2 also drive activation of GATOR1 through the suppression of GATOR2 (262, 263) in response to low levels of cytosolic leucine, which results in GDP-loaded RagA/B subunits (264, 265). The SAMTOR protein was identified as a direct sensor of the methionine metabolite, *S*-adenosylmethionine (SAM). Conversely, SAMTOR inhibits Rag heterodimer activity through binding and activating GATOR1 function upon SAM depletion, or methionine starvation (266).

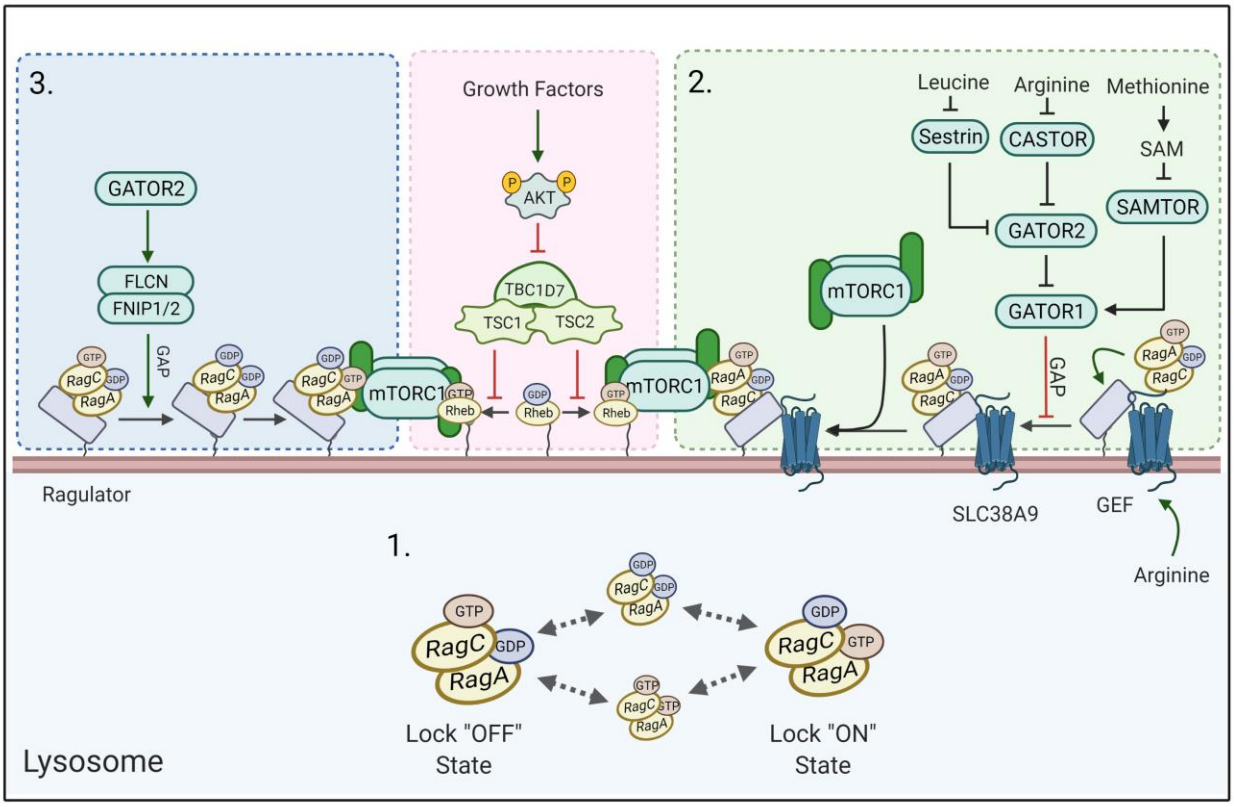

Figure 1. 10 Amino Acid-dependent Modulation of mTORC1 is Mediated by Rag GTPase Heterodimers. Intra-subunit communication between RagA/B and RagC/D governs intrinsic subunit GTPase activity and status of bound guanosine molecule (1). Abundant amino acids such as Leucine, Arginine and Methionine, mediate Rag heterodimer activity through the regulation of the GATOR complex and the Ragulator complex (2). Sufficient levels of amino acids also activate Rag heterodimers through activation of FLCN-FNIP1/2 complex (3).

1.8 Ras Family of Small GTPases

The Ras family of small GTPases is a collection of 36 members which act as signaling nodes that are activated in response a variety of extracellular stimuli to drive cellular events such as cell proliferation, survival and adhesion (267). These small GTPases function as molecular switches that transition between an active GTP-bound state and an inactive GDP-bound state. Upon acquisition of GTP, the small GTPase undergoes a conformational change to allow interaction with their respective effectors to initiate downstream signaling cascades. The GDP-GTP cycling within small GTPase is modulated by specific guanine nucleotide exchange factors (GEFs), and GTPase-activating proteins (GAPs). GAPs catalyze the conversion of GTP into

GDP within the small GTPase by stabilizing and positioning the water molecule used for hydrolysis. As seen in RasGAP (268) and RhoGAP (269), this is molecularly achieved by an "Arginine finger" whereby an arginine residue within the GAP involves a nearby glutamine residue within the GTPase to stabilize the nucleophilic water molecule. Alternatively, GTP-hydrolysis can be catalyzed by an "asparagine thumb" whereby an asparagine residue within the GAP directly stabilizes the nucleophilic water molecule as seen in Rap1GAP (270), and TSC2 (271). While GAPs drive the inactive GTPase conformation by facilitating the conversion of GTP into GDP, GEFs promotes the active GTPase conformation by eliciting the dissociation of the guanine nucleotide through opening of the binding pocket (272, 273). Consequentially, the vacant guanine nucleotide-binding pocket is subsequently filled by GTP due to the 10-fold higher intracellular levels of GTP than GDP (272, 273).

1.8.1 Members of the Ras family of small GTPase capable of activating mTORC1

1.8.1.1 Small GTPase Rheb1

Rheb1 is a member of the Ras family of small GTPases, and it is one of the few small GTPases reported to activate mTORC1. Akin to other members of the Ras family of small GTPases, Rheb1 contains a switch I and II domain which elicits interaction with its downstream effectors. Rheb1 also contains a P-loop motif which elicits GTP-binding, and a CAAX motif which directs proper subcellular localization of the small GTPase through farnesylation (274). It is well-established that the small GTPase Rheb1 is the obligatory activator of mTORC1, where activation requires a direct interaction between the small GTPase and the mTOR subunit (275). Early discoveries of dominant negative and hyperactivating Rheb1 mutants illustrated that despite exhibiting higher avidity within its GDP-bound state (275), mTORC1 activation is only achieved in the presence of GTP-bound Rheb1. Overlapping crystal structures of GDP- and GTP-bound Rheb1 reveals a conformation change within the switch I domain, which plays an important role in the activation of mTORC1(276, 277). While minimal conformational changes occur within the switch II domain during GDP-GTP cycling, the switch II domain does contribute to Rheb1 function where introducing Y67A/I69A and I76A/D77A mutant residues within the switch II motif diminishes capacity to activate mTORC1 (277). Despite these early observations, our knowledge of the molecular changes unfolding within mTORC1 subsequent binding of Rheb1 that leads to activation is still very limited. However, by contrasting the

recently published Cryo-EM reconstruction of Apo-mTORC1 and Rheb1-bound mTORC1 (88), it was revealed that binding of active Rheb1 causes displacement of the N-HEAT domain which allosterically reconfigures the catalytic cleft into a more compact conformation. Within the unbound form, mTORC1 exhibits a widened catalytic cleft which aligns residues in a conformation that is not conducive for ATP hydrolysis. The Rheb-mTOR interface is composed of N-HEAT, M-HEAT and the FAT domain where the Switch I motif interacts with M-HEAT and FAT domains, while Switch II of Rheb1 mediates interaction with all three domains. These recent mTORC1 structures also exposed the nature of the direct interaction between the switch II motif of Rheb1 and mTOR, which was previously determined critical for mTORC1 activation. These observations inspired the pioneering Rheb1-targeted small molecule inhibitor NR1 (278) in attempts to directly mitigate mTORC1 activity.

It is clear from *in vitro* kinase assays with recombinant mTORC1 that the sole addition of GTP-loaded Rheb1 is sufficient to induce increased kinase activity (275, 279, 280). Despite this observation, whether Rheb1 plays additional roles to further augment mTORC1 activation *in vivo* has not been explored. The phospholipase D1 (PLD1) has been demonstrated to be an effector of Rheb1, where PLD1-dependent production of Phosphatidic acid increases mTORC1 function (212). Direct supplementation of phosphatidic acid has been also shown to mediate dissociation of the mTOR inhibitor Deptor (207) and FK506 Binding Protein 38 (FKBP38) from mTORC1 (206). Whether active Rheb1 plays a prominent role in mediating the dissociation of Deptor and FKBP38 from mTOR remains to be addressed.

The canonical mechanism of Rheb1 regulation occurs predominantly through the modulation of its upstream GAP, the TSC complex which catalyzes GTPase activity. Interesting, the pool of Rheb1 molecules within the cell is highly populated by the GTP-bound state compared to other members of the Ras family of small GTPases (281). This is largely due its unique low intrinsic GTPase activity which is largely attributed to the presence of an arginine at residue 15 rather than a glycine like most members of the Ras GTPase family (276, 282). Although a few proteins have been shown to carry some Rheb1 GEF activity, including TCTP, a *bona fide* GEF has yet been identified. As such, evaluating the relative contribution of the GEF to regulation of Rheb1 activation has been thus far, rather elusive.

Non-canonical mechanisms of regulating Rheb1 function include PRAK-mediated phosphorylation. Phosphorylation of S183 results in dissociation of the bound nucleotide (227,

283). GAPDH plays a role in regulating Rheb1 function sequestering the small GTPase when glucose levels are low. Upon influx of glucose, GAPDH dissociates from Rheb1 thus allowing coupling of GLUT-mediated glucose influx with mTORC1 activation (284). Farnesylation of the CAAX motif of Rheb1 also plays a crucial role in eliciting this direct interaction, as it localizes the small GTPase into close proximity to mTORC1 at the lysosome (285-287). Early investigation into the therapeutic potential of targeting Rheb1 took advantage of the fact that proper localization was crucial for Rheb1 function through the use of farnesyltransferase inhibitors. Although FTIs also affected proper Ras localization, the inhibition of Rheb1 function did partially contribute to the anti-tumorigenic effects of FTI treatment. Although direct interaction between GTP-bound Rheb1 and mTOR is required for mTORC1 activation, GDP-bound Rheb1 has also been demonstrated to bind to mTOR. While the exact molecular mechanism is unknown, inactive Rheb1 paradoxically interaction with mTOR more than the active forms (275).

1.8.1.2 Small GTPase Rheb2

Unlike lower eukaryotic organisms, such as *Drosophila melanogaster (288),* the Rheb1 subfamily within mammalian cells consists of two isoforms, Rheb1 and the closely related Rheb2, also referred to as Rheb2 (289, 290). Both human and murine Rheb2 shares roughly 52% amino acid homology with Rheb1 with the highest similarity located within the Switch I and II domains, and demonstrates capacity to mediate mTORC1 activation within *in vitro* kinase assays (213). This biochemical evidence is consistent with observations that ectopic overexpression of Rheb2 within various cell models (Myeloid progenitor 32D, and HEK293 cells) elicits increased mTORC1 activity (280, 291). Nonetheless, Rheb1 remains the prominent isoform in mediating mTORC1 activation *in vivo* despite Rheb2 expression being detected within a wide range of tissues (292-294). Germline ablation of Rheb2 is viable and results in normal murine development (37), while germline ablation of Rheb1 or Raptor, the mTORC1-specific adaptor protein, leads to murine embryonic lethality (37, 39, 106). Additionally, neuronal-specific ablation of Rheb1 *in vivo* leads to myelination defects in postnatal brain development which is not recapitulated with Rheb2 ablation (37). Consistently, depletion of Rheb2 within various cell models (HEK293, HeLa and NIH3T3 cells) also reveals no change in mTORC1 function (279),

thus suggesting endogenous levels of Rheb2 may not play a prominent role in mediating mTORC1 activation.

Collectively, these observations suggest that Rheb2-mediated mTORC1 activation may occur at non-physiological levels of expression. Interestingly, overexpression of Rheb2 is clinically documented within cases of myeloid leukemia resulting from an in-frame DHH-RHEB2 gene fusion (295). While status of mTORC1 activity is not yet examined within the presence of DHH-RHEB2, occurrence of this gene fusion did correlate with poorer patient prognosis (295).

1.8.1.3 Small GTPase Ral

The Ral GTPases, which comprise of RalA and RalB, are another member of the Ras Superfamily of small GTPases reported to demonstrate some capacity to stimulate mTORC1 activation (267, 296). Synonymous to other small GTPase, GTP-GDP cycling of Ral GTPases is catalyzed by a Ral specific group of GTPase-Activating proteins and Guanine Exchange factors. The heterodimeric Ral GAP, which consists of the RalGAPβ subunit coupled with either a RalGAPα1 or RalGAPα2 subunit, catalyzes the hydrolysis of the GTP bound to Ral thus allowing transition into the inactive conformation (297). The various Ral GEFs catalyze the release of the guanine nucleotide to allow binding of GTP to the Ral GTPase. Once activated, Ral GTPases are known for their role in facilitating assembly of the octameric exocyst complex through interaction with Exo84 and Sec5, which occurs at the endomembrane of vesicles and the plasma membrane respectively (298). Assembly of the exocyst complex, which is composed of Sec3, Sec5, Sec6, Se8, Sec 10, Sec15, Exo70, and Exo84 (Reviewed in (299)), drives vesicle transport and tethering that precedes SNARE-mediated fusion to sites of active exocytosis. (Reviewed in (300)). Additionally, Ral GTPases are also involved in the regulation cell proliferation and migration (296, 301, 302).

The two isoforms RalA and RalB exhibit high homology with 82% similarity in amino acid identity, particularly within the switch I and II domains which elicits some functional redundancy between the two GTPases (303, 304). Despite having similar Switch I and II sequences, RalA and RalB do also execute distinct biological functions. This is partially attributed to the variable sequence regions directly upstream of the Switch domains within both isoforms that confer differential affinity for common effectors (305). In addition, some distinct

functionality can be attributed to the differential subcellular localization of RalA and RalB which is prompted by the variable C-terminal region of these two GTPases (305). While Ral GTPases are commonly enriched at the plasma membrane, PKCα and Aurora-A kinase mediated phosphorylation of S194 within the C-terminal region of Ral GTPase can divert subcellular enrichment towards the endomembrane system (301, 306)**.** Similar to Rheb1 and Rheb2, both RalA and RalB interact with PLD1 (307-309). RalA has demonstrated a prominent involvement in PLD1-mediated stimulation of mTORC1 activity (308). Although Ral GTPases have demonstrated involvement in stimulating mTORC1 activity, the capacity to which Ral GTPases can directly bind and activate mTORC1 is still unclear. While addition of either recombinant RalA or RalB does not elicit mTORC1 activation within *in vitro* kinase assays (280), hyperactivation of RalB through hyperactivating mutations within the GTPase or the genetic ablation of RalGAP does mediate direct activation of mTORC1 *in vivo* (296).

1.9 Dysregulation of the PI3K/Akt/mTORC1 pathway within Breast Cancer

Aberrant activation of mTORC1 is frequently observed within cancer, whereby hyperactivating mutations within the mTOR kinase are documented across various malignancies (310). Despite the infrequency of hyperactivating mTOR mutations within breast cancer, alteration within upstream modulators of the PI3K/ mTORC1 pathway including PIK3CA, AKT, PTEN, TSC1, TSC2 and LKB1 are commonly observed, and potentiate activation of the signalling cascade (311, 312). Suppression of PTEN function within breast cancer can be achieved through genomic alternations, promoter methylation as well as, mRNA and protein degradation (313, 314). Hyperactivating mutations within either the helical or kinase domain of *PIK3CA* are documented within one-third of breast cancers (315). Alternatively, increased PI3K and Akt activity is also achieved as a consequence of amplification and overexpression growth receptors such as HER2. In addition to growth factor driven activation, genetic aberrations within the amino acid-sensing modulators of mTORC1 are also apparent within metastatic breast cancer. Mutations within upstream regulators GATOR1 further potentiate mTORC1 activation (316-318).

Due to their frequent deregulation in cancer, these upstream modulators of mTORC1 activation become high-potential candidates for cancer therapeutics. In this section, I highlight some pharmacological compounds that suppress either mTORC1 activity or activation of

downstream mTORC1 effectors which are either applied within the clinical setting, or under development for clinical application **(Figure 1.11)**.

1.9.1 Small Molecule PI3K inhibitors

The heterodimeric lipid kinase PI3K is composed of a catalytic p110α, β or δ subunit along with a regulatory subunit p85, p55 or p50 (319). The stimulation of PI3K activity culminates in the robust activation of mTORC1 as a result of Akt-mediated suppression of the TSC complex and PRAS40. Buparlisib and Pictilisib are two pan-PI3K inhibitors **(Figure 1.11)** that have demonstrated high efficacy in treating patients with hormone-positive breast cancer carrying PIK3CA mutations (320, 321). Although the high toxicity did limit the therapeutic potential of pan-PI3K inhibitors, the onset of these small molecules did identify a patient population which exhibited considerable therapeutic benefit from PI3K-targeted treatment. The onset of pan-PI3K inhibitor did also inspire the development and clinical application of p110α-specific inhibitors in attempts to further improve therapeutic tolerability. Activating PIK3CA mutations which culminate in p110α hyperactivation are the most frequent molecular alterations of the PI3K signalling cascade within breast cancer (322), thus emphasizing this particular isoform above the others. The application of p110α-specific inhibitors such as Alpelisib and Taselisib, (323) within the clinical setting did achieve reduced overall toxicity while retaining the therapeutic efficacy of targeting PI3K (324). Similarly, other compounds that de-repressed TSC complex activity such as the Akt inhibitor MK2206, and MEK1/2 inhibitors AZD6244 and PD0325901 were also trialed as breast cancer therapeutics and demonstrated modest response (325).

1.9.2 The Anti-diabetic drug Metformin

While the biguanide Metformin was initially formulated as an anti-diabetic drug, the epidemiologic observation that chronic Metformin treatment reduced the incidence of cancer sparked the repurposing of the drug as an anti-cancer therapeutic agent (326). Phase II clinical trials demonstrated improved survival and tumor response within metastatic breast cancer patients upon treatment with metformin in combination with anthracyclines, taxanes or capecitabine (326). The anti-cancer effects of Metformin can be partially attributed to the suppression of systemic insulin, insulin-like growth factors levels (327), as well as reduced

hepatic glucose production (328). Metformin also elicits cell intrinsic anti-cancer effects by inhibiting the electron transport chain and suppressing ATP production. This cellular state of energy deficiency triggers AMPK-mediated suppression of mTORC1 activity in a TSC complex-dependent manner (329, 330) **(Figure 1.11)**. The suppression of mTORC1 activity upon Metformin treatment also partially achieved through increased nuclear retention of the RagC GAP folliculin in a TSC-independent manner. The nuclear sequestration of folliculin prolongs RagC within its GTP-bound state thus inhibiting Rag heterodimer activation (253, 331) **(Figure 1.10)**.

1.9.3 Small molecule mTOR inhibitors

The initial discovery of Rapamycin and the unravelling of its molecular mode of action were the pioneering advancements which launched the field of the mTORC1 signalling. Rapamycin and the derivative rapalogs Temsirolimus and Everolimus are considered first generation mTOR inhibitors, which allosterically suppress mTORC1 activity through the formation a gain-of-function complex with FKBP12 (332), as well as other FKBP members (333). Clinical cancer cases illustrating exemplary therapeutic efficacy of rapalogs can be found within varies cancers (334, 335) that demonstrate robust oncogenic addiction to mTORC1 function, such as malignancies carrying mTOR mutations or exhibiting functional loss of TSC complex (336, 337). Despite the therapeutic response, clinical efficacy of rapalogs is limited by the feedback Akt activation resulting from S6K suppression (190-192), and the partial inhibition of the mTORC1 effector 4EBP1 (338). Initiatives to bypass these two clinical challenges drove the development of ATP-competitive small molecule mTOR inhibitors Torin1, AZD2014, and PP242 (338, 339), as well as PI3K/mTOR dual inhibitors NVP-BEZ235 and LY3023414 (340, 341).

1.9.4 Inhibitors disrupting the initiation of cap-dependent mRNA translation

As described above, the assembly of the eIF4F complex crucial for cap-dependent mRNA translation is driven by eIF4E, which recruits the eIF4G scaffold along with the eIF4A RNA helicase. mTORC1 regulates eIF4E activation by modulating the dissociation of 4EBPs from the mRNA cap-binding protein, thus effectively unveiling the binding motif necessary for direct eIF4E-eIF4G interaction (342). Effectively, the pharmalogical inhibition of mTORC1 with

ATP-competitive mTOR inhibitors such as Torin1 or PP242, consequently results in suppression of the eIF4E-eIF4G interaction that is indispensable for eIF4F assembly. Within breast cancer, elevated 4EBP1 phosphorylation and eIF4E expression correlates with higher tumor grade and reduced survival (343). Given its prominent contribution to cancer progression (344, 345), extensive focus have been placed on the development of small molecules that perturb the eIF4E-eIF4G interaction. One concept of disrupting the eIF4E-eIF4G interaction involves directly antagonising the eIF4E-mRNA interaction with the antiviral drug Ribavirin, which structurally resembles the 7-Methyl GTP (344). While Phase I/II clinical trials for Ribavirin for breast cancer have yet to be conducted, application of the antiviral drug for treating and hepatocellular carcinoma have demonstrated therapeutic benefit (346). Alternatively, small synthetic peptides 4EGI-1 and 4EIRCat were developed to competitively bind the eIF4G-binding motif on eIF4E to inhibit cap-dependent translation (345, 347). While 4EGI-1 did demonstrate robust anti-cancer effects within pre-clinical models (118, 119, 345), further development of 4EGI-1 for clinical application are halted due to low therapeutic index and off-target effects (348).

mRNA transcripts crucial for cellular growth, such as Cyclin D1, Survivin and VEGF, frequently carry complex 5'UTR structures requiring extensive RNA helicase activity for efficient ribosome scanning (121). As a crucial component of the eIF4F complex, the RNA helicase eIF4A functions to unwind hindering secondary structures within the 5' UTR region. The natural products Silvestrol, Rocaglamide A, CR-1-31, along with compounds such as Pateamine A and Hippuristanol are small molecules that inhibit eIF4A function (349). Effectively, these small molecules function to deplete the free eIF4A available for assembly into the eIF4F complex by sequestrating eIF4A onto mRNA (350). While reports from breast cancer clinical trials are lacking, the use of eIF4A inhibitors Silvestrol and CR-31 have demonstrated robust anti-cancer response within various pre-clinical models of pancreatic (351), prostate, and breast cancer (352, 353).

Taken together, the aforementioned repertoire of pharmacological compounds illustrates a breadth of possibilities for disrupting the PI3K/mTORC1 pathway based on our current cumulative knowledge of the signalling cascade. Within the above section, I've highlighted some molecules in development for clinical application that target various members spanning from upstream regulators to key downstream effectors of mTORC1. Additionally, previously non-targetable members of the signalling cascade such as Rheb1 have become accessible for

therapeutic intervention with the onset of novel compound discovery (278). Despite our comprehensive knowledge concerning the canonical PI3K/mTORC1 pathway, expanding our understanding on the plasticity of this signalling cascade when confronted with the aforementioned pharmacological inhibitors, would further illuminate the potential resistance mechanisms and other therapeutic challenges that may develop.

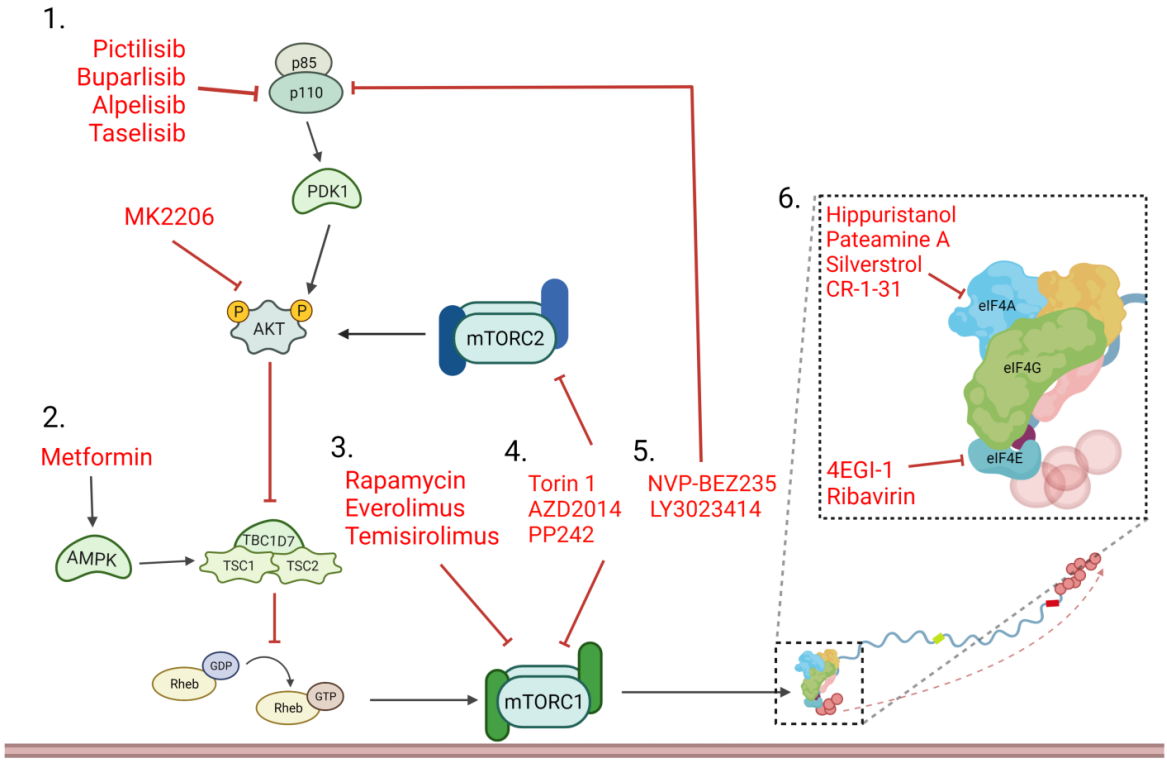

Figure 1.11 Pharmalogical compounds targeting various members of the PI3K/mTOR signalling cascade. Various pharmalogical inhibitors developed for clinical application, including PI3K inhibitors, Akt inhibitors (1) and the anti-diabetic drug metformin (2) are currently available to inhibit various upstream regulators of mTORC1. Rapalogs (3), ATP-competitive mTOR inhibitors, and PI3K/mTOR dual inhibitor are currently used to directly inhibit the mTOR kinase. eIF4A inhibitors Hippuristanol, Silverstrol, and Pateamine A, as well as eIF4E inhibitors Ribavirin and 4EGI-1 can be used to disrupt eIF4F function downstream of mTORC1.

1.10 Experimental Rationale:

Elevated rates of protein synthesis are frequently observed within various malignancies and contribute prominently to disease progression. Due to the strenuous demand of maintaining elevated protein synthesis and the evolutionary nature of cancer progression, tumors often develop various adaption mechanisms to maintain these increased rates.

mTORC1 is a multicomponent kinase which plays a prominent role in regulating protein synthesis primarily through the modulation of downstream effectors S6K and 4EBPs. While the role of mTORC1 in the maintenance of mammary tumor cells has been thoroughly studied, its contribution to the early stages of mammary tumor initiation remains unexplored. To address this, we used GEMMs of breast cancer that closely recapitulate the complex process of tumor initiation in combination with gene targeted strategies against mTORC1 to dissect its role within this process. Taking advantage of the evolutionary nature of mammary tumorigenesis within these GEMMs, we also examined the cell plasticity of mammary tumor cells at bypassing perturbation of mTORC1 activation in attempts to expand our understanding of alternative modes of activation.

1.11 References:

1. Chew HK (2001) Adjuvant therapy for breast cancer: who should get what? *The Western journal of medicine* 174(4):284-287.
2. Anonymous (2019) Release notice - Canadian Cancer Statistics 2019. *Health promotion and chronic disease prevention in Canada : research, policy and practice* 39(8-9):255.
3. Kaplan HG & Malmgren JA (2008) Impact of triple negative phenotype on breast cancer prognosis. *The breast journal* 14(5):456-463.
4. Prat A & Perou CM (2011) Deconstructing the molecular portraits of breast cancer. *Molecular oncology* 5(1):5-23.
5. Perou CM, *et al.* (2000) Molecular portraits of human breast tumours. *Nature* 406(6797):747-752.
6. Parker JS, *et al.* (2009) Supervised risk predictor of breast cancer based on intrinsic subtypes. *Journal of clinical oncology : official journal of the American Society of Clinical Oncology* 27(8):1160-1167.
7. Herschkowitz JI, *et al.* (2007) Identification of conserved gene expression features between murine mammary carcinoma models and human breast tumors. *Genome biology* 8(5):R76.
8. Sørlie T, *et al.* (2001) Gene expression patterns of breast carcinomas distinguish tumor subclasses with clinical implications. *Proceedings of the National Academy of Sciences of the United States of America* 98(19):10869-10874.
9. Cheang MC, *et al.* (2009) Ki67 index, HER2 status, and prognosis of patients with luminal B breast cancer. *Journal of the National Cancer Institute* 101(10):736-750.
10. Geyer CE, *et al.* (2006) Lapatinib plus capecitabine for HER2-positive advanced breast cancer. *The New England journal of medicine* 355(26):2733-2743.
11. Dias K, *et al.* (2017) Claudin-Low Breast Cancer; Clinical & Pathological Characteristics. *PloS one* 12(1):e0168669.
12. Prat A, *et al.* (2015) Clinical implications of the intrinsic molecular subtypes of breast cancer. *Breast (Edinburgh, Scotland)* 24 Suppl 2:S26-35.
13. Richert MM, Schwertfeger KL, Ryder JW, & Anderson SM (2000) An atlas of mouse mammary gland development. *Journal of mammary gland biology and neoplasia* 5(2):227-241.
14. Visvader JE & Stingl J (2014) Mammary stem cells and the differentiation hierarchy: current status and perspectives. *Genes & development* 28(11):1143-1158.
15. Deugnier MA, Moiseyeva EP, Thiery JP, & Glukhova M (1995) Myoepithelial cell differentiation in the developing mammary gland: progressive acquisition of smooth muscle phenotype. *Developmental dynamics : an official publication of the American Association of Anatomists* 204(2):107-117.
16. McNally S & Stein T (2017) Overview of Mammary Gland Development: A Comparison of Mouse and Human. *Methods in molecular biology (Clifton, N.J.)* 1501:1-17.
17. Macias H & Hinck L (2012) Mammary gland development. *Wiley interdisciplinary reviews. Developmental biology* 1(4):533-557.
18. Henry MD, Triplett AA, Oh KB, Smith GH, & Wagner KU (2004) Parity-induced mammary epithelial cells facilitate tumorigenesis in MMTV-neu transgenic mice. *Oncogene* 23(41):6980-6985.
19. Little JL, *et al.* (2014) A requirement for Nedd9 in luminal progenitor cells prior to mammary tumorigenesis in MMTV-HER2/ErbB2 mice. *Oncogene* 33(4):411-420.

20. Lo PK, *et al.* (2012) CD49f and CD61 identify Her2/neu-induced mammary tumor-initiating cells that are potentially derived from luminal progenitors and maintained by the integrin-TGFβ signaling. *Oncogene* 31(21):2614-2626.
21. Reya T, Morrison SJ, Clarke MF, & Weissman IL (2001) Stem cells, cancer, and cancer stem cells. *Nature* 414(6859):105-111.
22. Marjanovic ND, Weinberg RA, & Chaffer CL (2013) Cell plasticity and heterogeneity in cancer. *Clinical chemistry* 59(1):168-179.
23. Scheel C, *et al.* (2011) Paracrine and autocrine signals induce and maintain mesenchymal and stem cell states in the breast. *Cell* 145(6):926-940.
24. Morel AP, *et al.* (2008) Generation of breast cancer stem cells through epithelial-mesenchymal transition. *PloS one* 3(8):e2888.
25. Mani SA, *et al.* (2008) The epithelial-mesenchymal transition generates cells with properties of stem cells. *Cell* 133(4):704-715.
26. Nowell PC (1976) The clonal evolution of tumor cell populations. *Science (New York, N.Y.)* 194(4260):23-28.
27. Merlo LM, Pepper JW, Reid BJ, & Maley CC (2006) Cancer as an evolutionary and ecological process. *Nature reviews. Cancer* 6(12):924-935.
28. Maley CC, *et al.* (2017) Classifying the evolutionary and ecological features of neoplasms. *Nature reviews. Cancer* 17(10):605-619.
29. Andrechek ER, *et al.* (2000) Amplification of the neu/erbB-2 oncogene in a mouse model of mammary tumorigenesis. *Proceedings of the National Academy of Sciences of the United States of America* 97(7):3444-3449.
30. Golovkina TV, Dudley JP, & Ross SR (1998) B and T cells are required for mouse mammary tumor virus spread within the mammary gland. *Journal of immunology (Baltimore, Md. : 1950)* 161(5):2375-2382.
31. Hadjantonakis AK, Pirity M, & Nagy A (2008) Cre recombinase mediated alterations of the mouse genome using embryonic stem cells. *Methods in molecular biology (Clifton, N.J.)* 461:111-132.
32. Ray MK, Fagan SP, & Brunicardi FC (2000) The Cre-loxP system: a versatile tool for targeting genes in a cell- and stage-specific manner. *Cell transplantation* 9(6):805-815.
33. Zagozdzon AM, *et al.* (2012) Generation of a new bioluminescent model for visualisation of mammary tumour development in transgenic mice. *BMC cancer* 12:209.
34. Ahmed F, *et al.* (2002) GFP expression in the mammary gland for imaging of mammary tumor cells in transgenic mice. *Cancer research* 62(24):7166-7169.
35. Soriano P (1999) Generalized lacZ expression with the ROSA26 Cre reporter strain. *Nat Genet* 21(1):70-71.
36. Takeda K, *et al.* (1997) Targeted disruption of the mouse Stat3 gene leads to early embryonic lethality. *Proceedings of the National Academy of Sciences of the United States of America* 94(8):3801-3804.
37. Zou J, *et al.* (2011) Rheb1 is required for mTORC1 and myelination in postnatal brain development. *Dev Cell* 20(1):97-108.
38. Jones LM, *et al.* (2016) STAT3 Establishes an Immunosuppressive Microenvironment during the Early Stages of Breast Carcinogenesis to Promote Tumor Growth and Metastasis. *Cancer research* 76(6):1416-1428.
39. Goorden SM, *et al.* (2011) Rheb is essential for murine development. *Molecular and cellular biology* 31(8):1672-1678.

40. Van Keymeulen A, *et al.* (2011) Distinct stem cells contribute to mammary gland development and maintenance. *Nature* 479(7372):189-193.
41. Rios AC, Fu NY, Lindeman GJ, & Visvader JE (2014) In situ identification of bipotent stem cells in the mammary gland. *Nature* 506(7488):322-327.
42. Hennighausen L (1990) The mammary gland as a bioreactor: production of foreign proteins in milk. *Protein expression and purification* 1(1):3-8.
43. Stewart TA, Hollingshead PG, & Pitts SL (1988) Multiple regulatory domains in the mouse mammary tumor virus long terminal repeat revealed by analysis of fusion genes in transgenic mice. *Mol Cell Biol* 8(1):473-479.
44. Henrard D & Ross SR (1988) Endogenous mouse mammary tumor virus is expressed in several organs in addition to the lactating mammary gland. *Journal of virology* 62(8):3046-3049.
45. Wagner KU, *et al.* (1997) Cre-mediated gene deletion in the mammary gland. *Nucleic acids research* 25(21):4323-4330.
46. Guy CT, Cardiff RD, & Muller WJ (1992) Induction of mammary tumors by expression of polyomavirus middle T oncogene: a transgenic mouse model for metastatic disease. *Molecular and cellular biology* 12(3):954-961.
47. Siegel PM, Dankort DL, Hardy WR, & Muller WJ (1994) Novel activating mutations in the neu proto-oncogene involved in induction of mammary tumors. *Molecular and cellular biology* 14(11):7068-7077.
48. Knight JF, *et al.* (2013) Met synergizes with p53 loss to induce mammary tumors that possess features of claudin-low breast cancer. *Proceedings of the National Academy of Sciences of the United States of America* 110(14):E1301-1310.
49. Welm AL, Kim S, Welm BE, & Bishop JM (2005) MET and MYC cooperate in mammary tumorigenesis. *Proceedings of the National Academy of Sciences of the United States of America* 102(12):4324-4329.
50. Li Y, Hively WP, & Varmus HE (2000) Use of MMTV-Wnt-1 transgenic mice for studying the genetic basis of breast cancer. *Oncogene* 19(8):1002-1009.
51. Jang JW, Boxer RB, & Chodosh LA (2006) Isoform-specific ras activation and oncogene dependence during MYC- and Wnt-induced mammary tumorigenesis. *Mol Cell Biol* 26(21):8109-8121.
52. D'Cruz CM, *et al.* (2001) c-MYC induces mammary tumorigenesis by means of a preferred pathway involving spontaneous Kras2 mutations. *Nature medicine* 7(2):235-239.
53. Bertram R & Hillen W (2008) The application of Tet repressor in prokaryotic gene regulation and expression. *Microbial biotechnology* 1(1):2-16.
54. Orth P, Schnappinger D, Hillen W, Saenger W, & Hinrichs W (2000) Structural basis of gene regulation by the tetracycline inducible Tet repressor-operator system. *Nature structural biology* 7(3):215-219.
55. Gossen M & Bujard H (1992) Tight control of gene expression in mammalian cells by tetracycline-responsive promoters. *Proceedings of the National Academy of Sciences of the United States of America* 89(12):5547-5551.
56. Loew R, Heinz N, Hampf M, Bujard H, & Gossen M (2010) Improved Tet-responsive promoters with minimized background expression. *BMC biotechnology* 10:81.

57. Agha-Mohammadi S, *et al.* (2004) Second-generation tetracycline-regulatable promoter: repositioned tet operator elements optimize transactivator synergy while shorter minimal promoter offers tight basal leakiness. *The journal of gene medicine* 6(7):817-828.
58. Gossen M, *et al.* (1995) Transcriptional activation by tetracyclines in mammalian cells. *Science (New York, N.Y.)* 268(5218):1766-1769.
59. Das AT, *et al.* (2004) Viral evolution as a tool to improve the tetracycline-regulated gene expression system. *The Journal of biological chemistry* 279(18):18776-18782.
60. Zhou X, Vink M, Klaver B, Berkhout B, & Das AT (2006) Optimization of the Tet-On system for regulated gene expression through viral evolution. *Gene therapy* 13(19):1382-1390.
61. Moody SE, *et al.* (2002) Conditional activation of Neu in the mammary epithelium of transgenic mice results in reversible pulmonary metastasis. *Cancer cell* 2(6):451-461.
62. Rao T, *et al.* (2014) Inducible and coupled expression of the polyomavirus middle T antigen and Cre recombinase in transgenic mice: an in vivo model for synthetic viability in mammary tumour progression. *Breast cancer research : BCR* 16(1):R11.
63. Goel S, *et al.* (2016) Overcoming Therapeutic Resistance in HER2-Positive Breast Cancers with CDK4/6 Inhibitors. *Cancer cell* 29(3):255-269.
64. Fluck MM & Schaffhausen BS (2009) Lessons in signaling and tumorigenesis from polyomavirus middle T antigen. *Microbiology and molecular biology reviews : MMBR* 73(3):542-563, Table of Contents.
65. Izumchenko E, *et al.* (2009) NEDD9 promotes oncogenic signaling in mammary tumor development. *Cancer research* 69(18):7198-7206.
66. Lahlou H, *et al.* (2007) Mammary epithelial-specific disruption of the focal adhesion kinase blocks mammary tumor progression. *Proceedings of the National Academy of Sciences of the United States of America* 104(51):20302-20307.
67. Marcotte R, Smith HW, Sanguin-Gendreau V, McDonough RV, & Muller WJ (2012) Mammary epithelial-specific disruption of c-Src impairs cell cycle progression and tumorigenesis. *Proceedings of the National Academy of Sciences of the United States of America* 109(8):2808-2813.
68. Guy CT, *et al.* (1992) Expression of the neu protooncogene in the mammary epithelium of transgenic mice induces metastatic disease. *Proceedings of the National Academy of Sciences of the United States of America* 89(22):10578-10582.
69. Siegel PM & Muller WJ (1996) Mutations affecting conserved cysteine residues within the extracellular domain of Neu promote receptor dimerization and activation. *Proceedings of the National Academy of Sciences of the United States of America* 93(17):8878-8883.
70. Siegel PM, Ryan ED, Cardiff RD, & Muller WJ (1999) Elevated expression of activated forms of Neu/ErbB-2 and ErbB-3 are involved in the induction of mammary tumors in transgenic mice: implications for human breast cancer. *EMBO J* 18(8):2149-2164.
71. Dankort DL, Wang Z, Blackmore V, Moran MF, & Muller WJ (1997) Distinct tyrosine autophosphorylation sites negatively and positively modulate neu-mediated transformation. *Molecular and cellular biology* 17(9):5410-5425.
72. Schade B, *et al.* (2007) Distinct ErbB-2 coupled signaling pathways promote mammary tumors with unique pathologic and transcriptional profiles. *Cancer research* 67(16):7579-7588.

73. Mattoon DR, Lamothe B, Lax I, & Schlessinger J (2004) The docking protein Gab1 is the primary mediator of EGF-stimulated activation of the PI-3K/Akt cell survival pathway. *BMC biology* 2:24.
74. Ursini-Siegel J, *et al.* (2010) Receptor tyrosine kinase signaling favors a protumorigenic state in breast cancer cells by inhibiting the adaptive immune response. *Cancer research* 70(20):7776-7787.
75. Li J, Kim SG, & Blenis J (2014) Rapamycin: one drug, many effects. *Cell metabolism* 19(3):373-379.
76. Dumont FJ, *et al.* (1990) The immunosuppressive macrolides FK-506 and rapamycin act as reciprocal antagonists in murine T cells. *Journal of immunology (Baltimore, Md. : 1950)* 144(4):1418-1424.
77. Kuo CJ, *et al.* (1992) Rapamycin selectively inhibits interleukin-2 activation of p70 S6 kinase. *Nature* 358(6381):70-73.
78. Chung J, Kuo CJ, Crabtree GR, & Blenis J (1992) Rapamycin-FKBP specifically blocks growth-dependent activation of and signaling by the 70 kd S6 protein kinases. *Cell* 69(7):1227-1236.
79. Price DJ, Grove JR, Calvo V, Avruch J, & Bierer BE (1992) Rapamycin-induced inhibition of the 70-kilodalton S6 protein kinase. *Science (New York, N.Y.)* 257(5072):973-977.
80. Heitman J, Movva NR, & Hall MN (1991) Targets for cell cycle arrest by the immunosuppressant rapamycin in yeast. *Science (New York, N.Y.)* 253(5022):905-909.
81. Cafferkey R, *et al.* (1993) Dominant missense mutations in a novel yeast protein related to mammalian phosphatidylinositol 3-kinase and VPS34 abrogate rapamycin cytotoxicity. *Molecular and cellular biology* 13(10):6012-6023.
82. Koltin Y, *et al.* (1991) Rapamycin sensitivity in Saccharomyces cerevisiae is mediated by a peptidyl-prolyl cis-trans isomerase related to human FK506-binding protein. *Molecular and cellular biology* 11(3):1718-1723.
83. Kunz J, *et al.* (1993) Target of rapamycin in yeast, TOR2, is an essential phosphatidylinositol kinase homolog required for G1 progression. *Cell* 73(3):585-596.
84. Brown EJ, *et al.* (1994) A mammalian protein targeted by G1-arresting rapamycin-receptor complex. *Nature* 369(6483):756-758.
85. Sabatini DM, Erdjument-Bromage H, Lui M, Tempst P, & Snyder SH (1994) RAFT1: a mammalian protein that binds to FKBP12 in a rapamycin-dependent fashion and is homologous to yeast TORs. *Cell* 78(1):35-43.
86. Brown EJ, *et al.* (1995) Control of p70 s6 kinase by kinase activity of FRAP in vivo. *Nature* 377(6548):441-446.
87. Brunn GJ, *et al.* (1996) Direct inhibition of the signaling functions of the mammalian target of rapamycin by the phosphoinositide 3-kinase inhibitors, wortmannin and LY294002. *Embo j* 15(19):5256-5267.
88. Yang H, *et al.* (2017) Mechanisms of mTORC1 activation by RHEB and inhibition by PRAS40. *Nature* 552(7685):368-373.
89. Chen X, *et al.* (2018) Cryo-EM structure of human mTOR complex 2. *Cell research* 28(5):518-528.
90. Loewith R, *et al.* (2002) Two TOR complexes, only one of which is rapamycin sensitive, have distinct roles in cell growth control. *Molecular cell* 10(3):457-468.

91. Yang H, *et al.* (2013) mTOR kinase structure, mechanism and regulation. *Nature* 497(7448):217-223.
92. Gaubitz C, *et al.* (2015) Molecular Basis of the Rapamycin Insensitivity of Target Of Rapamycin Complex 2. *Molecular cell* 58(6):977-988.
93. Sarbassov DD, *et al.* (2006) Prolonged rapamycin treatment inhibits mTORC2 assembly and Akt/PKB. *Molecular cell* 22(2):159-168.
94. Hara K, *et al.* (2002) Raptor, a binding partner of target of rapamycin (TOR), mediates TOR action. *Cell* 110(2):177-189.
95. Kim DH, *et al.* (2002) mTOR interacts with raptor to form a nutrient-sensitive complex that signals to the cell growth machinery. *Cell* 110(2):163-175.
96. Yip CK, Murata K, Walz T, Sabatini DM, & Kang SA (2010) Structure of the human mTOR complex I and its implications for rapamycin inhibition. *Molecular cell* 38(5):768-774.
97. Beretta L, Gingras AC, Svitkin YV, Hall MN, & Sonenberg N (1996) Rapamycin blocks the phosphorylation of 4E-BP1 and inhibits cap-dependent initiation of translation. *Embo j* 15(3):658-664.
98. Brunn GJ, *et al.* (1997) Phosphorylation of the translational repressor PHAS-I by the mammalian target of rapamycin. *Science (New York, N.Y.)* 277(5322):99-101.
99. Shahbazian D, *et al.* (2006) The mTOR/PI3K and MAPK pathways converge on eIF4B to control its phosphorylation and activity. *Embo j* 25(12):2781-2791.
100. Dennis MD, Jefferson LS, & Kimball SR (2012) Role of p70S6K1-mediated phosphorylation of eIF4B and PDCD4 proteins in the regulation of protein synthesis. *The Journal of biological chemistry* 287(51):42890-42899.
101. Schalm SS, Fingar DC, Sabatini DM, & Blenis J (2003) TOS motif-mediated raptor binding regulates 4E-BP1 multisite phosphorylation and function. *Current biology : CB* 13(10):797-806.
102. Schalm SS & Blenis J (2002) Identification of a conserved motif required for mTOR signaling. *Current biology : CB* 12(8):632-639.
103. Nojima H, *et al.* (2003) The mammalian target of rapamycin (mTOR) partner, raptor, binds the mTOR substrates p70 S6 kinase and 4E-BP1 through their TOR signaling (TOS) motif. *The Journal of biological chemistry* 278(18):15461-15464.
104. Sancak Y, *et al.* (2007) PRAS40 is an insulin-regulated inhibitor of the mTORC1 protein kinase. *Molecular cell* 25(6):903-915.
105. Wang L, Harris TE, Roth RA, & Lawrence JC, Jr. (2007) PRAS40 regulates mTORC1 kinase activity by functioning as a direct inhibitor of substrate binding. *The Journal of biological chemistry* 282(27):20036-20044.
106. Guertin DA, *et al.* (2006) Ablation in mice of the mTORC components raptor, rictor, or mLST8 reveals that mTORC2 is required for signaling to Akt-FOXO and PKCalpha, but not S6K1. *Dev Cell* 11(6):859-871.
107. Kim DH, *et al.* (2003) GbetaL, a positive regulator of the rapamycin-sensitive pathway required for the nutrient-sensitive interaction between raptor and mTOR. *Molecular cell* 11(4):895-904.
108. Wang B, *et al.* (2017) TRAF2 and OTUD7B govern a ubiquitin-dependent switch that regulates mTORC2 signalling. *Nature* 545:365.
109. Frias MA, *et al.* (2006) mSin1 is necessary for Akt/PKB phosphorylation, and its isoforms define three distinct mTORC2s. *Current biology : CB* 16(18):1865-1870.

110. Sarbassov DD, *et al.* (2004) Rictor, a novel binding partner of mTOR, defines a rapamycin-insensitive and raptor-independent pathway that regulates the cytoskeleton. *Current biology : CB* 14(14):1296-1302.
111. Sarbassov DD, Guertin DA, Ali SM, & Sabatini DM (2005) Phosphorylation and regulation of Akt/PKB by the rictor-mTOR complex. *Science (New York, N.Y.)* 307(5712):1098-1101.
112. Jacinto E, *et al.* (2004) Mammalian TOR complex 2 controls the actin cytoskeleton and is rapamycin insensitive. *Nature cell biology* 6(11):1122-1128.
113. Pearce LR, *et al.* (2007) Identification of Protor as a novel Rictor-binding component of mTOR complex-2. *The Biochemical journal* 405(3):513-522.
114. Buttgereit F & Brand MD (1995) A hierarchy of ATP-consuming processes in mammalian cells. *The Biochemical journal* 312 (Pt 1):163-167.
115. Grüner S, *et al.* (2018) Structural motifs in eIF4G and 4E-BPs modulate their binding to eIF4E to regulate translation initiation in yeast. *Nucleic acids research* 46(13):6893-6908.
116. Haghighat A, Mader S, Pause A, & Sonenberg N (1995) Repression of cap-dependent translation by 4E-binding protein 1: competition with p220 for binding to eukaryotic initiation factor-4E. *Embo j* 14(22):5701-5709.
117. De A, *et al.* (2019) Inhibition of oncogenic cap-dependent translation by 4EGI-1 reduces growth, enhances chemosensitivity and alters genome-wide translation in non-small cell lung cancer. *Cancer gene therapy* 26(5-6):157-165.
118. Wang H, *et al.* (2015) The synergistic inhibition of breast cancer proliferation by combined treatment with 4EGI-1 and MK2206. *Cell cycle (Georgetown, Tex.)* 14(2):232-242.
119. Yi T, Kabha E, Papadopoulos E, & Wagner G (2014) 4EGI-1 targets breast cancer stem cells by selective inhibition of translation that persists in CSC maintenance, proliferation and metastasis. *Oncotarget* 5(15):6028-6037.
120. Ma XM & Blenis J (2009) Molecular mechanisms of mTOR-mediated translational control. *Nature reviews. Molecular cell biology* 10(5):307-318.
121. Pelletier J & Sonenberg N (1985) Insertion mutagenesis to increase secondary structure within the 5' noncoding region of a eukaryotic mRNA reduces translational efficiency. *Cell* 40(3):515-526.
122. Komar AA & Hatzoglou M (2005) Internal ribosome entry sites in cellular mRNAs: mystery of their existence. *The Journal of biological chemistry* 280(25):23425-23428.
123. Gingras AC, *et al.* (2001) Hierarchical phosphorylation of the translation inhibitor 4E-BP1. *Genes & development* 15(21):2852-2864.
124. Pause A, *et al.* (1994) Insulin-dependent stimulation of protein synthesis by phosphorylation of a regulator of 5'-cap function. *Nature* 371(6500):762-767.
125. Shveygert M, Kaiser C, Bradrick SS, & Gromeier M (2010) Regulation of eukaryotic initiation factor 4E (eIF4E) phosphorylation by mitogen-activated protein kinase occurs through modulation of Mnk1-eIF4G interaction. *Molecular and cellular biology* 30(21):5160-5167.
126. Muller D, *et al.* (2013) 4E-BP restrains eIF4E phosphorylation. *Translation (Austin)* 1(2):e25819.
127. Robichaud N, *et al.* (2015) Phosphorylation of eIF4E promotes EMT and metastasis via translational control of SNAIL and MMP-3. *Oncogene* 34(16):2032-2042.

128. Thoreen CC, *et al.* (2012) A unifying model for mTORC1-mediated regulation of mRNA translation. *Nature* 485(7396):109-113.
129. Averous J, Fonseca BD, & Proud CG (2008) Regulation of cyclin D1 expression by mTORC1 signaling requires eukaryotic initiation factor 4E-binding protein 1. *Oncogene* 27(8):1106-1113.
130. Larsson O, *et al.* (2012) Distinct perturbation of the translatome by the antidiabetic drug metformin. *Proceedings of the National Academy of Sciences of the United States of America* 109(23):8977-8982.
131. Wu LX, *et al.* (2005) CD28 regulates the translation of Bcl-xL via the phosphatidylinositol 3-kinase/mammalian target of rapamycin pathway. *Journal of immunology (Baltimore, Md. : 1950)* 174(1):180-194.
132. Wolfe AL, *et al.* (2014) RNA G-quadruplexes cause eIF4A-dependent oncogene translation in cancer. *Nature* 513(7516):65-70.
133. Dennis PB, Pullen N, Pearson RB, Kozma SC, & Thomas G (1998) Phosphorylation sites in the autoinhibitory domain participate in p70(s6k) activation loop phosphorylation. *The Journal of biological chemistry* 273(24):14845-14852.
134. Pearson RB, *et al.* (1995) The principal target of rapamycin-induced p70s6k inactivation is a novel phosphorylation site within a conserved hydrophobic domain. *Embo j* 14(21):5279-5287.
135. Pullen N, *et al.* (1998) Phosphorylation and activation of p70s6k by PDK1. *Science (New York, N.Y.)* 279(5351):707-710.
136. Yi SA, *et al.* (2016) S6K1 Phosphorylation of H2B Mediates EZH2 Trimethylation of H3: A Determinant of Early Adipogenesis. *Molecular cell* 62(3):443-452.
137. Bungard D, *et al.* (2010) Signaling kinase AMPK activates stress-promoted transcription via histone H2B phosphorylation. *Science (New York, N.Y.)* 329(5996):1201-1205.
138. Galan JA, *et al.* (2014) Phosphoproteomic analysis identifies the tumor suppressor PDCD4 as a RSK substrate negatively regulated by 14-3-3. *Proceedings of the National Academy of Sciences of the United States of America* 111(29):E2918-2927.
139. Roux PP, *et al.* (2007) RAS/ERK signaling promotes site-specific ribosomal protein S6 phosphorylation via RSK and stimulates cap-dependent translation. *The Journal of biological chemistry* 282(19):14056-14064.
140. Shima H, *et al.* (1998) Disruption of the p70(s6k)/p85(s6k) gene reveals a small mouse phenotype and a new functional S6 kinase. *Embo j* 17(22):6649-6659.
141. Ruvinsky I, *et al.* (2005) Ribosomal protein S6 phosphorylation is a determinant of cell size and glucose homeostasis. *Genes & development* 19(18):2199-2211.
142. Fingar DC, Salama S, Tsou C, Harlow E, & Blenis J (2002) Mammalian cell size is controlled by mTOR and its downstream targets S6K1 and 4EBP1/eIF4E. *Genes & development* 16(12):1472-1487.
143. Murakami M, *et al.* (2004) mTOR is essential for growth and proliferation in early mouse embryos and embryonic stem cells. *Molecular and cellular biology* 24(15):6710-6718.
144. Hentges KE, *et al.* (2001) FRAP/mTOR is required for proliferation and patterning during embryonic development in the mouse. *Proceedings of the National Academy of Sciences of the United States of America* 98(24):13796-13801.
145. Zhang H, Stallock JP, Ng JC, Reinhard C, & Neufeld TP (2000) Regulation of cellular growth by the Drosophila target of rapamycin dTOR. *Genes & development* 14(21):2712-2724.

146. Boye E & Grallert B (2020) eIF2α phosphorylation and the regulation of translation. *Current genetics* 66(2):293-297.
147. Pavitt GD, Ramaiah KV, Kimball SR, & Hinnebusch AG (1998) eIF2 independently binds two distinct eIF2B subcomplexes that catalyze and regulate guanine-nucleotide exchange. *Genes & development* 12(4):514-526.
148. Sudhakar A, *et al.* (2000) Phosphorylation of serine 51 in initiation factor 2 alpha (eIF2 alpha) promotes complex formation between eIF2 alpha(P) and eIF2B and causes inhibition in the guanine nucleotide exchange activity of eIF2B. *Biochemistry* 39(42):12929-12938.
149. Gandin V, *et al.* (2016) mTORC1 and CK2 coordinate ternary and eIF4F complex assembly. *Nature communications* 7:11127.
150. Vattem KM & Wek RC (2004) Reinitiation involving upstream ORFs regulates ATF4 mRNA translation in mammalian cells. *Proceedings of the National Academy of Sciences of the United States of America* 101(31):11269-11274.
151. Lu PD, Harding HP, & Ron D (2004) Translation reinitiation at alternative open reading frames regulates gene expression in an integrated stress response. *The Journal of cell biology* 167(1):27-33.
152. Baird TD, *et al.* (2014) Selective mRNA translation during eIF2 phosphorylation induces expression of IBTKα. *Molecular biology of the cell* 25(10):1686-1697.
153. Palam LR, Baird TD, & Wek RC (2011) Phosphorylation of eIF2 facilitates ribosomal bypass of an inhibitory upstream ORF to enhance CHOP translation. *The Journal of biological chemistry* 286(13):10939-10949.
154. Dikic I & Elazar Z (2018) Mechanism and medical implications of mammalian autophagy. *Nature reviews. Molecular cell biology* 19(6):349-364.
155. Egan DF, *et al.* (2015) Small Molecule Inhibition of the Autophagy Kinase ULK1 and Identification of ULK1 Substrates. *Molecular cell* 59(2):285-297.
156. Valvezan AJ, *et al.* (2017) mTORC1 Couples Nucleotide Synthesis to Nucleotide Demand Resulting in a Targetable Metabolic Vulnerability. *Cancer cell* 32(5):624-638.e625.
157. Ben-Sahra I, Howell JJ, Asara JM, & Manning BD (2013) Stimulation of de novo pyrimidine synthesis by growth signaling through mTOR and S6K1. *Science (New York, N.Y.)* 339(6125):1323-1328.
158. Peterson TR, *et al.* (2011) mTOR complex 1 regulates lipin 1 localization to control the SREBP pathway. *Cell* 146(3):408-420.
159. Duvel K, *et al.* (2010) Activation of a metabolic gene regulatory network downstream of mTOR complex 1. *Molecular cell* 39(2):171-183.
160. Land SC & Tee AR (2007) Hypoxia-inducible factor 1alpha is regulated by the mammalian target of rapamycin (mTOR) via an mTOR signaling motif. *The Journal of biological chemistry* 282(28):20534-20543.
161. Cunningham JT, *et al.* (2007) mTOR controls mitochondrial oxidative function through a YY1-PGC-1alpha transcriptional complex. *Nature* 450(7170):736-740.
162. Kim J, Kundu M, Viollet B, & Guan KL (2011) AMPK and mTOR regulate autophagy through direct phosphorylation of Ulk1. *Nature cell biology* 13(2):132-141.
163. Jung CH, *et al.* (2009) ULK-Atg13-FIP200 complexes mediate mTOR signaling to the autophagy machinery. *Molecular biology of the cell* 20(7):1992-2003.

164. McEwan DG, *et al.* (2015) PLEKHM1 regulates autophagosome-lysosome fusion through HOPS complex and LC3/GABARAP proteins. *Molecular cell* 57(1):39-54.
165. Palmieri M, *et al.* (2011) Characterization of the CLEAR network reveals an integrated control of cellular clearance pathways. *Human molecular genetics* 20(19):3852-3866.
166. Settembre C, *et al.* (2011) TFEB links autophagy to lysosomal biogenesis. *Science (New York, N.Y.)* 332(6036):1429-1433.
167. Napolitano G & Ballabio A (2016) TFEB at a glance. *Journal of cell science* 129(13):2475-2481.
168. Martina JA & Puertollano R (2013) Rag GTPases mediate amino acid-dependent recruitment of TFEB and MITF to lysosomes. *The Journal of cell biology* 200(4):475-491.
169. Martina JA, Chen Y, Gucek M, & Puertollano R (2012) MTORC1 functions as a transcriptional regulator of autophagy by preventing nuclear transport of TFEB. *Autophagy* 8(6):903-914.
170. Di Malta C, *et al.* (2017) Transcriptional activation of RagD GTPase controls mTORC1 and promotes cancer growth. *Science (New York, N.Y.)* 356(6343):1188-1192.
171. Horton JD, Goldstein JL, & Brown MS (2002) SREBPs: activators of the complete program of cholesterol and fatty acid synthesis in the liver. *The Journal of clinical investigation* 109(9):1125-1131.
172. Porstmann T, *et al.* (2008) SREBP activity is regulated by mTORC1 and contributes to Akt-dependent cell growth. *Cell metabolism* 8(3):224-236.
173. Rawson RB (2003) The SREBP pathway--insights from Insigs and insects. *Nature reviews. Molecular cell biology* 4(8):631-640.
174. Yabe D, Brown MS, & Goldstein JL (2002) Insig-2, a second endoplasmic reticulum protein that binds SCAP and blocks export of sterol regulatory element-binding proteins. *Proceedings of the National Academy of Sciences of the United States of America* 99(20):12753-12758.
175. Yang T, *et al.* (2002) Crucial step in cholesterol homeostasis: sterols promote binding of SCAP to INSIG-1, a membrane protein that facilitates retention of SREBPs in ER. *Cell* 110(4):489-500.
176. Yabe D, Xia ZP, Adams CM, & Rawson RB (2002) Three mutations in sterol-sensing domain of SCAP block interaction with insig and render SREBP cleavage insensitive to sterols. *Proceedings of the National Academy of Sciences of the United States of America* 99(26):16672-16677.
177. Brown AJ, Sun L, Feramisco JD, Brown MS, & Goldstein JL (2002) Cholesterol addition to ER membranes alters conformation of SCAP, the SREBP escort protein that regulates cholesterol metabolism. *Molecular cell* 10(2):237-245.
178. Pende M, *et al.* (2004) S6K1(-/-)/S6K2(-/-) mice exhibit perinatal lethality and rapamycin-sensitive 5'-terminal oligopyrimidine mRNA translation and reveal a mitogen-activated protein kinase-dependent S6 kinase pathway. *Molecular and cellular biology* 24(8):3112-3124.
179. Huffman TA, Mothe-Satney I, & Lawrence JC, Jr. (2002) Insulin-stimulated phosphorylation of lipin mediated by the mammalian target of rapamycin. *Proceedings of the National Academy of Sciences of the United States of America* 99(2):1047-1052.
180. Dibble CC, *et al.* (2012) TBC1D7 is a third subunit of the TSC1-TSC2 complex upstream of mTORC1. *Molecular cell* 47(4):535-546.

181. Castro AF, Rebhun JF, Clark GJ, & Quilliam LA (2003) Rheb binds tuberous sclerosis complex 2 (TSC2) and promotes S6 kinase activation in a rapamycin- and farnesylation-dependent manner. *The Journal of biological chemistry* 278(35):32493-32496.
182. Inoki K, Li Y, Xu T, & Guan KL (2003) Rheb GTPase is a direct target of TSC2 GAP activity and regulates mTOR signaling. *Genes & development* 17(15):1829-1834.
183. Ma L, Chen Z, Erdjument-Bromage H, Tempst P, & Pandolfi PP (2005) Phosphorylation and functional inactivation of TSC2 by Erk implications for tuberous sclerosis and cancer pathogenesis. *Cell* 121(2):179-193.
184. Tee AR, Anjum R, & Blenis J (2003) Inactivation of the tuberous sclerosis complex-1 and -2 gene products occurs by phosphoinositide 3-kinase/Akt-dependent and -independent phosphorylation of tuberin. *The Journal of biological chemistry* 278(39):37288-37296.
185. Ma L, *et al.* (2007) Identification of S664 TSC2 phosphorylation as a marker for extracellular signal-regulated kinase mediated mTOR activation in tuberous sclerosis and human cancer. *Cancer research* 67(15):7106-7112.
186. Inoki K, Li Y, Zhu T, Wu J, & Guan KL (2002) TSC2 is phosphorylated and inhibited by Akt and suppresses mTOR signalling. *Nature cell biology* 4(9):648-657.
187. Cai SL, *et al.* (2006) Activity of TSC2 is inhibited by AKT-mediated phosphorylation and membrane partitioning. *The Journal of cell biology* 173(2):279-289.
188. Manning BD, Tee AR, Logsdon MN, Blenis J, & Cantley LC (2002) Identification of the tuberous sclerosis complex-2 tumor suppressor gene product tuberin as a target of the phosphoinositide 3-kinase/akt pathway. *Molecular cell* 10(1):151-162.
189. Madigan JP, *et al.* (2018) The tuberous sclerosis complex subunit TBC1D7 is stabilized by Akt phosphorylation-mediated 14-3-3 binding. *The Journal of biological chemistry* 293(42):16142-16159.
190. Shah OJ, Wang Z, & Hunter T (2004) Inappropriate activation of the TSC/Rheb/mTOR/S6K cassette induces IRS1/2 depletion, insulin resistance, and cell survival deficiencies. *Current biology : CB* 14(18):1650-1656.
191. Harrington LS, *et al.* (2004) The TSC1-2 tumor suppressor controls insulin-PI3K signaling via regulation of IRS proteins. *The Journal of cell biology* 166(2):213-223.
192. Shah OJ & Hunter T (2006) Turnover of the active fraction of IRS1 involves raptor-mTOR- and S6K1-dependent serine phosphorylation in cell culture models of tuberous sclerosis. *Molecular and cellular biology* 26(17):6425-6434.
193. Dibble CC, Asara JM, & Manning BD (2009) Characterization of Rictor phosphorylation sites reveals direct regulation of mTOR complex 2 by S6K1. *Molecular and cellular biology* 29(21):5657-5670.
194. Liu P, *et al.* (2013) Sin1 phosphorylation impairs mTORC2 complex integrity and inhibits downstream Akt signalling to suppress tumorigenesis. *Nature cell biology* 15(11):1340-1350.
195. Yang G, Murashige DS, Humphrey SJ, & James DE (2015) A Positive Feedback Loop between Akt and mTORC2 via SIN1 Phosphorylation. *Cell reports* 12(6):937-943.
196. Wang L, *et al.* (2007) Peripheral disruption of the Grb10 gene enhances insulin signaling and sensitivity in vivo. *Molecular and cellular biology* 27(18):6497-6505.
197. Hsu PP, *et al.* (2011) The mTOR-regulated phosphoproteome reveals a mechanism of mTORC1-mediated inhibition of growth factor signaling. *Science (New York, N.Y.)* 332(6035):1317-1322.

198. Yu Y, *et al.* (2011) Phosphoproteomic analysis identifies Grb10 as an mTORC1 substrate that negatively regulates insulin signaling. *Science (New York, N.Y.)* 332(6035):1322-1326.
199. Liu M, *et al.* (2014) Grb10 promotes lipolysis and thermogenesis by phosphorylation-dependent feedback inhibition of mTORC1. *Cell metabolism* 19(6):967-980.
200. Katz M, Amit I, & Yarden Y (2007) Regulation of MAPKs by growth factors and receptor tyrosine kinases. *Biochimica et biophysica acta* 1773(8):1161-1176.
201. Meloche S & Pouysségur J (2007) The ERK1/2 mitogen-activated protein kinase pathway as a master regulator of the G1- to S-phase transition. *Oncogene* 26(22):3227-3239.
202. Carracedo A, *et al.* (2008) Inhibition of mTORC1 leads to MAPK pathway activation through a PI3K-dependent feedback loop in human cancer. *The Journal of clinical investigation* 118(9):3065-3074.
203. Kamioka Y, Yasuda S, Fujita Y, Aoki K, & Matsuda M (2010) Multiple decisive phosphorylation sites for the negative feedback regulation of SOS1 via ERK. *The Journal of biological chemistry* 285(43):33540-33548.
204. Eblen ST, *et al.* (2004) Mitogen-activated protein kinase feedback phosphorylation regulates MEK1 complex formation and activation during cellular adhesion. *Molecular and cellular biology* 24(6):2308-2317.
205. Fukami K & Takenawa T (1992) Phosphatidic acid that accumulates in platelet-derived growth factor-stimulated Balb/c 3T3 cells is a potential mitogenic signal. *The Journal of biological chemistry* 267(16):10988-10993.
206. Yoon MS, Sun Y, Arauz E, Jiang Y, & Chen J (2011) Phosphatidic acid activates mammalian target of rapamycin complex 1 (mTORC1) kinase by displacing FK506 binding protein 38 (FKBP38) and exerting an allosteric effect. *The Journal of biological chemistry* 286(34):29568-29574.
207. Yoon MS, *et al.* (2015) Rapid mitogenic regulation of the mTORC1 inhibitor, DEPTOR, by phosphatidic acid. *Molecular cell* 58(3):549-556.
208. Gao D, *et al.* (2011) mTOR drives its own activation via SCF(betaTrCP)-dependent degradation of the mTOR inhibitor DEPTOR. *Molecular cell* 44(2):290-303.
209. Zhao Y, Xiong X, & Sun Y (2011) DEPTOR, an mTOR inhibitor, is a physiological substrate of SCF(betaTrCP) E3 ubiquitin ligase and regulates survival and autophagy. *Molecular cell* 44(2):304-316.
210. Duan S, *et al.* (2011) mTOR generates an auto-amplification loop by triggering the betaTrCP- and CK1alpha-dependent degradation of DEPTOR. *Molecular cell* 44(2):317-324.
211. Peterson TR, *et al.* (2009) DEPTOR is an mTOR inhibitor frequently overexpressed in multiple myeloma cells and required for their survival. *Cell* 137(5):873-886.
212. Sun Y, *et al.* (2008) Phospholipase D1 is an effector of Rheb in the mTOR pathway. *Proceedings of the National Academy of Sciences of the United States of America* 105(24):8286-8291.
213. Parmar N & Tamanoi F (2010) Rheb G-Proteins and the Activation of mTORC1. *Enzymes* 27:39-56.
214. Hardie DG (2004) The AMP-activated protein kinase pathway--new players upstream and downstream. *Journal of cell science* 117(Pt 23):5479-5487.

215. Xiao B, *et al.* (2013) Structural basis of AMPK regulation by small molecule activators. *Nature communications* 4:3017.
216. Hawley SA, *et al.* (1996) Characterization of the AMP-activated protein kinase kinase from rat liver and identification of threonine 172 as the major site at which it phosphorylates AMP-activated protein kinase. *The Journal of biological chemistry* 271(44):27879-27887.
217. Shaw RJ, *et al.* (2004) The tumor suppressor LKB1 kinase directly activates AMP-activated kinase and regulates apoptosis in response to energy stress. *Proceedings of the National Academy of Sciences of the United States of America* 101(10):3329-3335.
218. Inoki K, Zhu T, & Guan KL (2003) TSC2 mediates cellular energy response to control cell growth and survival. *Cell* 115(5):577-590.
219. Inoki K, *et al.* (2006) TSC2 integrates Wnt and energy signals via a coordinated phosphorylation by AMPK and GSK3 to regulate cell growth. *Cell* 126(5):955-968.
220. Gwinn DM, *et al.* (2008) AMPK phosphorylation of raptor mediates a metabolic checkpoint. *Molecular cell* 30(2):214-226.
221. Degenhardt K, *et al.* (2006) Autophagy promotes tumor cell survival and restricts necrosis, inflammation, and tumorigenesis. *Cancer cell* 10(1):51-64.
222. White E (2015) The role for autophagy in cancer. *The Journal of clinical investigation* 125(1):42-46.
223. Amaravadi R, Kimmelman AC, & White E (2016) Recent insights into the function of autophagy in cancer. *Genes & development* 30(17):1913-1930.
224. Kazyken D, *et al.* (2019) AMPK directly activates mTORC2 to promote cell survival during acute energetic stress. *Science signaling* 12(585).
225. New L, *et al.* (1998) PRAK, a novel protein kinase regulated by the p38 MAP kinase. *Embo j* 17(12):3372-3384.
226. Zarubin T & Han J (2005) Activation and signaling of the p38 MAP kinase pathway. *Cell research* 15(1):11-18.
227. Zheng M, *et al.* (2011) Inactivation of Rheb by PRAK-mediated phosphorylation is essential for energy-depletion-induced suppression of mTORC1. *Nature cell biology* 13(3):263-272.
228. Wang L, Rhodes CJ, & Lawrence JC, Jr. (2006) Activation of mammalian target of rapamycin (mTOR) by insulin is associated with stimulation of 4EBP1 binding to dimeric mTOR complex 1. *The Journal of biological chemistry* 281(34):24293-24303.
229. Takahara T, Hara K, Yonezawa K, Sorimachi H, & Maeda T (2006) Nutrient-dependent multimerization of the mammalian target of rapamycin through the N-terminal HEAT repeat region. *The Journal of biological chemistry* 281(39):28605-28614.
230. Jain A, *et al.* (2014) Stoichiometry and assembly of mTOR complexes revealed by single-molecule pulldown. *Proceedings of the National Academy of Sciences of the United States of America* 111(50):17833-17838.
231. Kim SG, *et al.* (2013) Metabolic stress controls mTORC1 lysosomal localization and dimerization by regulating the TTT-RUVBL1/2 complex. *Molecular cell* 49(1):172-185.
232. David-Morrison G, *et al.* (2016) WAC Regulates mTOR Activity by Acting as an Adaptor for the TTT and Pontin/Reptin Complexes. *Dev Cell* 36(2):139-151.
233. Majmundar AJ, Wong WJ, & Simon MC (2010) Hypoxia-inducible factors and the response to hypoxic stress. *Molecular cell* 40(2):294-309.

234. Shi YH & Fang WG (2004) Hypoxia-inducible factor-1 in tumour angiogenesis. *World journal of gastroenterology* 10(8):1082-1087.
235. Semenza GL (2002) HIF-1 and tumor progression: pathophysiology and therapeutics. *Trends in molecular medicine* 8(4 Suppl):S62-67.
236. Sofer A, Lei K, Johannessen CM, & Ellisen LW (2005) Regulation of mTOR and cell growth in response to energy stress by REDD1. *Molecular and cellular biology* 25(14):5834-5845.
237. Wolff NC, *et al.* (2017) Correction for Wolff et al., "Cell-Type-Dependent Regulation of mTORC1 by REDD1 and the Tumor Suppressors TSC1/TSC2 and LKB1 in Response to Hypoxia". *Molecular and cellular biology* 37(13).
238. Cam H, Easton JB, High A, & Houghton PJ (2010) mTORC1 signaling under hypoxic conditions is controlled by ATM-dependent phosphorylation of HIF-1α. *Molecular cell* 40(4):509-520.
239. Brugarolas J, *et al.* (2004) Regulation of mTOR function in response to hypoxia by REDD1 and the TSC1/TSC2 tumor suppressor complex. *Genes & development* 18(23):2893-2904.
240. Demetriades C, Plescher M, & Teleman AA (2016) Lysosomal recruitment of TSC2 is a universal response to cellular stress. *Nature communications* 7:10662.
241. Smith EM, Finn SG, Tee AR, Browne GJ, & Proud CG (2005) The tuberous sclerosis protein TSC2 is not required for the regulation of the mammalian target of rapamycin by amino acids and certain cellular stresses. *The Journal of biological chemistry* 280(19):18717-18727.
242. de Araujo MEG, *et al.* (2017) Crystal structure of the human lysosomal mTORC1 scaffold complex and its impact on signaling. *Science (New York, N.Y.)* 358(6361):377-381.
243. Sancak Y, *et al.* (2010) Ragulator-Rag complex targets mTORC1 to the lysosomal surface and is necessary for its activation by amino acids. *Cell* 141(2):290-303.
244. Sekiguchi T, Hirose E, Nakashima N, Ii M, & Nishimoto T (2001) Novel G proteins, Rag C and Rag D, interact with GTP-binding proteins, Rag A and Rag B. *The Journal of biological chemistry* 276(10):7246-7257.
245. Gong R, *et al.* (2011) Crystal structure of the Gtr1p-Gtr2p complex reveals new insights into the amino acid-induced TORC1 activation. *Genes & development* 25(16):1668-1673.
246. Anandapadamanaban M, *et al.* (2019) Architecture of human Rag GTPase heterodimers and their complex with mTORC1. *Science (New York, N.Y.)* 366(6462):203-210.
247. Gao M & Kaiser CA (2006) A conserved GTPase-containing complex is required for intracellular sorting of the general amino-acid permease in yeast. *Nature cell biology* 8(7):657-667.
248. Sancak Y, *et al.* (2008) The Rag GTPases bind raptor and mediate amino acid signaling to mTORC1. *Science (New York, N.Y.)* 320(5882):1496-1501.
249. Shen K, Choe A, & Sabatini DM (2017) Intersubunit Crosstalk in the Rag GTPase Heterodimer Enables mTORC1 to Respond Rapidly to Amino Acid Availability. *Molecular cell* 68(4):821.
250. Wolfson RL, *et al.* (2017) KICSTOR recruits GATOR1 to the lysosome and is necessary for nutrients to regulate mTORC1. *Nature* 543(7645):438-442.
251. Shen K, *et al.* (2018) Architecture of the human GATOR1 and GATOR1-Rag GTPases complexes. *Nature* 556(7699):64-69.

252. Bar-Peled L, *et al.* (2013) A Tumor suppressor complex with GAP activity for the Rag GTPases that signal amino acid sufficiency to mTORC1. *Science (New York, N.Y.)* 340(6136):1100-1106.
253. Tsun ZY, *et al.* (2013) The folliculin tumor suppressor is a GAP for the RagC/D GTPases that signal amino acid levels to mTORC1. *Molecular cell* 52(4):495-505.
254. Shen K & Sabatini DM (2018) Ragulator and SLC38A9 activate the Rag GTPases through noncanonical GEF mechanisms. *Proceedings of the National Academy of Sciences of the United States of America* 115(38):9545-9550.
255. Bar-Peled L, Schweitzer LD, Zoncu R, & Sabatini DM (2012) Ragulator is a GEF for the rag GTPases that signal amino acid levels to mTORC1. *Cell* 150(6):1196-1208.
256. Zoncu R, *et al.* (2011) mTORC1 senses lysosomal amino acids through an inside-out mechanism that requires the vacuolar H(+)-ATPase. *Science (New York, N.Y.)* 334(6056):678-683.
257. Wyant GA, *et al.* (2017) mTORC1 Activator SLC38A9 Is Required to Efflux Essential Amino Acids from Lysosomes and Use Protein as a Nutrient. *Cell* 171(3):642-654.e612.
258. Wang S, *et al.* (2015) Metabolism. Lysosomal amino acid transporter SLC38A9 signals arginine sufficiency to mTORC1. *Science (New York, N.Y.)* 347(6218):188-194.
259. Jung J, Genau HM, & Behrends C (2015) Amino Acid-Dependent mTORC1 Regulation by the Lysosomal Membrane Protein SLC38A9. *Molecular and cellular biology* 35(14):2479-2494.
260. Chantranupong L, *et al.* (2016) The CASTOR Proteins Are Arginine Sensors for the mTORC1 Pathway. *Cell* 165(1):153-164.
261. Saxton RA, Chantranupong L, Knockenhauer KE, Schwartz TU, & Sabatini DM (2016) Mechanism of arginine sensing by CASTOR1 upstream of mTORC1. *Nature* 536(7615):229-233.
262. Wolfson RL, *et al.* (2016) Sestrin2 is a leucine sensor for the mTORC1 pathway. *Science (New York, N.Y.)* 351(6268):43-48.
263. Peng M, Yin N, & Li MO (2014) Sestrins function as guanine nucleotide dissociation inhibitors for Rag GTPases to control mTORC1 signaling. *Cell* 159(1):122-133.
264. Parmigiani A, *et al.* (2014) Sestrins inhibit mTORC1 kinase activation through the GATOR complex. *Cell reports* 9(4):1281-1291.
265. Chantranupong L, *et al.* (2014) The Sestrins interact with GATOR2 to negatively regulate the amino-acid-sensing pathway upstream of mTORC1. *Cell reports* 9(1):1-8.
266. Gu X, *et al.* (2017) SAMTOR is an S-adenosylmethionine sensor for the mTORC1 pathway. *Science (New York, N.Y.)* 358(6364):813-818.
267. Wennerberg K, Rossman KL, & Der CJ (2005) The Ras superfamily at a glance. *Journal of cell science* 118(Pt 5):843-846.
268. Scheffzek K, *et al.* (1997) The Ras-RasGAP complex: structural basis for GTPase activation and its loss in oncogenic Ras mutants. *Science (New York, N.Y.)* 277(5324):333-338.
269. Rittinger K, Walker PA, Eccleston JF, Smerdon SJ, & Gamblin SJ (1997) Structure at 1.65 A of RhoA and its GTPase-activating protein in complex with a transition-state analogue. *Nature* 389(6652):758-762.
270. Kupzig S, Bouyoucef-Cherchalli D, Yarwood S, Sessions R, & Cullen PJ (2009) The ability of GAP1IP4BP to function as a Rap1 GTPase-activating protein (GAP) requires

its Ras GAP-related domain and an arginine finger rather than an asparagine thumb. *Molecular and cellular biology* 29(14):3929-3940.
271. Li Y, Inoki K, & Guan KL (2004) Biochemical and functional characterizations of small GTPase Rheb and TSC2 GAP activity. *Molecular and cellular biology* 24(18):7965-7975.
272. Goody RS & Hofmann-Goody W (2002) Exchange factors, effectors, GAPs and motor proteins: common thermodynamic and kinetic principles for different functions. *European biophysics journal : EBJ* 31(4):268-274.
273. Itzen A & Goody RS (2011) GTPases involved in vesicular trafficking: structures and mechanisms. *Seminars in cell & developmental biology* 22(1):48-56.
274. Hanker AB, *et al.* (2010) Differential requirement of CAAX-mediated posttranslational processing for Rheb localization and signaling. *Oncogene* 29(3):380-391.
275. Long X, Lin Y, Ortiz-Vega S, Yonezawa K, & Avruch J (2005) Rheb binds and regulates the mTOR kinase. *Current biology : CB* 15(8):702-713.
276. Yu Y, *et al.* (2005) Structural basis for the unique biological function of small GTPase RHEB. *The Journal of biological chemistry* 280(17):17093-17100.
277. Long X, Lin Y, Ortiz-Vega S, Busch S, & Avruch J (2007) The Rheb switch 2 segment is critical for signaling to target of rapamycin complex 1. *The Journal of biological chemistry* 282(25):18542-18551.
278. Mahoney SJ, *et al.* (2018) A small molecule inhibitor of Rheb selectively targets mTORC1 signaling. *Nature communications* 9(1):548.
279. Bonneau A & Parmar N (2012) Effects of RhebL1 silencing on the mTOR pathway. *Molecular biology reports* 39(3):2129-2137.
280. Tee AR, Blenis J, & Proud CG (2005) Analysis of mTOR signaling by the small G-proteins, Rheb and RhebL1. *FEBS letters* 579(21):4763-4768.
281. Im E, *et al.* (2002) Rheb is in a high activation state and inhibits B-Raf kinase in mammalian cells. *Oncogene* 21(41):6356-6365.
282. Mazhab-Jafari MT, *et al.* (2012) An autoinhibited noncanonical mechanism of GTP hydrolysis by Rheb maintains mTORC1 homeostasis. *Structure (London, England : 1993)* 20(9):1528-1539.
283. Zheng M, *et al.* (2015) Rheb phosphorylation is involved in p38-regulated/activated protein kinase-mediated tumor suppression in liver cancer. *Oncology letters* 10(3):1655-1661.
284. Lee MN, *et al.* (2009) Glycolytic flux signals to mTOR through glyceraldehyde-3-phosphate dehydrogenase-mediated regulation of Rheb. *Molecular and cellular biology* 29(14):3991-4001.
285. Buerger C, DeVries B, & Stambolic V (2006) Localization of Rheb to the endomembrane is critical for its signaling function. *Biochemical and biophysical research communications* 344(3):869-880.
286. Basso AD, *et al.* (2005) The farnesyl transferase inhibitor (FTI) SCH66336 (lonafarnib) inhibits Rheb farnesylation and mTOR signaling. Role in FTI enhancement of taxane and tamoxifen anti-tumor activity. *The Journal of biological chemistry* 280(35):31101-31108.
287. Ding H, *et al.* (2014) Farnesyltransferase inhibitor tipifarnib inhibits Rheb prenylation and stabilizes Bax in acute myelogenous leukemia cells. *Haematologica* 99(1):60-69.
288. Zhang Y, *et al.* (2003) Rheb is a direct target of the tuberous sclerosis tumour suppressor proteins. *Nature cell biology* 5(6):578-581.

289. Tabancay AP, Jr., *et al.* (2003) Identification of dominant negative mutants of Rheb GTPase and their use to implicate the involvement of human Rheb in the activation of p70S6K. *The Journal of biological chemistry* 278(41):39921-39930.
290. Patel PH, *et al.* (2003) Drosophila Rheb GTPase is required for cell cycle progression and cell growth. *Journal of cell science* 116(Pt 17):3601-3610.
291. Campbell TB, Basu S, Hangoc G, Tao W, & Broxmeyer HE (2009) Overexpression of Rheb2 enhances mouse hematopoietic progenitor cell growth while impairing stem cell repopulation. *Blood* 114(16):3392-3401.
292. Baker MD, *et al.* (2014) The small GTPase Rheb is required for spermatogenesis but not oogenesis. *Reproduction (Cambridge, England)* 147(5):615-625.
293. Saito K, Araki Y, Kontani K, Nishina H, & Katada T (2005) Novel role of the small GTPase Rheb: its implication in endocytic pathway independent of the activation of mammalian target of rapamycin. *Journal of biochemistry* 137(3):423-430.
294. Yuan J, *et al.* (2005) Identification and characterization of RHEBL1, a novel member of Ras family, which activates transcriptional activities of NF-kappa B. *Molecular biology reports* 32(4):205-214.
295. Masetti R, *et al.* (2013) DHH-RHEBL1 fusion transcript: a novel recurrent feature in the new landscape of pediatric CBFA2T3-GLIS2-positive acute myeloid leukemia. *Oncotarget* 4(10):1712-1720.
296. Martin TD, *et al.* (2014) Ral and Rheb GTPase activating proteins integrate mTOR and GTPase signaling in aging, autophagy, and tumor cell invasion. *Molecular cell* 53(2):209-220.
297. Shirakawa R, *et al.* (2009) Tuberous sclerosis tumor suppressor complex-like complexes act as GTPase-activating proteins for Ral GTPases. *The Journal of biological chemistry* 284(32):21580-21588.
298. Moskalenko S, *et al.* (2003) Ral GTPases regulate exocyst assembly through dual subunit interactions. *The Journal of biological chemistry* 278(51):51743-51748.
299. Wu B & Guo W (2015) The Exocyst at a Glance. *Journal of cell science* 128(16):2957-2964.
300. Heider MR & Munson M (2012) Exorcising the exocyst complex. *Traffic (Copenhagen, Denmark)* 13(7):898-907.
301. Wang H, *et al.* (2010) Phosphorylation of RalB is important for bladder cancer cell growth and metastasis. *Cancer research* 70(21):8760-8769.
302. Martin TD & Der CJ (2012) Differential involvement of RalA and RalB in colorectal cancer. *Small GTPases* 3(2):126-130.
303. Fenwick RB, *et al.* (2009) Solution structure and dynamics of the small GTPase RalB in its active conformation: significance for effector protein binding. *Biochemistry* 48(10):2192-2206.
304. Nicely NI, Kosak J, de Serrano V, & Mattos C (2004) Crystal structures of Ral-GppNHp and Ral-GDP reveal two binding sites that are also present in Ras and Rap. *Structure (London, England : 1993)* 12(11):2025-2036.
305. Shipitsin M & Feig LA (2004) RalA but not RalB enhances polarized delivery of membrane proteins to the basolateral surface of epithelial cells. *Molecular and cellular biology* 24(13):5746-5756.

306. Martin TD, Mitin N, Cox AD, Yeh JJ, & Der CJ (2012) Phosphorylation by protein kinase Calpha regulates RalB small GTPase protein activation, subcellular localization, and effector utilization. *The Journal of biological chemistry* 287(18):14827-14836.
307. Cascone I, *et al.* (2008) Distinct roles of RalA and RalB in the progression of cytokinesis are supported by distinct RalGEFs. *Embo j* 27(18):2375-2387.
308. Xu L, *et al.* (2011) Phospholipase D mediates nutrient input to mammalian target of rapamycin complex 1 (mTORC1). *The Journal of biological chemistry* 286(29):25477-25486.
309. Luo JQ, *et al.* (1998) Functional association between Arf and RalA in active phospholipase D complex. *Proceedings of the National Academy of Sciences of the United States of America* 95(7):3632-3637.
310. Grabiner BC, *et al.* (2014) A diverse array of cancer-associated MTOR mutations are hyperactivating and can predict rapamycin sensitivity. *Cancer discovery* 4(5):554-563.
311. Paul MR, *et al.* (2020) Genomic landscape of metastatic breast cancer identifies preferentially dysregulated pathways and targets. *The Journal of clinical investigation* 130(8):4252-4265.
312. Zhang Y, *et al.* (2017) A Pan-Cancer Proteogenomic Atlas of PI3K/AKT/mTOR Pathway Alterations. *Cancer cell* 31(6):820-832.e823.
313. Zhang HY, Liang F, Jia ZL, Song ST, & Jiang ZF (2013) PTEN mutation, methylation and expression in breast cancer patients. *Oncology letters* 6(1):161-168.
314. García JM, *et al.* (2004) Promoter methylation of the PTEN gene is a common molecular change in breast cancer. *Genes, chromosomes & cancer* 41(2):117-124.
315. Li SY, Rong M, Grieu F, & Iacopetta B (2006) PIK3CA mutations in breast cancer are associated with poor outcome. *Breast cancer research and treatment* 96(1):91-95.
316. Lerman MI & Minna JD (2000) The 630-kb lung cancer homozygous deletion region on human chromosome 3p21.3: identification and evaluation of the resident candidate tumor suppressor genes. The International Lung Cancer Chromosome 3p21.3 Tumor Suppressor Gene Consortium. *Cancer research* 60(21):6116-6133.
317. Li J, *et al.* (2004) Functional characterization of the candidate tumor suppressor gene NPRL2/G21 located in 3p21.3C. *Cancer research* 64(18):6438-6443.
318. Seng TJ, *et al.* (2005) Complex chromosome 22 rearrangements in astrocytic tumors identified using microsatellite and chromosome 22 tile path array analysis. *Genes, chromosomes & cancer* 43(2):181-193.
319. Vanhaesebroeck B, Guillermet-Guibert J, Graupera M, & Bilanges B (2010) The emerging mechanisms of isoform-specific PI3K signalling. *Nature reviews. Molecular cell biology* 11(5):329-341.
320. Folkes AJ, *et al.* (2008) The identification of 2-(1H-indazol-4-yl)-6-(4-methanesulfonyl-piperazin-1-ylmethyl)-4-morpholin-4-yl-thieno[3,2-d]pyrimidine (GDC-0941) as a potent, selective, orally bioavailable inhibitor of class I PI3 kinase for the treatment of cancer. *Journal of medicinal chemistry* 51(18):5522-5532.
321. Krop IE, *et al.* (2016) Pictilisib for oestrogen receptor-positive, aromatase inhibitor-resistant, advanced or metastatic breast cancer (FERGI): a randomised, double-blind, placebo-controlled, phase 2 trial. *The Lancet. Oncology* 17(6):811-821.
322. Hanker AB, *et al.* (2013) Mutant PIK3CA accelerates HER2-driven transgenic mammary tumors and induces resistance to combinations of anti-HER2 therapies. *Proceedings of the National Academy of Sciences of the United States of America* 110(35):14372-14377.

323. Fritsch C, *et al.* (2014) Characterization of the novel and specific PI3Kα inhibitor NVP-BYL719 and development of the patient stratification strategy for clinical trials. *Molecular cancer therapeutics* 13(5):1117-1129.
324. André F, *et al.* (2019) Alpelisib for PIK3CA-Mutated, Hormone Receptor-Positive Advanced Breast Cancer. *The New England journal of medicine* 380(20):1929-1940.
325. Xing Y, *et al.* (2019) Phase II trial of AKT inhibitor MK-2206 in patients with advanced breast cancer who have tumors with PIK3CA or AKT mutations, and/or PTEN loss/PTEN mutation. *Breast cancer research : BCR* 21(1):78.
326. Lega IC, *et al.* (2013) Association between metformin therapy and mortality after breast cancer: a population-based study. *Diabetes care* 36(10):3018-3026.
327. Sonnenblick A, *et al.* (2017) Impact of Diabetes, Insulin, and Metformin Use on the Outcome of Patients With Human Epidermal Growth Factor Receptor 2-Positive Primary Breast Cancer: Analysis From the ALTTO Phase III Randomized Trial. *Journal of clinical oncology : official journal of the American Society of Clinical Oncology* 35(13):1421-1429.
328. Bailey CJ & Turner RC (1996) Metformin. *The New England journal of medicine* 334(9):574-579.
329. Pernicova I & Korbonits M (2014) Metformin--mode of action and clinical implications for diabetes and cancer. *Nature reviews. Endocrinology* 10(3):143-156.
330. Dowling RJ, Zakikhani M, Fantus IG, Pollak M, & Sonenberg N (2007) Metformin inhibits mammalian target of rapamycin-dependent translation initiation in breast cancer cells. *Cancer research* 67(22):10804-10812.
331. Wu L, *et al.* (2016) An Ancient, Unified Mechanism for Metformin Growth Inhibition in C. elegans and Cancer. *Cell* 167(7):1705-1718.e1713.
332. Liang J, Choi J, & Clardy J (1999) Refined structure of the FKBP12-rapamycin-FRB ternary complex at 2.2 A resolution. *Acta crystallographica. Section D, Biological crystallography* 55(Pt 4):736-744.
333. Lee SY, *et al.* (2016) Proximity-Directed Labeling Reveals a New Rapamycin-Induced Heterodimer of FKBP25 and FRB in Live Cells. *ACS central science* 2(8):506-516.
334. Baselga J, *et al.* (2012) Everolimus in postmenopausal hormone-receptor-positive advanced breast cancer. *The New England journal of medicine* 366(6):520-529.
335. Yardley DA, *et al.* (2013) Everolimus plus exemestane in postmenopausal patients with HR(+) breast cancer: BOLERO-2 final progression-free survival analysis. *Advances in therapy* 30(10):870-884.
336. Wagle N, *et al.* (2014) Activating mTOR mutations in a patient with an extraordinary response on a phase I trial of everolimus and pazopanib. *Cancer discovery* 4(5):546-553.
337. Iyer G, *et al.* (2012) Genome sequencing identifies a basis for everolimus sensitivity. *Science (New York, N.Y.)* 338(6104):221.
338. Feldman ME, *et al.* (2009) Active-site inhibitors of mTOR target rapamycin-resistant outputs of mTORC1 and mTORC2. *PLoS biology* 7(2):e38.
339. Meric-Bernstam F & Gonzalez-Angulo AM (2009) Targeting the mTOR signaling network for cancer therapy. *Journal of clinical oncology : official journal of the American Society of Clinical Oncology* 27(13):2278-2287.
340. Li T, *et al.* (2010) WJD008, a dual phosphatidylinositol 3-kinase (PI3K)/mammalian target of rapamycin inhibitor, prevents PI3K signaling and inhibits the proliferation of

transformed cells with oncogenic PI3K mutant. *The Journal of pharmacology and experimental therapeutics* 334(3):830-838.
341. Mazzoletti M, *et al.* (2011) Combination of PI3K/mTOR inhibitors: antitumor activity and molecular correlates. *Cancer research* 71(13):4573-4584.
342. Sekiyama N, *et al.* (2015) Molecular mechanism of the dual activity of 4EGI-1: Dissociating eIF4G from eIF4E but stabilizing the binding of unphosphorylated 4E-BP1. *Proceedings of the National Academy of Sciences of the United States of America* 112(30):E4036-4045.
343. Coleman LJ, *et al.* (2009) Combined analysis of eIF4E and 4E-binding protein expression predicts breast cancer survival and estimates eIF4E activity. *British journal of cancer* 100(9):1393-1399.
344. Kentsis A, Topisirovic I, Culjkovic B, Shao L, & Borden KL (2004) Ribavirin suppresses eIF4E-mediated oncogenic transformation by physical mimicry of the 7-methyl guanosine mRNA cap. *Proceedings of the National Academy of Sciences of the United States of America* 101(52):18105-18110.
345. Moerke NJ, *et al.* (2007) Small-molecule inhibition of the interaction between the translation initiation factors eIF4E and eIF4G. *Cell* 128(2):257-267.
346. Assouline S, *et al.* (2009) Molecular targeting of the oncogene eIF4E in acute myeloid leukemia (AML): a proof-of-principle clinical trial with ribavirin. *Blood* 114(2):257-260.
347. Cencic R, *et al.* (2011) Reversing chemoresistance by small molecule inhibition of the translation initiation complex eIF4F. *Proceedings of the National Academy of Sciences of the United States of America* 108(3):1046-1051.
348. Fan S, Li Y, Yue P, Khuri FR, & Sun SY (2010) The eIF4E/eIF4G interaction inhibitor 4EGI-1 augments TRAIL-mediated apoptosis through c-FLIP Down-regulation and DR5 induction independent of inhibition of cap-dependent protein translation. *Neoplasia (New York, N.Y.)* 12(4):346-356.
349. Bordeleau ME, *et al.* (2008) Therapeutic suppression of translation initiation modulates chemosensitivity in a mouse lymphoma model. *The Journal of clinical investigation* 118(7):2651-2660.
350. Bordeleau ME, *et al.* (2005) Stimulation of mammalian translation initiation factor eIF4A activity by a small molecule inhibitor of eukaryotic translation. *Proceedings of the National Academy of Sciences of the United States of America* 102(30):10460-10465.
351. Chan K, *et al.* (2019) eIF4A supports an oncogenic translation program in pancreatic ductal adenocarcinoma. *Nature communications* 10(1):5151.
352. Webb TE, Davies M, Maher J, & Sarker D (2020) The eIF4A inhibitor silvestrol sensitizes T-47D ductal breast carcinoma cells to external-beam radiotherapy. *Clinical and translational radiation oncology* 24:123-126.
353. Cencic R, *et al.* (2009) Antitumor activity and mechanism of action of the cyclopenta[b]benzofuran, silvestrol. *PloS one* 4(4):e5223.

Chapter 2: Rheb1-independent Activation of mTORC1 in Mammary Tumors Occurs through Activating Mutations in mTOR

2.1 Premise

mTORC1 hyperactivation is commonly observed within tumours pertaining to the HER2-positive breast cancers. At the time of this study, the contribution of mTORC1 function during the transition from pre-neoplastic mammary epithelia into transformed cells remained unexplored. To address this, we genetically deleted the upstream obligate activator Rheb1 within an ErbB2-driven and a PyV mT-driven mouse model of breast cancer to examine the effects of mTORC1 inhibition on mammary tumor initiation. Concomitantly, we also interrogated the state of mTORC1 regulation within the mammary tumours that ultimately developed, in attempts to identify any compensatory mechanisms of mTORC1 activation in the absence of $^{Rheb1.}$

2.2 Abstract

Mechanistic Target of Rapamycin Complex 1 (mTORC1) is a master modulator of cellular growth, and its aberrant regulation is recurrently documented within breast cancer. While the small GTPase Rheb1 is the canonical activator of mTORC1, Rheb1-independent mechanisms of mTORC1 activation have also been reported but have not been fully understood**.** Employing multiple transgenic mouse models of breast cancer, we report that ablation of Rheb1 significantly impedes mammary tumorigenesis. In the absence of Rheb1, a block in tumor initiation can be overcome by multiple independent mutations in *Mtor* to allow Rheb1-independent re-activation of mTORC1. We further demonstrate that the mTOR kinase is indispensable for tumor initiation as the genetic ablation of mTOR abolishes mammary tumorigenesis. Collectively, our findings demonstrate that mTORC1 activation is indispensable for mammary tumor initiation, and that tumours acquire alternative mechanisms of mTORC1 activation.

2.3 Introduction

Mammary tumorigenesis is a multistep evolutionary process involving the selection for genetic or epigenetic alternations that allow the pre-neoplastic epithelial cell population to subvert barriers to uncontrolled growth and survival, correlating within progression through a series of pathologic stages (1-4). The multistep evolutionary nature of mammary tumor initiation is closely recapitulated by genetically engineered mouse models (GEMMs) of breast cancer (5). For example, mammary-specific expression of the oncogenic receptor tyrosine ErbB2 or the Polyomavirus Middle T antigen (PyV mT) is sufficient to drive tumorigenesis through a series of pre-malignant stages that culminate in the formation of metastatic mammary tumors (6-9). However, despite intensive efforts to elucidate the molecular events crucial for mammary tumor initiation (10-12), many of the underlying mechanisms remain undefined.

The mechanistic Target of Rapamycin (mTOR) is a serine/threonine protein kinase that frequently undergoes aberrant activation in cancer (13). mTOR can form two multi-protein complexes, mTORC1 and mTORC2, which regulate distinct molecular processes (14). Specific functions of mTORC1 include stimulation of protein synthesis through phosphorylation of p70 S6 Kinases 1 and 2, and the eukaryotic initiation factor 4E-binding protein (4E-BP1-3) (15-17), whereas mTORC2 is best known for its role in regulation of the Akt family of kinases (18). Although regulation of mTORC2 is not well understood, mTORC1 is activated in response to diverse extracellular and intracellular stimuli including growth factors and amino acids (19). A critical mechanism by which these factors control mTORC1 involves the activation of the small GTPase Rheb1 (20). The Tuberous Sclerosis complex (TSC1/2), composed of TSC1 (hamartin) and TSC2 (tuberin) (21), functions as the GTPase-activating protein (GAP) that governs Rheb1 function by converting active GTP-bound Rheb1 into its inactive GDP-bound form (22, 23). The GAP activity of TSC1/2 is disabled by phosphorylation of TSC2 through PI3K-Akt (24), and ERK1/2-MAPK signaling pathways (25), allowing for de-repression of Rheb1 and activation of mTORC1 (21, 26). Although mTORC1 plays a prominent role in the growth of established tumors cells (27), its role in mammary tumor initiation has not been explored.

Herein, we report that Rheb1-mediated mTORC1 activation plays a crucial role in the initiation of mammary tumorigenesis in both an ErbB2 and Luminal B GEMM of breast cancer. Our data further indicate that in a subset of Rheb1-deficient mammary tumors, oncogenic mTORC1 activation occurs through mutations within the mTOR kinase. In contrast to ablation of Rheb1, abrogation of mTOR resulted in a complete block in mammary tumorigenesis. Collectively, our data suggest that the mTOR kinase is a critical signaling node required for mammary tumor initiation

2.4 Results

Mammary Ablation of Rheb1 Delays Mammary Tumorigenesis. To evaluate the involvement of mTORC1 signaling in mammary tumor initiation, we used mammary epithelial-specific conditional gene targeting to delete the upstream activator Rheb1 in two GEMMs representative of the ErbB2-positive and Luminal B breast cancer subtype (28). To explore the role of Rheb1 in ErbB2-positive breast cancer, mice carrying the loxP-flanked *Rheb1* allele ($Rheb1^{fl/fl}$) were crossed with a strain expressing bicistronic transgene containing activated ErbB2 and Cre recombinase linked by an internal ribosome entry sequence (IRES) under the transcriptional control of the Mouse Mammary Tumor Virus long terminal repeat (MMTV-LTR) (referred to as NIC) (9). This strategy couples the overexpression of ErbB2 with mammary-specific excision of the conditional knockout *Rheb1* allele within the $Rheb1^{fl/fl}$ NIC mice **(Fig 2.1A)**. Mammary deletion of Rheb1 significantly delayed ErbB2-driven mammary tumorigenesis in the $Rheb1^{fl/fl}$ NIC strain (TD_{50} = 375 days) compared to wildtype controls (TD_{50} = 125 days, $p<0.0001$) **(Fig 2.1B)**. Although tumor initiation is fully penetrant in the NIC strain (10, 29), only 60.7% of $Rheb1^{fl/fl}$ NIC mice **(Fig 2.1B)** developed tumors expressing both ErbB2 and Cre. Albeit with a reduced penetrance, ErbB2-positive tumors that do arise are lacking detectable Rheb1 expression **(Fig 2.1D & 2.1F)**. PCR designed to specifically detect the excision of Rheb1 allele **(Suppl Fig 2.2A)** revealed that the Rheb1 allele is excised within the tumor epithelium and retained with the tumor stroma **(Suppl Fig 2.2B & 2.2C)**. Given that defects in mammary gland development can greatly impair tumorigenesis (30), we further examined whether mammary deletion of *Rheb1* produced adverse effects on mammary ductal outgrowth.

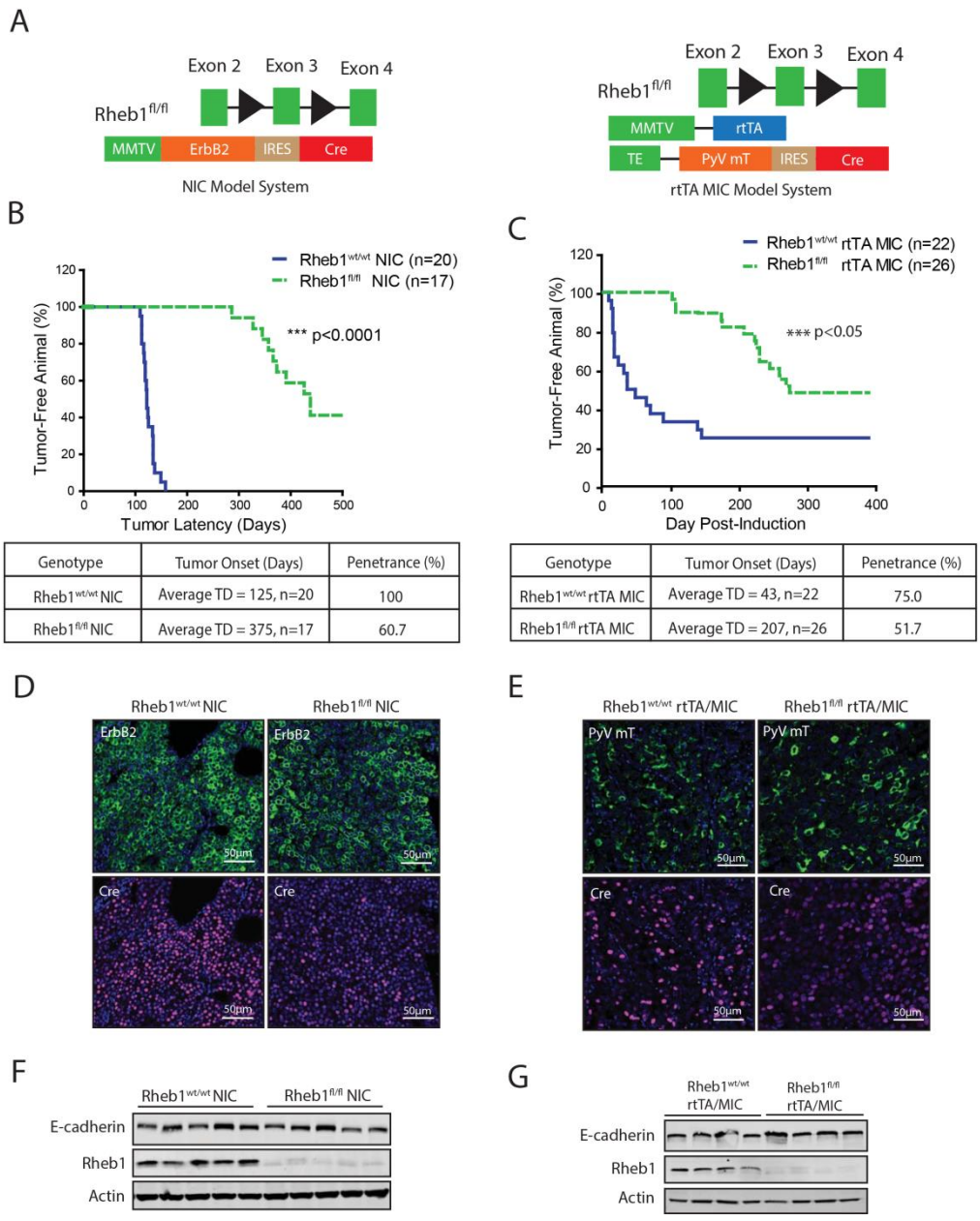

Genotype	Tumor Onset (Days)	Penetrance (%)
Rheb1$^{wt/wt}$ NIC	Average TD = 125, n=20	100
Rheb1$^{fl/fl}$ NIC	Average TD = 375, n=17	60.7

Genotype	Tumor Onset (Days)	Penetrance (%)
Rheb1$^{wt/wt}$ rtTA MIC	Average TD = 43, n=22	75.0
Rheb1$^{fl/fl}$ rtTA MIC	Average TD = 207, n=26	51.7

Figure 2. 1 Mammary Deletion of Rheb1 Delays Mammary Tumorigenesis. (A) Left: Schematic representation of the MMTV-driven activated ErbB2 transgenic mice (NIC strain) and the loxP-site flanked *Rheb1* allele. Right: Schematic representation of the Doxycycline-inducible MMTV-rtTA PyV mT transgenic mice (MIC strain), and the loxP-site flanked *Rheb1* allele. MMTV, Murine mammary tumor virus. IRES, Internal ribosomal entry site. TE, Tetracycline-responsive operator. rtTA, reverse tet-responsive transactivator. (B) Kaplan-Meier plot illustrating percentage of tumor-free Rheb1$^{wt/wt}$

NIC (n=20), and Rheb1$^{fl/fl}$ NIC mice (n=17). The p-values were calculated using a Mantel-Cox Test. (C) Kaplan-Meier plot illustrating percentage of tumor-free Rheb1$^{wt/wt}$ MIC (n=22), and Rheb1$^{fl/fl}$ MIC mice (n=26). The p-values were calculated using a Mantel-Cox Test. (D) Immunofluorescence staining of Rheb1$^{wt/wt}$ NIC and Rheb1$^{fl/fl}$ NIC tumor sections for ErbB2 and Cre. Scale bar represents 50μm. (E) Immunofluorescence staining of Rheb1$^{wt/wt}$ MIC and Rheb1$^{fl/fl}$ MIC tumor sections for PyV mT and Cre. Scale bar represents 50μm. (F) Western blot analysis of Rheb1$^{wt/wt}$ NIC and Rheb1$^{fl/fl}$ NIC tumor protein extract with indicated antibodies. (G) Western blot analysis of Rheb1$^{wt/wt}$ MIC, and Rheb1$^{fl/fl}$ MIC tumors protein extract with indicated antibodies.

Analysis of whole-mounted mammary glands of 7 and 11 week old Rheb1$^{fl/fl}$ MMTV-Cre mice confirmed that Rheb1 was dispensable for early mammary ductal development **(Suppl Fig. 2.3A-2.3C)**. To validate our observations in another GEMM of breast cancer, we crossed the Rheb1$^{fl/fl}$ mice with a doxycycline (Dox)-inducible PyV mT-IRES-Cre transgenic system (MIC strain) (31) which also closely recapitulate human breast cancer progression through defined pre-malignant stages, culminating in aggressive, metastatic disease (6) **(Fig 2.1A)**. To standardize the initial mammary epithelial content prior to oncogene expression, Rheb1$^{fl/fl}$ and Rheb1$^{wt/wt}$ MIC mice were placed under Dox induction at 8 weeks of age. As observed with the ErbB2-driven tumor model system, mammary deletion of Rheb1 also delayed mammary tumorigenesis in Rheb1$^{fl/fl}$ MIC mice (TD_{50} = 220 days) compared to their wildtype counterparts (TD_{50} = 60 days, $p<0.05$) **(Fig 2.1C)**. Despite this initial defect in tumor induction, mammary tumors ultimately do develop within the Rheb1$^{fl/fl}$ MIC strain albeit with reduced overall tumor penetrance (55%) compared to the wild-type control (75%) **(Fig 2.1C)**. Like the ErbB2 model system, mammary tumors arising within the Rheb1$^{fl/fl}$ MIC strain lacked detectable Rheb1 expression **(Fig 2.1G)** while maintaining expression of the PyV mT oncogene and Cre **(Fig 2.1E)**. Collectively, these results argue that ablation of Rheb1 elicits a significant delay in tumor onset in both ErbB2- and PyV mT-driven mammary tumorigenesis. However, a proportion of the Rheb1-deficient mammary epithelium

evolves mechanisms that permit tumor formation in the absence of Rheb1 in GEMMS representative of both ErbB2-amplified and luminal B breast cancer.

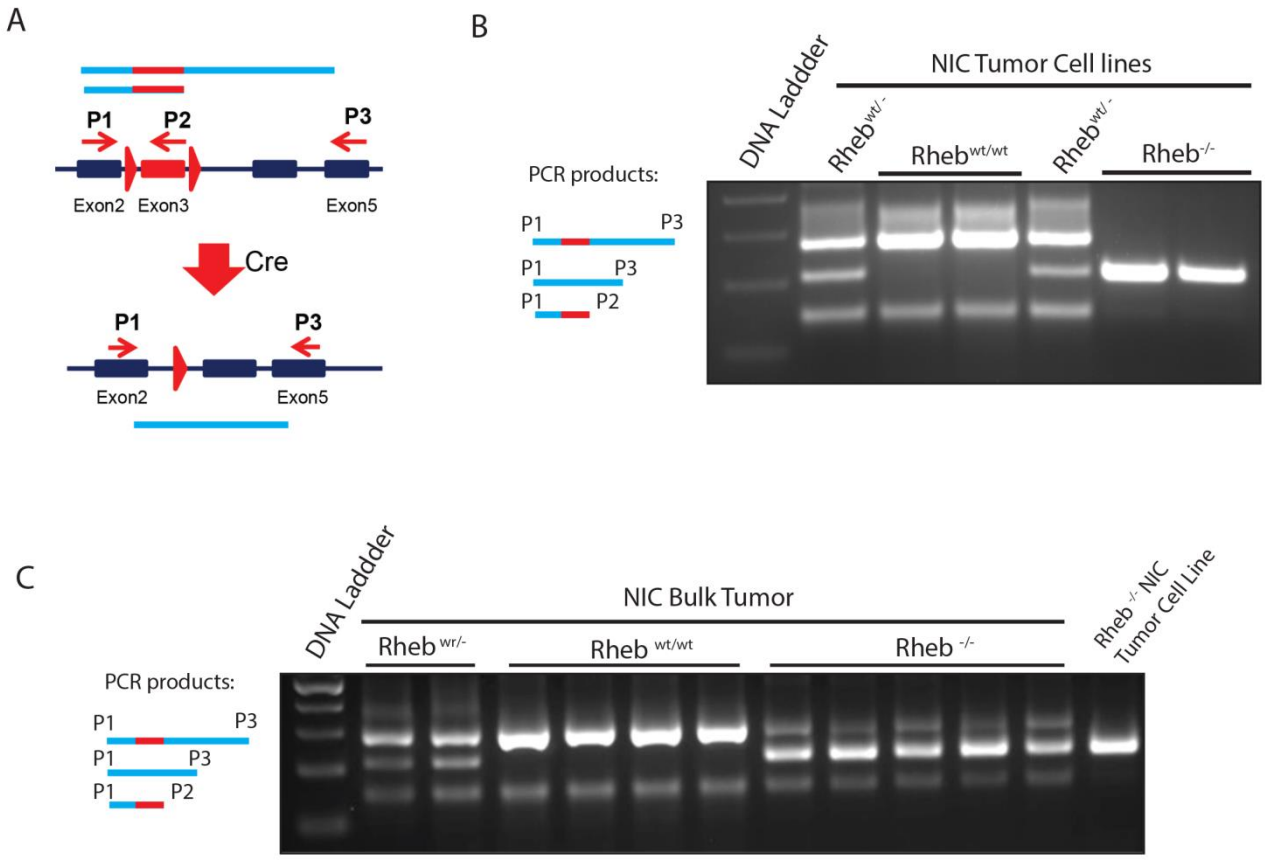

Figure 2. 2 Rheb1 NIC Tumors cells exhibit excision of Rheb1 allele. (A) Cartoon schematic depicting the conditional Rheb1 allele knockout strategy, and excision PCR detection strategy. Excision of the Rheb1 allele decreases the size of the top band (primer 1 and primer 3) while causing the lower band to disappear (primer 1 and primer 2). (B) Agarose gel showing excision detection PCR on cDNA collected from isolated Rheb1 $^{wt/fl}$ NIC, Rheb1$^{wt/wt}$ NIC and Rheb1$^{fl/fl}$ NIC tumor cells. (C) Agarose gel showing excision detection PCR on cDNA collected from Rheb1 $^{wt/fl}$ NIC, Rheb1$^{wt/wt}$ NIC and Rheb1$^{fl/fl}$ NIC bulk tumors and a Rheb1$^{fl/fl}$ NIC tumor cell line.

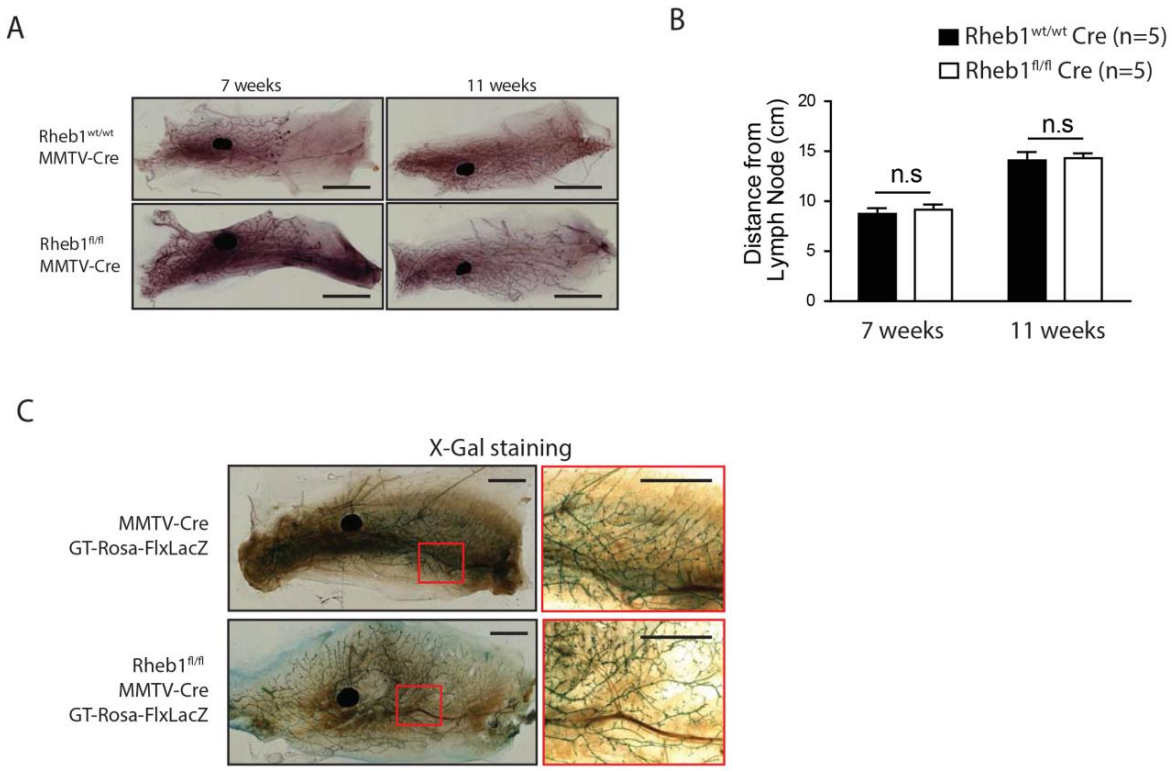

Figure 2. 3 Rheb1 is Dispensable for Mammary Ductal Outgrowth. (A) Representative whole mounts of mammary glands from 7 week and 11 week old Rheb1$^{wt/wt}$ MMTV-Cre and Rheb1$^{fl/fl}$ MMTV-Cre mice stained with Hematoxylin. Scale bar represents 1 cm. (B) Quantification of mammary ductal outgrowth in 7 week and 11 week-old Rheb1$^{wt/wt}$ MMTV-Cre and Rheb1$^{fl/fl}$ MMTV-Cre mice. Ductal outgrowth is represented as distance from leading terminal end bud to midpoint of the lymph node in the right No.4 mammary gland. Values represent mean (+/- SEM) of 5 mice per genotype at indicated timepoints. Statistical significance was assessed via two-tailed unpaired student's *t*-test. (C) Representative X-gal-stained whole mounts of Rheb1$^{wt/wt}$ Rosa26R-FlxSTOP LacZ MMTV-Cre and Rheb1$^{fl/fl}$ Rosa26R-FlxSTOP LacZ MMTV-Cre mice. Scale bar represents 500 μm. Right panel represents 35X magnification of boxed area.

Rheb1 function is required at the early stages of mammary tumor progression.

One important advantage of the Dox-inducible MIC model system **(Fig 2.1A)** is that it grants temporal control of PyV mT oncogene expression thereby allowing for interrogation of early pre-malignant stages of mammary tumorigenesis. As such, we evaluated the immediate effects of Rheb1 ablation on the early stages of mammary tumorigenesis by examining the mammary glands of Rheb1$^{fl/fl}$ MIC mice following 4 and 14 days of Dox induction. In contrast to rapid expansion of epithelial content, and induction of mammary epithelial hyperplasias and adenomas observed within Rheb1$^{wt/wt}$ MIC mice, mammary ablation of Rheb1 within Rheb1$^{fl/fl}$ MIC mice resulted in normal mammary ducts with scarce mammary hyperplasias **(Fig 2.4A & 2.4B)**. The block in mammary tumor progression as a result of Rheb1 ablation was also observed as early as four days post-induction, where early mammary hyperplasias were observed in the Rheb1$^{wt/wt}$ MIC mice **(Fig 2.4A)**. Consistent with the significant delay in tumor onset observed in Rheb1$^{fl/fl}$ MIC mice; these results indicate that Rheb1 is required at an early stage of mammary tumor induction.

To confirm that this early block in mammary tumor progression was also occurring within the ErbB2 model system, we performed histological analysis of mammary glands of at 120-125 day old Rheb1$^{wt/wt}$ NIC and Rheb1$^{fl/fl}$ NIC mice and examined for early hyperplasia and adenomas. While mammary glands of control mice at early time points exhibited signs of hyperplasia, and small pre-malignant lesions (**Fig 2.4C; black arrows**); we failed to detect any histological evidence of transformation in the absence of $^{Rheb1.}$ To determine which particular pathological stage tumor progression was stalled at following loss of Rheb1, we examined the frequencies of different types of lesions within adjacent mammary tissue from Rheb1$^{fl/fl}$ NIC and Rheb1$^{wt/wt}$ NIC mice at tumor endpoint. Under these conditions, we noted a wide range of pathology types including hyperplasias (4.4%), adenomas (5.8%), and even early carcinomas (2.5%) in wild-type control mice **(Fig. 2.4D)**, whereas in Rheb1$^{fl/fl}$ NIC mammary glands exhibited a normal histological appearance, with the rare instance of early hyperplasia (0.8%).Taken together, these observations along with the tumor onset data argues that Rheb1 plays a critical role in the initiation phase of tumor progression in both ErbB2- and PyV mT-driven GEMMS.

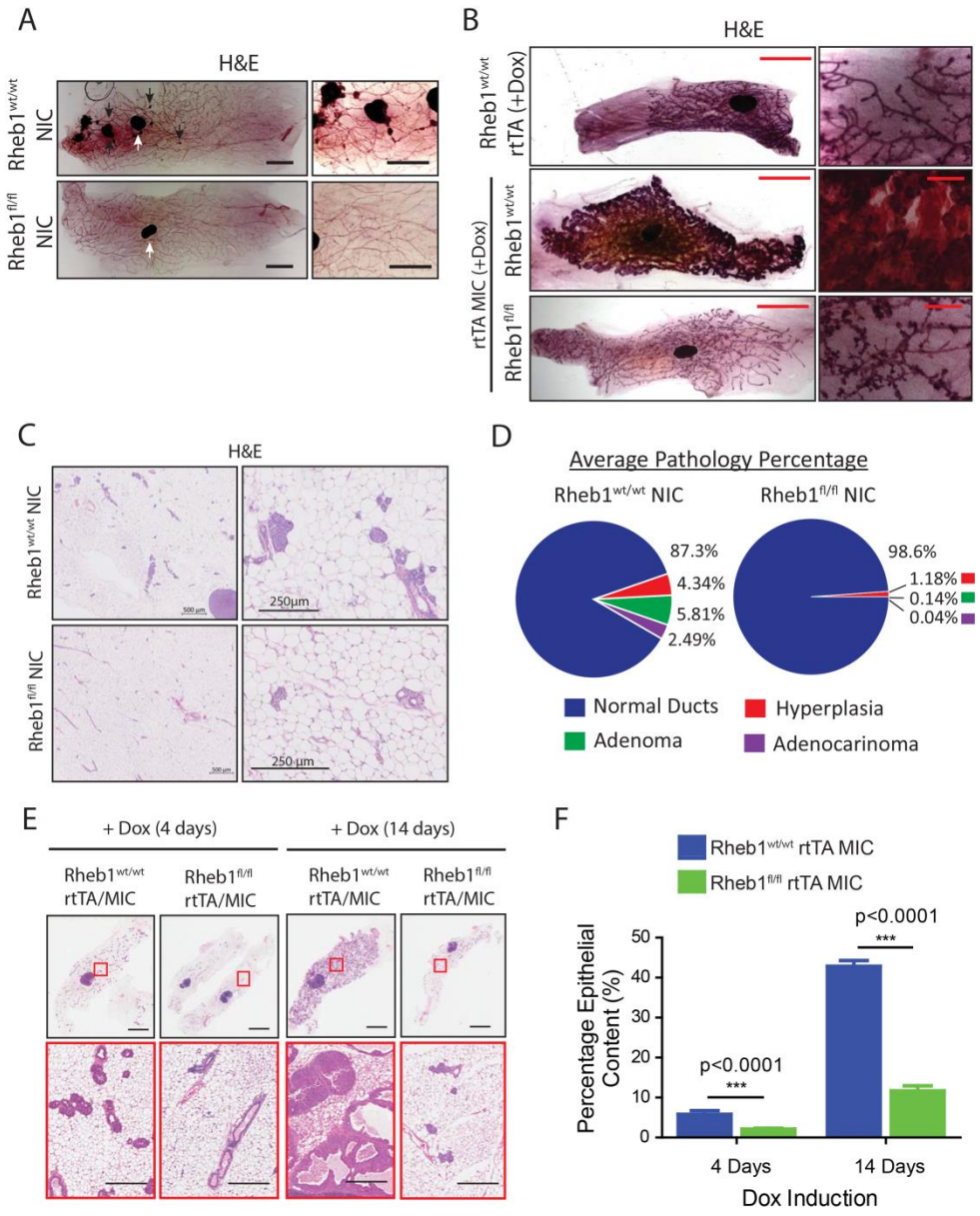

Figure 2.4 Ablation of Rheb1 Stalls Mammary Tumorigenesis at Early Stages of Progression. (A) Top: Representative H&E-stained histological sections of mammary glands collected from Rheb1$^{wt/wt}$ MIC and Rheb1$^{fl/fl}$ MIC mice following 4 days, or 14 days of Doxycycline induction. Scale bar represents 2mm. Bottom: panel is a 35X representation of area boxed in red in top panel. Scale bar represents 200 µm. (B) Top: Representative Immunohistofluorescence staining for E-Cadherin. Lymph node encircled by dash lines. Scale bars represent 100 µm. Bottom: Quantification of E-Cadherin IHC staining of mammary glands of Rheb1$^{wt/wt}$ MIC and Rheb1$^{fl/fl}$ MIC mice following 4-day or 14-day doxycycline administration. Values represent mean (+/- SEM) of 5 mice per

genotype at indicated timepoints. Statistical significance was assessed by two-tailed unpaired Student's *t*-test. (C) Left: Representative hematoxylin-stained whole mounts of mammary glands collected from Rheb1$^{wt/wt}$ NIC and Rheb1$^{fl/fl}$ NIC mice at 130 days of age. Scale bar represents 500 µm. Right: Panel is 35X magnification of left panel. Scale bar represents 100 µm. (D) Top: Representative H&E-stained mammary gland sections of Rheb1$^{wt/wt}$ NIC and Rheb1$^{fl/fl}$ NIC mice collected at tumor endpoint. Right panel is magnification of left panel. Scale bars represent 500 µm. Bottom: Quantification of pathology types found in the mammary glands collected from Rheb1$^{wt/wt}$ NIC (n=17) and Rheb1$^{fl/fl}$ NIC (n=20) mice at tumor endpoint. Frequency of normal ducts, Hyperplasia, Adenoma, and Adenocarcinomas is relative to total number of ductal structures per histology section, and values represents mean from at least 5 biological replicates per genotype.

Rheb1-dependent activation of mTORC1 is critical for the initiation phase of mammary tumor progression. While it is well established that Rheb1 is an obligate activator of mTORC1 in various *in vitro* systems (26, 32-34), the relative contribution of Rheb1 in regulating mTORC1 activity within mammary epithelium *in vivo* remains to be established. Since the downstream phosphorylation targets of mTORC1, p70 S6K1 and 4E-BP1 exhibit differential sensitivity to loss of mTORC1 activity (35, 36) we sought to establish the degree of mTORC1 inhibition upon Rheb1 ablation by monitoring the phosphorylation status of these targets. Given that the MMTV promoter of our transgenic models exhibits mosaic activity within the mammary epithelia, it is crucial to identify the epithelium within the mammary ducts that exhibit Rheb1 ablation to accurately discern the effects of gene loss. Using RNA probes to visualize intact and excised Rheb1 transcript **(Fig 2.5A-2.5C)**, we were able to detect an increasing amount of excised Rheb1 transcript **(Fig 2.5D)**, and decreasing amount of intact Rheb1 transcript **(Fig 2.5E)** within the Cre-expressing pre-neoplastic epithelium of Rheb1$^{fl/fl}$ MIC mice thus confirming that Cre expression can serve as an appropriate surrogate for Rheb1 excision. To this end, histological sections of mammary glands from Rheb1$^{fl/fl}$ NIC and Rheb1$^{wt/wt}$ NIC mice were subjected to immunohistochemistry analysis for Cre, phospho-4E-BP1

(S65) and phospho-S6 ribosomal protein (pS6 S240/244), which is a downstream target of S6Ks **(Fig 2.6C; Suppl Fig 2.7C)**. The Cre-positive, and hence ErbB2-expressing, mammary epithelium from

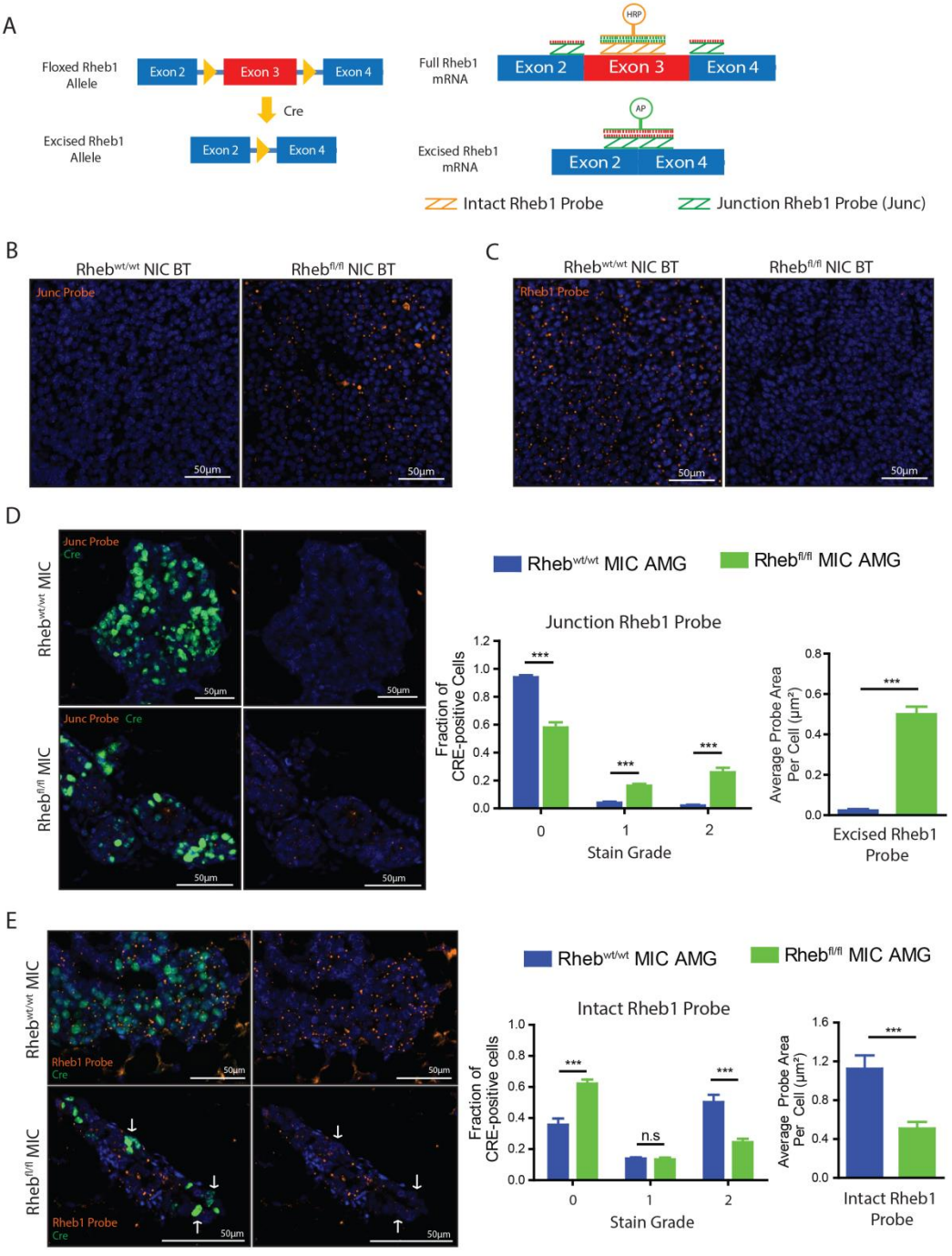

Figure 2.5 Excised Rheb1 Transcript is Enriched within Cre-positive Pre-Neoplastic Mammary Epithelium of Rheb1$^{fl/fl}$ MIC mice. (A) Cartoon schematic illustrating Basescope probe strategy for visualization of intact Rheb1 transcript (Rheb1 Probe) and excised Rheb1 transcript (Junc Probe). (B) Representative Basescope staining of Rheb1$^{wt/wt}$ NIC and Rheb1$^{fl/fl}$ NIC tumors for excised Rheb1 transcripts with the Junc Probe. (C) Representative Basescope staining of Rheb1$^{wt/wt}$ NIC and Rheb1$^{fl/fl}$ NIC tumors for intact Rheb1 transcripts with the Rheb1 Probe. (D) Left: Representative Basescope staining for excised Rheb1 transcript and immunohistochemistry staining for Cre in the mammary glands of Rheb1$^{wt/wt}$ MIC and Rheb1$^{fl/fl}$ MIC mice 2 weeks post-doxycycline induction. Right: Graphs illustrating grade of Junction Rheb1 probe staining, and average abundance of Junction Rheb1 probe within Cre-positive mammary epithelium. Values represents mean (+/- SEM) from at least 150 Cre-positive cells across at least three biological replicates per genotype. Statistical significance was assessed by two-tailed unpaired Student's *t*-test. (E) Left: Representative Basescope staining for intact Rheb1 transcript and immunohistochemistry staining for Cre in the mammary gland of Rheb1$^{wt/wt}$ MIC and Rheb1$^{fl/fl}$ MIC mice 2 weeks post-doxycycline induction. Right: Graphs illustrating grade of Rheb1 staining, and average abundance of Rheb1 probe within Cre-positive mammary epithelium. Values represents mean (+/- SEM) from at least 150 Cre-positive cells across at least three biological replicates.

Rheb1$^{fl/fl}$ NIC mice exhibited decreased levels of both p4E-BP1 and p-rpS6 compared to the Cre-positive mammary epithelium of their wildtype counterparts (**Fig 2.6A and 2.6D; Suppl Fig 2.7A & 2.7D**). Collectively, these results indicate that Rheb1 ablation *in vivo* resulted in loss of both p70 S6 kinase function and 4E-BP1 phosphorylation in the ErbB2-overexpressing mammary epithelium thus indicating an acute loss of mTORC1 activity. Similar observations were also made within the Rheb1$^{fl/fl}$ MIC mammary glands (**Fig 2.6B & 2.6D; Suppl Fig 2.7B & 2.7D**), and raptor$^{fl/fl}$ MIC mammary glands **(Suppl Fig 2.7E & 2.7F)**.

Subsequently, we sought to examine the proliferative capacity of the neoplastic mammary epithelium following ablation of Rheb1 by assessing the levels of the

proliferative marker PCNA **(Suppl Fig 2.8A)**. We observed a decrease in proliferation within the pre-neoplastic mammary epithelium following ablation of Rheb1, which was closely recapitulated with genetic ablation of Raptor **(Suppl Fig 2.8B-2.8C)**. Taken together, these observations argue that mammary ablation of Rheb1-dependent mTORC1 activity elicits an early block in the initiation of the tumorigenic process. While this correlative data implicates mTORC1 as the prominent output of Rheb1 function, we next sought to functionally evaluate contribution of mTORC1 function in the initiation of tumor progression. As such, we next examined if disruption of the mTORC1 scaffold raptor within the mammary epithelium elicits a comparable defect in mammary tumor induction. To address this, a conditional raptor knockout strain (37) was crossed with both the MIC and NIC model systems **(Fig. 2.9A)**.

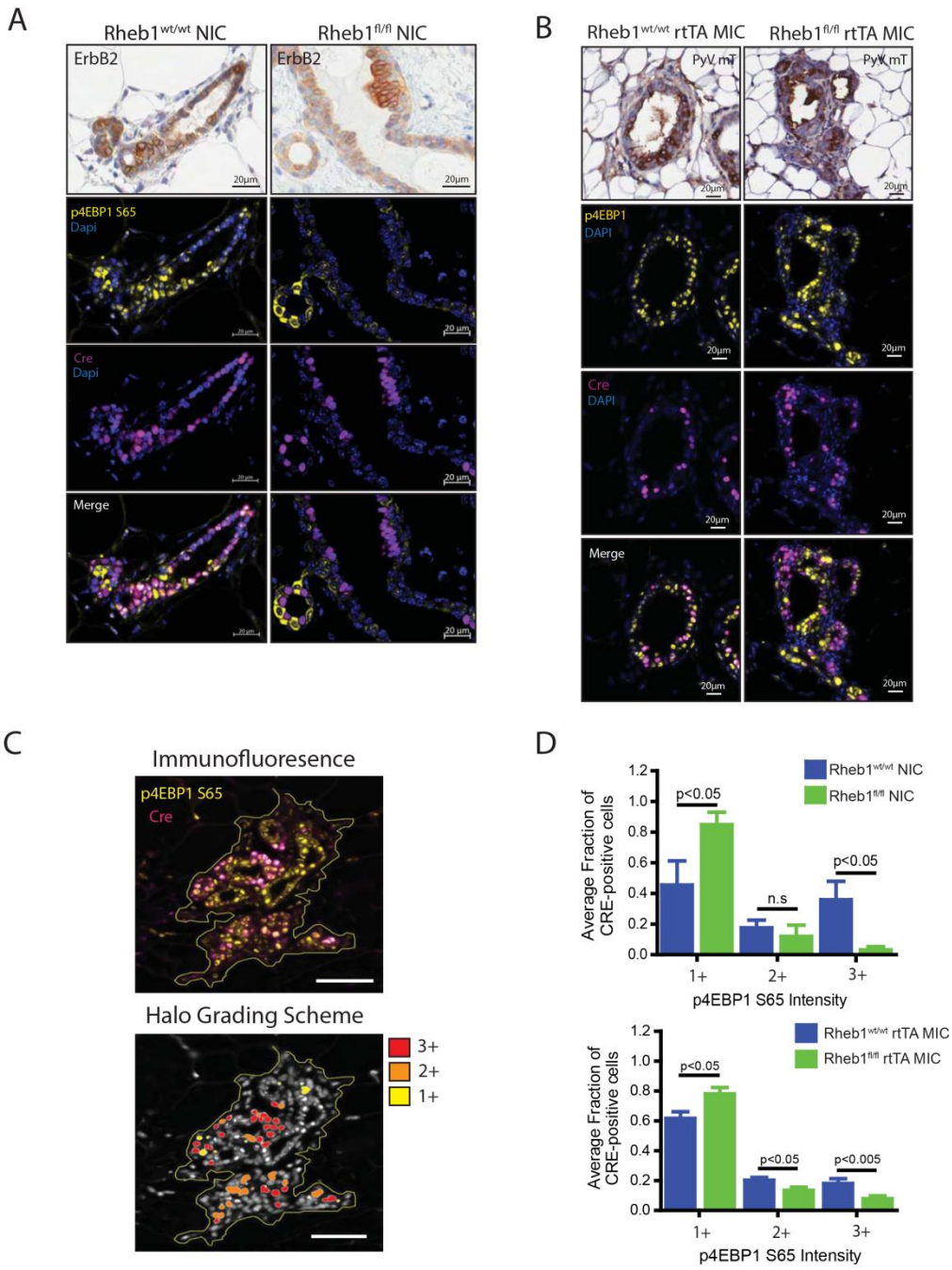

Figure 2. 6 Loss of Rheb1 inhibits ErbB2-mediated 4EBP1 phosphorylation in Mammary Epithelium. (A) Representative images of immunofluorescence and immunohistochemistry staining of mammary ductal structures from Rheb1$^{wt/wt}$ NIC and Rheb1$^{fl/fl}$ NIC mice at tumor endpoint for indicated antibodies. Scale bars represent 20 µm. (B) Representative images of immunohistofluorescence and immunohistochemistry staining of mammary ductal structures from Rheb1$^{wt/wt}$ MIC and Rheb1$^{fl/fl}$ MIC mice

after 14 days of Dox induction for indicated antibodies. Scale bars represent 20 μm. (C) Grading scheme of phospho-4EBP1 S65 IHC staining intensity in Cre-positive mammary epithelium. Scale bar represents 50 μm. (D) Graph depicting frequency of grade 1, 2 and 3 p4EBP1 S65 staining in Cre-positive mammary epithelium in adjacent mammary glands of Rheb1$^{wt/wt}$ NIC and Rheb1$^{fl/fl}$ NIC mice at tumor endpoint (top), and Rheb1$^{wt/wt}$ MIC and Rheb1$^{fl/fl}$ MIC mice after 14 days of Doxycycline induction (bottom). Values represent mean (+/- SEM) frequency of each grade within minimally 150 Cre-positive.

Consistent with our observations with Rheb1 ablation, mammary ablation of raptor within the raptor$^{fl/fl}$ NIC and raptor$^{fl/fl}$ MIC stains exhibited a dramatically delayed tumor onset **(Fig. 2.9B and 2.9C)** which was correlated with a block in the initiation of tumor progression **(Fig. 2.9D-2.9G)**. Collectively, these observations also argue that disruption of mTORC1 through Raptor deletion phenocopies the defect in mammary tumor initiation observed in our Rheb1$^{fl/fl}$ MIC and NIC model systems.

Mammary Tumors Evolve Different Rheb1-independent mechanisms of mTORC1 activation. Although initiation of mammary tumorigenesis is hindered in the absence of Rheb1 **(Fig 2.1F & 2.1G)**, Rheb1-deficient tumors do ultimately develop (**Fig. 2.1F and 2.1G)** which exhibit similar range of pathology and keratin expression profile as wildtype tumors **(Suppl Fig 2.10A)**. *In vivo* growth, as measured by changes in tumor volume, of Rheb1-deficient and Rheb1-proficent NIC tumors was comparable up to 6 weeks after initial tumor palpation **(Suppl Fig 2.10E)**. Similar trends were observed in immunohistochemical analyses of proliferative (Ki67 and PCNA) and apoptotic markers (Cleaved Caspase 3) **(Suppl Fig 2.8D-2.8E & Suppl Fig 2.10B-2.10D)**. Given that we observed loss of p70 S6K1 activity and 4E-BP1 phosphorylation observed in the pre-malignant mammary epithelium of Rheb1$^{fl/fl}$ NIC and Rheb1$^{fl/fl}$ MIC mice **(Fig 2.6A and 2.6B)**, we next examined the phosphorylation of rpS6 and 4E-BP1 in endpoint Rheb1-deficient NIC and MIC tumors. In contrast to the lack of mTORC1 activity in early lesions, the Rheb1-deficient NIC and NIC end-stage tumors exhibited robust

phosphorylation of 4E-BP1 that was comparable to Rheb1-proficient controls **(Fig 2.11A and 2.11B; Suppl Fig. 2.14B & 2.14C)**. However, examination of rpS6 phosphorylation in the Rheb1-deficient NIC and MIC tumors reveals two distinct subsets exhibiting either

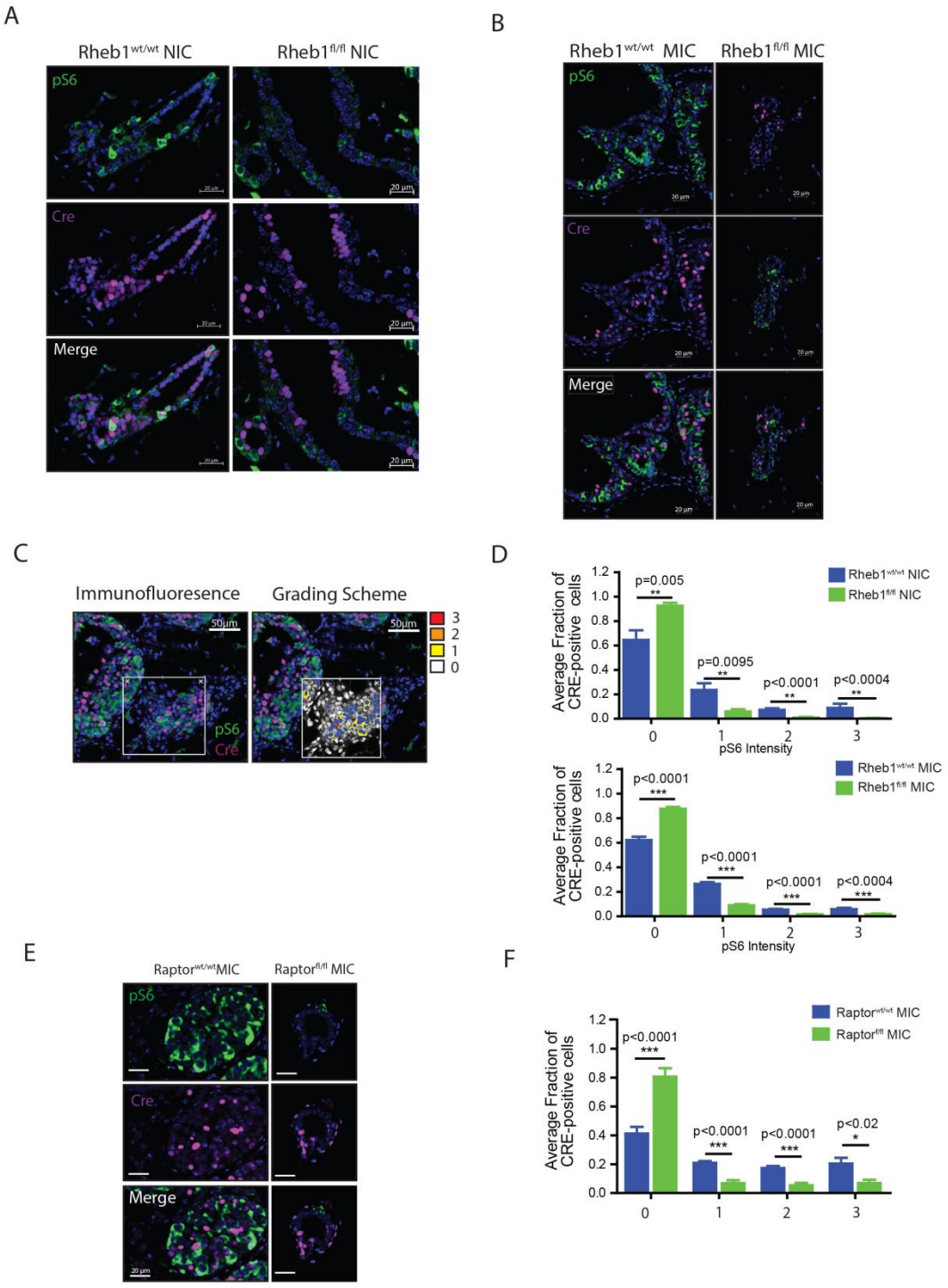

Figure 2. 7 Loss of Rheb1 Inhibits p70 S6K Activity in the Neoplastic Mammary Epithelium. (A) Representative images of Immunohistochemistry staining of mammary ductal structures from Rheb1$^{wt/wt}$ NIC and Rheb1$^{fl/fl}$ NIC mice at tumor endpoint for indicated antibodies. (B) Representative images of Immunohistochemistry staining of

mammary ductal structures from Rheb1$^{wt/wt}$ MIC and Rheb1$^{fl/fl}$ MIC mice after 14 days of doxycycline induction. (C) Grading scheme of phospho-S6 S240/S244 Immunohistochemistry staining intensity in Cre-positive mammary epithelium. (D) Graph depicting frequency of 0, 1, 2 and 3 pS6 S240/S244 staining in Cre-positive mammary epithelium in adjacent mammary glands of Rheb1$^{wt/wt}$ NIC and Rheb1$^{fl/fl}$ NIC mice at tumor endpoint (top), and Rheb1$^{wt/wt}$ MIC and Rheb1$^{fl/fl}$ MIC mice after 14 days of Doxycycline induction (bottom). Values represent mean frequency of each grade from at least 150 Cre-positive cells across at least five biological replicates per genotype. Statistical significance was assessed by two-tailed unpaired Student's *t* test. (E) Representative images of Immunohistochemistry staining of mammary ductal structures from Raptor$^{wt/wt}$ MIC and Raptor$^{fl/fl}$ MIC mice after 14 days of doxycycline induction. (F) Graph depicting frequency of 0, 1, 2 and 3 pS6 S240/S244 staining in Cre-positive mammary epithelium in mammary glands of Raptor$^{wt/wt}$ MIC and Raptor$^{fl/fl}$ MIC mice after 14 days of Doxycycline induction. Values represent mean frequency of each grade from at least 150 Cre positive cells across at least five biological replicates per genotype. Statistical significance was assessed by two-tailed unpaired Student's *t*-test.

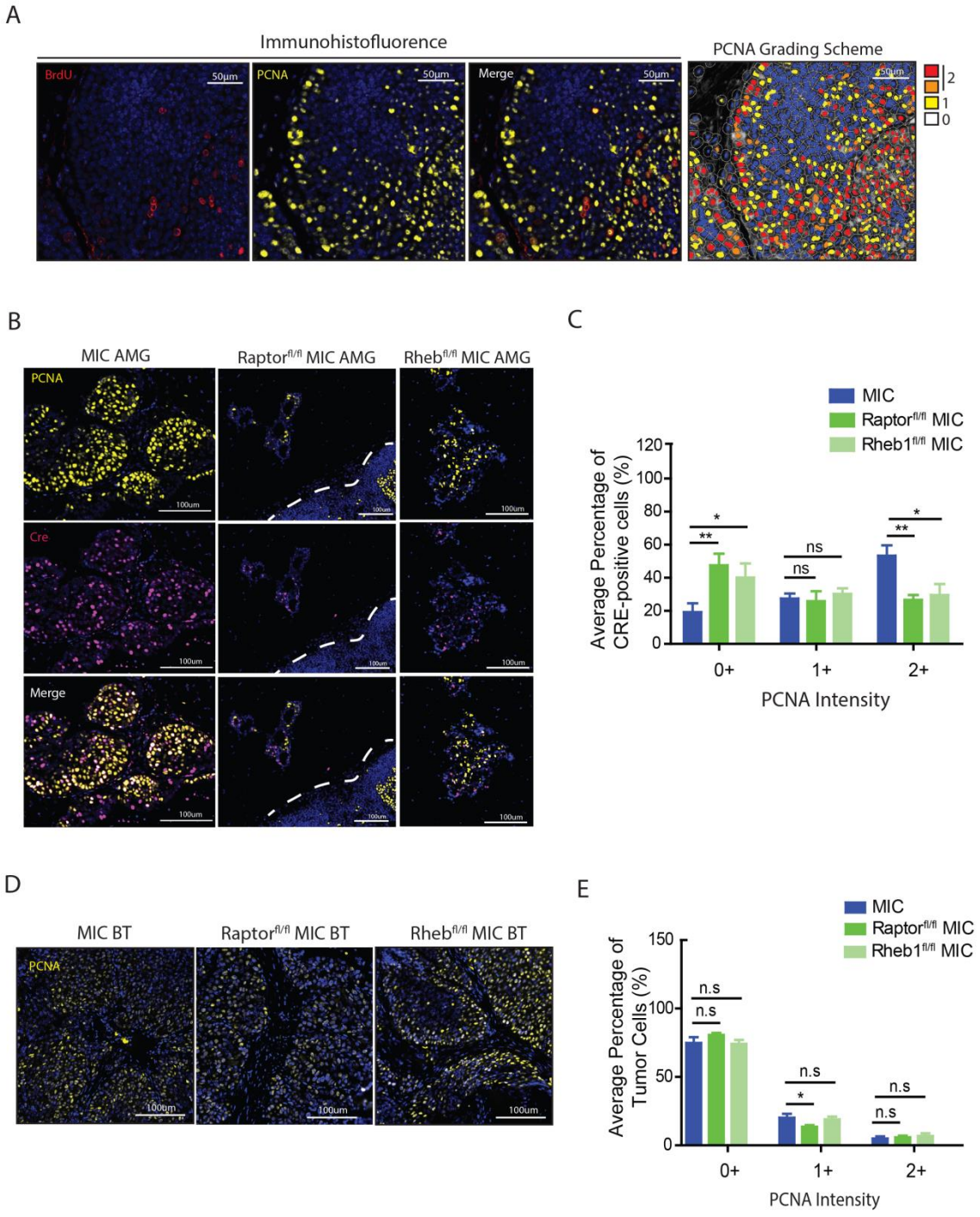

Figure 2. 8 Inhibition of mTORC1 reduces the Proliferative Capacity of the Pre-Neoplastic Mammary Epithelium. (A) Representative images of Immunohistochemistry staining of BrdU and PCNA, along with the grading scheme for PCNA staining intensity in Rheb$^{wt/wt}$ MIC tumor. (B) Representative images of

immunohistochemistry staining of PCNA and Cre in mammary ductal structures from Rheb1$^{wt/wt}$ MIC, Rheb1$^{fl/fl}$ MIC and Raptor$^{fl/fl}$ mice after 14 days of doxycycline induction. (C) Graphs depicting frequency of 0, 1, and 2 grade PCNA staining in Cre-positive mammary epithelium in mammary glands of Rheb1$^{wt/wt}$ MIC, Rheb1$^{fl/fl}$ MIC, and Raptor$^{fl/fl}$ MIC mice after 4 days of doxycycline induction. Values represent mean frequency of each grade from at least 150 Cre-positive cells across five biological replicates per genotype. Statistical significance was assessed by two-tailed unpaired Student's *t*-test. (D) Representative images of immunohistochemistry staining of PCNA wildtype MIC, Rheb1$^{fl/fl}$ MIC and Raptor$^{fl/fl}$ MIC end-stage tumors. (E) Graph depicting frequency of 0, 1, and 2 PCNA staining in tumor cells of wildtype MIC, Rheb1$^{fl/fl}$ MIC and Raptor$^{fl/fl}$ MIC end-stage tumors. Values represent mean frequency of each grade from at least five biological replicates per genotype, and statistical significance was assessed by two-tailed unpaired Student's *t*-test.

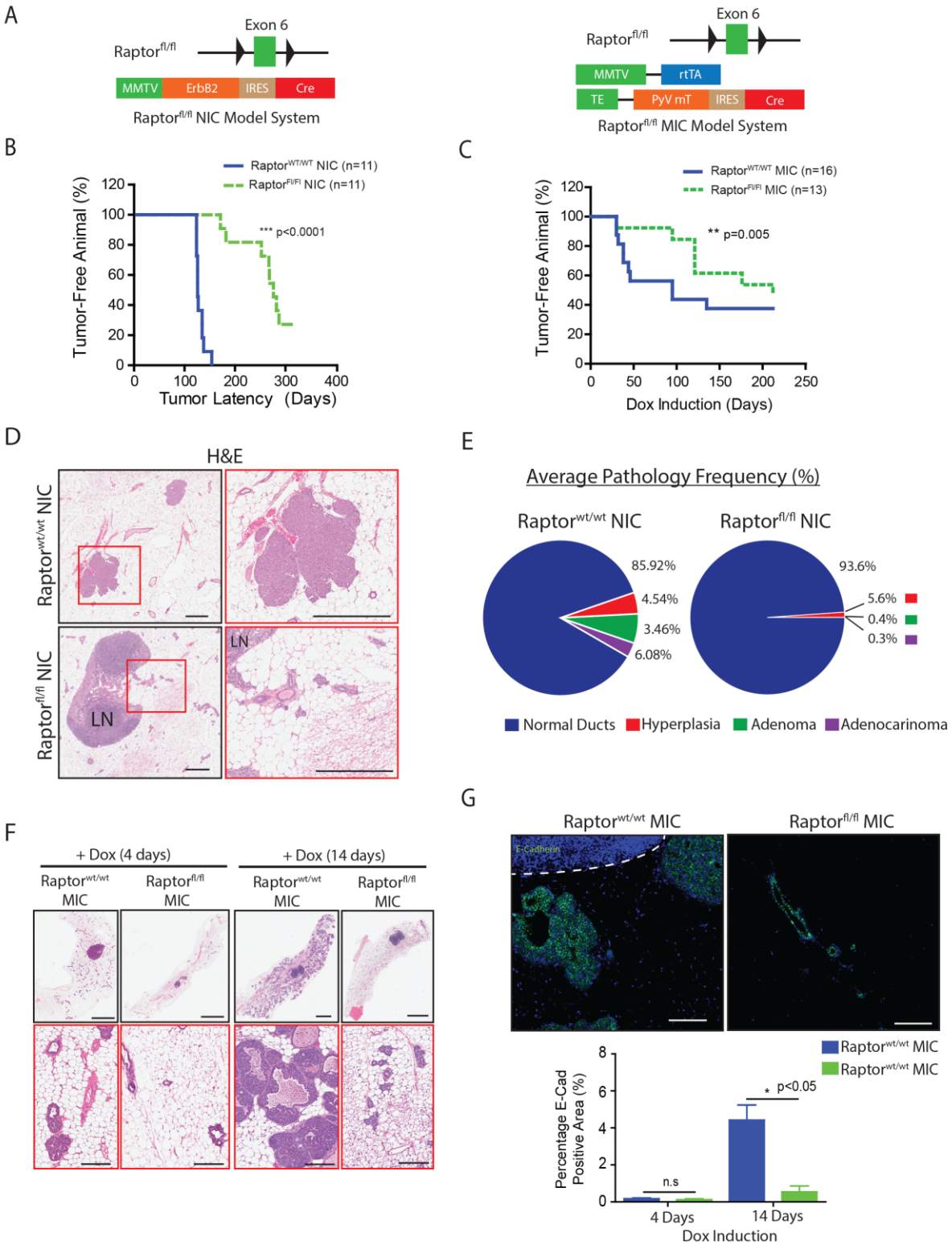

Figure 2. 9 Loss of Raptor Delays Mammary Tumor Initiation. (A) Left: Schematic representation of the MMTV-driven activated ErbB2 transgenic mice (NIC strain) and the loxP-site flanked *Rheb1* allele. Right: Schematic representation of the Doxycycline-

inducible MMTV-rtTA PyV mT transgenic mice (MIC strain), and the loxP-site flanked *Rptor* allele. (B) Kaplan-Meier plot illustrating percentage of tumor-free Raptor$^{wt/wt}$ NIC (n=11), and Raptor$^{fl/fl}$ NIC mice (n=11). The p-values were calculated using a Mantel-Cox Test. (C) Kaplan-Meier plot illustrating percentage of tumor-free Raptor$^{wt/wt}$ MIC (n=16), and Raptor$^{fl/fl}$ MIC mice (n=13). The p-values were calculated using a Mantel-Cox Test. (D) Representative H&E-stained mammary gland sections of Raptor$^{wt/wt}$ NIC and Raptor$^{fl/fl}$ NIC mice collected at tumor endpoint. Right panel is magnification of left panel. Scale bars represent 500 μm. (E) Quantification of pathology types found in the mammary glands collected from Raptor$^{wt/wt}$ NIC (n=17) and Raptor$^{fl/fl}$ NIC (n=20) mice at tumor endpoint. Frequency of normal ducts, Hyperplasia, Adenoma, and Adenocarcinomas is relative to total number of ductal structures per histology section, and values represents mean from at least 5 biological replicates per genotype. (F) Top: Representative H&E-stained histological sections of mammary glands collected from Raptor$^{wt/wt}$ MIC and Raptor$^{fl/fl}$ MIC mice following 4 days, or 14 days of Doxycycline induction. Scale bars represent 2mm. Bottom: 35X representations of area in top panel. Scale bars represent 200 μm. (G) Top: Representative Immunohistochemistry staining for E-Cadherin. Lymph node encircled by dash lines. Scale bars represent 100μm. Bottom: Quantification of E-Cadherin staining of mammary glands of Raptor$^{wt/wt}$ MIC and Raptor$^{fl/fl}$ MIC mice following 4-day or 14-day doxycycline administration. Values represent mean (+/- SEM) of 5 mice per genotype at indicated timepoints. Statistical significance was assessed by two-tailed unpaired Student's *t*-test.

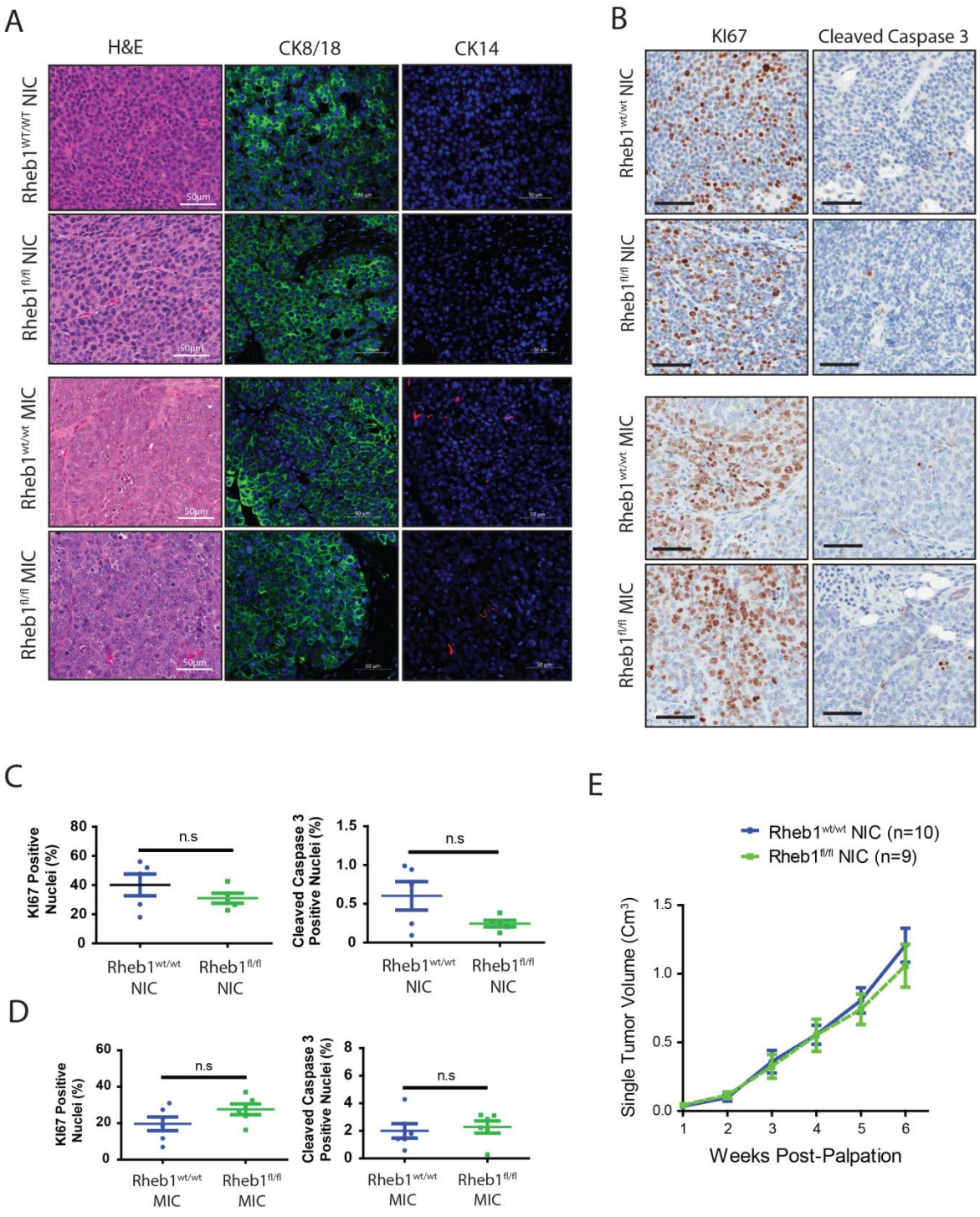

Figure 2. 10 Rheb1$^{wt/wt}$ NIC and Rheb1$^{fl/fl}$ NIC Mammary Tumors Exhibit Comparable Growth. (A) Top: Representative H&E, CK14, and CK8/18 immunohistoflorescence staining of Rheb1$^{wt/wt}$ NIC and Rheb1$^{fl/fl}$ NIC tumors. Bottom:

Representative H&E, CK14, and CK8/18 immunohistochemistry staining of $Rheb1^{wt/wt}$ MIC and $Rheb1^{fl/fl}$ MIC tumors. (B) Top: Representative KI67 and Cleaved Caspase 3 immunohistochemistry staining of $Rheb1^{wt/wt}$ NIC, and $Rheb1^{fl/fl}$ NIC tumors. Bottom: Representative KI67 and Cleaved Caspase 3 immunohistochemistry staining of $Rheb1^{wt/wt}$ MIC, and $Rheb1^{fl/fl}$ MIC tumors. (C) Graphs depicting average percentage KI67 or Cleaved Caspase 3 positive nuclei in end-stage $Rheb1^{wt/wt}$ NIC and $Rheb1^{fl/fl}$ NIC tumors. (D) Graphs depicting average percentage KI67 or Cleaved Caspase 3 positive nuclei in end-stage $Rheb1^{wt/wt}$ MIC and $Rheb1^{fl/fl}$ MIC tumors. Error bars represent SEM and statistical significance was assessed by two-tailed unpaired Student's *t*-test across five biological replicates per genotype. (E) Graph depicting change in volume of single tumor from $Rheb1^{wt/wt}$ NIC (n=10) and $Rheb1^{fl/fl}$ NIC (n=9) mice. Values represents mean tumor volume of single tumor as measured with calliper with error bars representing SEM.

low rpS6 phosphorylation **(Fig 2.11A; lanes 6-11 & Suppl Fig 2.14B; lanes 7-9 & 12)**, or levels of S6 phosphorylation comparable to wildtype NIC or MIC tumors **(Fig 2.11A; lanes 12-14, and Suppl Fig 2.14B; lanes 10-11 and 13-14).**

Since mTORC1 activity can be influenced by insulin stimulation (21), and fluctuations in systemic insulin levels contribute to varying translational rates within tissue (38), we also examined levels of p-rpS6 and p4E-BP1 in four Rheb1-deficient NIC tumor cell lines under constant growth factor conditions. Consistent with our *in vivo* analyses, we observed a similar bifurcation in phospho-rpS6 S240/244 levels among the Rheb1-deficient NIC cell lines thus indicating the cell intrinsic nature of this phenotype **(Fig 2.11C)**. In addition, Rheb1-deficient NIC cells also exhibited levels of p4E-BP1 comparable to Rheb1-proficient NIC cells. Consistent with these observations, global translation monitored by puromycin incorporation and production of puromycin-labelled cyclin D1 and Bcl_{XL}, known to be translated by mTORC1-sensitive mRNAs (39, 40), were also comparable between Rheb1-deficient and proficient NIC cells **(Fig 2.11D & 2.11E)**. Given that other kinases such as CDK1 (41), were reported to phosphorylate 4E-

BP1 independently of mTORC1, we further examined the mTORC1-dependence of 4E-BP1 phosphorylation in these Rheb1-deficient NIC tumors cells. We observed comparable inhibition of 4E-BP1 and rpS6 phosphorylation in both Rheb1-proficient and Rheb1-deficient NIC cells following 48hr treatment with either the rapalog everolimus, or the ATP-competitive mTOR inhibitor torin1 **(Fig 2.11F)**, indicating that 4E-BP1 regulation in Rheb1-deficient NIC cells remained mTORC1 dependent. Similarly,

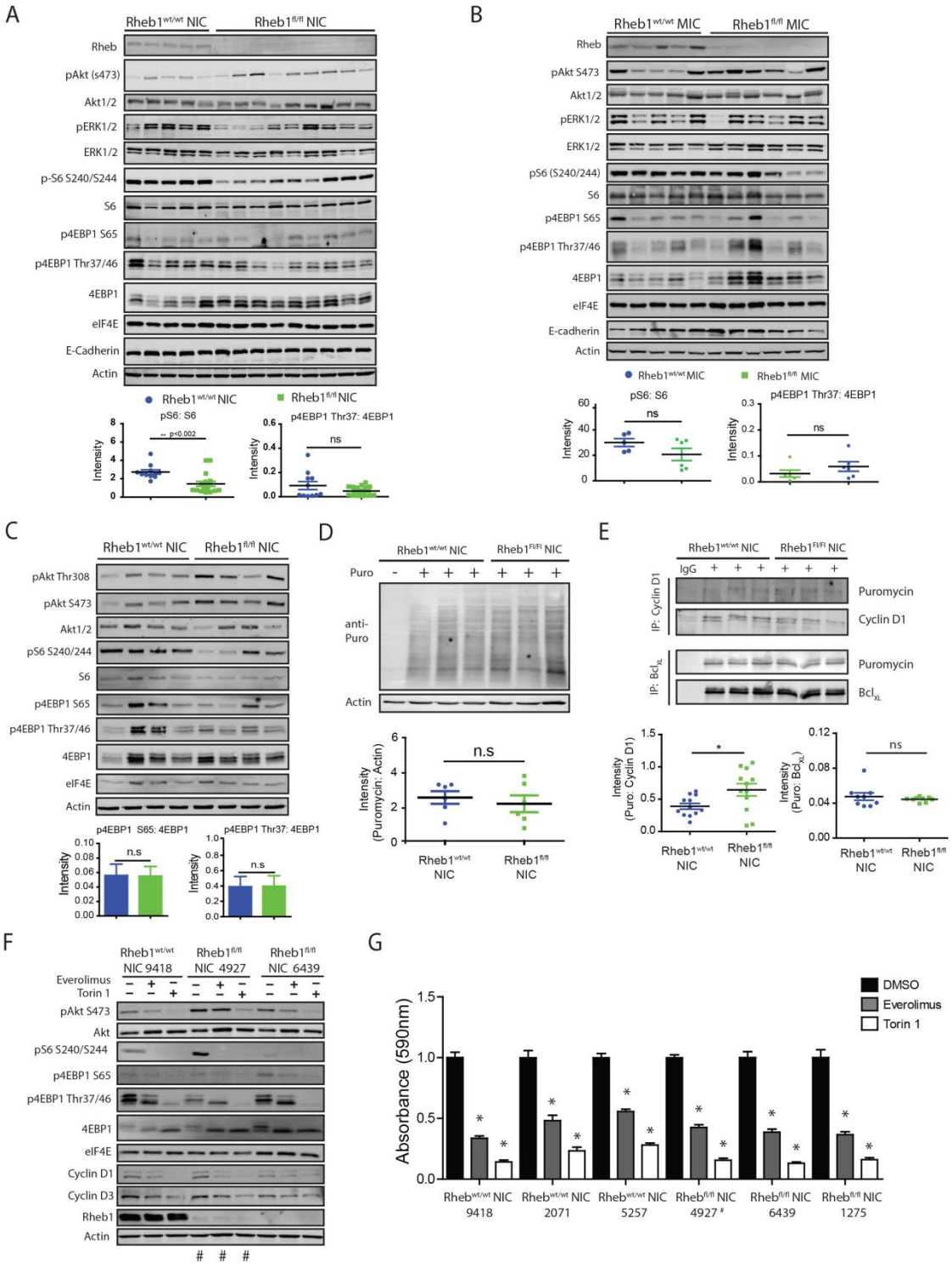

Figure 2. 11 Rheb1-deficient Mammary Tumors Maintain mTORC1 Activation and Function. (A) Immunoblot of protein extracts from end-stage Rheb1$^{wt/wt}$ NIC and Rheb1$^{fl/fl}$ NIC mammary tumors, with antibodies against indicated proteins. Bottom:

Quantification of immunoblots for indicated proteins in (A). Error bars represents SEM (B) Immunoblots of protein extracts from end-stage Rheb1$^{wt/wt}$ MIC and Rheb1$^{fl/fl}$ MIC mammary tumors, with antibodies against indicated proteins. Bottom: Quantification of immunoblots for indicated proteins in (B). (C) Immunoblots of protein extracts from Rheb1$^{wt/wt}$ NIC and Rheb1$^{fl/fl}$ NIC tumors cell lines, with antibodies against indicated proteins. Bottom: Quantification of immunoblots for indicated proteins in (A). (D) Immunoblot showing puromycin incorporation within Rheb1$^{wt/wt}$ NIC and Rheb1$^{fl/fl}$ NIC tumor cell lines. Actin was detected as loading control. Bottom: Graph represents mean level of puromycin incorporation within three Rheb1$^{wt/wt}$ NIC and Rheb1$^{fl/fl}$ NIC tumor cell lines from three independent experiments. (E) Immunoblot showing puromycin labelled Cyclin D1 and Bcl-XL within three Rheb1$^{wt/wt}$ NIC and Rheb1$^{fl/fl}$ NIC tumor cell lines after Cyclin D1 or Bcl-XL immunoprecipitation. Bottom: Graph represents mean level of puromycin-labelled cyclin D1 and Bcl-XL within three Rheb1$^{wt/wt}$ NIC and Rheb1$^{fl/fl}$ NIC tumor cell lines from three independent experiments. * p-value <0.05. Error bars represent SEM, and statistical significance was assessed by two-tailed unpaired Student's *t*-test for blot quantifications (A-E). (F) Immunoblot of Rheb1$^{wt/wt}$ NIC and Rheb1$^{fl/fl}$ NIC tumor cell lysate treated with Everolimus and Torin 1 probed using the antibodies indicated. Data are representative of three independent experiments. Rheb$^{fl/fl}$ NIC cell line carrying mTOR mutation indicated by #. (G) Graph showing cell viability of Rheb1$^{wt/wt}$ NIC and Rheb1$^{fl/fl}$ NIC tumor cells treated with Everolimus, or Torin 1. Values represent mean value (+/- SEM) of three biological replicates per genotype, with eight replicates per each treatment. The growth assay was repeated independently three times. Statistical significance was assessed by two-tailed unpaired Student's *t*-test where * represents p-value <0.05.

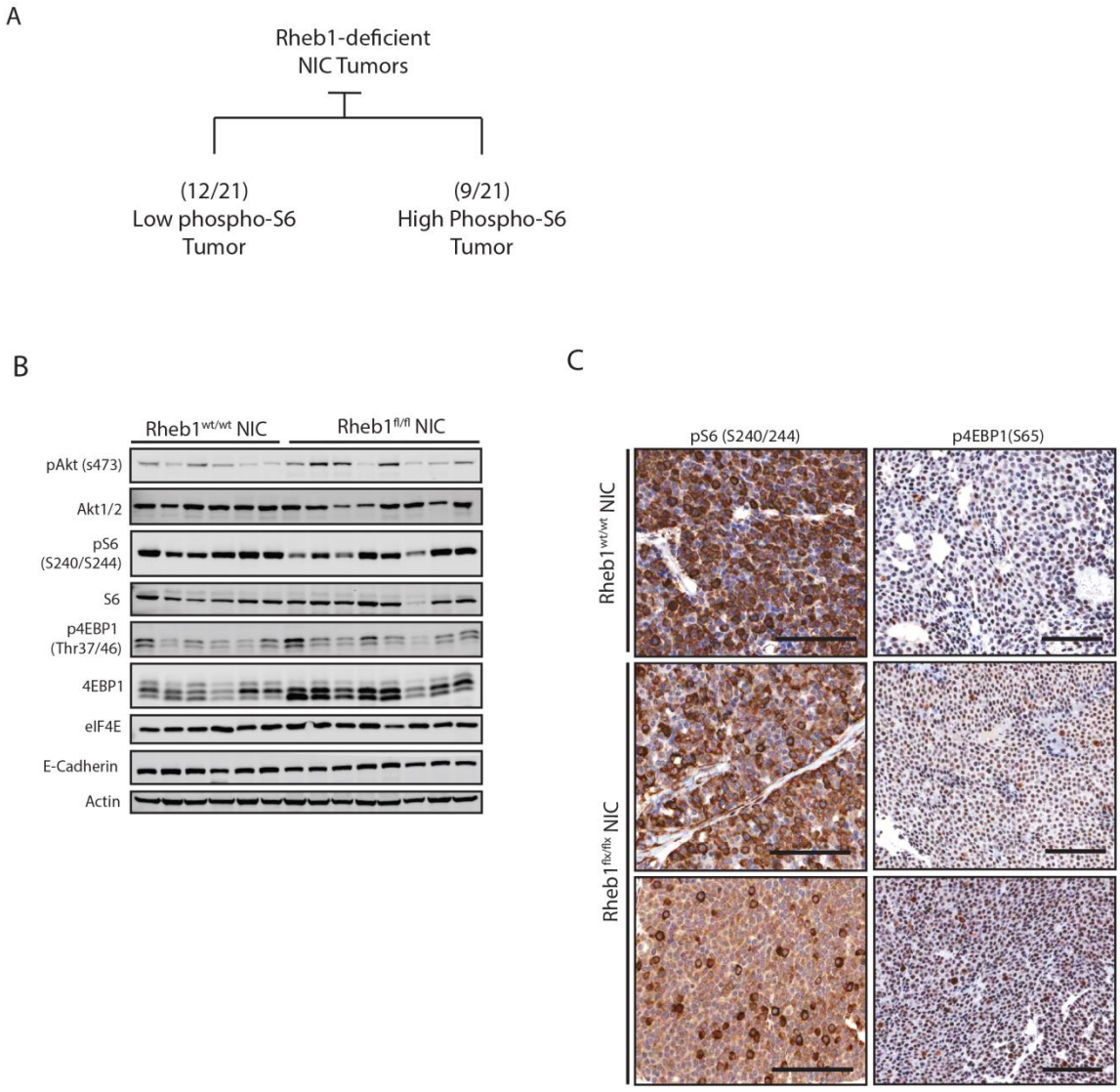

Figure 2. 12 mTORC1 activity in Endstage Rheb1-depleted NIC Mammary Tumors. **(**A) Schematic illustrating stratification of Rheb1-depleted NIC tumors based on levels of phospho-S6 (240/244). 12/21 Rheb1-depleted NIC tumors were stratified into low pS6 subset. 9/21 Rheb-depleted NIC tumors were grouped into high pS6 subset. (B) Western blot analysis of protein extracts from end-stage Rheb1$^{wt/wt}$ NIC and Rheb1$^{fl/fl}$ NIC mammary tumors, with antibodies against indicated proteins. Rheb1$^{fl/fl}$ NIC tumors carrying mTOR mutations depicted by asterisk. (C) Representative pS6 S240/244 and p4EBP1 S65 Immunohistochemistry staining on Rheb1$^{wt/wt}$ NIC and Rheb1$^{fl/fl}$ NIC

mammary tumors. Representative images of high Phospho-S6, and low phospho-S6 Rheb1$^{fl/fl}$ NIC tumor subset are shown.

Activating *MTOR* mutations Occur in Rheb1-Deficient Mammary Tumors. Given that mTORC1 activity is fully restored within a subset of Rheb1-deficient tumors **(Fig 2.11A; Suppl Fig. 2.14B)**, we next sought to determine the underlying Rheb1-independent molecular mechanism of mTORC1 re-activation. Notably Akt S473 phosphorylation, a marker of mTORC2 function (42), was elevated in end-stage Rheb1-deficient NIC tumors compared to their wildtype counterparts. This trend was conserved within the primary Rheb1-deficient NIC tumor cells, and demonstrated mTORC2-dependency as long-term treatment with either everolimus or torin 1 ablated Akt phosphorylation **(Fig 2.11F)**. The elevated mTORC2 function in Rheb1-deficient NIC tumor cells is likely attributable to alleviation of a negative feedback loop involving p70 S6K (43) as most Rheb1-deficient NIC tumors cells have lower p70 S6K activity compared to their wildtype counterpart **(Fig 2.11C)**. Noticeably, two of the Rheb1-deficient NIC cell lines displayed concurrent elevation in mTORC2 activity and restoration of p70 S6K activity as measured by p-rpS6 (S240/244) levels **(Fig 2.11C)**. This phenotype was reminiscent of the effects of activating mutations in *mTOR,* which drive increased basal activity of both mTORC1 and mTORC2 (44). Although it has been shown that mutant TOR supports the growth of Rheb1-null yeast cells (45), this has not previously been examined as a mechanism of compensation for loss of Rheb1 function in mammalian cells. This prompted us to examine the *Mtor* mutational status within a cohort of Rheb1-deficient NIC tumors. The sequencing analysis revealed four different *Mtor* mutations were uncovered in the subset of Rheb1-deficient NIC tumors with comparable rpS6 phosphorylation to wild-type controls while no mutations in *Mtor* were detected in NIC tumors **(Suppl Fig 2.14A)**. Interestingly, the mTOR F1888C mutation was discovered in two independent Rheb1-deficient NIC tumors, and their corresponding cell lines **(Suppl Fig 2.14A)**. Given that the concurrent increase in pAkt (S473), and p-rpS6 (S240/244) was also observed in Rheb1-deficient MIC tumors **(Fig 2.11B)**, the

mutational status of *Mtor* was also examined in the PyV mT-driven tumors. Three additional *Mtor* mutations were discovered in the Rheb1-deficient MIC tumors exhibiting high p-rpS6 (S240/244), while no mutations were detected in either wildtype MIC tumors or Rheb1-deficient MIC tumors exhibiting low p-rpS6 phosphorylation **(Suppl Fig 2.15B)**. Of clinical relevance, many of these mTOR mutations uncovered have been previously reported within human disease **(Fig 2.13B)**. All mTOR mutations uncovered from both transgenic tumor models **(Fig 2.13A)** were shown to confer elevated mTORC1 activity following ectopic expression in 293T cells **(Fig 2.13C)**. These results are consistent with other studies as the mTOR T1977K mutation has been previously reported to confer elevated mTORC1 activity (44, 46, 47). In addition to exhibiting comparable levels of mTORC1 activity as the wildtype counterparts **(Fig 2.13D)**, Rheb1-deficient NIC tumors carrying mTOR mutations also exhibited comparable expression of the mTORC1-sensitive targets cyclin D1 (39), cyclin D3 (48) and Bcl-X_L (40). These observations argue that one of the compensatory mechanisms that restore mTORC1 activity in the absence of the Rheb1 GTPase involves the occurrence of activating mutations within the mTOR kinase. Given that transgenic mammary tumors accumulate multiple molecular alterations along tumor progression, we wondered if mTOR mutations alone were sufficient to elicit Rheb1-independence within our Rheb1-deficient tumor models, or these genetic alterations required additional factors present in our tumor system. While technical challenges limited us from directly re-introducing wildtype mTOR into primary Rheb1-deficient tumor cells carrying mutant mTOR to evaluate the relative contribution of mTOR mutation to mTORC1 reactivation, we examined if expression of mutant mTOR were sufficient to elicit Rheb1-independent mTORC1 activation in 293T cells. To address this, 293T cells were depleted of Rheb1 via siRNA after ectopic expression of either wildtype mTOR or a panel of mutant mTOR uncovered within our Rheb1-deficient mammary tumors. While 293T cells ectopically expressing wildtype mTOR exhibited decreased rpS6 and 4EBP1 phosphorylation following Rheb1 depletion via siRNA, we observed that mTORC1 activity within 293T

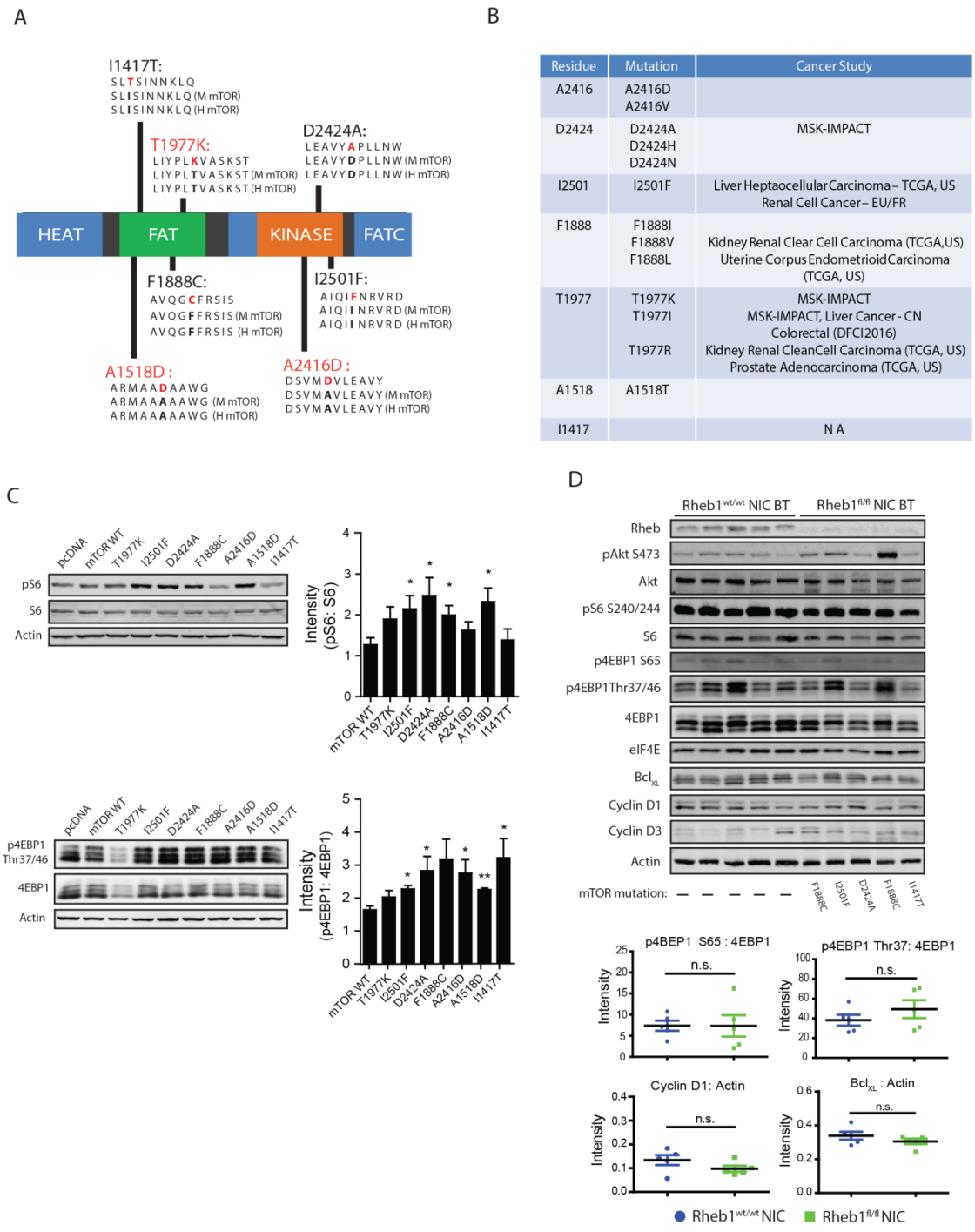

Residue	Mutation	Cancer Study
A2416	A2416D A2416V	
D2424	D2424A D2424H D2424N	MSK-IMPACT
I2501	I2501F	Liver Heptaocellular Carcinoma – TCGA, US Renal Cell Cancer – EU/FR
F1888	F1888I F1888V F1888L	Kidney Renal Clear Cell Carcinoma (TCGA,US) Uterine Corpus Endometrioid Carcinoma (TCGA, US)
T1977	T1977K T1977I T1977R	MSK-IMPACT MSK-IMPACT, Liver Cancer - CN Colorectal (DFCI2016) Kidney Renal CleanCell Carcinoma (TCGA, US) Prostate Adenocarcinoma (TCGA, US)
A1518	A1518T	
I1417		N A

Figure 2. 13 Gain-of-Function *Mtor* Mutations Develop in Subset of Rheb1-deficient Mammary Tumors. (A) Schematic illustrating *MTOR* mutations discovered in Rheb1-deficient NIC (Black) and Rheb1-deficient MIC (Red) mammary tumors along with surrounding amino acids in murine and human mTOR. (B) Table depicting human

mTOR mutations found in cancer patients similar to mTOR mutations uncovered within Rheb1$^{fl/fl}$ MIC and Rheb1$^{fl/fl}$ NIC tumors. (C) Top: Representative Immunoblots of 293T cells expressing either wildtype or mutant mTOR probed with indicated antibodies. Bottom: Graphs of quantification of S6 and 4EBP1 phosphorylation within 293T cells expressing either wildtype or mutant mTOR. Values represent mean (+/-STEM) of three independent experiments. Statistical significance was assessed by two-tailed unpaired student's *t*-test where * represents $p<0.05$. (D) Immunoblot analysis of Rheb1$^{fl/fl}$ NIC tumors carrying mTOR mutations, and Rheb1$^{wt/wt}$ NIC controls with indicated antibodies. Bottom: Quantification of p4EBP1 Thr37, p4EBP1 S65, Cyclin D1, and Bcl-XL from (D). Values represent mean (+/- SEM) where statistical significance was assessed by two-tailed unpaired Student's *t*-test.

cells expressing the mTOR I2501F and I1417T mutations exhibited insensitivity to Rheb1 depletion by siRNA **(Suppl Fig 2.15A)**. Conversely, we observed that 293T cells expressing the mTOR T1977K, F1888C, A2416D, A1518D and D2424A mutations displayed variable sensitivity to Rheb1 depletion **(Suppl Fig 2.15A)**. These results suggest that certain mTOR mutations may confer Rheb1-independent mTORC1 activation which is consistent with previous reports that different mTOR mutations elicit distinct mechanistic functions (46). Furthermore, it is feasible that other mTOR mutations may require the presence of additional factors within the mammary tumor setting to elicit Rheb1-independence, which requires further elucidation in future work. Additionally, given that mTOR mutations were only uncovered within a subset of Rheb1-deficient tumors exhibiting comparable p-rpS6 levels as wildtype controls, the underlying molecular mechanism leading to mTORC1 re-activation within other subsets of Rheb1-deficient tumors may be distinct.

mTOR function is indispensable for ErbB2 mammary tumor induction. Our studies with the Rheb1$^{fl/fl}$ MIC and Rheb1$^{fl/fl}$ NIC strains have demonstrated that mammary tumors ultimately evolve molecular mechanisms to allow mTORC1 re-activation. Despite our observations with the conditional Rheb1 knockout model systems, whether the

mTOR kinase itself is dispensable for mammary tumor progression is unclear. To directly address the contribution of the mTOR kinase in mammary tumor induction, we crossed the conditional mTOR knockout mice ($mTOR^{fl/fl}$ strain) (49) with our NIC strain **(Fig 2.16A)**. In contrast to the conditional Rheb1 knockout GEMMs **(Fig 2.1A)**, mammary ablation of mTOR resulted in the abrogation of tumor formation within the $mTOR^{fl/fl}$ NIC

A

Genotype	mTOR Mutation
Rheb1$^{wt/wt}$ NIC – 1243	No mutation
Rheb1$^{wt/wt}$ NIC – 1473	No mutation
Rheb1$^{wt/wt}$ NIC – 1825	No mutation
Rheb1$^{wt/wt}$ NIC – 901	No mutation
Rheb1$^{wt/wt}$ NIC – 9422	No mutation
Rheb1$^{wt/wt}$ NIC – 4071	No mutation
Rheb1$^{wt/wt}$ NIC – 8966	No mutation
Rheb1$^{wt/wt}$ NIC – 9910	No mutation
Rheb1$^{wt/wt}$ NIC – 9955	No mutation
Rheb1$^{fl/fl}$ NIC – 1062	I2501F
Rheb1$^{fl/fl}$ NIC – 4927	D2424A
Rheb1$^{fl/fl}$ NIC – 2444	I1417T
Rheb1$^{fl/fl}$ NIC – 7052	F1888C
Rheb1$^{fl/fl}$ NIC – 6445	F1888C
Rheb1$^{fl/fl}$ NIC – 1476	No mutation
Rheb1$^{fl/fl}$ NIC – 4928	No mutation
Rheb1$^{fl/fl}$ NIC – 5651A	No mutation
Rheb1$^{fl/fl}$ NIC – 1429	No mutation
Rheb1$^{fl/fl}$ NIC – 2940	No mutation
Rheb1$^{fl/fl}$ NIC – 5565	No mutation

B

Genotype	mTOR Mutation
Rheb1$^{wt/wt}$ MIC – 1489	No mutation
Rheb1$^{wt/wt}$ MIC – 290	No mutation
Rheb1$^{wt/wt}$ MIC – 681	No mutation
Rheb1$^{wt/wt}$ MIC– 780	No mutation
Rheb1$^{wt/wt}$ MIC– 8926	No mutation
Rheb1$^{fl/fl}$ MIC – 8924	A1518D
Rheb1$^{fl/fl}$ MIC – 7546	T1977K
Rheb1$^{fl/fl}$ MIC – 7656	A2416D
Rheb1$^{fl/fl}$ MIC – 7707	No mutation
Rheb1$^{fl/fl}$ MIC – 7712	No mutation
Rheb1$^{fl/fl}$ MIC– 1487	No mutation
Rheb1$^{fl/fl}$ MIC– 7543	No mutation
Rheb1$^{fl/fl}$ MIC– 7729	No mutation
Rheb1$^{fl/fl}$ MIC– 7954	No mutation
Rheb1$^{fl/fl}$ MIC– 8920	No mutation

C

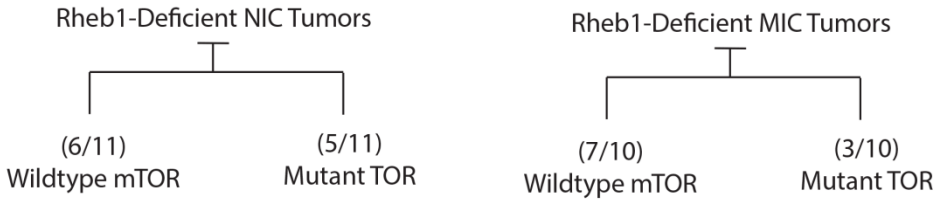

Figure 2. 14 *Mtor* Mutations occur uniquely within Rheb1-deficient Mammary Tumors. (A) Table depicting the mutational status of *Mtor* within a panel of Rheb1$^{wt/wt}$ NIC and Rheb1$^{fl/fl}$ NIC mammary tumors. (B) Table depicting the mutational status of *Mtor* within a panel of Rheb1$^{wt/wt}$ MIC and Rheb1$^{fl/fl}$ MIC mammary tumors. (C)

Hierarchical graph illustrating fraction of Rheb1-deficient NIC and MIC tumors carrying mTOR mutation

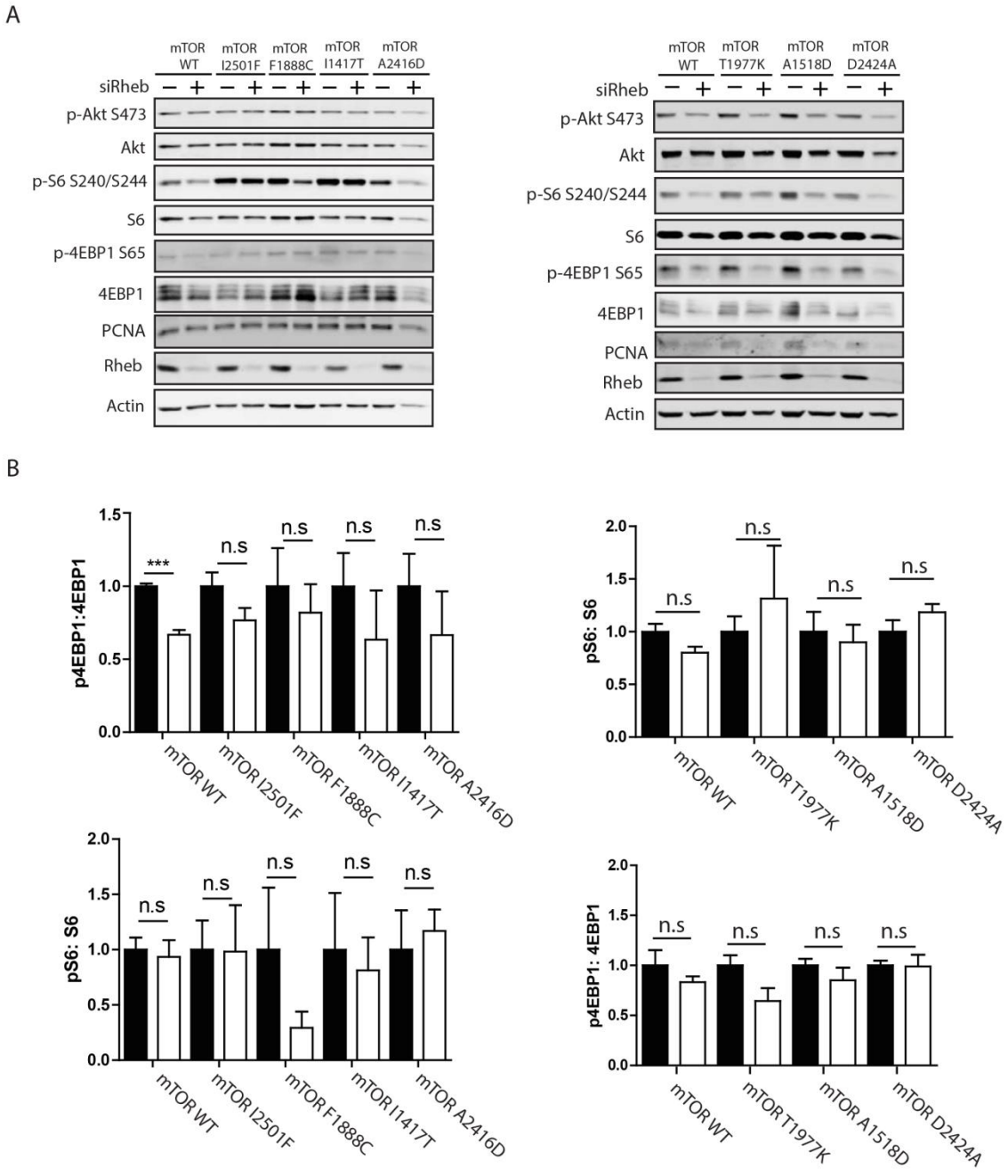

Figure 2. 15 mTOR mutations elicit variable insensitivity to Rheb1 depletion in 293T cells. (A) Representative Immunoblots of cell lysate collected from 293T cells expressing either wildtype mTOR or mutant mTOR following transfection for siRNA for Rheb1, probed with indicated antibodies. (B) Quantification of phospho-4EBP1 S65 and phosphor-S6 from (A). Graph represents average values (+/- SEM) from three

independent experiments, and statistical significance was assessed by two-tailed unpaired student's *t*-test.

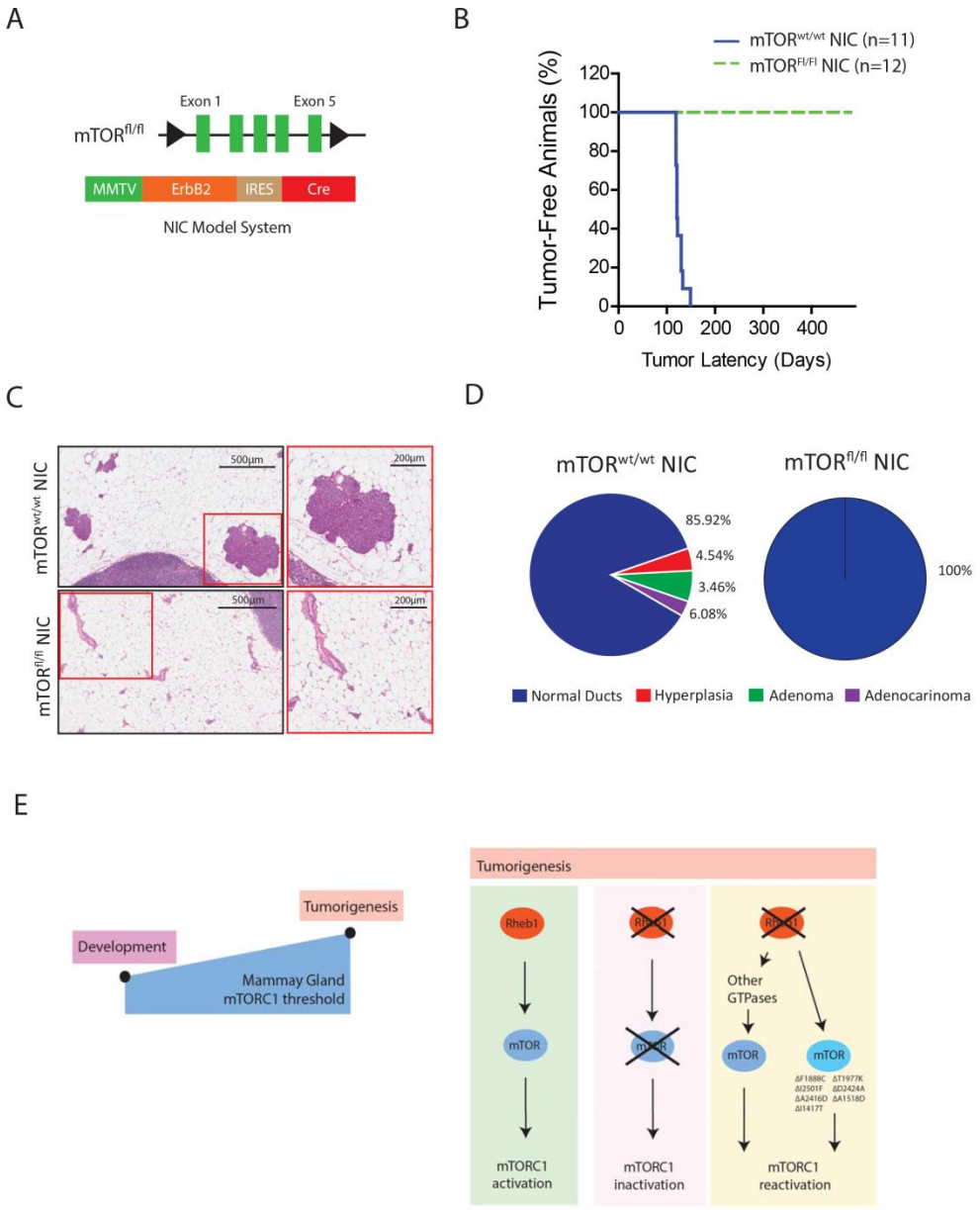

Figure 2. 16 mTOR is Indispensable for Mammary Tumorigenesis. (A) Schematic representation of the MMTV-driven activated ErbB2 transgenic mice (NIC strain) and the loxP-site flanked *Mtor* allele. (B) Kaplan-Meier plot illustrating percentage of tumor-free mTOR$^{wt/wt}$ NIC (n=11), and mTOR$^{fl/fl}$ NIC mice (n=12). (C) Left: Representative

H&E-stained mammary gland sections of mTOR$^{wt/wt}$ NIC and mTOR$^{fl/fl}$ NIC mice collected at tumor endpoint. Scale bar represents 500μm Right: Panel is magnification of left panel. Scale bar represents 200μm. (D) Quantification of pathology types found in the mammary glands collected from mTOR$^{wt/wt}$ NIC (n=17) and mTOR$^{fl/fl}$ NIC (n=11) mice at tumor endpoint. Frequency of normal ducts, Hyperplasia, Adenoma, and Adenocarcinomas is relative to total number of ductal structures per histology section, and values represents mean from at least 5 biological replicates per genotype. (E) Cartoon representation of working model for mTORC1 re-activation in Rheb1-deficient tumors. A high threshold for mTORC1 activity is required for mammary tumorigenesis than normal mammary gland development. In the absence of Rheb1-mediated mTORC1 activation, alternative mechanisms of mTORC1 activation arise within the pre-neoplastic tissue to allow for tumor initiation.

strain within the 1-year observation period **(Fig 2.16B)**. Consistent with the indispensable role of mTOR in mammary tumor formation, histological examination of mammary glands from end-point mTOR$^{fl/fl}$ NIC failed to reveal any evidence of abnormal histology **(Fig 2.16C and 2.16D)**. Altogether, these observations argue that in contrast to Rheb1, the mTOR kinase is an essential signaling node within ErbB2-driven mammary tumor progression.

2.5 Discussion

The adaptive selection of molecular features crucial for tumor cell survival and growth associated with mammary tumor progression, is closely recapitulated within GEMMs of breast cancer (50). Following loss of genes or disruption of processes typically required for tumorigenesis, molecular compensation frequently occurs within the pre-neoplastic mammary epithelium, allowing the adoption of alternative mechanisms of transformation (51-53). We demonstrate using two GEMMs of breast cancer that loss of Rheb1 within the pre-neoplastic mammary epithelium stalls tumor progression at early stages. Although recent *in vitro* evidence indicate that other alternative small GTPases exhibit the capacity to activate mTORC1 (54, 55), mTORC1 function within the pre-

neoplastic mammary epithelium of the *in vivo* models examined here is diminished upon Rheb1 ablation **(Fig. 2.6A & 2.6B)**. Consistent with the importance of Rheb1-dependent mTORC1 activation in the early phase of tumor induction, targeted deletion of Raptor in both MIC and NIC models resulted in a similar delay in the initiation of mammary tumors **(Fig. 2.9A & 2.9C)**. Interestingly, despite the critical role of mTORC1 function during the initial stages of tumor progression with these GEMMS, normal mammary gland development was refractory to Rheb1 ablation. These observations suggest that mTORC1 function may be required at different thresholds within normal and malignant cells. Consistent with this concept, haploid insufficiency in the downstream of mTORC1 signaling eIF4E, had little impact on normal development but resulted in severe impairment of lung tumor progression (56). Given the key role of 4E-BPs in regulating translation of specific mRNAs crucial to oncogenesis such as cyclin D1 and D3 (39, 53), these observations stress the importance of maintaining an oncogenic threshold of translation within tumor cells. While mTORC1-mediated regulation of the 4EBP1-eIF4E axis is disrupted with Rheb1 ablation within these two selected GEMMs, the resultant delay in tumorigenesis may derive from the disruption of additional mTORC1-dependent processes including regulation of autophagy (57), and cell metabolism (58, 59). While not the focus of this study, the relative contribution of these mTORC1-dependent processes to tumor initiation requires further investigation.

Despite the initial delay in tumor initiation observed in the conditional Rheb1 knockout MIC and NIC strains, tumors eventually developed with variable penetrance in both model systems. Biochemical analyses of Rheb1-deficient tumors revealed that they had recovered mTORC1's capacity to phosphorylate downstream target such as S6 kinase and 4E-BP1 **(Fig. 2.11A & 2.11B)**. The Rheb1-deficient tumors originating from both GEMMS exhibited variable levels of rpS6 phosphorylation, while 4E-BP1 phosphorylation was comparable to the wildtype controls. An important facet of the Rheb1-deficient NIC cell lines is that phosphorylation of rpS6 and 4E-BP1 is abrogated by either rapamycin or torin 1 **(Fig 2.11C)**, which indicates a requirement of mTORC1 kinase. While the mTOR mutations L2185A/C, A2034V and F2108L have been reported to confer resistance to mTORC1 and mTOR inhibitors (60-62), the Rheb-deficient NIC

cell line 4927 which carried mutant mTOR still retains sensitivity to mTORC1 inhibition **(Fig. 2.11F)**.

Although mTORC1 function is restored to varying degrees within arising Rheb1-deficient tumors, we did observe restoration of mTORC1 activity to comparable level as wildtype controls within a subset of mammary tumors **(Fig 2.11A & 2.11B)**. The use of GEMMs of breast cancer provided an opportunity to interrogate these processes in a biologically relevant setting. In a proportion of these tumors, restoration of mTORC1 activity was associated with activating mutations within mTOR kinase **(Fig. 2.13A)**. Recent clinical studies have identified mTOR-activating mutations to be associated with therapeutic benefit in both urothelial/bladder cancer and renal cell carcinoma (63, 64). Despite the identification of these mTORC1-hyperactivating mTOR mutations in numerous cancers in the clinical setting (44, 63), their exact mode of action is still unclear (44, 46). Although, mTOR mutations that arise in cells while under the selective pressure of mTORC1 or mTOR inhibitors elicit specialized modes of action in disrupting inhibitor function. In the presence of mTOR ATP-competitive inhibitor AZD8055, mTOR mutations arise in the kinase domain leading to altered kinetic properties of the kinase (62), while mTOR mutations that disrupt binding of the FKBP12 complex arise in cells under Rapalog treatment (60, 62). Additionally, the L2185A mTOR mutation in the ATP-binding pocket has also been demonstrated to confer resistance to mTOR inhibitor AZD8055 (61). Taken together, the mTOR mutations that developed in the absence of Rheb1 in our transgenic system may elicit a specialized mode of action to confer activation. Of clinical relevance, the mTOR mutations discovered from both Rheb1-deficient tumor systems have been previously reported within human malignant disease **(Fig 2.13B)**. Considering the evolutionary nature of tumor progression within GEMMs, these mTOR mutations likely play a compensatory role in the reactivation of mTORC1 in the absence of Rheb1 **(Fig 2.16E)**. While molecular mechanism of Rheb1-mediated mTORC1 activation is lacking, it is well established that activation requires direct interaction between Rheb1 and mTOR (65). Recent structures of Rheb-bound mTORC1 reveal that mTORC1 undergoes a conformational change to adopt a conformation primed for ATP hydrolysis upon binding to Rheb1 (66). Yang et al., also demonstrated that a lower dose of Rheb1 is required for activation of mutant mTORC1 which suggests that

the Rheb1-mTOR complex forms more efficiently in the presence of mutant mTOR. Conceivably, the mTOR mutations discovered within our Rheb1-deficient tumor systems may support a similar conformational change. While Rheb1 is absent within our tumor systems, alternative small GTPases such as RalB GTPases have demonstrated a modest binding capacity to mTOR and increasing RalB-mTOR interaction does elicit more robust mTORC1 activation (54). It is also plausible that acute activation of this or other closely related GTPases may provide an additional compensatory role that allows restoration of mTORC1 function (55). Future studies will focus on establishing the contribution of alternative small GTPases to mTORC1 activation within the reported Rheb1-deficient NIC cell lines**.** Although mammary tumors evolved in the absence of Rheb1, mammary ablation of mTOR within the NIC model resulted in complete abrogation of tumors. These observations indicate that the kinase component of mTORC1, mTOR is indispensable for mammary tumor formation. Using our model systems, we highlight that compensatory mechanisms can occur to allow re-activation of mTORC1 upon deletion of $^{Rheb1.}$ Given the essential role of mTOR in mammary tumorigenesis, future development of mTOR targeted therapeutics may have important clinical implications in treatment and management of breast cancer.

2.6 Experimental Procedure

Experimental Animal Models. Generation of MMTC-Cre, MMTV-NIC and TetO-MIC mice was described previously (5, 31, 67). The MMTV-rtTA strain was obtained from Dr. Lewis Chodosh as previously described (68). The ROSA26 Cre-activated b-galactosidase reporter strain was obtained from Dr. Phillipe Soriano as previously described (69). The conditional Rheb1 knockout mice were obtained from Dr. Richard Lamb, University of Liverpool. The conditional Raptor knockout and conditional mTOR knockout mice were obtained from Dr. Nahum Sonnenberg, McGill University. The study of mice was approved by the Animal Resources Centre at McGill University and follows with the guidelines set by the Canadian Council of Animal Care. All mice were backcrossed to a pure FVB/N. Female mice were monitored for tumor formation by physical palpation 8 week after birth, and were necropsied 6 weeks post tumor onset with exception when tumor burden exceeded maximal volume allowed by our animal protocol.

Primary Cell Culture and Cell Lines. Primary tumor cells were generated from transgenic tumors as previously described (10), and maintained in culture in DMEM media supplemented with 5% FBS, 5ng/mL EGF, 35 ug/mL bovine pituitary extract, 5ug/mL Insulin, 1ug/mL Hydrocortisone. 293T cells were cultured HEK-293T cells were obtained from ATCC® (ATCC® CRL-3216), and cultured in DMEM supplemented with 10% FBS.

Histological and Immunohistochemical Analysis. Tumors were fixed in 10% neutral buffered formalin for 24hrs, and transferred to cold 70% ethanol. Samples were paraffin-embedded and sectioned at 4um. Sections were de-paraffinized with xylene, and antigen retrieval was performed in 10mM Citrate buffer (pH6) using a pressure cooker. Endogenous peroxidase was quenched with 3% Hydrogen Peroxide. Sections were blocked with 10% Power Block agent (BioGenex) in PBS for 10 mins, and incubated with primary antibody overnight at 4^{o}C. Subsequently three PBS washes, sections were incubated with secondary antibody (Vector Elite) for 1hr at room temperature. For immunohistochemistry, staining was visualized with Vectastain ABC kit (Vector Laboratories) per manufacturer's instructions follow by Hematoxylin counterstaining. For immunofluorescence, staining was visualized with either Tyraminde Signal Amplification reagent (Thermo Fisher Scientific) for 10 minutes per manufacturer's instructions, followed by DAPI stain for 5 minutes. Immunohistochemistry images were acquired using Aperio-XT Slide scanner (Aperio Technologies). Immunofluorescent images were acquired using an LSM510 Confocal Microscope (Carl Zeiss), and analyzed using ZEN software.

Whole-mount Mammary Glands and X-Gal Staining. No 4. Mammary glands were dissected, spread on glass slide and placed within acetone overnight. Mammary glands were incubated in Harris Modified Hematoxylin stain (Fischer Chemical) overnight, and destained in 1% HCl in 70% ethanol. Mammary glands were washed with ethanol, and cleared in xylene for 1 day before mounting with ClearMount (American Mastertech Scientific). For X-Gal staining, mammary glands were dissected, fixed in Fixing buffer

(2% paraformaldehyde, 0.25% glutaraldehyde, 0.01% NP-40 in PBS) for 2hr, incubated within PreStain buffer (2mM $MgCl_2$, 0.01% Na-deoxycholate, 0.02% NP-40 in PBS) for 2hrs. Subsequently, glands were added to Staining buffer (500mM $K_4Fe(CN)_6$, and 40mg/ml in Prestaining buffer) for 24hrs at room temperature. Mammary glands were dehydrated in 70% EtOH followed by 100% EtOH, and cleared in xylene before being mounted with Clear Mount (American Mastertech Scientific).

Immunoblotting. Tumor lysates were prepared from flash-frozen tumor pieces in RIPA buffer (150mM sodium chloride, 50mM Tris-HCl pH7.4, 2mM EDTA,10m NaF, 10mM Sodium pyrophosphate, 1% sodium deoxycholate, 1% NP-40) supplemented with 1mM sodium orthovanadate, 1mM PMSF, 10mM NaF, 10ug/ul leupeptin and 10ug/ul apotinin. Whole cell lysate was also prepared in RIPA buffer. Protein concentration was quantified by Bradford Assay (Bio-Rad) and 25ug of total protein was resolved by SDS-PAGE, and transferred to Immobilion FL PVDF membranes (Millipore), and block with Odyssey Blocking buffer (Li-COR Biosciences). Primary antibodies were diluted in Odyssey Blocking buffer overnight at 4^oC. Secondary fluorophore-conjugated antibodies, IRDye 800 anti-rabbit, IRDye 680 anti-goat and IRDye 680 anti-mouse were incubated for 1hr at room temperature. Immunoblots were scanned with Odyssey CL-X imaging system, and images were processed with Image Studio Lite V4.0.

Antibodies. Antibodies used for immunoblots include Rheb1 (Cell signalling, Cat# 1387, 1:1000), Cre (Cell signalling, Cat# 12830, IHC/IHF - 1:50), Cleaved Caspase 3 (Cell signaling, Cat# 9661, IHC - 1:500), pAkt S473 (Cell signaling, Cat# 4060, 1:1000), pAkt Thr308 (Cell signaling, Cat# 13038, 1:1000), pS6 S240/244 (Cell signaling, Cat# 5364, WB - 1:1000, IHC/IHF – 1:500), Total S6 (Cell signaling, Cat# 2317), p4EBP1 S65 (Cell signaling, Cat# 13443, WB-1:1000, IHC/IHF-1:500), p4EBP1 Thr37/46 (Cell signaling, Cat# 2855, WB-1:1000, IHC/IHF-1:500), 4EBP1 (Cell signaling, Cat# 9644, WB-1:1000), eIF4E (Cell signaling, Cat# 9742, 1:1000), Cyclin D1 (Cell signaling, Cat# 2978, 1:1000), Cyclin D1 (Cell signaling, Cat# 2922, IP-1:50), Cyclin D3 (Cell signaling, Cat# 2936, 1:1000), Actin (Sigma, A5316, 1:5000), PyV mT (clone 762, a gift from Dr. Steven Dilworth, IHC/IHF-1:100), Akt1/2 (Santa Cruz, SC-1619, 1:200), E-Cadherin

(BD Bioscience, Cat# 610182, 1:1000), Neu (Dako, A0485 , 1:500), Ki67 (Abcam, ab15580, 1:500), Cytokeratin 8/18 (Fitzgerald, 20R-CP004, 1:500), Cytokeratin 14 (BioLegend, PRB-155P, 1:500), and Anti-puromycin (Millipore, Clone 12010 – MABE343, 1:1000). Goat anti-rabbit IRDye 800, Goat anti-mouse IRDye 680, Donkey anti-goat IRDye 800 (Li-COR, 925-32211, 925-68070, 925-68074, 1:10 000)

DNA extraction and Sanger Sequencing. Genomic DNA was collected from mammary tumors using the DNA/RNA All Prep Mini kit (Qiagen. Cat No. 80204). All Exons of *mTOR* gene were sequenced by Sanger sequencing as conducted by the Genome Quebec Innovation Centre.

Cloning and Cell Transfection. pcDNA3.1 Puro+ V2 was generated by subcloning small DNA fragment carrying XbaI-NotI-XhoI-KpnI restriction sites into pcDNA3.1Puro+ using NheI and KpnI sites. *MTOR* was subcloned pcDNA3-Flag mTOR WT (70) (Addgene; #26603) into pBluescript (Agilent Technologies) and the pcDNA3.1Puro+ V2. Part I of *MTOR* was subcloned into pBluescript using NotI and KpnI. Part II of *MTOR* was subcloned into pcDNA3.1Puro+ V2 using KpnI and XbaI. Mutant fragments of *mTOR* were generated by two part PCR strategy using primer sequences provided, and subcloned into pBluescript or pcDNA3.1Puro+ V2. Complete *MTOR* was reassembled within pcDNA3.1Puro+ V2 using NotI and KpnI. Point mutations were verified using Sanger sequencing as conducted by the Genome Quebec Innovation Centre using primer sequences provided. Wildtype and mutant pcDNA3.1Puro+ V2 mTOR was transfected into 293T cells (ATCC) using Lipofectamine 3000 per manufacturer's instructions, and subsequently lysed in RIPA buffer 48hrs post-transfection.

Drug Treatment and Cell Viability Assay. Tumors cells were seeded in 96-well plates with 8 replicates at 5,000 cells per well. 24hrs later, tumor cells were treated with either DMSO, 50uM Everolimus (LC Laboratories, E-4040), or 250nM Torin 1 (Selleckem, S2827) in growth medium for 72hrs. Tumor cells were fixed with 2% PFA and stained

with 0.05% Crystal Violet (Sigma, HT90132) subsequent to treatment. Crystal violet staining was visualized in 10% acetic acid at 590nm.

SUnSET Assay and Immunoprecipitation. Tumor cells were starved overnight and stimulated with full growth medium for 9hrs before being pulsed with 10ug/mL of Puromycin for 3hr. Whole cell lysate was collected in modified RIPA buffer supplemented with protease inhibitors. For Cyclin D1 immunoprecipitation (IP), 500µg of whole cell lysate was incubated with primary antibody overnight at 4^{o}C under continuous agitation. Immune complexes were recovered with magnetic beads (Millipore, LSKMAGAG10), washed three times in lysis buffer, and resuspended in 50 µl of Laemmli buffer before separation by SDS PAGE. Analysis of Puromycin incorporation was detected with anti-puromycin antibody. IP experiments were repeated three times with three independent tumor lines per genotype.

siRNA transfection

Wildtype and mutant pcDNA3.1Puro+ V2 mTOR plasmids were transfected into 293T cells (ATCC) using Lipofectamine 3000 per manufacturer's instructions. Subsequently, 100µM of siRNA Rheb1 was transfected into 293T cells carrying either wildtype or mutant pcDNA3.1Puro+ V2 mTOR plasmids using HiPerfect transfection reagent per manufacturer's instructions. 293T cells were lysed in RIPA buffer 48hrs post-transfection of siRNA.

Quantification and Statistical Analysis

All statistical analysis was completed using GraphPad software. Two-tailed Student *t*-tests, and log-rank Mantel-Cox tests were applied accordingly. The results of the statistical tests can be found within the figures, and the figure legends.

2.7 References

1. Liggett WH, Jr. & Sidransky D (1998) Role of the p16 tumor suppressor gene in cancer. *Journal of clinical oncology : official journal of the American Society of Clinical Oncology* 16(3):1197-1206.

2. Sherr CJ & McCormick F (2002) The RB and p53 pathways in cancer. *Cancer cell* 2(2):103-112.
3. Wright WE & Shay JW (2000) Telomere dynamics in cancer progression and prevention: fundamental differences in human and mouse telomere biology. *Nature medicine* 6(8):849-851.
4. Visvader JE (2011) Cells of origin in cancer. *Nature* 469(7330):314-322.
5. Andrechek ER, *et al.* (2003) Gene expression profiling of neu-induced mammary tumors from transgenic mice reveals genetic and morphological similarities to ErbB2-expressing human breast cancers. *Cancer research* 63(16):4920-4926.
6. Guy CT, Cardiff RD, & Muller WJ (1992) Induction of mammary tumors by expression of polyomavirus middle T oncogene: a transgenic mouse model for metastatic disease. *Molecular and cellular biology* 12(3):954-961.
7. Guy CT, *et al.* (1992) Expression of the neu protooncogene in the mammary epithelium of transgenic mice induces metastatic disease. *Proceedings of the National Academy of Sciences of the United States of America* 89(22):10578-10582.
8. Guy CT, Cardiff RD, & Muller WJ (1996) Activated neu induces rapid tumor progression. *The Journal of biological chemistry* 271(13):7673-7678.
9. Schade B, *et al.* (2013) beta-Catenin signaling is a critical event in ErbB2-mediated mammary tumor progression. *Cancer research* 73(14):4474-4487.
10. Huck L, Pontier SM, Zuo DM, & Muller WJ (2010) beta1-integrin is dispensable for the induction of ErbB2 mammary tumors but plays a critical role in the metastatic phase of tumor progression. *Proceedings of the National Academy of Sciences of the United States of America* 107(35):15559-15564.
11. Ursini-Siegel J, *et al.* (2010) Receptor tyrosine kinase signaling favors a protumorigenic state in breast cancer cells by inhibiting the adaptive immune response. *Cancer research* 70(20):7776-7787.
12. Pontier SM, *et al.* (2010) Integrin-linked kinase has a critical role in ErbB2 mammary tumor progression: implications for human breast cancer. *Oncogene* 29(23):3374-3385.
13. Zoncu R, Efeyan A, & Sabatini DM (2011) mTOR: from growth signal integration to cancer, diabetes and ageing. *Nature reviews. Molecular cell biology* 12(1):21-35.
14. Laplante M & Sabatini DM (2012) mTOR signaling in growth control and disease. *Cell* 149(2):274-293.
15. Nojima H, *et al.* (2003) The mammalian target of rapamycin (mTOR) partner, raptor, binds the mTOR substrates p70 S6 kinase and 4E-BP1 through their TOR signaling (TOS) motif. *The Journal of biological chemistry* 278(18):15461-15464.
16. Ma XM & Blenis J (2009) Molecular mechanisms of mTOR-mediated translational control. *Nature reviews. Molecular cell biology* 10(5):307-318.
17. Schalm SS, Fingar DC, Sabatini DM, & Blenis J (2003) TOS motif-mediated raptor binding regulates 4E-BP1 multisite phosphorylation and function. *Current biology : CB* 13(10):797-806.
18. Sarbassov DD, Guertin DA, Ali SM, & Sabatini DM (2005) Phosphorylation and regulation of Akt/PKB by the rictor-mTOR complex. *Science (New York, N.Y.)* 307(5712):1098-1101.

19. Long X, Ortiz-Vega S, Lin Y, & Avruch J (2005) Rheb binding to mammalian target of rapamycin (mTOR) is regulated by amino acid sufficiency. *The Journal of biological chemistry* 280(25):23433-23436.
20. Dibble CC & Cantley LC (2015) Regulation of mTORC1 by PI3K signaling. *Trends Cell Biol* 25(9):545-555.
21. Garami A, *et al.* (2003) Insulin activation of Rheb, a mediator of mTOR/S6K/4E-BP signaling, is inhibited by TSC1 and 2. *Molecular cell* 11(6):1457-1466.
22. Inoki K, Li Y, Xu T, & Guan KL (2003) Rheb GTPase is a direct target of TSC2 GAP activity and regulates mTOR signaling. *Genes & development* 17(15):1829-1834.
23. Zhang Y, *et al.* (2003) Rheb is a direct target of the tuberous sclerosis tumour suppressor proteins. *Nature cell biology* 5(6):578-581.
24. Inoki K, Li Y, Zhu T, Wu J, & Guan KL (2002) TSC2 is phosphorylated and inhibited by Akt and suppresses mTOR signalling. *Nature cell biology* 4(9):648-657.
25. Ma L, Chen Z, Erdjument-Bromage H, Tempst P, & Pandolfi PP (2005) Phosphorylation and functional inactivation of TSC2 by Erk implications for tuberous sclerosis and cancer pathogenesis. *Cell* 121(2):179-193.
26. Sato T, Nakashima A, Guo L, & Tamanoi F (2009) Specific activation of mTORC1 by Rheb G-protein in vitro involves enhanced recruitment of its substrate protein. *The Journal of biological chemistry* 284(19):12783-12791.
27. Mosley JD, Poirier JT, Seachrist DD, Landis MD, & Keri RA (2007) Rapamycin inhibits multiple stages of c-Neu/ErbB2 induced tumor progression in a transgenic mouse model of HER2-positive breast cancer. *Molecular cancer therapeutics* 6(8):2188-2197.
28. Herschkowitz JI, *et al.* (2007) Identification of conserved gene expression features between murine mammary carcinoma models and human breast tumors. *Genome biology* 8(5):R76.
29. Utermark T, *et al.* (2012) The p110alpha and p110beta isoforms of PI3K play divergent roles in mammary gland development and tumorigenesis. *Genes & development* 26(14):1573-1586.
30. Marcotte R, Smith HW, Sanguin-Gendreau V, McDonough RV, & Muller WJ (2012) Mammary epithelial-specific disruption of c-Src impairs cell cycle progression and tumorigenesis. *Proceedings of the National Academy of Sciences of the United States of America* 109(8):2808-2813.
31. Rao T, *et al.* (2014) Inducible and coupled expression of the polyomavirus middle T antigen and Cre recombinase in transgenic mice: an in vivo model for synthetic viability in mammary tumour progression. *Breast cancer research : BCR* 16(1):R11.
32. Long X, Lin Y, Ortiz-Vega S, Yonezawa K, & Avruch J (2005) Rheb Binds and Regulates the mTOR Kinase. *Current Biology* 15(8):702-713.
33. Parmar N & Tamanoi F (2010) Rheb G-Proteins and the Activation of mTORC1. *Enzymes* 27:39-56.
34. Buerger C, DeVries B, & Stambolic V (2006) Localization of Rheb to the endomembrane is critical for its signaling function. *Biochemical and biophysical research communications* 344(3):869-880.

35. Kang SA, *et al.* (2013) mTORC1 phosphorylation sites encode their sensitivity to starvation and rapamycin. *Science (New York, N.Y.)* 341(6144):1236566.
36. Yang H, *et al.* (2013) mTOR kinase structure, mechanism and regulation. *Nature* 497(7448):217-223.
37. Polak P, *et al.* (2008) Adipose-specific knockout of raptor results in lean mice with enhanced mitochondrial respiration. *Cell metabolism* 8(5):399-410.
38. Baillie AG & Garlick PJ (1991) Responses of protein synthesis in different skeletal muscles to fasting and insulin in rats. *The American journal of physiology* 260(6 Pt 1):E891-896.
39. Averous J, Fonseca BD, & Proud CG (2008) Regulation of cyclin D1 expression by mTORC1 signaling requires eukaryotic initiation factor 4E-binding protein 1. *Oncogene* 27(8):1106-1113.
40. Wu LX, *et al.* (2005) CD28 regulates the translation of Bcl-xL via the phosphatidylinositol 3-kinase/mammalian target of rapamycin pathway. *Journal of immunology (Baltimore, Md. : 1950)* 174(1):180-194.
41. Shuda M, *et al.* (2015) CDK1 substitutes for mTOR kinase to activate mitotic cap-dependent protein translation. *Proceedings of the National Academy of Sciences of the United States of America* 112(19):5875-5882.
42. Sarbassov DD, *et al.* (2006) Prolonged rapamycin treatment inhibits mTORC2 assembly and Akt/PKB. *Molecular cell* 22(2):159-168.
43. Liu P, *et al.* (2013) Sin1 phosphorylation impairs mTORC2 complex integrity and inhibits downstream Akt signalling to suppress tumorigenesis. *Nature cell biology* 15(11):1340-1350.
44. Grabiner BC, *et al.* (2014) A diverse array of cancer-associated MTOR mutations are hyperactivating and can predict rapamycin sensitivity. *Cancer discovery* 4(5):554-563.
45. Urano J, *et al.* (2007) Point mutations in TOR confer Rheb-independent growth in fission yeast and nutrient-independent mammalian TOR signaling in mammalian cells. *Proceedings of the National Academy of Sciences of the United States of America* 104(9):3514-3519.
46. Xu J, *et al.* (2016) Mechanistically distinct cancer-associated mTOR activation clusters predict sensitivity to rapamycin. *The Journal of clinical investigation* 126(9):3526-3540.
47. Ghosh AP, *et al.* (2015) Point mutations of the mTOR-RHEB pathway in renal cell carcinoma. *Oncotarget* 6(20):17895-17910.
48. Larsson O, *et al.* (2012) Distinct perturbation of the translatome by the antidiabetic drug metformin. *Proceedings of the National Academy of Sciences of the United States of America* 109(23):8977-8982.
49. Risson V, *et al.* (2009) Muscle inactivation of mTOR causes metabolic and dystrophin defects leading to severe myopathy. *The Journal of cell biology* 187(6):859-874.
50. Ursini-Siegel J, Schade B, Cardiff RD, & Muller WJ (2007) Insights from transgenic mouse models of ERBB2-induced breast cancer. *Nature reviews. Cancer* 7(5):389-397.

51. Tung B, *et al.* (2017) beta-Catenin haploinsufficiency promotes mammary tumorigenesis in an ErbB2-positive basal breast cancer model. *Proceedings of the National Academy of Sciences of the United States of America* 114(5):E707-e716.
52. Simond AM, Rao T, Zuo D, Zhao JJ, & Muller WJ (2017) ErbB2-positive mammary tumors can escape PI3K-p110alpha loss through downregulation of the Pten tumor suppressor. *Oncogene* 36(43):6059-6066.
53. Zhang Q, *et al.* (2011) Cyclin D3 compensates for the loss of cyclin D1 during ErbB2-induced mammary tumor initiation and progression. *Cancer research* 71(24):7513-7524.
54. Martin TD, *et al.* (2014) Ral and Rheb GTPase activating proteins integrate mTOR and GTPase signaling in aging, autophagy, and tumor cell invasion. *Molecular cell* 53(2):209-220.
55. Tee AR, Blenis J, & Proud CG (2005) Analysis of mTOR signaling by the small G-proteins, Rheb and RhebL1. *FEBS letters* 579(21):4763-4768.
56. Truitt ML, *et al.* (2015) Differential requirements for eIF4E dose in normal development and cancer. *Cell* 162(1):59-71.
57. Kim J, Kundu M, Viollet B, & Guan KL (2011) AMPK and mTOR regulate autophagy through direct phosphorylation of Ulk1. *Nature cell biology* 13(2):132-141.
58. Li S, Brown MS, & Goldstein JL (2010) Bifurcation of insulin signaling pathway in rat liver: mTORC1 required for stimulation of lipogenesis, but not inhibition of gluconeogenesis. *Proceedings of the National Academy of Sciences of the United States of America* 107(8):3441-3446.
59. Land SC & Tee AR (2007) Hypoxia-inducible factor 1alpha is regulated by the mammalian target of rapamycin (mTOR) via an mTOR signaling motif. *The Journal of biological chemistry* 282(28):20534-20543.
60. Wagle N, *et al.* (2014) Response and acquired resistance to everolimus in anaplastic thyroid cancer. *The New England journal of medicine* 371(15):1426-1433.
61. Wu TJ, *et al.* (2015) Identification of a Non-Gatekeeper Hot Spot for Drug-Resistant Mutations in mTOR Kinase. *Cell reports* 11(3):446-459.
62. Rodrik-Outmezguine VS, *et al.* (2016) Overcoming mTOR resistance mutations with a new-generation mTOR inhibitor. *Nature* 534(7606):272-276.
63. Wagle N, *et al.* (2014) Activating mTOR mutations in a patient with an extraordinary response on a phase I trial of everolimus and pazopanib. *Cancer discovery* 4(5):546-553.
64. Kwiatkowski DJ, *et al.* (2016) Mutations in TSC1, TSC2, and MTOR Are Associated with Response to Rapalogs in Patients with Metastatic Renal Cell Carcinoma. *Clinical cancer research : an official journal of the American Association for Cancer Research* 22(10):2445-2452.
65. Long X, Lin Y, Ortiz-Vega S, Yonezawa K, & Avruch J (2005) Rheb binds and regulates the mTOR kinase. *Current biology : CB* 15(8):702-713.
66. Yang H, *et al.* (2017) Mechanisms of mTORC1 activation by RHEB and inhibition by PRAS40. *Nature* 552(7685):368-373.
67. Ursini-Siegel J, *et al.* (2008) ShcA signalling is essential for tumour progression in mouse models of human breast cancer. *The EMBO journal* 27(6):910-920.

68. Gunther EJ, *et al.* (2002) A novel doxycycline-inducible system for the transgenic analysis of mammary gland biology. *Faseb j* 16(3):283-292.
69. Soriano P (1999) Generalized lacZ expression with the ROSA26 Cre reporter strain. *Nat Genet* 21(1):70-71.
70. Vilella-Bach M, Nuzzi P, Fang Y, & Chen J (1999) The FKBP12-rapamycin-binding domain is required for FKBP12-rapamycin-associated protein kinase activity and G1 progression. *The Journal of biological chemistry* 274(7):4266-4272.

Chapter 3: Rheb1-deficient ErbB2 tumors switch dependency to alternative GTPases for mTORC1 activation

3.1 Premise

While regulation of S6 kinase activation and stimulation of eIF4E-driven eIF4F assembly are well known processes of mTORC1, the relative contribution of these downstream effectors during early stages of mammary tumorigenesis have yet to be thoroughly examined. Within Chapter 2, we demonstrated that ablation of mTORC1 activation stalls mammary tumorigenesis at the early stages of progression within our GEMMs of breast cancer. Expanding from Chapter 3, we employed our Dox-inducible PyV mT-driven tumor system to evaluate the relative contribution of the eIF4E signalling axis within the early stages of tumor progression, both *in vivo*, and using *in vitro* organoid system derived from the mammary epithelia of our Dox-inducible MIC mice. Consequently, we identified a robust Myc transcriptional signature along with the up-regulation of a large panel of ribosomal proteins early upon induction of PyV mT expression.

In addition, the work completed in Chapter 2 also highlighted restored mTORC1 activity within the mammary tumors, which ultimately developed in the absence of Rheb1. While mTOR mutations were identified as a contributing factor within a subset of Rheb1-deficient mammary tumours, a large portion of these tumours exhibited wildtype mTOR. This observation argues for the presence of distinct mechanisms of mTORC1 re-activation, we further explored other mechanisms of mTORC1 re-activation within Rheb1-deficient mammary tumours within Chapter 3.

3.2 Abstract

An elevated rate of protein synthesis which is essential for the aberrant proliferation of cancer cells is commonly observed within breast cancer. Increased protein synthesis can be achieved through either enhancing the efficiency of scanning ribosomes as well as the concurrent up-regulation of both eIF4E and functional ribosomes. mTORC1 is a master regulator of cell proliferation, and plays a prominent role in the regulation of mRNA translation. Employing the use of a doxycycline-inducible PyV mT-driven mouse model, we dissect the relative contribution of mTORC1 downstream effectors S6K and eIF4E, during early stages of mammary tumor initiation. We demonstrate that restoring eIF4E-function partially alleviates the block in tumor initiation brought on by inhibition of mTORC1. We demonstrated that hyperactivation of ribosome biogenesis occurs during early stages of PyV mT-driven tumorigenesis and inhibition of mTORC1 activation this elevation. In order to overcome the block in tumor initiation brought on by Rheb1 ablation, Rheb1-deficient tumours develop dependency on alternative small GTPases to mediate mTORC1 activation.

3.3 Introduction

Genetically engineered mouse models (GEMMs) of breast cancer are well capable of closely recapitulating the complex process of tumorigenesis, and as such, have become invaluable tools for studying disease progression (1). Tumour formation can be invoked through the mammary-specific expression of various oncogenes including the receptor tyrosine kinase ErbB2, or the Polyomavirus Middle T antigen (PyV mT) (2, 3). By coupling a gene-targeting strategy to the model systems, these GEMMs have allowed for a detailed interrogation of the molecular processes crucial for the initiation of tumorigenesis (4, 5).

Protein synthesis is a high energy-consuming demanding process, and as such, it befalls tight molecular regulation within the cell (6-8). Elevated rates of protein synthesis are closely associated with the increased cell proliferation that occurs during early stages of tumour initiation. An elevation in protein synthesis can be achieved either through the enhancement of mRNA translation efficiency, or through the increased abundance of functional ribosomes. The mechanistic Target of Rapamycin (mTOR) is a serine/threonine kinase which nucleates into two functionally distinct complexes, mTORC1 and mTORC2 (9). mTORC1 plays prominent roles in regulation of both translation initiation, and ribosomal biogenesis (7, 10). Upon binding of the small GTPase Rheb1 (11, 12), active mTORC1 mediates phosphorylation of downstream effectors, 4EBP1-3 and S6K. mTORC1 drives assembly of the eIF4F complex through the phosphorylation of the 4EBPs, which alleviates the suppression of eIF4E-dependent recruitment of the eIF4G scaffold and the eIF4A helicase . The incorporation of eIF4A helicase into the eIF4F complex enhances the efficiency of ribosome scanning by unwinding secondary structures within the 5’ UTR (13). Alternatively, the rate of protein synthesis can be enhanced through hyperactivation of ribosome biogenesis thus driving the production of more ribosomes. The process of ribosome biogenesis initiates with the production of pre-47S ribosomal RNA (rRNA) which is further cleaved and assembled with various ribosomal proteins into a pre-60S and a pre-40S subunit within the nucleolus (10). Subsequent export into the cytosol, mature 60S and 40S subunits are processed and ultimately assembled into a functional 80S ribosome at the initiation of translation elongation. mTORC1 has been shown to play a role in driving expression of rRNA required for ribosomal biogenesis within various cellular contexts either directly (14) or indirectly through the downstream effector S6K1 (15, 16).

We previously demonstrated that genetic ablation of Rheb1-mediated mTORC1 activation blocked tumor initiation within our tumor model systems (17), and Rheb1-deficient mammary tumors adopt alternative mechanisms of mTORC1 activation to permit tumorigenesis. Using an inducible PyV mT-driven mouse model of breast cancer, we further evaluated the relative contributions of eIF4E within the early stages of mammary tumor initiation through the genetic ablation of both 4EBP1 and 4EBP2.

Using a novel *in vitro* model system of tumor initiation derived from the mammary epithelia of doxycycline-inducible PyV mT mouse model (18), we demonstrated that S6K1 function contributes prominently during PyV mT-driven tumor initiation. In order for tumorigenesis to progress, the Rheb1-deficient pre-neoplastic epithelia developed dependency on alternative small GTPase such as RalB, to confer mTORC1 activation.

3.4 Results

mTORC1 activity is largely restored in Rheb1-deficient mammary tumors.

Our previous work had demonstrated that Rheb1-mediated mTORC1 activation is crucial for the initiation of both PyV mT-driven and ErbB2-driven mammary tumorigenesis. Genetic ablation of the small GTPase Rheb1 blocked tumor formation at early stages of progression within both models systems (17). While mTORC1 activation is well-established to be Rheb1-dependent, the mTORC1 activity within the mammary tumors that ultimately developed from the $Rheb1^{fl/fl}$ MIC and $Rheb1^{fl/fl}$ NIC models systems were largely restored, and Rheb1-independent. The levels of 4EBP1 Thr 37/46, and Ser 65 phosphorylation as well as rpS6 Ser240/244 phosphorylation, both well-established functional markers of mTORC1 activity, were comparable between Rheb1-deficient MIC tumors and their Rheb1-proficient counterparts **(Fig 3.1A)**. A similar trend within these two functional markers was also observed between the Rheb1-deficient NIC tumors compared to the Rheb1-proficient NIC tumors **(Fig 3.1B)**. In attempts to gain insight into the underlying molecular mechanism driving restored mTORC1 activation in the absence of Rheb1 within the MIC tumor system, we performed RNAseq analysis on RNA collected from both the Rheb1-deficient, and Rheb1-proficient mammary tumors. RNAseq analysis revealed a total of 93 genes differentially expressed between Rheb1-deficient mammary tumors in comparison to the wildtype controls **(Fig 3.2A)**.

Although the gene expression profiling

The minimal variation within the transcriptional profiles between Rheb1-deficient and Rheb1-proficient mammary tumors **(Figure 3.2A; Figure 3.10A),** in addition to their comparable growth capacity, argues for the highly compensated nature within these tumors for the loss of Rheb1.

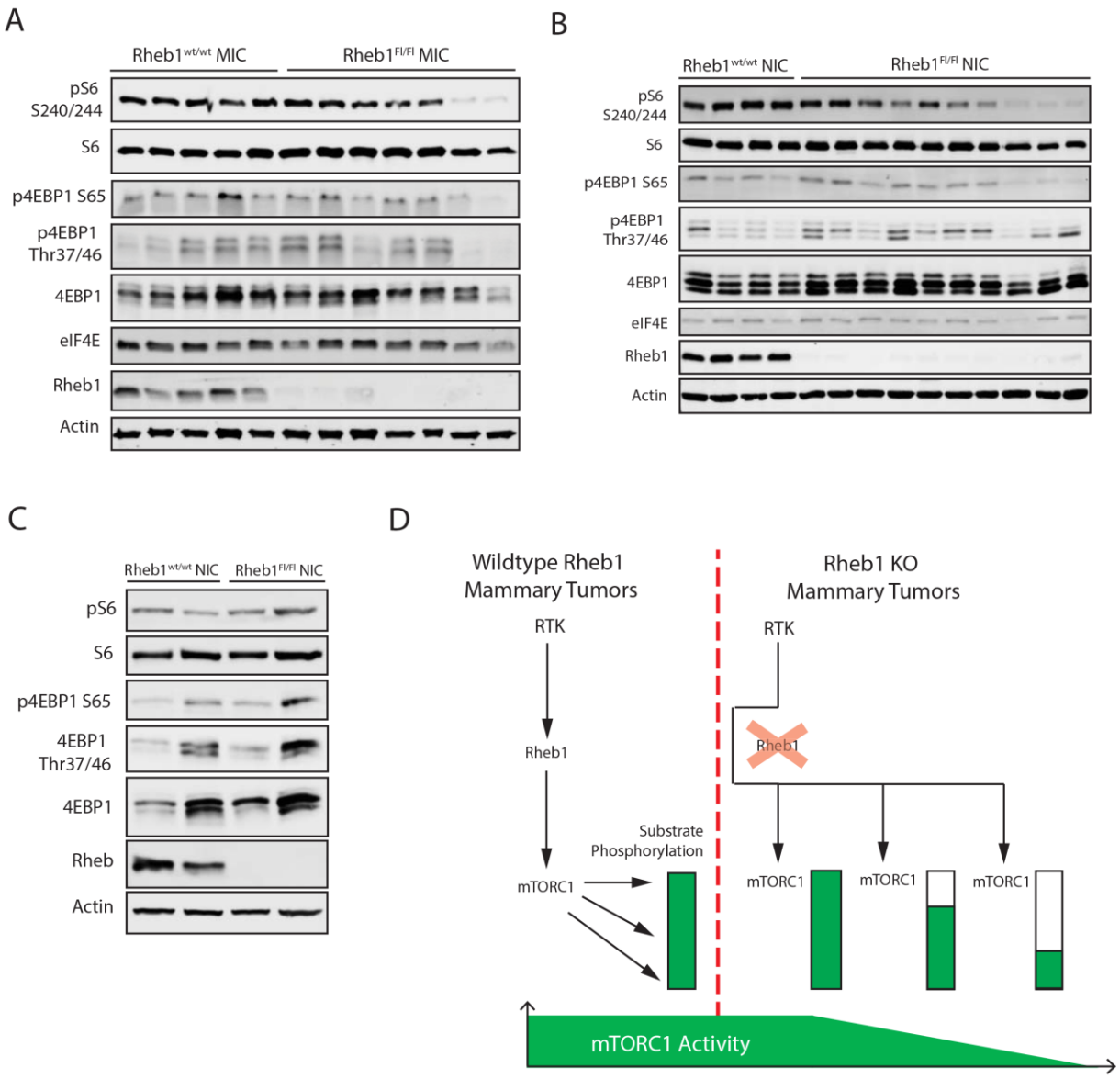

Figure 3. 1 mTORC1 function within Rheb1-deficient mammary tumors is variably restored. (A) Representative immunoblots of end-stage PyV mT-positive mammary tumors collected from Rheb1$^{wt/wt}$ MIC and Rheb1$^{fl/fl}$ MIC mice, probed with the indicated antibodies. (B) Representative immunoblots of end-stage ErbB2-positive mammary tumors collected from Rheb1$^{wt/wt}$ NIC and Rheb1$^{fl/fl}$ NIC mice, probed with the indicated antibodies. Representative immunoblots illustrating mTORC1 activity within Rheb1-deficient ErbB2-positive mammary tumor lines. (D) Cartoon schematic summary of the restored mTORC1 activity within the Rheb1-deficient tumor systems.

The observed Rheb1-independent mTORC1 activity was also retained within the tumor-derived Rheb1-deficient NIC cell lines, which suggests for a cell-intrinsic molecular mechanism driving the phenomenon **(Fig 3.1C; Fig 3.8A)**.While we previously demonstrated that a subset of these Rheb1-deficient mammary tumors developed hyperactivating mTOR mutations that contributed to restoring mTORC1 activation, a large subset of Rheb1-deficient tumors exhibited wildtype mTOR. This observation argues for the presence of other distinct mechanisms of compensation for Rheb1 loss **(Fig 3.1D)** which will be one of the main focuses of this study.

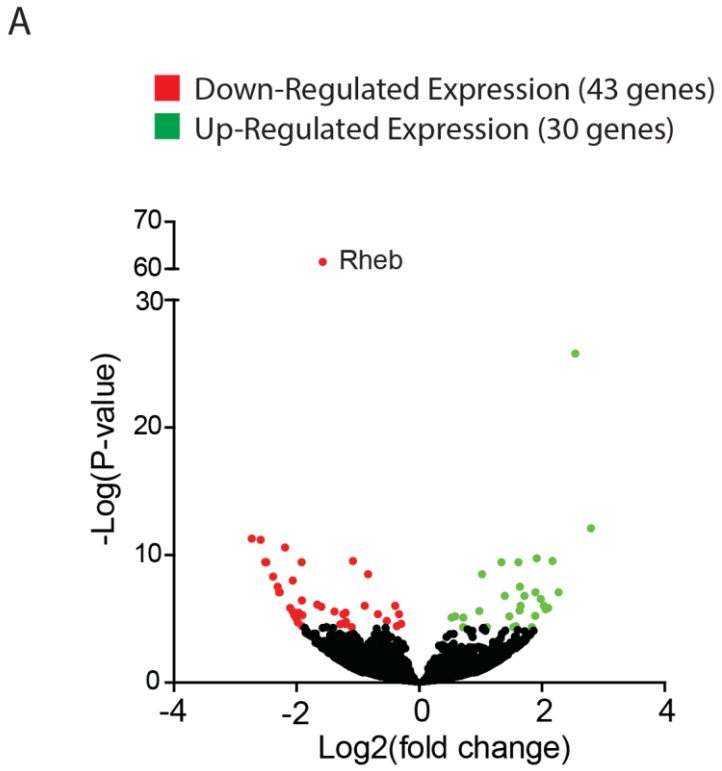

Figure 3. 2 RNAseq Analysis Reveals minimal transcriptional alterations between end-stage Rheb1-deficient and Rheb1-proficient tumors. (A) Volcano plot illustrating genes differentially expressed between Rheb1-deficient MIC and Rheb1-proficient MIC tumors. Red and green dots represent down-regulated and up-regulated genes respectively. Statistical analysis was performed by Student *t*-test and statistical significance was considered p-value < 0.05. The fold change threshold was set to -/+ log2 (0.4). RNAseq analysis was conducts on RNA collected from five independent tumors from the two genotypes. Statistical significance was assessed at adjacent p-value <0.05.

Ablation of 4EBP1 and 4EBP2 partially alleviates Block in Tumor Initiation Attributed to Rheb1 Ablation.

One of the well-established downstream effectors of mTORC1 is the 4EBPs, whereby mTORC1-mediated phosphorylation of 4EBP1-3 relieves the suppression of eIF4E-mediated assembly of the eIF4F complex to allow initiation of cap-dependent translation (19). The observation that 4EBP1 phosphorylation was restored within the Rheb1-deficient mammary tumors despite the initially the loss within the pre-neoplastic epithelia, argues that mTORC1-mediated eIF4E function is crucial for tumor formation within our mouse models. eIF4E-dependent mRNA translation has demonstrated prominent roles in the initiation of lung cancer and prostate cancer, by allowing for efficient translation of specific pro-tumorigenic transcripts (20). While evaluation of eIF4E function in the context of mammary tumor initiation is lacking, overexpression of eIF4E is sufficient to elicit transformation of established human mammary epithelial cells *in vitro* (21). As such, we wanted to ascertain if restoring eIF4E function was sufficient to alleviate the tumorigenic defect within the Rheb1-deficient pre-neoplastic epithelia. Since eIF4F assembly is largely dictated by the eIF4E/4EBP ratio and genetic ablation of both 4EBP1 and 4EBP2 was sufficient to alleviate the suppression of eIF4E-mediated translation caused by mTOR inhibitors (22, 23), we sought to address this by crossing conditional 4EBP1 and 4EBP2 knockout mice ($4EBP1^{fl/fl}$ $4EBP2^{fl/fl}$ strain) with our $Rheb1^{fl/fl}$ MIC mice **(Fig 3.3A-3.3C)**. We examined the acute effects of 4EBP1/2 ablation on early stages of PyV mT-induced mammary tumorigenesis within Rheb1-deficient mammary epithelia, which are identified vicariously through Cre expression. Firstly, we evaluated the epithelial content within the mammary glands of the $Rheb1^{fl/fl}$ $4EBP1^{fl/fl}$ $4EBP2^{fl/fl}$ MIC mice in comparison to both the $Rheb1^{fl/fl}$ MIC and wildtype MIC strains, following 14 days of doxycycline administration. The mammary epithelia undergo massive expansion within the wildtype MIC mice as a consequence of PyV mT expression, which is unaffected by genetic ablation of 4EBP1 and 4EBP2 within the

4EBP1$^{fl/fl}$ 4EBP2$^{fl/fl}$ MIC mice **(Fig 3.3D-3.3E)**. This epithelial expansion is severely blocked following ablation of Rheb1 and is only partially restored with genetic ablation

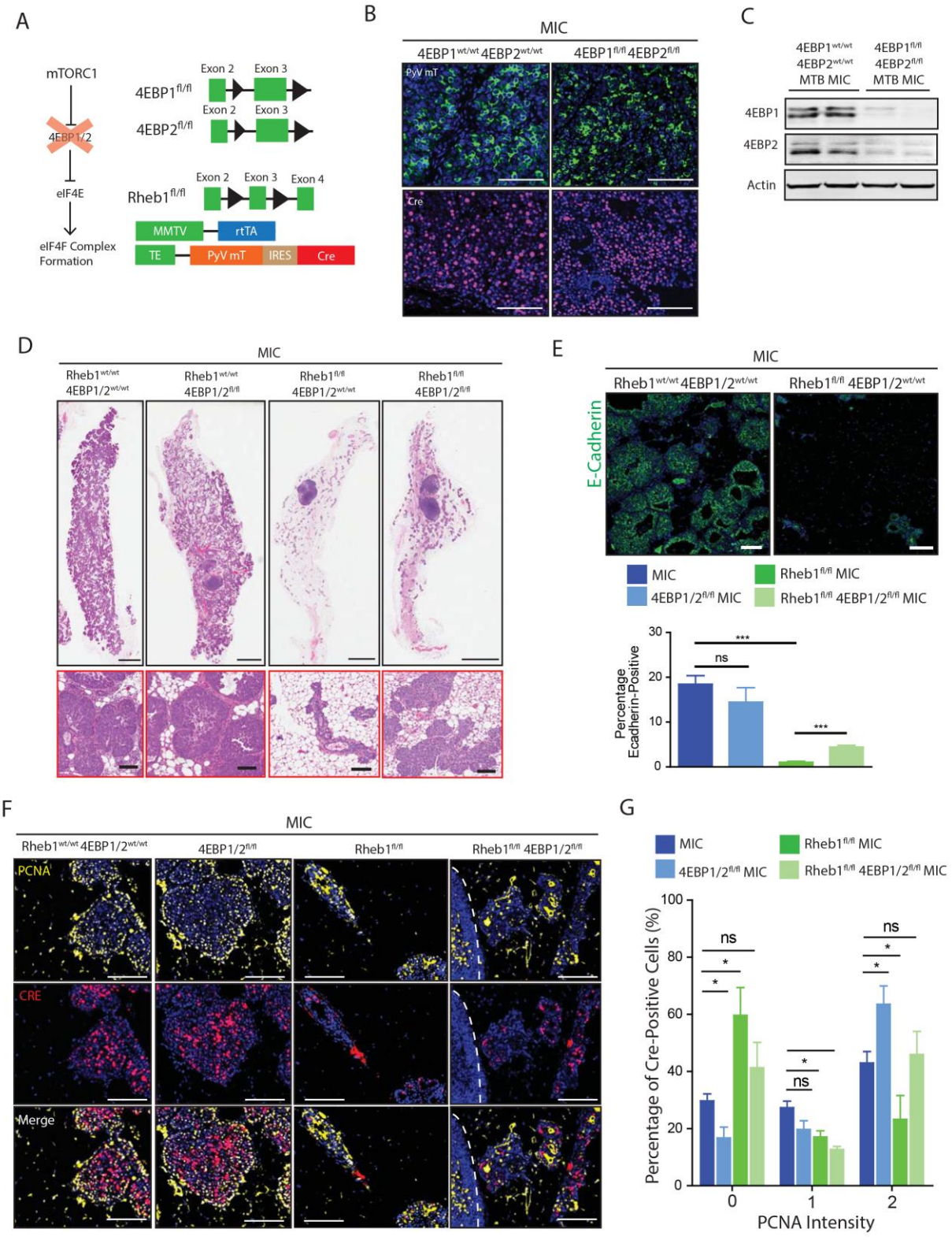

Figure 3. 3 Ablation of 4EBP1 and 4EBP2 partially rescues of the block in tumor initiation caused by Rheb1 ablation. (A) Schematic representation of the Doxycycline-inducible MMTV-

rtTA PyV mT transgenic mice (MIC strain), the loxP-site flanked *Rheb1* allele, and the loxP-site flanked *Eif4ebp1* and *Eif4ebp2* allele. MMTV, Murine mammary tumor virus. IRES, Internal ribosomal entry site. TE, Tetracycline-responsive operator. rtTA, reverse tet-responsive transactivator. (B) Immunofluorescence staining of wildtype MIC and 4EBP1$^{fl/fl}$ 4EBP2 $^{fl/fl}$ MIC mammary gland sections for PyV mT and Cre. Scale bars represents 100μm. (C) Western blot analysis of wildtype MIC and 4EBP1$^{fl/fl}$ 4EBP2 $^{fl/fl}$ MIC tumor protein extracts with indicated antibodies. (D) Top: Representative H&E-stained histological sections of mammary glands collected from mice of the indicated genotypes following 14 days of Doxycycline induction. Scale bar represents 2mm. Bottom: panel is a 35X representation of area boxed in red in top panel. Scale bar represents 200 μm. (E) Top: Representative Immunohistofluorescence staining for E-Cadherin. Scale bars represent 100 μm. Bottom: Quantification of E-Cadherin IHC staining of mammary glands of mice from indicated genotypes following 14-day doxycycline administration. Values represent mean (+/- SEM) of at least 5 mice per genotype. Statistical significance was assessed by two-tailed unpaired Student's *t*-test. (F) Representative immunohistochemistry staining for PCNA and Cre within mammary ductal from mice of indicated genotypes after 14 days of doxycycline induction. (G) Graphs depicting frequency of 0, 1, and 2 grade of PCNA staining within Cre-positive mammary epithelium from mice of the indicated genotypes after 14 days of doxycycline induction. Values represent mean frequency of each grade from at least 300 Cre-positive cells across three biological replicates per genotype. Statistical significance was assessed by two-tailed unpaired Student's *t*-test.

of 4EBP1 and 4EBP2 within the Rheb1$^{fl/fl}$ 4EBP1$^{fl/fl}$ 4EBP2$^{fl/fl}$ MIC mice in comparison to the Rheb1$^{fl/fl}$ MIC mice **(Fig 3.3D-3.3E)**. Provided that we observed only a partial restoration in PyV mT-induced expansion of the Rheb1-deficient pre-neoplastic cells upon ablation of both 4EBP1 and 4EBP2, we wanted to examine the proliferative status of the pre-neoplastic epithelia within the Rheb1$^{fl/fl}$ 4EBP1$^{fl/fl}$ 4EBP2$^{fl/fl}$ MIC mice. To address this, mammary gland sections were analyzed with immunohistochemistry staining for Cre and PCNA from both Rheb1$^{fl/fl}$ 4EBP1$^{fl/fl}$ 4EBP2$^{fl/fl}$ MIC and Rheb1$^{fl/fl}$ MIC mice and compared to the mammary glands of 4EBP1$^{fl/fl}$ 4EBP2$^{fl/fl}$ MIC and wildtype MIC mice. A higher frequency of strong PCNA intensity along with the concomitant lower frequency of weak PCNA intensity could be observed within the pre-neoplastic mammary epithelia of 4EBP1$^{fl/fl}$ 4EBP2$^{fl/fl}$ MIC mice relative to wildtype MIC mice **(Fig 3.3F-3.3G)**. This observation suggested an increased proliferative capacity within the epithelial cells upon loss of 4EBP1 and 4EBP2 despite comparable epithelial content between 4EBP1$^{fl/fl}$ 4EBP2$^{fl/fl}$ MIC mice and their wildtype counterparts. Conversely, a lower frequency of strong PCNA intensity along with a concomitant higher frequency of weak PCNA intensity was observed within the pre-neoplastic epithelia of Rheb1$^{fl/fl}$ MIC mice relative to wildtype MIC mice, which is consistent with the previously observed impaired proliferative capacity within the

Rheb1-deficient pre-neoplastic epithelia (17). Interestingly, although frequency of strong PCNA intensity was increased within the Rheb1-deficient pre-neoplastic epithelial upon ablation of 4EBP1 and 4EBP2 relative to Rheb1-deficient cells, the frequency of strong PCNA intensity was not comparable to the Rheb1-proficient 4EBP1/2-deficient epithelial cells **(Fig 3.3G)**. This intermediate trend in PCNA expression argues that genetic ablation of 4EBP1 and

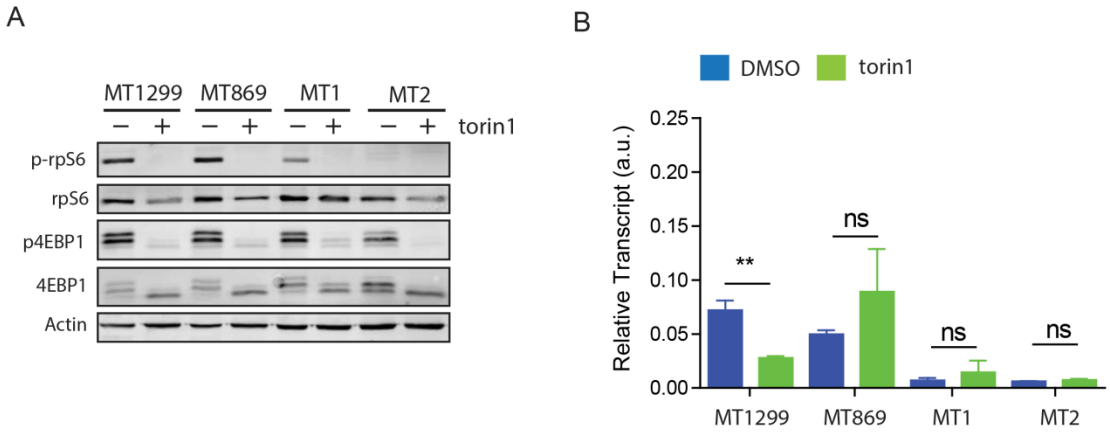

Figure 3. 4 Expression of 4EBP3 is not elevated within PyV MT-driven urine tumor cells following long-term mTORC1 inhibition. (A) Immunoblot of lysates collected from PyV mT-driven murine tumor cells following long-term torin1 treatment, probed with the indicated antibodies. (B) Transcript levels of *Eif4bp3* were assessed within PyV mT-driven tumor cells from (A). Data was normalized to *Gapdh*, and represents average values across three independent experiments. Error bars represent SEM. Statistical significance was assess by Student's *t* test.

4EBP2 only partially restored the proliferative capacity within the Rheb1-deficient epithelial cells. Taken together, the partial rescue in mammary epithelial expansion along with the intermediate restoration in proliferative capacity argues that other molecular factors aside from activation of the eIF4E signaling axis are required for tumor initiation to progress in the absence of Rheb1.

PyV mT-driven up-regulation of ribosome transcriptional program within *in vitro* model of tumor initiation.

Mammary ductal epithelia can be extracted from the mammary gland and propagated within a gel matrix composed of extracellular matrix (ECM). This *in vitro* assay allows for

growth and development of these mammary epithelial cells into acinar structures that closely mimics the ductal structures observed within the mammary gland (24). Through coupling of this *in vitro* model with the temporal control of PyV mT expression from our Dox-inducible GEMM, we wanted to assess the early transcriptional changes within the pre-neoplastic epithelia upon induction of oncogene in attempts to identify early processes that occur during tumor initiation.

As such, mammary epithelial cells from wildtype MIC mice were extracted and expanded within an ECM gel matrix to allow the development of acinar structures containing a lumen core, prior to induction of PyV mT expression. Subsequent the formation of acinar structures, doxycycline was administered and the organoids were monitored for morphological changes prior to cell fixation **(Fig 3.5A)**. Closely recapitulating the MIC mouse strain, we can start observing morphological abnormalities within these organoid structures, which is largely caused by the expansion of the epithelial cells and collapse of the lumen, just 7 days post Dox-induction **(Fig 3.5B-3.5C)**. Given that morphological changes were observed after 7 days of Dox induction, RNA was collected from organoids at this particular stage, and subjected to gene expression profiling via RNAseq analysis. Transcriptome profiling of these organoids revealed dramatic alterations in gene expression whereby 635 genes were up-regulated and 728 genes were down-regulated upon induction of PyV mT expression **(Fig 3.5D)**. Within these transcriptional changes, we uncovered an enrichment of a Myc gene signature along with up-regulation of a panel of 53 ribosomal proteins **(Fig 3.5E)**. Taken together, these observations

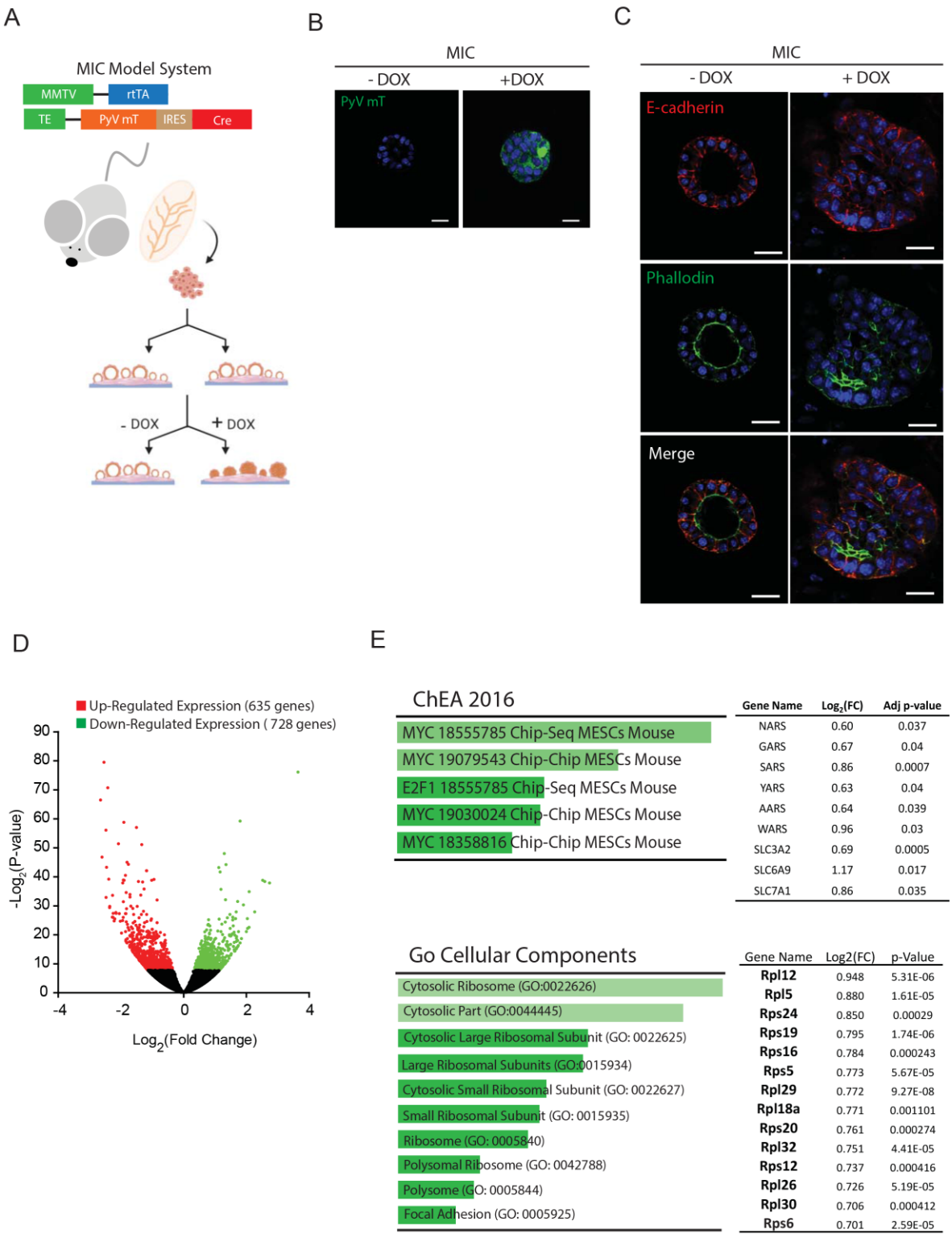

Gene Name	Log_2(FC)	Adj p-value
NARS	0.60	0.037
GARS	0.67	0.04
SARS	0.86	0.0007
YARS	0.63	0.04
AARS	0.64	0.039
WARS	0.96	0.03
SLC3A2	0.69	0.0005
SLC6A9	1.17	0.017
SLC7A1	0.86	0.035

Gene Name	Log2(FC)	p-Value
Rpl12	0.948	5.31E-06
Rpl5	0.880	1.61E-05
Rps24	0.850	0.00029
Rps19	0.795	1.74E-06
Rps16	0.784	0.000243
Rps5	0.773	5.67E-05
Rpl29	0.772	9.27E-08
Rpl18a	0.771	0.001101
Rps20	0.761	0.000274
Rpl32	0.751	4.41E-05
Rps12	0.737	0.000416
Rpl26	0.726	5.19E-05
Rpl30	0.706	0.000412
Rps6	0.701	2.59E-05

Figure 3. 5 PyV mT-driven *in vitro* organoid model of mammary tumor initiation. (A) Cartoon schematic of *in vitro* organoid system derived from mammary ductal epithelia of Dox-inducible PyV mT-driven GEMM. Created with BioRender.com. (B) Representative images of

mammary ductal organoids following 8 days of doxycycline induction stained with indicated antibodies. Scale bar represents 25um. (C) Representative images illustrating altered morphology of mammary organoids following PyV mT induction stained with indicated antibodies. Scale bar represents 25um. (D) Volcano plot illustrating genes differentially expressed within mammary ductal organoids following 8 days of doxycycline induction. The green and red dots represent significantly up-regulated and down-regulated genes respectively. The fold change threshold was set to -/+ log2 (0.4). Statistical analysis was performed by Student *t*-test and statistical significance was considered p-value < 0.05. (E) Top: ChEA analysis of differentially up-regulated genes within mammary organoids upon PyV mT induction illustrating Myc gene signature. Table partially lists the differentially expressed genes comprising gene signatures. Bottom: Go Cellular Components analysis was conducted with EnrichR illustrating enrichment of transcriptional gene signatures for ribosomal proteins. Table partially listing the differentially expressed ribosomal genes comprising gene signatures. Bars represent adjacent p-value.

suggests a potential increase in Myc activity and ribosome production within these organoids upon induction of PyV mT expression.

S6 Kinase activity remains disrupted within Rheb1-deficient pre-neoplastic mammary epithelia of Rheb1$^{fl/fl}$ 4EBP1$^{fl/fl}$ 4EBP2 $^{fl/fl}$ MIC mice.

Regulation of S6K is governed through a cascade of phosphorylation events which triggers the unraveling of the kinase into a structurally active conformation (25). mTORC1 propagates this cascade of phosphorylation events that ultimately permit robust S6K activation, by eliciting S6K Thr389 phosphorylation (26). Genetic ablation of both S6K1 and S6K2 isoforms elicits anti-proliferative effects *in vivo*, resulting in stunted murine developmental growth as well as blunted hepatic regeneration (27, 28). Given the persistent defect in mammary epithelial expansion and cell proliferation observed within the Rheb1-deficient pre-neoplastic epithelia following ablation of both 4EBP1 and 4EBP2, we wanted to evaluate the status S6K activity within the mammary glands of Rheb1$^{fl/fl}$ 4EBP1$^{fl/fl}$ 4EBP2$^{fl/fl}$ MIC mice. While rpS6 Ser235/236 can be phosphorylated by both S6K and RSK, rpS6 Ser240/244 phosphorylation is uniquely regulated by S6K and as such serves as biomarker of kinase activity (29). To this end, histological sections of mammary glands from Rheb1$^{fl/fl}$ 4EBP1$^{fl/fl}$ 4EBP2$^{fl/fl}$ MIC and Rheb1$^{fl/fl}$ MIC mice were subjected to immunohistochemistry analysis for rpS6 S240/244 phosphorylation along with Cre expression, in comparison with both the 4EBP1$^{fl/fl}$ 4EBP2$^{fl/fl}$ MIC and wildtype MIC controls. The pre-neoplastic epithelia exhibited decreased rpS6 S240/244 phosphorylation

within Rheb1$^{fl/fl}$ MIC mice in comparison to wildtype MIC mice. The decrease in rpS6 phosphorylation was also persistent upon ablation of 4EBP1 and 4EBP2 within the epithelia of Rheb1$^{fl/fl}$ 4EBP1$^{fl/fl}$ 4EBP2$^{fl/fl}$ MIC mice relative to wildtype MIC controls **(Fig 3A-3B)**. Taken together, these results largely confirm that both mTORC1 activity and consequently S6K function remains perturbed within the Rheb1-deficient mammary epithelia within Rheb1$^{fl/fl}$ 4EBP1$^{fl/fl}$ 4EBP2$^{fl/fl}$ MIC.

c-Myc plays a well-established role in driving expression of both rRNA and various ribosome factors during ribosomal biogenesis (30). The transcriptome analysis of our mammary organoid system revealed an increase in Myc activity, along with an up-regulation of various ribosomal proteins **(Fig 3.5E)**, which argues for increased ribosome biogenesis as an early molecular change within the mammary epithelia upon PyV mT induction. Myc-driven rRNA transcription and ribosomal biogenesis within *Drosophila* whereby activation of the RNA polymerase I transcription factor TIF-1A has been shown to be dependent on S6K function (15, 16). Additionally, S6K has also been shown to be involved in regulating ribosomal biogenesis within hepatocytes through transcriptional modulation of various ribosomal RNA processing protein involved in regulating expression and processing of rRNA such as Rrp15, Rrp12, and Rrp9 (31). Since mTORC1 along with S6K activity remains perturbed within the Rheb1$^{fl/fl}$ 4EBP1$^{fl/fl}$ 4EBP2$^{fl/fl}$ MIC mice that exhibit a persistent a defect in tumor initiation, we sought to examine if S6K or mTORC1 function elicits a prominent contribution to PyV mT-driven tumor initiation independent of eIF4E activation. To address this, we ablated S6K and mTORC1 function with the ATP-mimetic inhibitor Ly2584702 and Rapamycin respectively within our mammary organoid model system derived from the epithelia of wildtype MIC mice. Following the development of mammary acinar structures, PyV mT expression was induced along with the administration of the various inhibitors within the organoid structures for 7 days. Subsequent collection, the growth capacity within the organoid structures was assessed by measuring the average diameter of the organoid structures. Following treatment with either LY2584702 or Rapamycin, we observed reduction in the average size of organoids derived from either wildtype MIC or 4EBP1$^{fl/fl}$ 4EBP2$^{fl/fl}$ MIC mice **(Fig 3.7 C-3.7D)**.

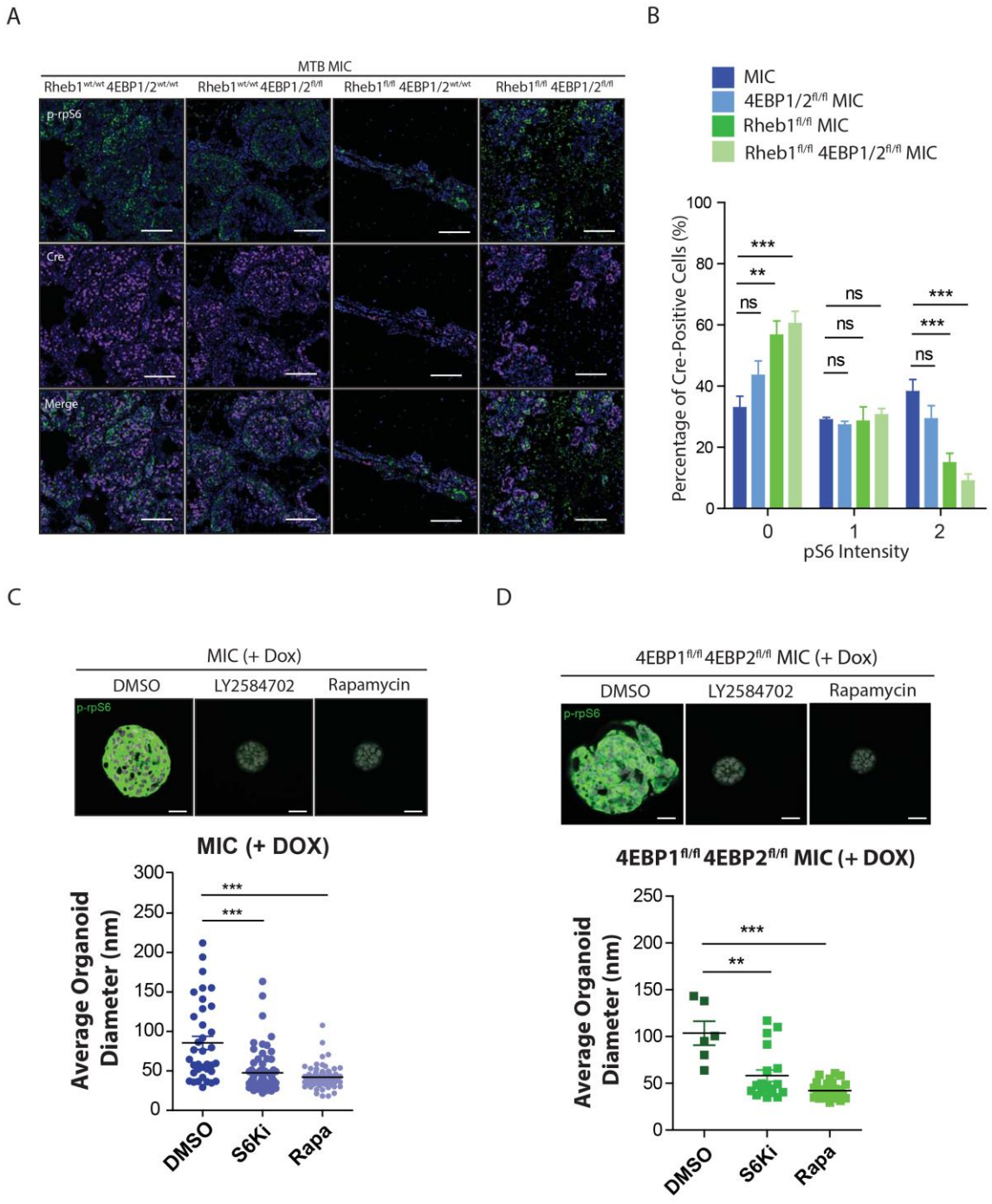

Figure 3. 6 S6 Kinase function is defective within Rheb-deficient pre-neoplastic mammary epithelia within Rheb1$^{fl/fl}$ 4EBP1$^{fl/fl}$ 4EBP2 $^{fl/fl}$ MIC mice. (A) Representative immunohistochemistry staining for p-rpS6 S240/S244 and Cre of mammary ductal structures from mice of the indicated genotypes after 14 days of doxycycline induction. Scale bars represent 100 µm. (B) Graph depicting frequency of intensity grade 0, 1 and 2 of p-rpS6

S240/S244 staining in Cre-positive mammary epithelium from mice of the indicated genotypes after 14 days of doxycycline induction. Values represent mean frequency from at least 300 Cre-positive cells across at least three biological replicates per genotype. Statistical significance was assessed by two-tailed unpaired Student's *t*-test. (C) (D) Top: Representative images of mammary organoids following 8 days of doxycycline induction stained with indicated antibodies. Scale bar represents 25um. Bottom: Graph illustrating average diameter of organoids derived from either wildtype MIC or 4EBP1$^{fl/fl}$ 4EBP2 $^{fl/fl}$ MIC mice, treated with either LY2584702 or Rapamycin. Statistical significance was assessed by Student *t*-test and statistical significance was considered p-value < 0.05.

Taken together these results demonstrate a role for S6K activation is required during the early stages of PyV mT-induced tumor initiation which remains perturbed within Rheb1-deficient pre-neoplastic mammary epithelia of Rheb1$^{fl/fl}$ 4EBP1$^{fl/fl}$ 4EBP2$^{fl/fl}$ MIC mice. Given that we observe S6K activity is rescued within the Rheb1-deficient mammary tumors, the restoration of the S6K signaling axis in addition to de-repression of eIF4E activity may be required to permit tumor initiation of Rheb1-deficient pre-neoplastic epithelia.

A subset of Rheb1-deficient mammary tumors depends on the small GTPase RalB to mediate mTORC1 activation.

Due to the strict temporal control of PyV mT expression within the doxycycline-inducible MIC model system, we are granted more meticulous dissections of the molecular events occurring during early stages of tumor initiation, in addition to the late stages of malignant disease. Molecular events and cellular processes crucial for tumor progression can be accurately inferred by contrasting the changes in tumor biology between these two stages of disease progression. While the PyV mT oncogene is not observed within human cancer, the viral protein does govern growth signalling cascade common to mammalian receptor tyrosine kinases such as HER2 (32). Consequently, we observe common histological and molecular alternation within the developed mammary tumors across both the MIC and NIC model systems. Rheb1-deficient MIC tumours largely exhibited re-activation of mTORC1 in the absence of Rheb1, which is closely recapitulated within the Rheb1-deficient NIC tumours. Across both tumor

systems, a large subset of Rheb1-deficient mammary tumours developed hyperactivating mTOR mutations. Despite this discovery, a distinct subset of Rheb1-deficient mammary tumours carrying wildtype mTOR also exhibited restored mTORC1 activation **(Fig 2.14A-B)**. This observation argues for the presence of a distinct molecular mechanism for mTORC1 activation within these particular Rheb1-deficient mammary tumours. As described previously, amino acid levels govern the recruitment of mTORC1 to the lysosome in proximity to Rheb1 via the Rag heterodimers (33). While amino acid starvation triggers the initial inhibition of mTORC1 activity through the initiating recruitment of TSC1/2 to the lysosome to inhibit Rheb1 (34), prolonged amino acid starvation abrogates the Rheb1-mTOR interaction by ablating lysosomal recruitment of mTORC1 (33, 35). In addition to retaining sensitivity to Akt and ERK1/2 inhibition, mTORC1 activation within the Rheb1-deficient tumour cells also remained sensitive to amino acid withdrawal **(Fig. 3.8B-D)**. As such, we sought to determine if mTORC1 activation within these tumour cells were dependent upon interaction with an alternative small GTPase.

Given the presence of literary *in vivo* evidence for RalB in conferring mTORC1 activation within RalGAP-deficient cells (36), we directed our initial focus on evaluating RalB as a candidate for maintaining mTORC1 activation within Rheb1-deficient mammary tumors. Although RalB expression was not elevated within Rheb1-deficient tumors, we sought to determine level of active RalB within Rheb1-deficient NIC tumors. To address this, Rheb1-deficient NIC tumor lysates along with their wildtype controls were subjected to a RalBP1-GST pulldown assay whereby active RalB is uniquely isolated with the RalBP1 for immunoblot analysis. Despite the variable degree of RalB activation within Rheb1-deficient NIC tumors, some tumors exhibit an enrichment for active RalB **(Fig 3.9A)**. Although RalB hyperactivation is not definitive of functional dependency for mTORC1 activation, this observation at least suggests that regulation of the small GTPase is altered within a subset of Rheb1-deficient NIC tumors in comparison to wildtype NIC controls. As such, we proceeded to functionally assess sensitivity of mTORC1 activity to the small molecule Ral inhibitors BQU57 and RBC8 (37), within a panel of Rheb1-deficient NIC tumor lines. It was demonstrated that ligand-independent assembly of a β3-integrin-RalGDS complex could serve as a mechanism of RalB activation within pancreatic cancer (38). We did observe β3-integrin overexpression within a subset of Rheb1-deficient NIC tumors in comparison with wildtype controls **(Figure 3.10A-30.10B)**, and there was considerable overlap between high β3-integrin expression and high RalB activity

within these tumors **(Fig 3.9A)**. While only a small subset of Rheb1-deficient tumors were preserved as allografts, the Rheb1-deficient NIC tumor line 6333 retained elevated expression of β3-integrin. mTORC1 activity within cell lines derived from this tumor demonstrated greater sensitivity to Ral inhibition than wildtype NIC tumor cells **(Figure 3.10C-3.10F)**. Taken together, these results serve as proof-of-concept that there is a subset of Rheb1-deficient mammary tumors that have developed a dependency on alterative small GTPases such as Ral GTPases, to mediate mTORC1 activation.

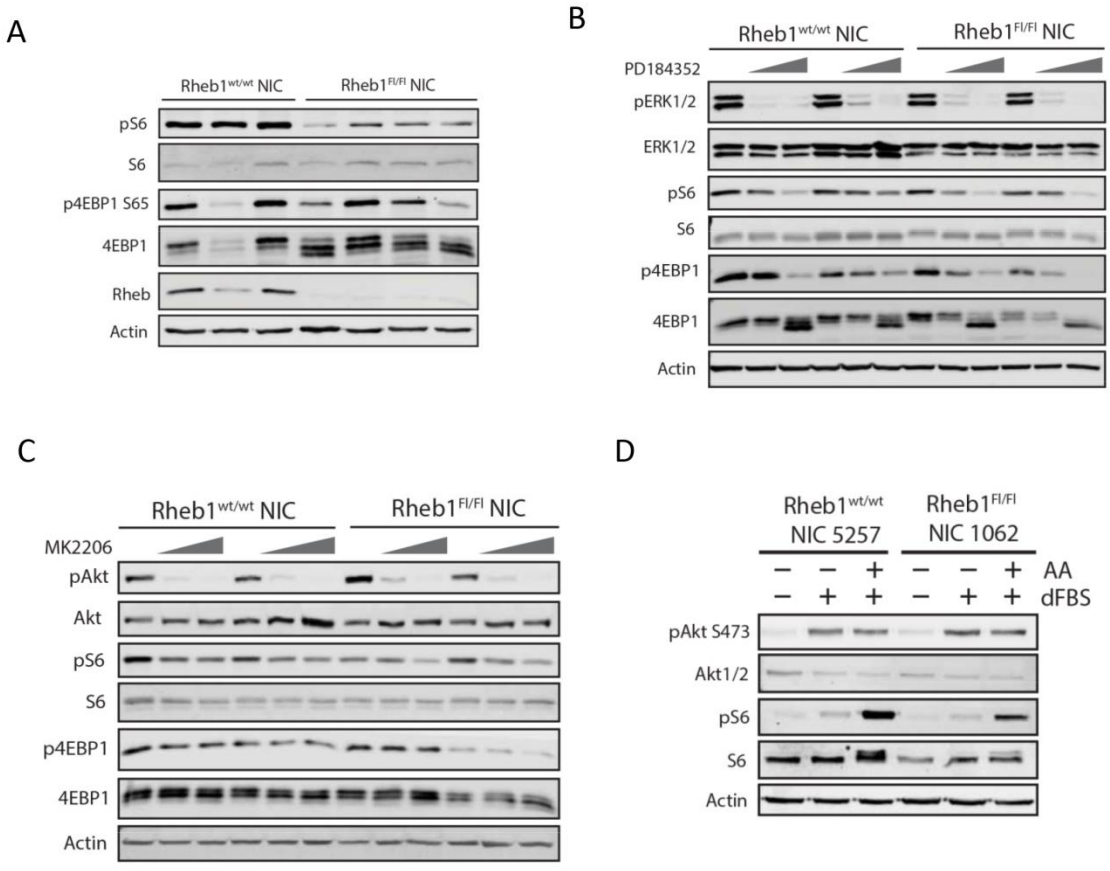

Figure 3. 7 mTORC1 activity within Rheb1-deficient NIC tumor cells are still dependent on Akt and ERK1/2 function, and Amino acid starvation. (A) Immnuoblot of lysate collect primary cell lines dissociated from Rheb1-proficient NIC and Rheb1-deficient NIC tumors probed with the indicated antibodies. (B) Immunoblot of lysate collected from Rheb1$^{wt/wt}$ NIC and Rheb1$^{fl/fl}$ NIC tumor cells treated with MK2206 probed with the indicated antibodies. (C) Immunoblot of lysate collected from

Rheb1-proficient NIC and Rheb1-deficient NIC tumor cells treated with PD058059 probed with the indicated antibodies. Immunoblots within (B) and (C) are representative of three independent experiments. (D) Immunoblot of lysate collected from Rheb1-proficient NIC and Rheb1-deficient NIC tumors cells starved of amino acid, and probed with indicated antibodies.

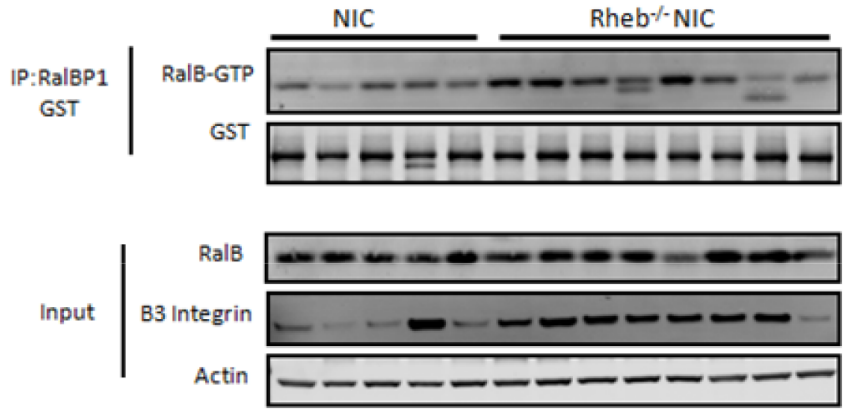

Figure 3. 8 RalBP1-GST pulldown assay reveal elevated RalB activity within a subset of Rheb1-deficient NIC tumors. (A) Pull-down of active GTP-bound Ral GTPase from tumor lysate of Rheb1$^{wt/wt}$ NIC and Rheb1$^{fl/fl}$ NIC tumors with RalBP-GST beads. Input and pull-down samples were analyzed by immunoblot and probed with indicated antibodies.

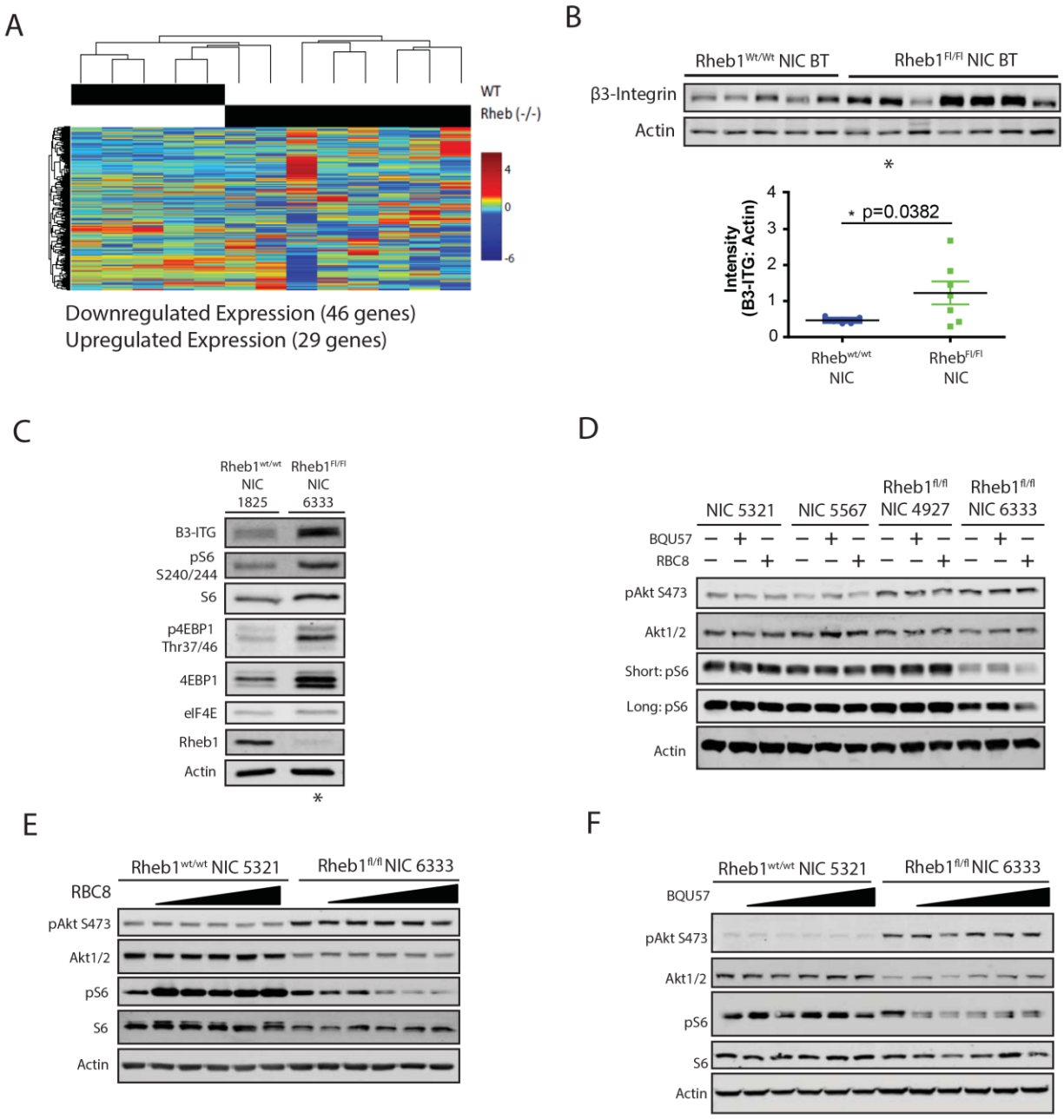

Figure 3. 9 Subset of Rheb1-deficient mammary tumors develops dependency on small GTPase RalB for mTORC1 activation. (A) Heatmap illustrating unsupervised hierarchical clustering of end-stage wildtype NIC and Rheb1-deficient NIC tumors. (B) Immunoblot of lysates collected from end-stages Rheb1-proficient NIC and Rheb1-deficient NIC tumors, probed

with indicated antibodies. **Bottom:** Quantification of immunoblots for indicated protein in (B). Statistical significance was assessed by two-tailed unpaired Student's *t*-test and statistical significance was set at p-value <0.05. (C) Immunoblot analysis of GEMM-derived allografts from Rheb1-proficient NIC and Rheb1-deficient NIC tumors with indicated antibodies. The Rheb1-deficient NIC tumor examined in (C) is derived from the tumor annotated by * in (B). (D) Immunoblot analysis of Rheb1-proficient NIC and Rheb1-deficient NIC tumor cell lines treated with Ral inhibitor BQU57 or RBC8 for 6hrs, probed using the indicated antibodies. Rheb1-deficient NIC tumor cell line 4927 was validated to carry a mTOR mutation via Sanger sequencing. Immunoblot is representative of two independent experiments. (E) (F) Immunoblot analysis of Rheb1-proficient NIC and Rheb1-deficient NIC tumor cell lines treated with varying doses of Ral inhibitor BQU57 or RBC8 for 48hrs, probed using the indicated antibodies.

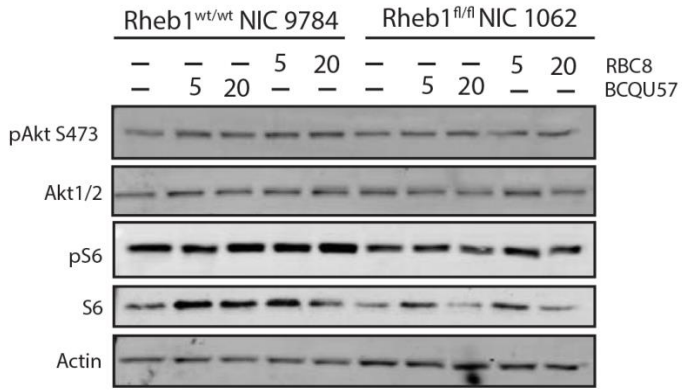

Figure 3. 10 Primary Rheb1-deficient NIC tumor line carrying mTOR mutation exhibit insensitivity to Ral inhibition. (A) Immnuoblot of lysate collect primary cell lines derived from Rheb1-proficient NIC tumor 9784 and Rheb1-deficient NIC tumor 1062 treated with Ral inhibitors RBC8 and BQU57 for 48hrs, probed with the indicated antibodies. Rheb1-deficient NIC tumor 1062 was validated to carry mTOR I2501F mutation by Sanger sequencing. Immunoblot is representative of two independent experiments.

1.5 Discussion

Previously, we demonstrated that disruption of Rheb1-mediated mTORC1 activation blocked mammary tumor initiation within GEMMs of breast cancer (17), and the Rheb1-

deficient mammary tumors that ultimately developed exhibited restored 4EBP1 phosphorylation comparable to Rheb1-proficient tumors. Despite the prominent oncogenic role of eIF4E in the transformation of human mammary epithelial cells *in vitro* (21), we demonstrate through genetic ablation of both 4EBP1 and 4EBP2 that restoring eIF4E activity within the Rheb1-deficient mammary epithelia was insufficient to completely alleviate the defect in tumor initiation **(Fig 3.3D-3.3E)**. While genetic ablation of both 4EBP1 and 4EBP2 proves sufficient to rescue eIF4E-mediated mRNA translation within mouse embryonic fibroblast (39), up-regulation of the 4EBP3 is observed within various human cell lines following long-term mTOR inhibition (40). Although we failed to detect up-regulation of 4EBP3 following long-term mTORC1 inhibition within our model system **(Fig 3.4A-3.4B)**, we cannot exclude the contribution of basal expression of 4EBP3 to eIF4E activity within our model system. Although outside of the scope of this study, it is feasible to speculate that mammary tumors, which develop from $4EBP1^{fl/fl}$ $4EBP2^{fl/fl}$ MIC mice, may gravitate towards up-regulated 4EBP3 expression to maintain homeostatic levels of protein synthesis. Aside from its anti-tumorigenic properties (21), 4EBPs also serve a role in maintaining cell survival by suppressing the energy costly process of mRNA translation during inadequate situations. Taken together, these observations argue that other mTORC1-dependent processes in addition to eIF4E-driven mRNA translation are required to permit formation of mammary tumors in the absence of Rheb1. Through the use of rpS6 S240/S244 phosphorylation, we confirmed that mTORC1 activity and consequentially S6K function remains perturbed within Rheb1-deficient pre-neoplastic epithelia of $Rheb1^{fl/fl}$ $4EBP1^{fl/fl}$ $4EBP2^{fl/fl}$ MIC mice.

In attempts to better dissect the early stages of tumorigenesis, we capitalized on the inducible nature of PyV mT expression within our MIC mouse strain to derive an *in vitro* organoid system for PyV mT-driven tumor initiation. Transcriptome analysis of our organoid system revealed an enrichment for a Myc gene signature which was suggestive of increased Myc activity upon PyV mT induction, along with up-regulation of a ribosome transcriptional program involving various ribosomal proteins **(Fig 3.5D-3.5E)**. Hyper-activated ribosomal biogenesis which entails elevated expression of rRNA as well as increased expression of ribosomal proteins is frequently observed within malignancy (14, 16). Myc is well-established to drive expression of ribosomal RNA (rRNA), which partially composes the ribosome. Given that increased ribosome content supports increased cell proliferation, enhanced ribosomal biogenesis within the pre-

neoplastic epithelia of the inducible PyV mT model would support the rapid expansion of mammary epithelia induced by oncogene expression **(Fig 3.7A)**. Ribosomal protein mRNA including rpS6, frequently contain a 5' TOP motif and exhibit sensitivity to mTORC1 inhibition (41). While S6K were initially implicated in the translation of mRNA containing 5' TOP motifs, that role is challenged by the observation of persistent 5' TOP mRNA translation in the absence of both S6K isoforms (28), as well as within mice carrying non-phosphorylatable rpS6 (42). Meanwhile, the decreased size of PyV mT-driven organoids following LY2584702 treatment **(Fig 3.7C-3.7D)** could be attributed to the reduced ribosome biogenesis brought on by impaired S6K-dependent rRNA expression (16), which is largely eIF4E-independent.

Rheb1-deficient mammary tumors exhibit restored S6K function through re-activation of mTORC1 in a Rheb1-independnent manner **(Fig 3.1A-3.1B)**. We illustrate the possibility that Rheb1-deficient NIC tumours can adopt dependency on alternative small GTPases, such as Ral GTPases, to maintain oncogenic levels of mTORC1 activation. It is of interest to highlight that Rheb1-deficient NIC tumors lines 4927 and 1062 which carry mTOR D2424A and mTOR I2501F mutations, did not exhibit sensitivity to Ral inhibitors BQU57 and RBC8 **(Fig 3.11A)**. This observation demonstrates that the mechanism of mTORC1 re-activation within these Rheb1-deficient tumor lines is independent of RalB. While sensitivity of mTORC1 activity to Ral inhibitors was observed within a limited amount of Rheb1-deficient tumors cell lines, it does demonstrate that certain Rheb1-deficient tumor cells can adopt dependency on distinct small GTPases. Although not addressed within this study, the possibility of Rheb2 contributing to mTORC1 activation within these Rheb1-deficient tumors cannot be excluded. Future work will focus on identifying these alternative small GTPases functioning to maintain mTORC1 activation within Rheb1-deficient NIC tumors.

Through the use of our mouse models of breast cancer, we expanded on our previous finding that genetic ablation of Rheb1 block mammary tumorigenesis within the early stages of tumor initiation. Herein, we demonstrate that restoring eIF4E function was insufficient to permit tumor initiation within the Rheb1-deficient pre-neoplastic epithelia. Mammary tumors ultimately develop by switching dependency to alternative small GTPase such as Ral GTPase, to ensure re-activation of mTORC1 in the absence of Rheb1.

1.6 Experimental Procedure

Experimental Animals. All mice used in study were backcrossed to a pure FVB/N and study was approved by the Animal Resources Centre at McGill University and abided to the guidelines set by the Canadian Council of Animal Care. Female mice were monitored by physical palpation 8 week after birth for tumor development, and were necropsied either 6 weeks post tumor onset or upon exceeding maximal tumor burden allowed by our animal protocol. The MMTV-rtTA strain was obtained from Dr. Lewis Chodosh as previously described (43), and the production of the TetO-MIC mice was described previously (17). The conditional Rheb1 knockout mice were obtained from Dr. Richard Lamb, University of Liverpool. The conditional 4EBP1 and 4EBP2 knockout mice were obtained from Dr. Nahum Sonnenberg, McGill University.

Cell Culture and Cell Lines. Primary cell lines were derived from transgenic tumors as previously described (5), and culture in DMEM media supplemented with 5% FBS, 5ng/mL EGF, 35 ug/mL bovine pituitary extract, 5ug/mL Insulin, 1ug/mL Hydrocortisone. HEK-293T cells were obtained from ATCC® (ATCC® CRL-3216), and cultured in DMEM supplemented with 10% FBS, and penicillin/streptomycin. Amino acid starvation conditions were achieved with amino acid-free DMEM (Multicell, Cat No. 319-004-CL) supplemented with Insulin and Hydrocortisone.

Histological and Immunohistochemical Analysis. Tissue samples were fixed with 10% neutral buffered formalin for 24 hrs and stored in cold 70% ethanol before being paraffin-embedded and sectioned at 4um. Tissue sections were de-paraffinized with xylene, and antigen retrieval was performed in 10mM Citrate buffer (pH 6) using a pressure cooker. Endogenous peroxidase was quenched with 3% Hydrogen Peroxide and sections were blocked with 10% Power Block agent (BioGenex) in PBS for 10 mins prior to overnight incubation with primary antibody at 4^{o}C. Subsequent three PBS washes, sections were incubated with secondary antibody (Vector Elite) for 1hr at room temperature. For fluorescent detection, immunohistochemistry staining was visualized with Tyraminde Signal Amplification reagent (Thermo Fisher Scientific) for 10 minutes per manufacturer's instructions, followed by DAPI stain for 5 minutes. Images of H&E stained tissue sections were obtained using Aperio-XT Slide scanner (Aperio Technologies).

Immunofluorescent images were acquired using an LSM510 Confocal Microscope (Carl Zeiss), and assessed with ZEN software.

Immunoblotting. Lysates were prepared from flash-frozen tumor pieces in RIPA buffer (150mM sodium chloride, 50mM Tris-HCl pH7.4, 2mM EDTA,10m NaF, 10mM Sodium pyrophosphate, 1% sodium deoxycholate, 1% NP-40) supplemented with 1mM sodium orthovanadate, 1mM PMSF, 10mM NaF, 10ug/ul leupeptin and 10ug/ul apotinin. Whole cell lysate was also prepared in RIPA buffer. Protein concentration was quantified by Bradford Assay (Bio-Rad) and 25ug of total protein was resolved by SDS-PAGE, and transferred to Immobilion FL PVDF membranes (Millipore), and block with blocking buffer composed of 3% Casein and 5% BSA. Primary antibodies were diluted in blocking buffer and incubated overnight at 4^{o}C. Secondary fluorophore-conjugated antibodies, IRDye 800 anti-rabbit, IRDye 680 anti-goat and IRDye 680 anti-mouse were incubated for 1hr at room temperature. Immunoblots were scanned with Odyssey CL-X imaging system, and images were processed with Image Studio Lite V4.0.

Antibodies. Immunoblot antibodies include pS6 S240/244 (Cell signaling, Cat# 5364, WB - 1:1000, IHC/IHF – 1:500), Total S6 (Cell signaling, Cat# 2317), p4EBP1 S65 (Cell signaling, Cat# 13443, WB-1:1000, IHC-1:500), p4EBP1 Thr37/46 (Cell signaling, Cat# 2855, WB-1:1000, IHC/IHF-1:500), 4EBP1 (Cell signaling, Cat# 9644, WB-1:1000), 4EBP2 (Cell Signaling, Cat# 2845, WB-1:500), eIF4E (Cell signaling, Cat# 9742, 1:1000), Rheb1 (Cell signalling, Cat# 1387, 1:1000), Cre (Cell signalling, Cat# 12830, IHC/IHF - 1:50), Actin (Sigma, A5316, 1:5000), PyV mT (SC-53481, IHC -1:100), Anti-puromycin (Millipore, Clone 12010 – MABE343, 1:1000), E-Cadherin (BD Bioscience, Cat# 610182, 1:100), PCNA (Cell Signaling, Cat# 13110) and Alexa Fluor 488 Phallodin stain (ThermoFisher Scientific, A12379). Goat anti-rabbit IRDye 800, and Goat anti-mouse IRDye 680 secondary antibody (Li-COR, 925-32211, 925-68070, 1:10 000).

RNA analysis.

RNA was collected from mammary tumors and organoid using the RNEasy mini Kit (Qiagen, Cat# NC9677589). cDNA for qRT-PCR was prepared using TransScript All-in-One First-Strand cDNA Synthesis kit (Civic Bioscience, AH341) according to the manufacturer's protocol. RT-

PCR was conducted using LightCycler 480 and SYBR Green I master mix (Roche, Cat# 04707516001). RNAseq analysis and bioinformatics analysis was conducted through Novogene. The microarray analysis was conducted with Genome Quebec Innovation Centre.

Isolation of Primary Mammary Epithelia and Growth of Mammary Organoids.

The 2nd, 3rd, 4th and 5th pairs of mammary glands were collected from mouse necropsy. Collectively, the mammary glands were minced using scissors and incubated within digestion medium (DMEM/F12 supplied with 100µg/ml Pen/Strep, 50µg/ml Gentamicin, and 20mg of Collagenase) for 1.5hrs at 37^{o}c with constant mixing. After the 1.5hr incubation, the epithelial cells were pelleted by centrifugation at 1000rpm for 5 minutes and subjected to repeated washes with PBS with 5% FBS 5 times. The organoids were subjected to trypsin/EDTA treatment with frequent mixing. Subsequently, trypsin was neutralized with calf serum and the supernatant was passed through a 45µm strainer. The single cells pelleted and re-suspended in Mammary Epithelial Cell growth medium and seeded on sterile coverslips layered with 15µl of Geltrex. Primary epithelial cells were growth for 7 days to allow development of

Quantification and Statistical Analysis

All statistical analysis was completed using GraphPad software. Two-tailed Student *t*-tests, and log-rank Mantel-Cox tests were applied accordingly. The results of the statistical tests can be found within the figures, and the figure legends.

1.7 Reference

1. Andrechek ER, *et al.* (2003) Gene expression profiling of neu-induced mammary tumors from transgenic mice reveals genetic and morphological similarities to ErbB2-expressing human breast cancers. *Cancer research* 63(16):4920-4926.
2. Guy CT, Cardiff RD, & Muller WJ (1992) Induction of mammary tumors by expression of polyomavirus middle T oncogene: a transgenic mouse model for metastatic disease. *Molecular and cellular biology* 12(3):954-961.
3. Guy CT, *et al.* (1992) Expression of the neu protooncogene in the mammary epithelium of transgenic mice induces metastatic disease. *Proceedings of the National Academy of Sciences of the United States of America* 89(22):10578-10582.
4. Huck L, Pontier SM, Zuo DM, & Muller WJ (2010) beta1-integrin is dispensable for the induction of ErbB2 mammary tumors but plays a critical role in the metastatic phase of tumor progression. *Proceedings of the National Academy of Sciences of the United States of America* 107(35):15559-15564.

5. Bui T, *et al.* (2019) Functional Redundancy between β1 and β3 Integrin in Activating the IR/Akt/mTORC1 Signaling Axis to Promote ErbB2-Driven Breast Cancer. *Cell reports* 29(3):589-602.e586.
6. Buttgereit F & Brand MD (1995) A hierarchy of ATP-consuming processes in mammalian cells. *The Biochemical journal* 312 (Pt 1):163-167.
7. Ma XM & Blenis J (2009) Molecular mechanisms of mTOR-mediated translational control. *Nature reviews. Molecular cell biology* 10(5):307-318.
8. Pelletier J & Sonenberg N (1985) Insertion mutagenesis to increase secondary structure within the 5' noncoding region of a eukaryotic mRNA reduces translational efficiency. *Cell* 40(3):515-526.
9. Laplante M & Sabatini DM (2012) mTOR signaling in growth control and disease. *Cell* 149(2):274-293.
10. Thomson E, Ferreira-Cerca S, & Hurt E (2013) Eukaryotic ribosome biogenesis at a glance. *Journal of cell science* 126(Pt 21):4815-4821.
11. Yang H, *et al.* (2017) Mechanisms of mTORC1 activation by RHEB and inhibition by PRAS40. *Nature* 552(7685):368-373.
12. Long X, Lin Y, Ortiz-Vega S, Yonezawa K, & Avruch J (2005) Rheb binds and regulates the mTOR kinase. *Current biology : CB* 15(8):702-713.
13. Wolfe AL, *et al.* (2014) RNA G-quadruplexes cause eIF4A-dependent oncogene translation in cancer. *Nature* 513(7516):65-70.
14. Mayer C & Grummt I (2006) Ribosome biogenesis and cell growth: mTOR coordinates transcription by all three classes of nuclear RNA polymerases. *Oncogene* 25(48):6384-6391.
15. Mitchell NC, *et al.* (2015) S6 Kinase is essential for MYC-dependent rDNA transcription in Drosophila. *Cellular signalling* 27(10):2045-2053.
16. Hannan KM, *et al.* (2003) mTOR-dependent regulation of ribosomal gene transcription requires S6K1 and is mediated by phosphorylation of the carboxy-terminal activation domain of the nucleolar transcription factor UBF. *Molecular and cellular biology* 23(23):8862-8877.
17. Xiao B, *et al.* (2020) Rheb1-Independent Activation of mTORC1 in Mammary Tumors Occurs through Activating Mutations in mTOR. *Cell reports* 31(4):107571.
18. Rao T, *et al.* (2014) Inducible and coupled expression of the polyomavirus middle T antigen and Cre recombinase in transgenic mice: an in vivo model for synthetic viability in mammary tumour progression. *Breast cancer research : BCR* 16(1):R11.
19. Sonenberg N & Hinnebusch AG (2009) Regulation of translation initiation in eukaryotes: mechanisms and biological targets. *Cell* 136(4):731-745.
20. Furic L, *et al.* (2010) eIF4E phosphorylation promotes tumorigenesis and is associated with prostate cancer progression. *Proceedings of the National Academy of Sciences of the United States of America* 107(32):14134-14139.
21. Avdulov S, *et al.* (2004) Activation of translation complex eIF4F is essential for the genesis and maintenance of the malignant phenotype in human mammary epithelial cells. *Cancer cell* 5(6):553-563.
22. Thoreen CC, *et al.* (2012) A unifying model for mTORC1-mediated regulation of mRNA translation. *Nature* 485(7396):109-113.
23. Alain T, *et al.* (2012) eIF4E/4E-BP ratio predicts the efficacy of mTOR targeted therapies. *Cancer research* 72(24):6468-6476.

24. Mroue R & Bissell MJ (2013) Three-dimensional cultures of mouse mammary epithelial cells. *Methods in molecular biology (Clifton, N.J.)* 945:221-250.
25. Hannan KM, Thomas G, & Pearson RB (2003) Activation of S6K1 (p70 ribosomal protein S6 kinase 1) requires an initial calcium-dependent priming event involving formation of a high-molecular-mass signalling complex. *The Biochemical journal* 370(Pt 2):469-477.
26. Pearson RB, *et al.* (1995) The principal target of rapamycin-induced p70s6k inactivation is a novel phosphorylation site within a conserved hydrophobic domain. *Embo j* 14(21):5279-5287.
27. Espeillac C, *et al.* (2011) S6 kinase 1 is required for rapamycin-sensitive liver proliferation after mouse hepatectomy. *The Journal of clinical investigation* 121(7):2821-2832.
28. Pende M, *et al.* (2004) S6K1(-/-)/S6K2(-/-) mice exhibit perinatal lethality and rapamycin-sensitive 5'-terminal oligopyrimidine mRNA translation and reveal a mitogen-activated protein kinase-dependent S6 kinase pathway. *Molecular and cellular biology* 24(8):3112-3124.
29. Roux PP, *et al.* (2007) RAS/ERK signaling promotes site-specific ribosomal protein S6 phosphorylation via RSK and stimulates cap-dependent translation. *The Journal of biological chemistry* 282(19):14056-14064.
30. van Riggelen J, Yetil A, & Felsher DW (2010) MYC as a regulator of ribosome biogenesis and protein synthesis. *Nature reviews. Cancer* 10(4):301-309.
31. Chauvin C, *et al.* (2014) Ribosomal protein S6 kinase activity controls the ribosome biogenesis transcriptional program. *Oncogene* 33(4):474-483.
32. Fluck MM & Schaffhausen BS (2009) Lessons in signaling and tumorigenesis from polyomavirus middle T antigen. *Microbiology and molecular biology reviews : MMBR* 73(3):542-563, Table of Contents.
33. Sancak Y, *et al.* (2008) The Rag GTPases bind raptor and mediate amino acid signaling to mTORC1. *Science (New York, N.Y.)* 320(5882):1496-1501.
34. Demetriades C, Plescher M, & Teleman AA (2016) Lysosomal recruitment of TSC2 is a universal response to cellular stress. *Nature communications* 7:10662.
35. Sancak Y, *et al.* (2010) Ragulator-Rag complex targets mTORC1 to the lysosomal surface and is necessary for its activation by amino acids. *Cell* 141(2):290-303.
36. Martin TD, *et al.* (2014) Ral and Rheb GTPase activating proteins integrate mTOR and GTPase signaling in aging, autophagy, and tumor cell invasion. *Molecular cell* 53(2):209-220.
37. Yan C, *et al.* (2014) Discovery and characterization of small molecules that target the GTPase Ral. *Nature* 515(7527):443-447.
38. Seguin L, *et al.* (2014) An integrin β_3-KRAS-RalB complex drives tumour stemness and resistance to EGFR inhibition. *Nature cell biology* 16(5):457-468.
39. Dowling RJ, *et al.* (2010) mTORC1-mediated cell proliferation, but not cell growth, controlled by the 4E-BPs. *Science (New York, N.Y.)* 328(5982):1172-1176.
40. Tsukumo Y, Alain T, Fonseca BD, Nadon R, & Sonenberg N (2016) Translation control during prolonged mTORC1 inhibition mediated by 4E-BP3. *Nature communications* 7:11776.
41. Meyuhas O & Kahan T (2015) The race to decipher the top secrets of TOP mRNAs. *Biochimica et biophysica acta* 1849(7):801-811.

42. Ruvinsky I, *et al.* (2005) Ribosomal protein S6 phosphorylation is a determinant of cell size and glucose homeostasis. *Genes & development* 19(18):2199-2211.
43. Gunther EJ, *et al.* (2002) A novel doxycycline-inducible system for the transgenic analysis of mammary gland biology. *Faseb j* 16(3):283-292.

4.0 General Discussion

At the start of this thesis work, the small GTPase Rheb1 was already well-established uniquely as the obligatory activator of mTORC1. mTORC1 is a master regulator of cellular growth which is frequently dysregulated within cancer, thus rendering it an enticing therapeutic target. This was illustrated through studies examining the effects of mTORC1 inhibition on cancer cell growth through either a pharmacological approach with the inhibitor Rapamycin (1, 2), or a genetic approach of targeting the mTORC1 scaffolding protein Raptor (3, 4).Within the context of breast cancer, studies were mostly centered around already transformed cells (1, 5-7) while evaluation of mTORC1 function during the transition of pre-neoplastic cells into transformed state was still lacking. To address this, we decided to interrogate this unexplored avenue within a biologically relevant context using mouse models of breast cancer.

4.1 Rheb1-dependent mTORC1 activation is crucial within the pre-neoplastic mammary epithelia during tumor initiation.

It is of interest to highlight that Rheb1-dependent, but mTORC1-independent functions of the small GTPase have been documented within the literature. Such functions include mediating mitophagy (8) and regulating subcellular segregation of misfolded proteins (9). Amidst these Rheb1-dependent functions, we demonstrated in Chapter 2 that disruption of mTORC1 activation was sufficient to closely recapitulate the block in tumor progression caused by Rheb1 ablation **(Fig 2.9A-D)**. This was not entirely unexpected as mTORC1 serves as a crucial signaling node in conveying growth signals required for cell proliferation, by modulating various cellular processes described above. Although the relative contribution of these mTORC1-mediated processes have yet to be dissected during the early stages of the tumor initiation, this thesis work is mainly focused around its role in the regulation of mRNA translation over this particular stage of tumor progression.

As aforementioned above, the small GTPase Rheb1 was unique in its capacity to activate mTORC1 within biochemical *in vitro* kinase assays (10). This is also highlighted within *in vivo* observations from germ-line deletion of either Rheb1 or the Raptor subunit, whereby genetic ablation of either genes phenocopied embryonic lethality (11, 12). Although the closely related isoform Rheb2 (or RhebL1) demonstrated the capacity to activate mTORC1 within an *in vitro* kinase assay, it remains controversial whether Rheb2 prominently contributes to mTORC1

regulation *in vivo* as mTORC1 activity is sustained upon ablation of Rheb2 (13). Thus far, a thorough interrogation into Rheb1-independent modes of mTORC1 activation is still lacking and may be limited by the lethality of Rheb1 ablation. Nevertheless, it was demonstrated that hyperactivation of the small GTPase RalB through genetic ablation of RalGAP did result in mTORC1 activation in a Rheb1-independent manner within pancreatic cancer cells (14). While this does conflict with previous *in vitro* mTOR kinase results, these *in vivo* observations do highlight the potential of alternative small GTPases driving mTORC1 activation. Despite this, we demonstrated within Chapter 2 that genetic ablation of Rheb1 was sufficient to ablate mTORC1 activation within the pre-neoplastic mammary epithelia of both a PyV mT-driven, and an ErbB2-driven model system (15). These observations argue that amidst the presence of alternative small GTPases, Rheb1 remains unique for its role within mammary tumor initiation. This may be attributed to differences between the preferential subcellular localization of Rheb1 and RalB. While active RalB is concentrated at the plasma membrane (16-18), Rheb1 and Rheb2 are localized to the endomembranes due to their CAAX motif sequences (19). Given its unique role, Rheb1 cancer therapeutics was previously evaluated through as cancer therapeutic target through the use of farnesyltransferase inhibitors (FTI) which disrupted the proximal localization of Rheb1 to mTORC1 (20). Albeit disrupting the Rheb1-mTORC1 interaction did demonstrate anti-cancer effects (21, 22), a major caveat within this therapeutic strategy was that FTIs also disrupted proper localization of the small GTPase Ras. However, future therapeutic interventions specifically targeting the small GTPase have become more plausible with the recent discovery of a small molecule inhibitor for Rheb1 (23).

4.2 Differential contribution of the S6K and eIF4E signaling axis within mammary tumor initiation.

The contribution of mTORC1 to the regulation of mRNA translation stems primarily from modulating the downstream effectors S6K1/2 and the 4EBPs. Since S6K1/2 and the 4EBPs contribute different roles to protein synthesis as detailed within Chapter 1, the translation of various transcripts have demonstrated differential sensitivity to perturbation of either S6K or eIF4E (24, 25). Consequentially, the relative contribution between these two mTORC1 effectors to tumor initiation varies across different tumor types. Disruption of S6K-mediated suppression of eEFK was sufficient to significantly perturb the initiation of intestinal tumorigenesis in a

eIF4E-independent manner (24), while alteration to eIF4E function was sufficient to perturb the initiation of prostate cancer, Ras-mediated lung cancer and Myc-driven lymphomas (26-28). Thus far, a detailed dissection of the relative contribution for these two mTORC1 effectors within mammary tumors initiation is still lacking. Stemming from our initial observations from Chapter 2, whereby ablation of Rheb1 resulted in suppression of both S6K and eIF4E function, we decided to evaluate the relative contribution of eIF4E activity to the block in PyV mT-driven tumor initiation exhibited by the Rheb1-deficient pre-neoplastic epithelia. Due to the evolutionary nature of tumorigenesis, cellular processes crucial for cancer cell growth tend to be preserved during disease progression. Based on this tenet, we can infer which processes would be indispensable for the development of Rheb1-deficient tumors, by contrasting the status of the downstream effectors of mTORC1 between the Rheb1-deficient pre-neoplastic state, and Rheb1-deficient neoplastic state. Within Chapter 2, we observed comparable levels of 4EBP1 phosphorylation, along with restored translation of eIF4E-sensitive targets within the arising Rheb1-deficient mammary tumors compared to Rheb1-proficient mammary tumors. Meanwhile, S6K activity was restored to comparable levels as Rheb1-proficient mammary tumors within only a portion of the Rheb1-deficient tumors **(Fig 2.11A-2.11B)**. Based on these observations, we initially speculated that PyV mT-driven mammary tumor initiation may be highly dependent on eIF4E activity; as such the re-activation of eIF4E activation was the driving event in permitting tumor progression in the absence of Rheb1. While we did observe a modest rescue in the PyV mT-driven expansion of mammary epithelia within the $Rheb1^{fl/fl}$ $4EBP1^{fl/fl}$ $4EBP2^{fl/fl}$ MIC mice relative to the $Rheb1^{fl/fl}$ MIC controls; however, tumor initiation remained perturbed despite restoring eIF4E function **(Fig 3.3 D-3.3E)** This observation argues that solely restoring eIF4E function alone is insufficient to drive PyV mT-mediated tumor initiation in the absence of Rheb1, whereby other mTORC1-dependent or Rheb1-dependent functions are required in conjunction to permit tumor progression.

In attempts to gain a deeper insight of the cellular processes altered during the early stages of PyV mT-driven tumor initiation, we examined the transcriptional changes within an *in vitro* organoid system derived from the mammary epithelia of wildtype MIC mice upon induction of PyV mT. Transcriptome analysis revealed an enrichment of a Myc gene signature along with increased expression of a large panel of ribosomal proteins within the mammary organoids upon induction of PyV mT expression in comparison with un-induced controls **(Fig**

3.5E). Taken together, these observations suggested for an up-regulation of Myc activity early on within the pre-neoplastic epithelia during tumor initiation.

Upon induction of PyV mT expression within the mammary epithelia of the MIC strain, we can observe increased cell proliferation and rapid expansion of the mammary epithelia from 1-2% to 20-30% of total area of the mammary gland within a 14 day period. Given that elevated protein synthesis creates the necessary cell mass to sustain increased cellular growth, we thought restoring eIF4E-mediated protein synthesis would be sufficient to support this aggressive epithelial expansion. Increased ribosomal biogenesis which would additionally support the increase demand in cell mass required for such aggressive cellular growth. S6K has been established to participate in various roles during ribosomal biogenesis, including driving transcriptional up-regulation of a large panel of ribosomal proteins (29), as well as inducing expression of the 47S pre-RNA (30-32). Correspondingly, targeting S6K with either the S6K-specific inhibitor Ly-2584702, or Rapamycin, decreased the average size of PyV mT-driven mammary organoids **(Fig 3.7C-3.7D)**. Given S6K activity remained inhibited within the Rheb1-deficient pre-neoplastic epithelial cells of Rheb1$^{fl/fl}$ 4EBP1$^{fl/fl}$ 4EBP2$^{fl/fl}$ MIC mice; we speculated that the persistent disruption in tumor initiation may also be attributed to a block in PyV mT-driven induction of ribosomal biogenesis.

It is well-established that up-regulated eIF4E activity, either through inhibition of 4EBPs or though increase of eIF4E:4EBP ratio, increases rates of protein synthesis by enhancing the ribosome scanning efficiency. Increased ribosome biogenesis may alter the translatome by increasing the abundance of the ribosome machinery recruited to transcripts in an eIF4E-independent manner. Given these two processes function distinctly to modulate the translatome, it is feasible to speculate that S6K-mediated stimulation of ribosomal biogenesis in conjunction with increased eIF4E-dependent mRNA translation could provide compounded effects on tumor initiation. As such, further investigation involving the restoration of S6K function within the Rheb1-deficient pre-neoplastic epithelia of Rheb1$^{fl/fl}$ 4EBP1$^{fl/fl}$ 4EBP2$^{fl/fl}$ MIC mice is necessary, and the details of generating such a novel mouse strain to fulfill the aforementioned criteria are described within my future directions.

4.3 Hyperactivating mTOR mutations contribute to eliciting Rheb1-independent mTORC1 activation.

Various components of the PI3K-mTOR signaling cascade are frequently altered within cancer. Hyperactivating mutations within mTOR have been previously documented from various cancer types including renal carcinoma, lung cancer and breast cancer (33-37). Within Chapter 2, we uniquely uncovered mTOR mutations within the Rheb1-deficient tumors which originated from both the NIC and MIC model systems through Sanger sequencing **(Fig 2.14A-2.14B)**. Across the panel of mTOR mutations uncovered, we demonstrated that the mTOR I2501F and I1417T mutations were sufficient to elicit Rheb1-independence within the 293T cell system, whereas other mTOR mutations retained sensitivity to Rheb1 depletion **(Fig 2.15A-2.15B)**. This discrepancy between the two cell systems can potentially be attributed to additional alterations accumulated along tumor progression by Rheb1-deficient mammary tumors which would confer complete Rheb1-independent mTORC1 activation in conjunction with mTOR mutations. An inherent limitation to the study was that the mTOR mutations could only be exogenously introduced into the 293T system due to technical limitations, but would have been more representative within a breast cancer cell line such as BT474 or SkBr3 could be potential accomplished through CRISPR-mediated gene editing.

Multiple working models have been proposed to better understand the hyperactivating nature of various mTOR mutations, including intrinsic increased kinase activity (34) and decreased avidity for the inhibitor Deptor (33, 35). These examples begin to illustrate the heterogeneous nature of mTOR mutations whereby distinct mutations along the kinase can elicit distinct functional consequences, in the meanwhile a large subset of these documented mTOR mutations have not been characterized (36, 37). Given all mutations uncovered within Rheb1-deficient tumors were not localized to the ATP-catalytic pocket, the mode of action of these mTOR mutations and how they would confer Rheb1-independence within our tumor context was not intuitive. Recent Cryo-EM structure of Rheb1-bound mTORC1 have provided insight into the Rheb1-induced conformational changes within mTOR (38), whereby mTOR mutations were inferred to recapitulate some of these conformational changes elicited by Rheb1 binding. Based on that, it is feasible to think activation of mTORC1 may become less dependent on Rheb1 binding in the presence of certain mTOR mutations, albeit certain mTOR mutations alone as

such mTOR T1977K (15) or mTOR T1977R (34) are insufficient to confer complete Rheb1-independency within the 293T cell system.

While it is well-established that the direct Rheb1-mTOR interaction is crucial for mTORC1 activation and structural details of this interaction are now available, it would be of interest to explore how mTOR mutations could either directly or allosterically alter this interaction. While this avenue remains to be addressed within the literature, it is tantalizing to speculate that certain mTOR mutations could alter the avidity for Rheb1 or potentially other small GTPases, as mTOR mutations that confer altered avidity to other interactors such as Deptor (mTOR L1460P and C1483F) and FKBP12 (mTOR A2034V and F2108L) have been reported (33, 35, 39).

Alternatively, the unique capacity of Rheb1 to activate mTORC1 amidst the two reported alternative GTPases RalB and Rheb2, could be attributed to different avidities within each GTPase for mTOR. It has been demonstrated that the hyperactive RalB Q72L mutant, which exhibits persistent GTP-bound status due to reduced intrinsic and GAP-mediated GTPase activity (40), confers increased avidity to mTOR in comparison to wildtype RalB, and is sufficient to elicit more robust mTORC1 activation (14). While we did demonstrate mTORC1 activation responding to Ral inhibitors within a small subset of Rheb1-deficient NIC tumor lines, the underlying mechanism behind this phenomenon is still lacking. Based on our observations with Ral inhibitor response **(Fig 3.10D; Fig 3.11A)**, it is feasible to speculate that mTORC1 activation within distinct Rheb1-deficient mammary tumors may be dependent on these alternative small GTPases. The further elucidation on the exact identity of these other alternative GTPases acting on mTORC1 within distinct Rheb1-deficient mammary tumors is required.

4.4 mTOR functions are indispensable for mammary tumor initiation.

Provided that mTOR conveys a kinase function central to both mTORC1 and mTORC2, it wasn't unexpected that genetic ablation of mTOR would prominently disrupt mammary tumor initiation with our ErbB2-driven tumor system **(Fig 2.16B)**. Disruption of mTORC2 function through genetic ablation of the scaffolding component Rictor delayed ErbB2-driven mammary tumorigenesis (41), while disruption of mTORC1 function through genetic ablation of the scaffolding component Raptor, demonstrated within Chapter 2, also drastically impaired the initiation of mammary tumors. Nuclear roles of mTOR also have been documented, within

prostate cancer, which contribute to transcriptional regulation of cellular glucose metabolism and lipid synthesis (42). While nuclear mTOR is not prominently present within our mammary tumor system, we cannot exclude its involvement within the early stages of mammary tumor initiation within mTOR$^{fl/fl}$ NIC mice. Regardless, the complete abolishment of tumor development as a result of genetic ablation of mTOR argues for the uniqueness of its kinase role.

The scaffolding protein Raptor is absolutely crucial for mTORC1 function as it elicits the unique role of recruiting downstream effectors (43-45). While we did observe loss of mTORC1 activity within the pre-neoplastic epithelia of Raptor$^{fl/fl}$ MIC mice **(Fig 2.7E-2.7F)**, mTORC1 activity was ultimately restored within the mammary tumors that arose from both the conditional Raptor$^{fl/fl}$ MIC and Raptor$^{fl/fl}$ NIC mouse strains **(Fig 4.1D-F)**. This observation along with the observation that mTORC1 function is restored within our Rheb1-deficient tumor models, argues for the strong selection for events that allow mTORC1 activation in order to permit tumor initiation within our mouse models. Intrigued by this observation, we investigated further into the molecular mechanisms allowing for the maintenance of mTORC1 activity within these mammary tumors. Through biochemical analyses and Sanger sequencing, we uncovered that Raptor expression was being retained within the arising mammary tumors due to the ablation of Cre-mediated excision of the LoxP site-flanked DNA segments. While this is the first documentation of this phenomenon within our model system where both oncogene and Cre recombinase are co-expressed, all mammary tumors that developed from both Raptor$^{fl/fl}$ MIC and Raptor$^{fl/fl}$ NIC mouse strains seemingly retained expression of Raptor. Although our interrogation into the underlying molecular mechanism was not extensive, we did uncover genetic loss of a LoxP site along within flanking DNA segments, within one tumor sample. Taken together, these observations further emphasize the requirement for mTORC1 activation during tumor initiation as only pre-neoplastic epithelium with retained Raptor expression ultimately proceed into end-stage tumors.

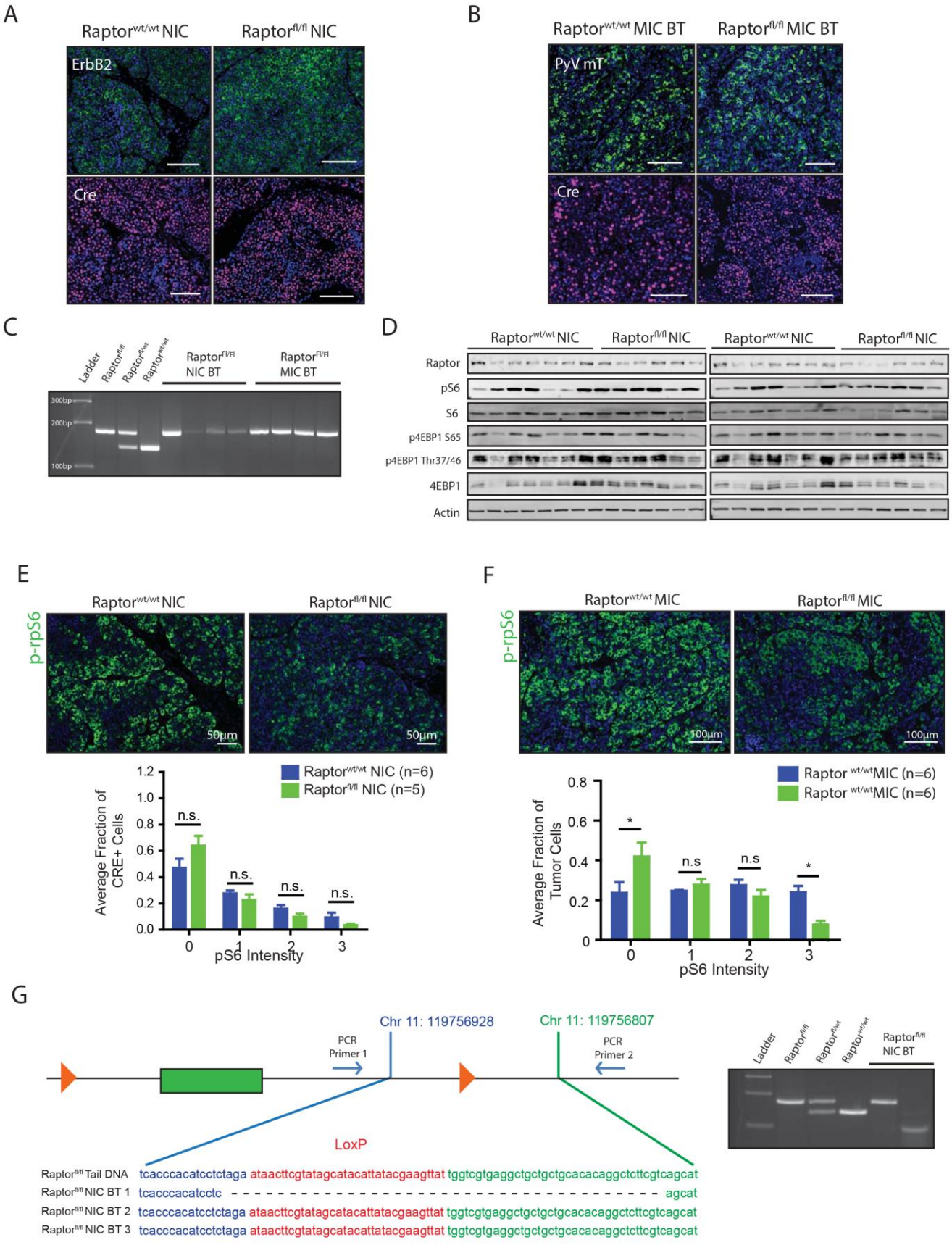
A
Raptor^wt/wt NIC
Raptor^fl/fl NIC
ErbB2
Cre
B
Raptor^wt/wt MIC BT
Raptor^fl/fl MIC BT
PyV mT
Cre
C
Ladder
Raptor^fl/fl
Raptor^fl/wt
Raptor^wt/wt
Raptor^Fl/Fl NIC BT
Raptor^Fl/Fl MIC BT
300bp
200bp
100bp
D
Raptor^wt/wt NIC
Raptor^fl/fl NIC
Raptor^wt/wt NIC
Raptor^fl/fl NIC
Raptor
pS6
S6
p4EBP1 S65
p4EBP1 Thr37/46
4EBP1
Actin
E
Raptor^wt/wt NIC
Raptor^fl/fl NIC
p-rpS6
50μm
50μm
Raptor^wt/wt NIC (n=6)
Raptor^fl/fl NIC (n=5)
Average Fraction of CRE+ Cells
n.s.
pS6 Intensity
F
Raptor^wt/wt MIC
Raptor^fl/fl MIC
p-rpS6
100μm
100μm
Raptor ^wt/wt MIC (n=6)
Raptor ^wt/wt MIC (n=6)
Average Fraction of Tumor Cells
*
n.s
pS6 Intensity
G
Chr 11: 119756928
Chr 11: 119756807
PCR Primer 1
PCR Primer 2
LoxP
Raptor^fl/fl Tail DNA tcacccacatcctctaga ataacttcgtatagcatacattatacgaagttat tggtcgtgaggctgctgctgcacacaggctcttcgtcagcat
Raptor^fl/fl NIC BT 1 tcacccacatcctc - agcat
Raptor^fl/fl NIC BT 2 tcacccacatcctctaga ataacttcgtatagcatacattatacgaagttat tggtcgtgaggctgctgctgcacacaggctcttcgtcagcat
Raptor^fl/fl NIC BT 3 tcacccacatcctctaga ataacttcgtatagcatacattatacgaagttat tggtcgtgaggctgctgctgcacacaggctcttcgtcagcat
Ladder
Raptor^fl/fl
Raptor^fl/wt
Raptor^wt/wt
Raptor^fl/fl NIC BT

Figure 4. 1 Mammary Tumors Arising from Raptor$^{fl/fl}$ NIC and Raptor$^{fl/fl}$ MIC mice retain Raptor expression. (A) Immunofluorescence staining of Raptor$^{wt/wt}$ NIC and Raptor$^{fl/fl}$ NIC tumor sections for ErbB2 and Cre. Scale bar represents 50µm. (B) Immunofluorescence staining of Raptor$^{wt/wt}$ MIC and Raptor$^{fl/fl}$ MIC tumor sections for PyV mT and Cre. Scale bar represents 50µm. (C) Agarose gel showing genotyping PCR on DNA isolated from Raptor$^{fl/fl}$ NIC and Raptor$^{fl/fl}$ MIC tumor. (D) Western blot analysis of Rheb1$^{wt/wt}$ NIC and Rheb1$^{fl/fl}$ NIC tumor protein extract with indicated antibodies. (E) Top: Immunofluorescence staining of Raptor$^{wt/wt}$ NIC and Raptor$^{fl/fl}$ NIC tumor sections for p-rpS6 S240/244. Scale bar represents 50µm. Bottom: Graph depicting frequency of grade 1, 2 and 3 p-rpS6 S240/244 staining in mammary tumors collected from Raptor$^{wt/wt}$ NIC and Raptor$^{fl/fl}$ NIC mice at tumor endpoint. Statistical significance was assess by Student *t*-test and significance was set at $p<0.05$. (F) Top: Immunofluorescence staining of Raptor$^{wt/wt}$ MIC and Raptor$^{fl/fl}$ MIC tumor sections for p-rpS6 S240/244. Scale bar represents 50µm. Bottom: : Graph depicting frequency of grade 1, 2 and 3 p-rpS6 S240/244 staining in mammary tumors collected from Raptor$^{wt/wt}$ NIC and Raptor$^{fl/fl}$ NIC mice at tumor endpoint. Statistical significance was assess by Student *t*-test and significance was set at $p<0.05$. (G) Cartoon schematic illustrating the region of one LoxP site within Raptor gene from DNA collected from Raptor$^{fl/fl}$ NIC tumors, as determined by Sanger sequencing.

4.5 Experimental Limitations and Future Directions

Within this section, I highlighted some experimental limitations and additional suggestion to the described thesis work which future studies could improve and expand upon.

While we were able to uncover mTOR mutations within our Rheb1-deficient tumor models within Chapter 2, an inherent limitation at the time of this study was that the frequency of mTOR mutations within the tumor cell population could not be ascertained through Sanger sequencing. A single-cell sequencing approach would have allowed for examination of the frequency of tumor cells carrying mTOR mutations within our bulk Rheb1-deficient NIC tumors. Since mTORC1 remained crucial within our Rheb1-deficient tumor, it was feasible to speculate that the development of mTOR mutations would be an early event that would permit tumor progression in the absence of Rheb1. As such, the entire tumor cell population would be

populated by cells encompassing a common mTOR mutation. Conversely, mTOR mutations could have also developed during a later stage of tumor progression where theses genetic alterations simply conferred a growth advantage to Rheb1-deficient tumor cells, thus allowing enrichment of this cell population within the tumor. Single-cell sequencing would reveal a large portion of the tumor cell population would carry a common mTOR mutation but not all tumor cells. While mTOR mutations were not detected within Rheb1-proficient tumors by Sanger sequencing **(Fig 2.14A-2.14B)**, we cannot exclude the possibility of a low occurrence of mTOR mutations which may not be enriched within a tumor system where mTORC1 activation is already quite robust.

In Chapter 3, we attempted to evaluate the relative contribution of the eIF4E signaling axis downstream of mTORC1 to PyV mT-driven mammary tumor initiation. As genetic ablation of both 4EBP1 and 4EBP2 was sufficient to restore eIF4E-sensitive translation in the presence of mTOR inhibition (46-48), we sought to restore eIF4E function within Rheb1-deficient pre-neoplastic epithelia in a similar manner. At the time of breeding the conditional 4EBP1$^{fl/fl}$ 4EBP2$^{fl/fl}$ mouse strain into the Rheb1$^{fl/fl}$ MIC strain, it was not known that long-term mTORC1 inhibition resulted in increased TFE3-driven expression of the third isoform 4EBP3 within various human cell lines (49). Despite this, we did not observed increase in 4EBP3 expression following long-term treatment with torin1 within our PyV mT-driven tumors cell lines **(Fig 3.4B)**. These observations suggest that this molecular mechanism of 4EBP3 regulation is not prominent within our murine PyV mT-driven model system. Meanwhile, genetic ablation of both 4EBP1 and 4EBP2 did elicit a modest restoration in mammary epithelia expansion driven by PyV mT expression within the Rheb1$^{fl/fl}$ 4EBP1$^{fl/fl}$ 4EBP2$^{fl/fl}$ MIC mice. Regardless, we cannot disregard the contribution to eIF4E suppression caused by the basal levels of 4EBP3 expression within the epithelia within the Rheb1$^{fl/fl}$ 4EBP1$^{fl/fl}$ 4EBP2$^{fl/fl}$ MIC mice. Although, future work could attempt to evaluate the abundance of eIF4E-eIF4G interaction by a proximity ligation assay within either mammary tissue, or organoid structures derived from Rheb1$^{fl/fl}$ 4EBP1$^{fl/fl}$ 4EBP2$^{fl/fl}$ MIC mice in comparison to 4EBP1$^{fl/fl}$ 4EBP2$^{fl/fl}$ MIC or wildtype MIC controls.

As aforementioned within Chapter 3, we observed that genetic ablation of both 4EBP1 and 4EBP2 resulted in modest restoration of PyV mT-driven epithelial expansion within the Rheb1-deficient pre-neoplastic epithelia. Additionally, we did observe the persistent inhibition of

mTORC1 and consequentially the perturbation of S6K within the Rheb1-deficient 4EBP1/2-deficient pre-neoplastic epithelia. Future work could potentially focus on differentiating the effects attributed to S6K inhibition from mTORC1 inhibition during the early stages of tumor initiation, in attempts to evaluate the contribution of cellular processes uniquely governed between these two kinases. Such a feat could be achieved through the expression of a Rapamycin-insensitive S6K mutant, whereby the S6K T398E is mutated along with the deletion of the auto-inhibitory C-terminus (44). Since robust LacZ expression was achieved from the GTRosa Flx-Stop-Flx LacZ reporter mouse strain used in Chapter 2 **(Fig 2.3C)**, integration of this Rapamycin-insensitive S6K mutant downstream the GTRosa Flx-Stop-Flx construct would couple robust expression of the mutant kinase with the presence of Cre **(Fig 4.2A)**. This strategy would help highlight the contributions mTORC1-dependent, S6K-independent functions that remain perturbed within the Rheb1-deficient pre-neoplastic epithelia. Such functions could include the suppression of autophagy through ULK1/2 phosphorylation (50). The limitation would be that the Rheb1-dependent and mTORC1-independent processes cannot be distinguished within this Rheb1-deficient model system and would require additional investigation.

Additionally, we can further the dissection of S6K function within PyV mT-driven mammary tumor initiation by evaluating the relative contribution of S6K-dependent regulation of translation elongation through the suppression of eEF2 kinase, and consequential de-repression of the eEF2 GTP-dependent translocase. This aspect can be approached *in vitro*, whereby we can target the eEF2 kinase with either the inhibitor A-484954 or an RNAi strategy within our organoid tumor initiation system derived from the Rheb1-deficient pre-neoplastic epithelia within Rheb1$^{fl/fl}$ 4EBP1$^{fl/fl}$ 4EBP2$^{fl/fl}$ MIC mice. Assessment of S6K-mediated suppression of eEF2K within PyV mT-driven tumor initiation could also be approached *in vivo*, by crossing the Rheb1$^{fl/fl}$ 4EBP1$^{fl/fl}$ 4EBP2$^{fl/fl}$ MIC mice with the *Eef2k* knockout strain (51) and examining the resultant pathology within the mammary gland following 2 weeks of doxycycline administration.

Lastly, we also demonstrated within Chapter 3 that a distinct subset of Rheb1-deficient NIC tumors develop a dependency for RalB for mTORC1 activation as a proof-of-concept that alternative small GTPases function to compensate for the loss of Rheb1. Since our initial approach was mostly literature-based, we were limited by the alternative small GTPases that

were previously documented to mediate mTORC1 activation. However, future work could adopt a more exploratory approach and focus on identifying unique interactors bound to mTORC1 within Rheb1-deficient tumors.

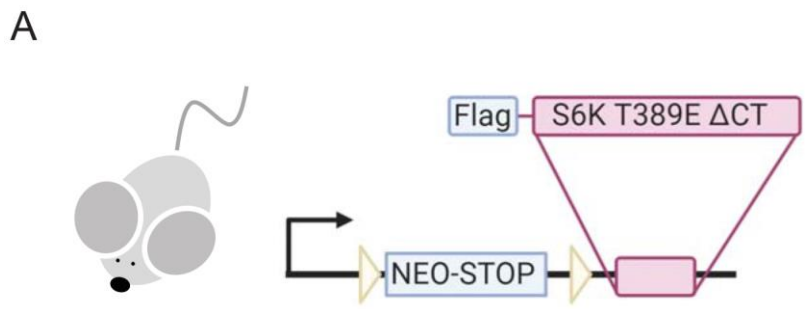

Fig 4.2 Transgenic system for Conditional Expression of mTORC1-independent S6K mutant. (A) Cartoon schematic of transgenic mouse system for conditional overexpression of hyperactivating S6 Kinase mutant. NEO-STOP represents neomycin stop cassette.

From my work in Chapter 2, we generated a few established Rheb1-deficient NIC tumors cell lines which retained comparable levels of mTORC1 activation as their wildtype counterparts. In addition, we established a small repertoire of allografts derived from both Rheb1-deficient NIC and MIC tumors, which can also be generated into primary tumor cell lines **(Fig 3.1C; Fig 3.8A)**. Feasibly, intact mTORC1 could be isolated from lysate generated from these tumor lines by immunoprecipitating the scaffolding protein Raptor, and the various components subjected to mass spectrometry analysis in attempts to identify its interactors. Since co-immunoprecipitation of endogenous Rheb1 with mTORC1 has been documented within the literature to be rather elusive, the Rheb1-deficient tumor cells would be subjected to protein crosslinking in order to further stabilize the potential mTOR-GTPase interaction.

While transcriptome analysis of the Rheb1-deficient mammary tumors in comparison with Rheb1-proficient tumors has been the driving our interrogation the changes within tumor biology, it doesn't provide insight into the changes within the mTORC1 interactome that could drive Rheb1-independent mTORC1 activation in the absence of any transcriptional changes. BioID has been previously employed for various proteins including mTORC2 (52) in attempts to

identify novel interactors, but studies investigating the mTORC1 interactome is still lacking. It would be of interest to examine how the mTORC1 interactome is altered within Rheb1-deficient NIC tumor cells relative to Rheb1-proficient NIC tumor cells. This interrogation may highlight enriched interactions between potentially novel activators and mTORC1, or diminished interactions between inhibitors and mTORC1.

4.6 Closing Remarks

Taken together, this thesis work highlights the unique role of the small GTPase Rheb1 in eliciting mTORC1 activation, despite the presence of alternative small GTPase capable of the similar feat, within mammary tumor initiation. My work has led to the development of various mammalian cell and allograft system, whereby mTORC1 activation is maintained in the absence of Rheb1. Our forward genetics dissection of mTORC1 activation within the Rheb1-deficient mammary tumours uncovered multiple mechanisms of Rheb1-independency, including the development of hyperactivating mTOR mutations and establishing dependency on alternative small GTPases including RalB. While Rheb1-targeted therapeutic potential was reignited upon the discovery of the first Rheb1 small molecule inhibitor (23), this thesis work highlights the potential mechanisms of drug resistance that may hinder future therapeutic efficacy.

4.7 Reference

1. Boulay A, *et al.* (2005) Dual inhibition of mTOR and estrogen receptor signaling in vitro induces cell death in models of breast cancer. *Clinical cancer research : an official journal of the American Association for Cancer Research* 11(14):5319-5328.
2. Shi Y, *et al.* (1995) Rapamycin enhances apoptosis and increases sensitivity to cisplatin in vitro. *Cancer research* 55(9):1982-1988.
3. Wu WK, *et al.* (2011) RNA interference targeting raptor inhibits proliferation of gastric cancer cells. *Experimental cell research* 317(10):1353-1358.
4. Gulhati P, *et al.* (2009) Targeted inhibition of mammalian target of rapamycin signaling inhibits tumorigenesis of colorectal cancer. *Clinical cancer research : an official journal of the American Association for Cancer Research* 15(23):7207-7216.
5. Miller TW, *et al.* (2009) Inhibition of mammalian target of rapamycin is required for optimal antitumor effect of HER2 inhibitors against HER2-overexpressing cancer cells. *Clinical cancer research : an official journal of the American Association for Cancer Research* 15(23):7266-7276.
6. Yan C, *et al.* (2014) The mTOR inhibitor rapamycin synergizes with a fatty acid synthase inhibitor to induce cytotoxicity in ER/HER2-positive breast cancer cells. *PloS one* 9(5):e97697.

7. Mosley JD, Poirier JT, Seachrist DD, Landis MD, & Keri RA (2007) Rapamycin inhibits multiple stages of c-Neu/ErbB2 induced tumor progression in a transgenic mouse model of HER2-positive breast cancer. *Molecular cancer therapeutics* 6(8):2188-2197.
8. Melser S, *et al.* (2013) Rheb regulates mitophagy induced by mitochondrial energetic status. *Cell metabolism* 17(5):719-730.
9. Zhou X, *et al.* (2009) Rheb controls misfolded protein metabolism by inhibiting aggresome formation and autophagy. *Proceedings of the National Academy of Sciences of the United States of America* 106(22):8923-8928.
10. Sato T, Nakashima A, Guo L, & Tamanoi F (2009) Specific activation of mTORC1 by Rheb G-protein in vitro involves enhanced recruitment of its substrate protein. *The Journal of biological chemistry* 284(19):12783-12791.
11. Goorden SM, *et al.* (2011) Rheb is essential for murine development. *Molecular and cellular biology* 31(8):1672-1678.
12. Guertin DA, *et al.* (2006) Ablation in mice of the mTORC components raptor, rictor, or mLST8 reveals that mTORC2 is required for signaling to Akt-FOXO and PKCalpha, but not S6K1. *Dev Cell* 11(6):859-871.
13. Zou J, *et al.* (2011) Rheb1 is required for mTORC1 and myelination in postnatal brain development. *Dev Cell* 20(1):97-108.
14. Martin TD, *et al.* (2014) Ral and Rheb GTPase activating proteins integrate mTOR and GTPase signaling in aging, autophagy, and tumor cell invasion. *Molecular cell* 53(2):209-220.
15. Xiao B, *et al.* (2020) Rheb1-Independent Activation of mTORC1 in Mammary Tumors Occurs through Activating Mutations in mTOR. *Cell reports* 31(4):107571.
16. Wang H, *et al.* (2010) Phosphorylation of RalB is important for bladder cancer cell growth and metastasis. *Cancer research* 70(21):8760-8769.
17. Martin TD, Mitin N, Cox AD, Yeh JJ, & Der CJ (2012) Phosphorylation by protein kinase Calpha regulates RalB small GTPase protein activation, subcellular localization, and effector utilization. *The Journal of biological chemistry* 287(18):14827-14836.
18. Gentry LR, *et al.* (2015) Divergent roles of CAAX motif-signaled posttranslational modifications in the regulation and subcellular localization of Ral GTPases. *The Journal of biological chemistry* 290(37):22851-22861.
19. Hanker AB, *et al.* (2010) Differential requirement of CAAX-mediated posttranslational processing for Rheb localization and signaling. *Oncogene* 29(3):380-391.
20. Buerger C, DeVries B, & Stambolic V (2006) Localization of Rheb to the endomembrane is critical for its signaling function. *Biochem Biophys Res Commun* 344(3):869-880.
21. Basso AD, *et al.* (2005) The farnesyl transferase inhibitor (FTI) SCH66336 (lonafarnib) inhibits Rheb farnesylation and mTOR signaling. Role in FTI enhancement of taxane and tamoxifen anti-tumor activity. *The Journal of biological chemistry* 280(35):31101-31108.
22. Ding H, *et al.* (2014) Farnesyltransferase inhibitor tipifarnib inhibits Rheb prenylation and stabilizes Bax in acute myelogenous leukemia cells. *Haematologica* 99(1):60-69.
23. Mahoney SJ, *et al.* (2018) A small molecule inhibitor of Rheb selectively targets mTORC1 signaling. *Nature communications* 9(1):548.
24. Faller WJ, *et al.* (2015) mTORC1-mediated translational elongation limits intestinal tumour initiation and growth. *Nature* 517(7535):497-500.

25. Larsson O, *et al.* (2012) Distinct perturbation of the translatome by the antidiabetic drug metformin. *Proceedings of the National Academy of Sciences of the United States of America* 109(23):8977-8982.
26. Wendel HG, *et al.* (2007) Dissecting eIF4E action in tumorigenesis. *Genes & development* 21(24):3232-3237.
27. Furic L, *et al.* (2010) eIF4E phosphorylation promotes tumorigenesis and is associated with prostate cancer progression. *Proceedings of the National Academy of Sciences of the United States of America* 107(32):14134-14139.
28. Truitt ML, *et al.* (2015) Differential Requirements for eIF4E Dose in Normal Development and Cancer. *Cell* 162(1):59-71.
29. Chauvin C, *et al.* (2014) Ribosomal protein S6 kinase activity controls the ribosome biogenesis transcriptional program. *Oncogene* 33(4):474-483.
30. Mitchell NC, *et al.* (2015) S6 Kinase is essential for MYC-dependent rDNA transcription in Drosophila. *Cellular signalling* 27(10):2045-2053.
31. Hannan KM, *et al.* (2003) mTOR-dependent regulation of ribosomal gene transcription requires S6K1 and is mediated by phosphorylation of the carboxy-terminal activation domain of the nucleolar transcription factor UBF. *Molecular and cellular biology* 23(23):8862-8877.
32. Mayer C, Zhao J, Yuan X, & Grummt I (2004) mTOR-dependent activation of the transcription factor TIF-IA links rRNA synthesis to nutrient availability. *Genes & development* 18(4):423-434.
33. Ghosh AP, *et al.* (2015) Point mutations of the mTOR-RHEB pathway in renal cell carcinoma. *Oncotarget* 6(20):17895-17910.
34. Xu J, *et al.* (2016) Mechanistically distinct cancer-associated mTOR activation clusters predict sensitivity to rapamycin. *The Journal of clinical investigation* 126(9):3526-3540.
35. Grabiner BC, *et al.* (2014) A diverse array of cancer-associated MTOR mutations are hyperactivating and can predict rapamycin sensitivity. *Cancer discovery* 4(5):554-563.
36. Cerami E, *et al.* (2012) The cBio cancer genomics portal: an open platform for exploring multidimensional cancer genomics data. *Cancer discovery* 2(5):401-404.
37. Gao J, *et al.* (2013) Integrative analysis of complex cancer genomics and clinical profiles using the cBioPortal. *Science signaling* 6(269):pl1.
38. Yang H, *et al.* (2017) Mechanisms of mTORC1 activation by RHEB and inhibition by PRAS40. *Nature* 552(7685):368-373.
39. Rodrik-Outmezguine VS, *et al.* (2016) Overcoming mTOR resistance mutations with a new-generation mTOR inhibitor. *Nature* 534(7606):272-276.
40. Lim KH, *et al.* (2005) Activation of RalA is critical for Ras-induced tumorigenesis of human cells. *Cancer cell* 7(6):533-545.
41. Morrison Joly M, *et al.* (2016) Rictor/mTORC2 Drives Progression and Therapeutic Resistance of HER2-Amplified Breast Cancers. *Cancer research* 76(16):4752-4764.
42. Audet-Walsh É, *et al.* (2017) Nuclear mTOR acts as a transcriptional integrator of the androgen signaling pathway in prostate cancer. *Genes & development* 31(12):1228-1242.
43. Schalm SS, Fingar DC, Sabatini DM, & Blenis J (2003) TOS motif-mediated raptor binding regulates 4E-BP1 multisite phosphorylation and function. *Current biology : CB* 13(10):797-806.
44. Schalm SS & Blenis J (2002) Identification of a conserved motif required for mTOR signaling. *Current biology : CB* 12(8):632-639.

45. Nojima H, *et al.* (2003) The mammalian target of rapamycin (mTOR) partner, raptor, binds the mTOR substrates p70 S6 kinase and 4E-BP1 through their TOR signaling (TOS) motif. *The Journal of biological chemistry* 278(18):15461-15464.
46. Thoreen CC, *et al.* (2012) A unifying model for mTORC1-mediated regulation of mRNA translation. *Nature* 485(7396):109-113.
47. Morita M, *et al.* (2013) mTORC1 controls mitochondrial activity and biogenesis through 4E-BP-dependent translational regulation. *Cell metabolism* 18(5):698-711.
48. Dowling RJ, *et al.* (2010) mTORC1-mediated cell proliferation, but not cell growth, controlled by the 4E-BPs. *Science (New York, N.Y.)* 328(5982):1172-1176.
49. Tsukumo Y, Alain T, Fonseca BD, Nadon R, & Sonenberg N (2016) Translation control during prolonged mTORC1 inhibition mediated by 4E-BP3. *Nature communications* 7:11776.
50. Kim J, Kundu M, Viollet B, & Guan KL (2011) AMPK and mTOR regulate autophagy through direct phosphorylation of Ulk1. *Nature cell biology* 13(2):132-141.
51. Ryazanov AG (2002) Elongation factor-2 kinase and its newly discovered relatives. *FEBS letters* 514(1):26-29.
52. Kovalski JR, *et al.* (2019) The Functional Proximal Proteome of Oncogenic Ras Includes mTORC2. *Molecular cell* 73(4):830-844.e812.